



The University of Reading

Regulation of Focal Adhesions by PtdIns(4,5)P₂ and PtdIns(3,4,5)P₃ in Cancer Cell Migration

Thesis submitted for the degree of Doctor of Philosophy
(PhD)

By

Dhurgham Al-Fahad

School of Biological Sciences

Ph.D. Thesis

April 2018

Declaration

I confirm that this is my own work and the use of all materials from other sources has been properly and fully acknowledged.

Signature:

Date:

Table of contents

Abstract	17
-----------------------	----

Chapter 1 Literature Review

1.1 Cancer overview.....	18
1.2 Cancer metastasis.....	21
1.3 Focal adhesions.....	26
1.4 FA assembly.....	31
1.5 Actin polymerisation	33
1.6 Myosin.....	35
1.7 FA disassembly.....	37
1.8 Phospholipids.....	40
1.9 Lipid kinases and phosphatases in PI cycle	42
1.10 Types of kinases and phosphatase involved in PIs cycle.....	42
1.11 PH domains and phosphoinositide.....	48
1.12 Role of the PI cycle in cancer.....	50
1.13 Role of the PI in FAs.....	51
1.14 Hypothesis and aims.....	62

Chapter 2: Materials and Methods

2.1 Reagents.....	63
2.2 Methods.....	69
2.2.1 Molecular biology and cloning.....	69
2.2.1. I Ampicillin and Kanamycin stock.....	69
2.2.1. II LB Agar.....	69
2.2.1. III Agar Plates.....	70
2.2.1. III Plasmid DNA purification.....	70
2.2.1. V Determination of DNA concentration and purity.....	72
2.2.2 Construction of fluorescent biosensors.....	72

2.2.2. I Digestion of plasmids.....	72
2.2.2. II Separation of digested plasmid.....	73
2.2.2. III agarose gel purification and gel extraction.....	74
2.2.2. IV Construction of primers.....	75
2.2.2. V Amplification of PH domain-PCR conditions.....	76
2.2.2. VI Transformation.....	77
2.2.2. VII Miniprep.....	77
2.3 Cell culture.....	83
2.3. I Routine cell passaging	83
2.4. Co-localisation Assay.....	85
2.4. I Coating wells plate with ECM.....	85
2.4. II Transfection.....	86
2.4 III. Immunofluorescence Staining.....	86
2.4 IV Confocal microscopy.....	87
2.4 V Co-localisation analysis.....	88
2.5 Local generation of lipids within FA turnover assay.....	89
2.5. I Co-transfection.....	89
2.5. II Confocal microscopy and live image.....	90
2.6 Inhibitor treatment.....	91
2.6. I Co-Transfection.....	92
2.6. II Live-cell time-lapse microscopy.....	92
2.6. III Wound Healing Assay.....	93
2.7 Immunoprecipitation and western blotting (IP and WB).....	94

2.7. I Cell lysate preparation.....	94
2.7. II Bradford protein assay.....	94
2.7. III Immunoprecipitation.....	95
2.7. IV Western blotting.....	95
2.8 Statistical analysis.....	97
Chapter 3: Spatial organisation between PtdIns(4,5)P2 / PtdIns(3,4,5)P3 and FAs	
3.1 Introduction.....	98
3.2 Results.....	101
3.2.1 Visualisation of PtdIns(4,5)P2 and PtdIns(3,4,5)P3 by PLC δ 1-PH-GFP/mCherry and Btk-PH-GFP/mCherry biosensor respectively in fixed and live cells.....	101
3.2.3 Effect of Btk-PH-GFP overexpression on PtdIns(3,4,5)P3 localisation.....	104
3.2.4 Comparison between antibodies and PH-domains to detect PtdIns(3,4,5)P3 and PtdIns(4,5)P2.....	107
3.2.5 Spatial regulation of PtdIns(4,5)P2 within a single FA in live and fixed cells.....	110
3.2.6 Spatial regulation of PtdIns(3,4,5)P3 within a single FA in live and fixed cells.....	114
3.2.7 Spatial regulation of PtdIns(4,5)P2 and PtdIns(3,4,5)P3 at the leading and trailing edges of cell within a single FA.....	118
3.2.8 Effect of PI3K and PLC inhibitors on co-localisation of PtdIns(4,5)P2 and PtdIns(3,4,5)P3 within FAs..	124
3.3 Discussion	129
Chapter 4: Temporal organisation of PtdIns(4,5)P2 and PtdIns(3,4,5)P3 within FAs	
4.1 Introduction.....	141
4.2 Results	144
4.2.1 Temporal regulation of PtdIns(4,5)P2 during assembly and disassembly of a single FA	144

4.2.2 Temporal regulation of PtdIns(3,4,5)P3 during assembly and disassembly of a single FA.....	150
4.2.3 Discussion.	155
Chapter five: The role of the PLC and PI3K signalling in FA turnover and cell migration	
5.1 Introduction.....	166
5.2 Results.....	168
5.2.1 PLC and PI3K inhibitors reduce the decline of PtdIns(4,5)P2 during FAs disassembly.	168
5.2.2 Effect of PLC and PI3K inhibition on FAs turnover.....	174
5.2.3 Effect PLC and PI3K inhibition on cell migration and wound healing.....	174
5.2.4 Interaction of PLC and PI3K with FAs.....	183
5.2.5 Discussion.....	190
Chapter 6: General discussion.....	208
Bibliography.....	214

Table of Tables:

Table 1.1: Mammalian phosphoinositide kinases.....	46
Table 1.2: Mammalian phosphoinositide phosphatases.....	47
Table 2.1: Cell culture reagents.....	63
Table 2.2: Molecular Biology Reagents.....	63
Table 2.3: Biochemical assay reagents.....	64
Table 2.4: Materials and solutions for biochemical assays.....	65
Table 2.5: Antibodies.....	67
Table 3.1: Data showing co-localisation values \pm standard deviation (SD) between PtdIns(4,5)P2 and FAs.....	112
Table 3.2: Data showing co-localisation values \pm (SD) between PtdIns(4,5)P2 and paxillin on collagen, fibronectin and gelatine.....	113
Table 3.3: Data show co-localisation values \pm (SD) between PtdIns(3,4,5)P3 and FAs.....	116
Table 3.4: Data showing co-localisation values \pm (SD) between PtdIns(3,4,5)P3 and paxillin on collagen, fibronectin and gelatine.....	117
Table 3.5: Data show co-localisation values \pm standard deviation between PtdIns(4,5)P2 and paxillin at the leading and trailing edge on collagen and fibronectin.....	120
Table 3.6: Data shows Co-localisation values \pm SD between PtdIns(4,5)P2 and paxillin at the leading and trailing edge on collagen and fibronectin.....	122
Table 3.7: Data showing Co-localisation values \pm standard deviation between PtdIns(4,5)P2 and zyxin	126
Table 3.8: Data showing Co-localisation values \pm SD between PtdIns(4,5)P2 and zyxin.....	128
Table 4.1: Percentage dynamic change of local levels of PtdIns(4,5)P2 within and around during zyxin turnover.....	147
Table 4.2: Percentage dynamic change of local levels of PtdIns(4,5)P2 within and around during paxillin turnover.....	148

.

Table 4.3: Percentage dynamic change of local generation level of PtdIns(3,4,5)P3 within and around zyxin turnover.....	153
Table 4.4: Percentage dynamic change of local levels of PtdIns(4,5)P2 within and around paxillin turnover.....	154
Table 5.1: Percentage decrease of local levels of PtdIns(4,5)P2 within zyxin disassembly.....	171
Table 5.2: Percentage decrease of local generation level of PtdIns(4,5)P2 within zyxin disassembly.....	173
Table 5.3: Effect of PLC inhibitor on FAs turnover time.....	177
Table 5.4: Effect of PI3K (LY294002) inhibitor on FAs turnover time.....	179

Table of Figures

Figure (1.1): The hallmarks of cancer.....	20
Figure (1.2): The metastatic cascade.....	22
Figure (1.3): The tumour microenvironment.....	25
Figure (1.4): The integrin subunits and their ECM interactions.....	27
Figure (1.5): Focal adhesion.....	30
Figure (1.6): Actin polymerisation.....	34
Figure (1.7): Adhesive signalling in cell migration.....	36
Figure (1.8): Traditional view of cell migration.....	39
Figure (1.9): Structure of PI and its phosphoinositide derivatives.....	41
Figure (1.10): molecular structure of mammalian phosphoinositide 3-kinases.....	43
Figure (1.11): Structure of mammalian of PLC isoforms	44
Figure (1.12): PI cycle.....	46
Figure (1.13): PI cycle.....	47
Figure (1.14): Structure of PH domain in complex with PI.....	49
Figure (1.15): PtdIns(4,5)P ₂ may enhance talin-integrin interaction.....	52
Figure (1.16): A model showing a possible role of PI3K and PLC signalling in cancer cell migration.	54
Figure (1.17): The cryo Vt–F-actin structure.....	58
Figure (1.18): PtdIns(4,5)P ₂ leads vinculin oligomerisation by unfolding the N terminus of Vt.....	60
Figure (2.1): Construction of PLC δ 1-PH-mCherry.....	80
Figure (2.2): Construction of Btk-PH-mCherry.....	82

Figure (2.3): showing A) spatial co-localisation between PtdIns(4,5)P2 and paxillin. B) Reverse spatial co-localisation measurement between paxillin and PI(4,5)P2.....	89
Figure (3.1): visualisation of PtdIns(4,5)P2 and PtdIns(3,4,5)P3 on the variety of surfaces in fixed cells.....	102
Figure (3.2): Visualisation of PtdIns(4,5)P2 and PtdIns(3,4,5)P3 on the variety of surfaces in live cells ..	103
Figure (3.3): Effect of Btk-PH-GFP overexpression in the fixed cell.....	105
Figure (3.4): Effect of Btk-PH-GFP overexpression in live cells.....	106
Figure (3.5): Quantification of PtdIns(3,4,5)P3 localisation.....	108
Figure (3.6): Quantification of PtdIns(4,5)P2 localisation.....	109
Figure (3.7): Spatial co-localisation between PtdIns(4,5)P2 and a single FA in MDA-MB-231 cells on the variety of surfaces.....	111
Figure (3.8). Quantification the spatial co-localisation of PtdIns(4,5)P2 within single FA.....	112
Figure (3.9). Quantification of spatial co-localisation between PtdIns(4,5)P2 and paxillin.....	113
Figure (3.10): Spatial co-localisation between PtdIns(3,4,5)P3 and a single FAs.....	115
Figure (3.11). Quantification of spatial co-localisation between PtdIns(3,4,5)P3 and paxillin.....	117
Figure (3.12) : Spatial co-localisation between PtdIns(4,5)P2 and paxillin at the leading and trailing edges of MDA-MB-231 cells on variety of surfaces.....	120
Figure (3.13): Quantification of spatial co-localisation between PtdIns(4,5)P2 and paxillin at the leading and trailing edges.....	121
Figure (3.14): Spatial co-localisation between PtdIns(3,4,5)P3 and paxillin at the leading and trailing edges of MDA-MB-231 cells on a variety of surfaces.....	122

Figure (3.15): Quantification of spatial co-localisation between PtdIns(3,4,5)P3 and paxillin at the leading and trailing edges.....	123
Figure (3.16): Effect PI3K and PLC inhibitors on spatial co-localisation between PtdIns(4,5)P2 and zyxin.....	125
Figure (3.17): PI3K inhibitors reduce spatial co-localisation between PtdIns(3,4,5)P3 and Zyxin.....	126
Figure (3.18): Effect PI3K and PLC inhibitors on spatial co-localisation between PtdIns(4,5)P2 and zyxin.....	127
Figure (3.19): PI3K inhibitors reduce spatial co-localisation between PtdIns(3,4,5)P3 and Zyxin.....	128
Figure (3.20): Showing Btk-PH and PLC δ 1-PH domains which are recruited by PtdIns(3,4,5)P3 and PtdIns(4,5)P2 respectively.....	132
Figure (3.21): Illustrating the effect of overexpression of PH domain and the abundance of lipids.....	133
Figure (3.22): Schematic model of the spatial organisation of FA-Phosphatidylinositol interactions within cell membrane.....	136
Figure (3.24): Illustrating of PtdIns(4,5)P2 and PtdIns(3,4,5)P3 metabolic pathways on plasma membrane and the effect PLC and PI3K inhibitors on local generation level of PtdIns(4,5)P2 and PtdIns(3,4,5)P3.....	139
Figure (4.1): Quantification of the local levels of PtdIns(4,5)P2 within a single FA.....	145
Figure (4.2): Quantification of the local levels of PtdIns(4,5)P2 within and around a single FA.....	147
Figure (4.3): Quantification of the local levels of PtdIns(4,5)P2 within and around a single FA.....	148
Figure (4.4): The dynamic change of local levels of PtdIns(4,5)P2 during zyxin turnover:.....	149

Figure (4.5): Quantification of the local levels of PtdIns(3,4,5)P3 within a single FA.....	151
Figure (4.6): The dynamic change of local levels of PtdIns(3,4,5)P3 during zyxin turnover.....	153
Figure (4.7): The dynamic change of local levels of PtdIns(3,4,5)P3 during paxillin turnover.....	154
Figure (4.8): Schematic of the recruitment and release of talin and vinculin by PtdIns(3,4,5)P3 during FA assembly and disassembly:.....	157
Figure (4.9): Proposed model of the interaction between PtdIns(4,5)P2 and FA proteins during assembly and disassembly process:.....	158
Figure (5.1): Effect of PLC on the decline of PtdIns(4,5)P2 during FA disassembly.....	170
Figure (5.2): PLC (U73122) inhibitor reduces the decline of PtdIns(4,5)P2 during FA disassembly.....	171
Figure (5.3): Effect of PI3K on the decline of PtdIns(4,5)P2 during FA disassembly.....	172
Figure (5.4): PI3K (LY294002) inhibitor reduces the decline of PtdIns(4,5)P2 during FA disassembly.....	173
Figure (5.5): Effect of PLC inhibitor (U73122) on FA turnover:.....	176
Figure (5.6): Effect of PLC inhibitor (U73122) on FA turnover.....	177
Figure (5.7): Effect of PI3K inhibitor (LY294002) on FA turnover:.....	178
Figure (5.8): Effect of PI3K inhibitor (LY294002) on FA turnover.....	179
Figure (5.9): Effect of PLC U73122 inhibitor on cell migration and wound healing in MDA-MB-231 cells on a fibronectin surface.....	180
Figure (5.10): Effect of PLC LY294002 inhibitor on cell migration and wound healing in MDA-MB-231 cells on a fibronectin surface.....	181

Figure (5.11): Effect of PLC Wormannin inhibitor on cell migration and wound healing in MDA-MB-231 cells on a fibronectin surface.....	182
Figure (5.12): Co-immunoprecipitates(IP) of FA complex.	184
Figure (5.13): co-immunoprecipitates(IP) of PI3K110 α and FAs.....	185
Figure (3.14): Spatial co-localisation between anti-PI3K110 α and vinculin MDA-MB-231 cells on the fibronectin.....	186
Figure (5.15): Co-localisation and co-immunoprecipitates(IP) of PI3K85 and FAs.....	187
Figure (3.16): Spatial co-localisation between anti-PI3Kp85 and vinculin MDA-MB-231 cells on the fibronectin.....	188
Figure (5.17): co-immunoprecipitates(IP) of PLC β 1 and FAs.....	189
Figure (4.18): A model showing a possible role of PLC within FA disassembly.....	191
Figure (5.19): A model showing a possible role of PLC and PI3K within FA disassembly.....	197
Figure (5.20): Effect of PI3K and PLC on FA turnover and cell migration.....	203

Table of abbreviations

ANOVA	Analysis of variance
APS	Ammonium persulphate
Arp2/3	Actin-Related Proteins 2/3
Btk	Bruton's tyrosine kinase
BM	Basement membrane
BSA	Bovine serum albumin
CAFs	Cancer associated fibroblasts
CaMK-II	Calmodulin dependent protein kinase-II
Cas	Crk-associated substrate
CAT	Collective to amoeboid transition
DAG	Diacylglycerol
DAPI	4,6-diamidino-2-phenylindole
DMEM	Dulbecco's modified Eagle's medium
DMSO	Dimethyl sulfoxide
DNA	Deoxyribonucleic acid
ECL	Enhanced chemiluminescence
ECM	Extracellular matrix
EDTA	Ethylenediaminetetra acetic acid
EGF	Epidermal growth factor
EMT	Epithelial-mesenchymal transition
ER	Endoplasmic reticulum
ERK	Extracellular signal-regulated kinase
FAK	Focal adhesion kinase
FAs	Focal adhesions
FBS	Foetal bovine serum
FLIM	Fluorescence lifetime imaging microscopy
FRET	Fluorescence resonance energy transfer
GFP	Green fluorescent protein
HR2	Helical domain
IP	Immunoprecipitation
IP3	Inositol trisphosphate
LB	Luria-Bertani
LPA	Lysophosphatidic acid
MAT	Mesenchymal to amoeboid transition
MLC	Myosin light chain
MLCK	MLC kinase

MMP	Matrix metalloproteinase
MOC	Mander's overlap coefficient
mTOR	Mammalian target of rapamycin
PA	Phosphatidic acid
PAGE	Polyacrylamide gel electrophoresis
PBS	Phosphate-buffered saline
PCC	Pearson coefficient correlation
PDGF	Platelet-derived growth factor
PDK1	3-phosphoinositide-dependent protein kinase 1
PEI	Polyethylenimine
PFA	Paraformaldehyde
PH	Pleckstrin homology
PI3K	Phosphoinositide-3-kinase
PI4Ks	Phosphatidylinositol-4 kinases
PIC	Protease inhibitor cocktail
PtdIns(4,5)P2	Phosphoinositide 4,5-bisphosphate
PtdIns(3,4,5)P3	Phosphoinositide 3,4,5-trisphosphate
PIP5K	Phosphatidylinositol 4-phosphate 5-kinase
PIPKs	Phosphatidylinositol phosphate kinases
PIs	Phosphatidylinositols
PKA	Protein kinase A
PKC	Protein kinase C
PLC	Phospholipase C
PLC δ	Phospholipase C delta
PLD	Phospholipase D
PR	Proline-rich region
PTEN	Phosphatase and tensin homolog deleted on chromosome ten
PVDF	Polyvinylidene fluoride
PX	Phox homology domain
Pyk2	Proline-rich tyrosine kinase2
RA	Ras-association
RIPA	Radio-Immunoprecipitation Assay
RNA	Ribonucleic acid
RPTP- α	Receptor tyrosine phosphatase α
SDS	Sodium dodecyl sulphate
SFKs	Src-family kinases
SOCS6	Suppressor of Cytokine Signalling 6
Src	Proto-oncogene tyrosine-protein kinase

TAMs	Tumour associated macrophages
TEMED	N N N'N'-tetramethylethylenediamine
TGF- β	Transforming growth factor beta
VEGF	Vascular endothelial growth factor
Vps34	Vacuolar protein sorting 34
WB	Western blotting
γ -SA	γ -specific array

Abstract

Phosphoinositides and their downstream signalling molecules are involved in adhesion, proliferation and invasion. In this study, MDA-MB-231 breast cancer has been used to investigate the possible role of PtdIns(4,5)P2 and PtdIns(3,4,5)P3 in the regulation of FA turnover.

Firstly, PtdIns(4,5)P2 and PtdIns(3,4,5)P3 have been visualised by PLC δ 1-PH-GFP or mCherry and Btk-PH-GFP or mCherry respectively. Then, the spatial organisation of PtdIns(4,5)P2 and PtdIns(3,4,5)P3 with FA proteins was directly studied. PtdIns(4,5)P2 and PtdIns(3,4,5)P3 were moderately co-localised with FA proteins, such as talin, vinculin, FAK, paxillin and zyxin. PLC inhibition increased co-localisation between PtdIns(4,5)P2 and FA, while PI3K inhibition had no effect.

Temporal organisation between PtdIns(4,5)P2 and PtdIns(3,4,5)P3 and FAs was studied. The local levels of PtdIns(4,5)P2 within a single FA increased gradually during assembly and declined gradually during the disassembly process. Whereas, PtdIns(3,4,5)P3 levels within FA were almost at a constant level during FAs assembly and disassembly. PLC inhibition significantly reduced the decline in PtdIns(4,5)P2 levels within single FA disassembly, while PI3K inhibition had only a small effect. Additionally, PLC and PI3K significantly inhibited FA turnover, cell migration and wound healing.

Finally, Co-IP studies showed that PI3K p110 α and PLC β 1 directly associated with vinculin and talin, while PI3K p85 did not interact with them. Reverse co-IP was used to confirm the interaction of PLC and PI3K with FA proteins.

In summary, PtdIns(4,5)P2 plays a role in the regulation of FA turnover and cell migration.

Keywords: focal adhesions, cell migration, PtdIns(4,5)P2, PtdIns(3,4,5)P3, PI3K, PLC.

Chapter One: Literature review

1.1. Cancer overview

Cancer is a group of diseases and disorders characterized by uncontrolled cell division with its ability to invade nearby tissues and metastasize to distant sites of the body. Cancer is caused by alterations in genes and expression, such as impaired tumour suppressor genes, leading to dysregulation of normal cell differentiation and cell division (Steege, 2006, Valastyan and Weinberg, 2011).

The factors that enable cancer cells to metastasize throughout the body are summarised to a number of traits often termed the hallmarks of cancer (Figure 1.1). Normal cells divide and grow under the control of many signalling molecules, such as hormones. However, cancer cells use different mechanisms to generate or activate signalling for themselves often known autocrine signalling which allow them to grow and divide continually, a process called as self-sufficiency in growth signals (Hanahan and Weinberg, 2011, Evan and Vousden, 2001). Normal cells respond to the surrounding environment or signals that inform them to discontinue division in the event of any defect, this process is controlled by tumour suppressor genes. However, cancer cells do not respond to these signals due to alterations and mutations in tumour suppressor genes. Add to that normal cells respond to contact inhibition to stop division and growth, while cancer cells do not have this feature and become more resistant, a process known as insensitivity to anti-growth signals (Hanahan and Weinberg, 2011, McClatchey and Yap, 2012).

In the occurrence of any defect in the cells, normal cells undergo programmed cell death (apoptosis) to stop them from division and growth and protect the cells from damage.

However, cancer cells have the ability to avoid apoptosis and this trait is called evading programmed cell death (Elmore, 2007, Hanahan and Weinberg, 2011). Normal cells possess a limited number of divisions due to telomeres which shorten during the process of division and activates senescence. Cancer cells, however, do not undergo this process as they activate telomerase which in turn increases the telomere length in the chromosomes, thus they divided continuously without interruption, this process is often termed limitless replicative potential (Greenberg, 2005, Hanahan and Weinberg, 2011).

The metabolic pathway in cancer cells is also quite different from normal cells. The production of energy in the cancer cells occurs through upregulating glycolysis. For example, mitochondria do not use normal aerobic respiration (oxidation of pyruvate, the citric acid cycle, and the electron transport chain), and do not entirely oxidize the glucose to ATP. This process is known as deregulated metabolism (Forrest, 2015, Gottlieb et al., 2003).

Furthermore, cancerous cells evade the immune system through avoidance of the immune signals that kill them. Sustained angiogenesis process plays an important role in the sustainability of tumour via formation of new blood vessels to deliver enough oxygen and nutrients (Bergers and Benjamin, 2003, Hanahan and Weinberg, 2011). Cancerous cells suffer from frequent mutations in the chromosomes which is known as genome instability, therefore, cancer cells are characterized from normal cells in faster cell proliferation and migration (Figure 1.1) (Hanahan and Weinberg, 2011).

Cancer cells undergo many changes that enable them to invade tissues and metastasize to distant sites, which is known as tissue invasion and metastasis (Hanahan and Weinberg, 2011, van Zijl et al., 2011).

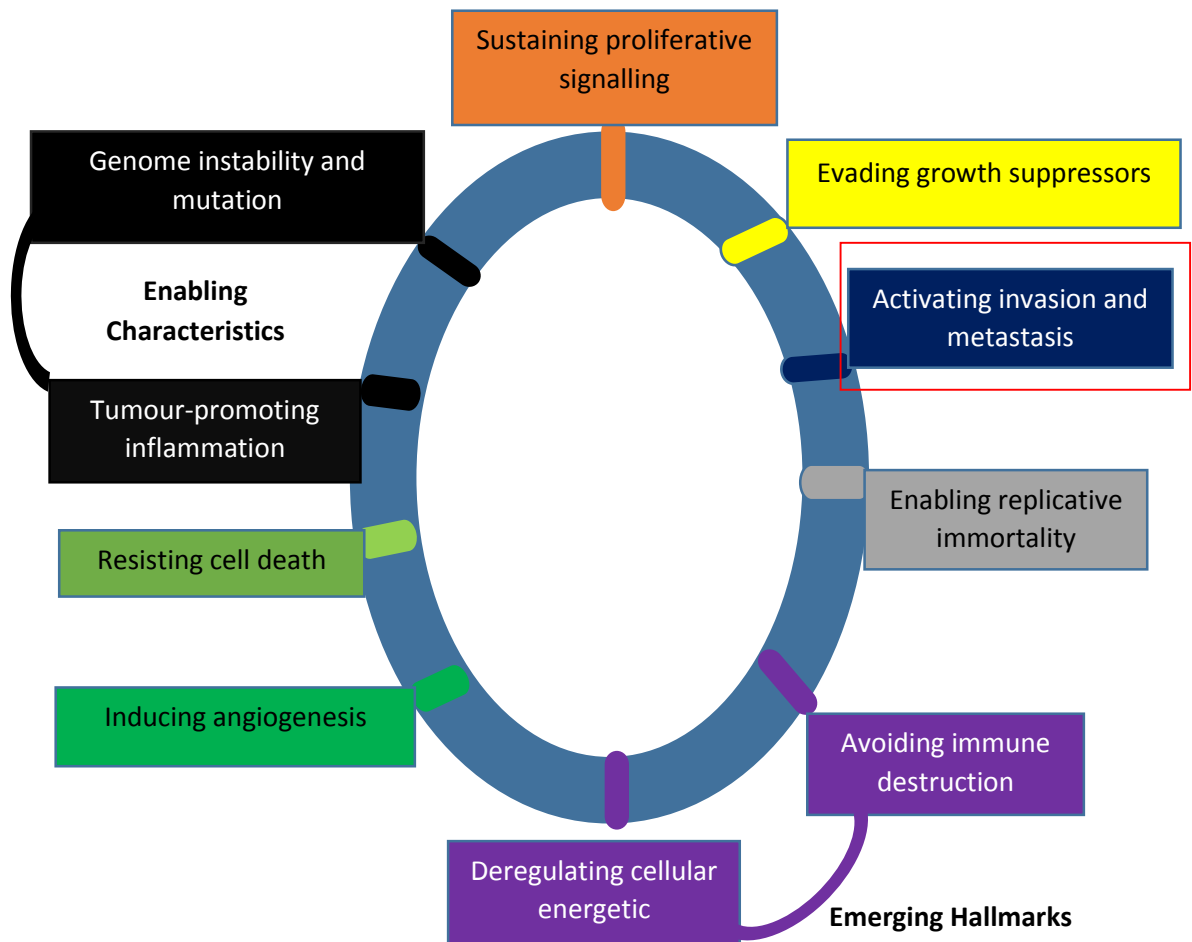


Figure (1.1): The hallmarks of cancer. The acquired capabilities are responsible for transforming normal cells into malignant tumour and metastasize to secondary site. The activation and metastasis will be the important part for this study, Modified: from Hanahan and Weinberg (2011).

1.2. Cancer metastasis

Cancer cells disseminate from the primary tumour (their original site) to distant sites to constitute a secondary tumour through process termed metastasis (Brooks et al., 2010). There are several complex biological processes that form metastasis through a progression of premalignant cells to a malignant tumour, a process known as the invasion metastasis cascade. Primary tumour invades stromal and extracellular matrix (ECM) layers locally through increasing the expression of proteases, such as matrix metalloproteinases (MMPs) which can degrade the ECM and basement membrane (BM) and decrease the expression of cellular adhesion molecules, such as focal adhesions and cell–cell junctions. Tumour cells then have the ability to enter blood vessels and transport to different organs. In this stage, many tumour cells die in the circulation. Surviving tumour cells transfer through vasculature and invade tissue at a distant site, then extend to form invadopodia to penetrate between endothelial cells and degrade ECM and BM by using MMPs to across into the parenchyma tissue (Valastyan and Weinberg, 2011). After extravasation the tumour cells will face difficulties in their new microenvironment which differs from their normal tissue. Therefore, tumour cells respond to growth factors or generate their own growth factor in order to survive and form micrometastasis. During this process the tumour cells will be extremely susceptible to the immune system and therefore must survive it to form micrometastasis. Some micrometastasis have the ability to grow and proliferate through inducing angiogenesis to provide nutrients and eventually form macrometastasis (Figure 1.2). Some micrometastasis, however, cannot grow to macrometastasis due to undergoing apoptosis (Valastyan and Weinberg, 2011).

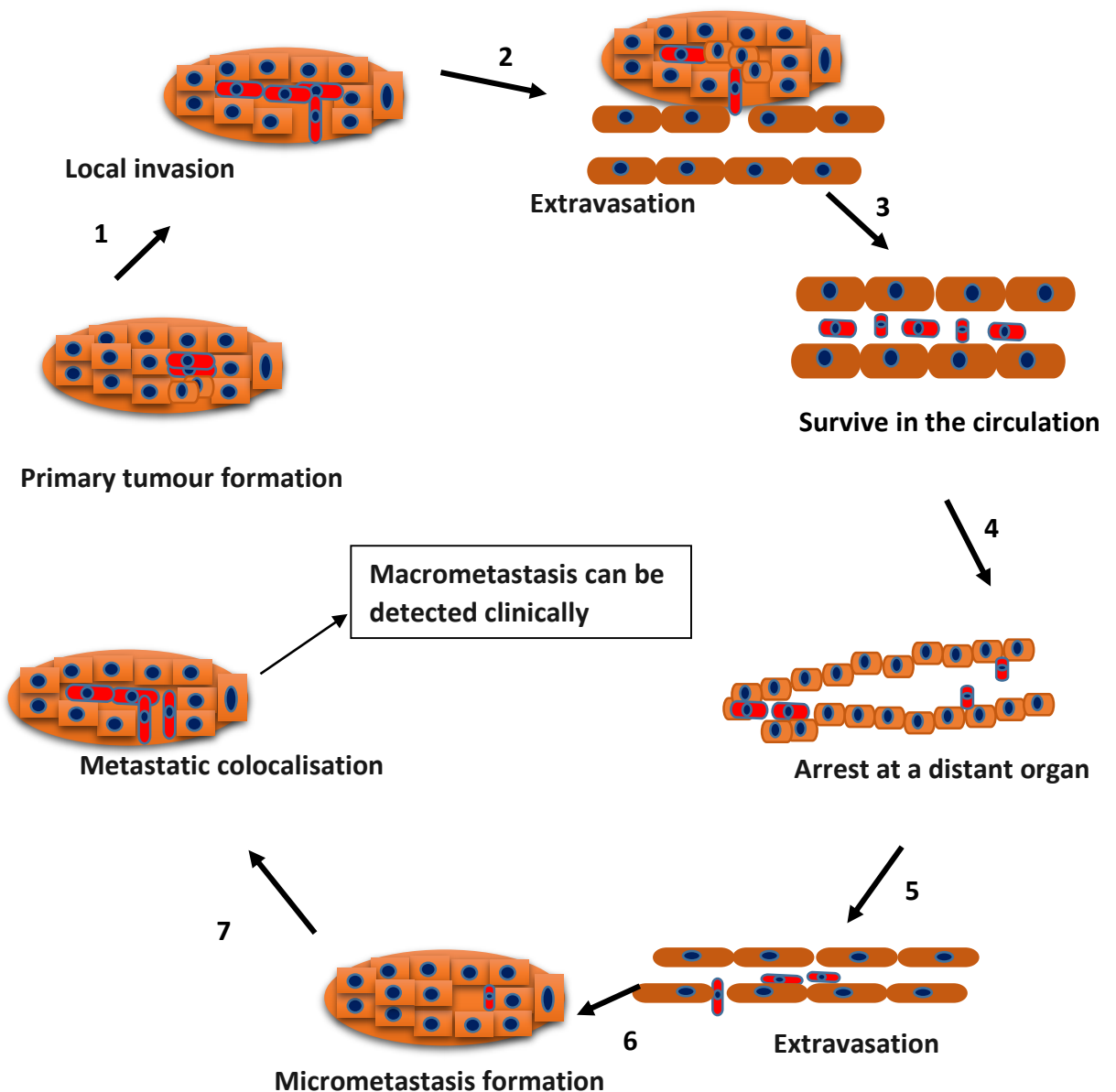


Figure (1.2): The metastatic cascade. The metastatic cascade including eight complex biological steps leading to form metastasis. Initially, cells detach from adjacent cells and grow as a mass to form primary tumour, then breach the BM and break down the ECM. The tumour cells then enter the blood vessel and travel to distant organs, and penetrate the endothelial of target organ. This process is called extravasation. Ultimately, cells form new colonises and constitute micrometastases at the distant organ.

Tumour cells undergo extreme changes in their plasticity during metastasis via transformation in morphology and phenotype, such as the mesenchymal to amoeboid transition (MAT) when they invade the tissue as single cells, the epithelial to mesenchymal transition (EMT) when they invade the tissue as detached clusters and collective to amoeboid transition (CAT). The tumour microenvironment contains many types of cells, such as endothelial cells including the lymph and blood vessels, stromal, fibroblasts, macrophages, neutrophils and mesenchymal stem cells.

The tumour microenvironment participates in tumour development by ECM rearrangement and releasing extracellular signals including growth factors, chemokines and cytokines (Wan et al., 2013, van Zijl et al., 2011). Transforming growth factor beta (TGF- β) stimulates EMT, releases MMPs and synthesizes the connective tissue. The density of connective tissue matrix affects the morphology of mammary epithelium (Wan et al., 2013, van Zijl et al., 2011). TGF- β also plays an important role in the tumour microenvironment through enhancing the interaction between tumour and stroma, proliferation of myofibroblasts, generation of autocrine platelet-derived growth factor (PDGF) that stimulates the division of tumour associated macrophage (TAM) and avoidance of immunity by targeting CD8 T cells (Figure 1.3) (Wan et al., 2013, van Zijl et al., 2011).

Furthermore, the tumour microenvironment also enhances tumour progression via rearrangement of ECM through releasing MMPs which degrade the ECM proteins, cleave cell adhesions, and activate cytokines and growth factors. This, enables tumour cells to metastasize (Wan et al., 2013, van Zijl et al., 2011). Cancer associated fibroblasts (CAFs) secrete MMPs, cytokines (e.g. IL-8 and VEGF) and chemokines (e.g. CXCL12) to enhance proliferation, invasion and neoangiogenesis. Tumour associated macrophages (TAMs) generate growth factors and matrix-degrading enzymes that enhance angiogenesis, cell invasion and haematogenous intravasation. The interaction between tumour cells and TAMs can be induced by factors, such as EGF that are produced by macrophages (Figure 1.3) (Wan et al., 2013, van Zijl et al., 2011).

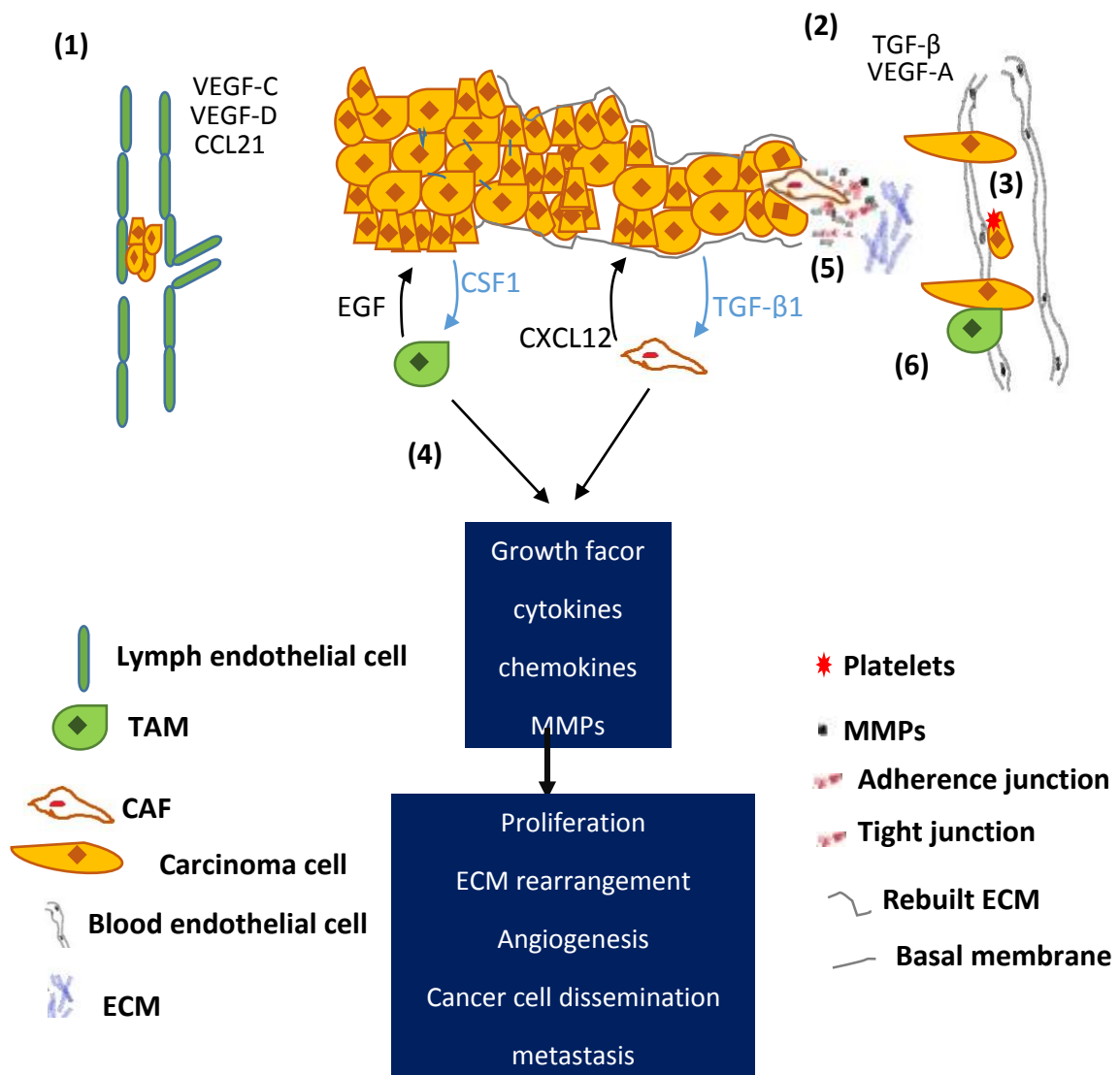


Figure (1.3): The tumour microenvironment. (1) Epithelial cancer cells into lymph vessels may happen via intercellular gaps and active attraction of lymph endothelial cells upon secretion of VEGF-C, VEGF-D and CCL21. (2) TGF- β induced EMT and the secretion of VEGF-A mediates hematogeneous dissemination. (3) Tumour cells can use platelets to avoid shear forces and natural killer (NK) cell attacks. (4) Two prominent cell types of the tumour microenvironment are TAMs and CAFs both generate components which induce cancer progression. (5) Myofibroblasts and ECM rearrangement able to constitute a track through which epithelial tumour cells can migrate. (6) In close interaction with tumour cells macrophages able to promote hematogenous transmigration. Modified: from van Zijl et al.

1.3. Focal adhesions (FAs)

Focal adhesions (FAs) are specialised assemblies of macromolecules that connect cells to the ECM (Wu, 2007). The cell-ECM interaction is an essential process through which cells can communicate with its surrounding environment (Wu, 2007). It also regulates many cellular functions, such as migration, survival, proliferation and cellular morphology that are necessary for the maintenance and repairing of tissue (Nagano et al., 2012). Integrins act as a mediator between FA proteins and the ECM (Wu, 2007). The integrins have non-covalently correlated subunits often termed α - and β -subunits. There are different types of α - and β -subunits, approximately eighteen in total and around 24 isoforms have been identified and each of these types binds with a particular type of ECM molecule (Figure 1.4) (van der Flier and Sonnenberg, 2001, Luo et al., 2007). Once the integrins bind to the appropriate ECM molecule, their inactive conformation changes to an active state. Thus, their shape is changed which allows recruitment of intracellular proteins. Integrins are the main intermediary between the ECM and intracellular proteins due to their extracellular domain (subunits) that links ECM to intracellular proteins through recruitment of them to the cell membrane (van der Flier and Sonnenberg, 2001, Luo et al., 2007).

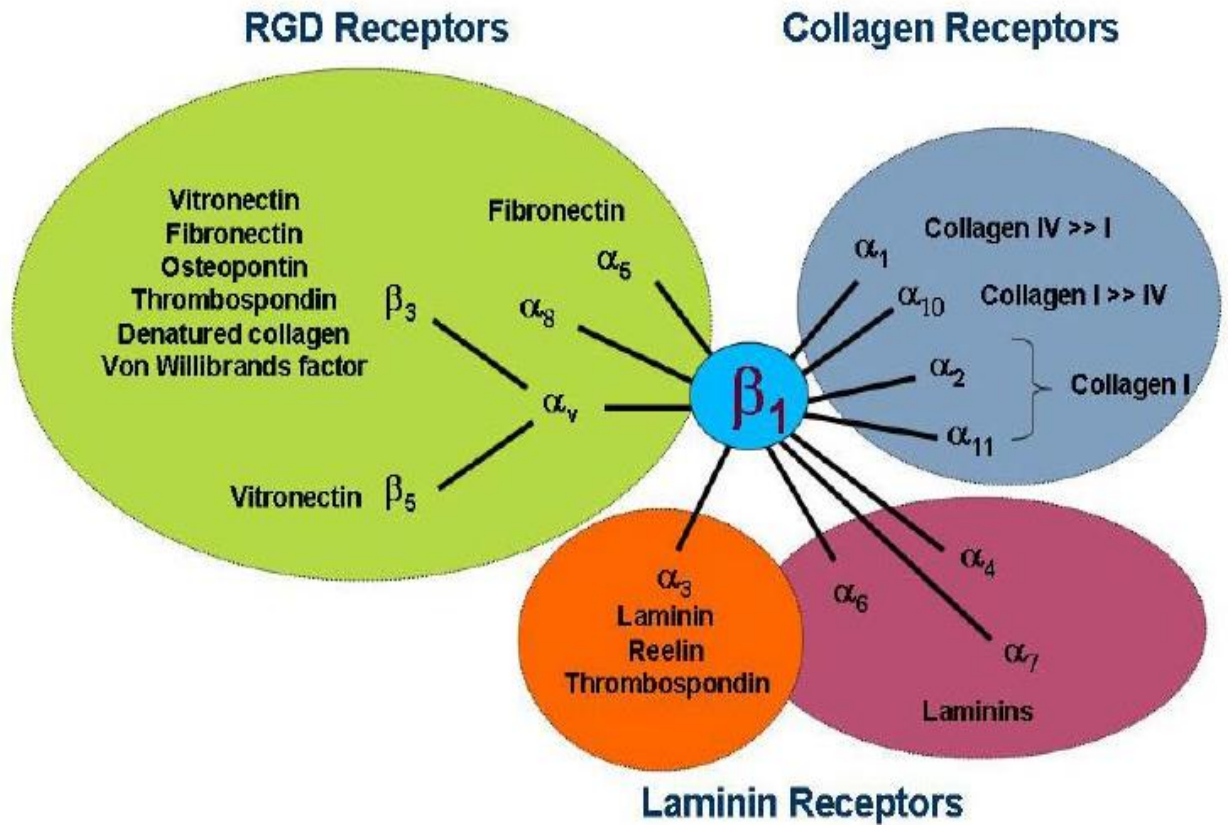


Figure (1.4): The integrin subunits and their ECM interactions (Lal et al., 2007).

Some types of FA proteins that are recruited into the FA complexes are shown in Figure 1.5;

Talin: a cytoskeletal protein of around 272 KDa in size, talin consists of a homodimer and links the actin cytoskeleton with integrin (Kanchanawong et al., 2010). Talin is cleaved into a rod and head domain by calpain II during disassembly of FAs (Nayal et al., 2004). Integrin and phospholipids interact with talin via its N-terminal FERM domain. The binding between talin and integrins is not only important for cytoskeleton morphology, but is also important for integrin activation (Nayal et al., 2004). Talin also

binds with the head domain of vinculin through its C-terminal rod which has a molecular weight of (220kDa) and consists of 13 helical bundles (Yao et al., 2014).

Vinculin: consists of a head and tail domain and plays an important role in the interconnecting signals of FAs. The head domain regulates integrin dynamics and integrin clustering, while the tail domain regulates mechanotransduction force machinery via phosphorylation of cell-cell or cell-matrix adhesion and the transfer of mechanical forces to the cell. The head region of vinculin induces FA growth dramatically via direct interaction with talin, this interaction leads to clustering of integrins and increases the residency time of integrin in FAs (Humphries et al., 2007).

Focal adhesions kinase (FAK): is a protein tyrosine kinase, and is considered a fundamental component in the assembly process of FAs by binding the ECM-integrin complex with the actin cytoskeleton (Feng and Mertz, 2015). FAK is activated through disruption of an auto-inhibitory binding between its terminal domain FERM and central kinase domain, then the activated FAK interacts with Src family kinases and participates in many signalling events via phosphorylation of other proteins and enzymes, such as PI3K, Src and Cas to regulate cell migration and invasion (Zhao and Guan, 2011).

Paxillin: a FA protein with a molecular weight 68-75 kDa (Turner et al., 1990). It interacts with other proteins through its domains, such as LD motifs and LIM domains. LIM domains named by their initial in the proteins Lin11, Isl-1 and Mec-3 and facilitate the interaction between proteins (Bach, 2000). LIM domains are protein structural domain contained of two attached zinger finger domain and divided by a two amino acid residue (Kadmas and Beckerle, 2004). N-terminal of paxillin contains five leucine-rich called LD

motifs that directly interact to FAK (Wade and Vande Pol, 2006). LD motifs play a role in protein-protein interaction and regulate cell motility and cell adhesion (Tumbarello et al., 2002).

These domains act as docking sites for GTPases, tyrosine kinases and serine/threonine kinases into FAs complex. Thus, it plays a crucial role in the regulation of cell migration by coordinating this signalling (Schaller, 2001). It binds to tubulin via its C-terminal domain which contains zinc finger LIM motifs (Herreros et al., 2000) and binds with FAK via its N-terminal region which contains LD domains (Tumbarello et al., 2002, Brown et al., 1998), and interacts with the cytoplasmic domain of $\beta 1$, $\beta 3$ and $\alpha 4$ integrins (Schaller, 2001).

Zyxin: a FA protein consists of two regions a N-terminal region contains proline-rich domain and C-terminal region contains three LIM domains. The proline-rich domain may bind with SH3 domains of proteins implicated in signal transduction, and LIM domains are possible involved in protein-protein interactions. It also localises within FA complexes (Wang and Gilmore, 2003).

FA dynamics play a crucial role in cancer cell migration through the assembly and disassembly process. FA complexes are formed in a highly regulated manner to perform their function which is to act as a mechanical and physical linkage between the ECM and actin bundles, and transduction of the biochemical signals between intracellular and extracellular regions (Figure 1.5) (Chen et al., 2003, Zaidel-Bar et al., 2004). These functions are achieved through defined steps, including initiation, assembly, maturation and disassembly which happen during the FA life cycle (Partridge and Marcantonio,

2006). FAs are stable in non-motile cells under normal conditions to maintain the shape of the cell. By contrast, in the migrating cell the FAs become dynamic by disassembly and then forming new FAs (Partridge and Marcantonio, 2006, Morgan et al., 2007).

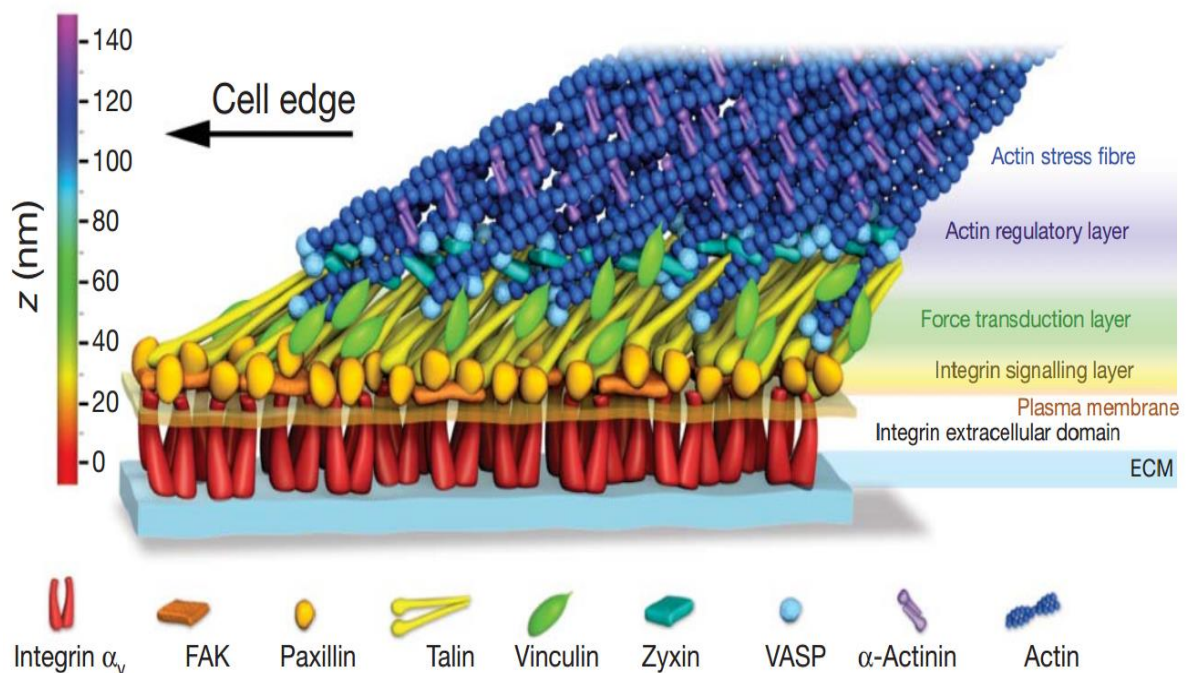


Figure (1.5): Focal adhesion. The first layer is the integrin signalling layer which is the nearest to the ECM containing paxillin, FAK and integrin cytoplasmic tails. The second layer is the force transduction layer that transmits the signals from actin to integrin and contains vinculin and talin. The third layer is the actin regulatory layer containing zyxin and α -actinin (Kanchanawong et al., 2010).

1.3. I. FA assembly

The initial stage of life cycle of FA is assembly at the leading edge of the cell. During this stage a large and flat structure is formed often called the lamellipodium which contains adapter proteins, such as talin, paxillin, vinculin and integrin. Once the lamellipodium has formed, FA complexes adhere to the integrin receptors to support the cell and produce traction. The front edge of the cell is then adhered to the ECM via the integrins. Thus, the cell has the force to generate traction and to pull the cell body forwards via stretching of the internal cytoskeleton (Nagano et al., 2012).

Cell-ECM adhesion stimulates the pooling of integrin and leads to recruitment of the intracellular FA proteins to the inner surface of the membrane (Petit and Thiery, 2000, Galbraith and Sheetz, 1998), including talin, vinculin, paxillin, tensin, alpha actinin. (Humphries et al., 2007, Burridge et al., 1992). Signalling proteins, such as kinases and phosphatases transfer the signals between the FA and the cell to control multiple cellular processes including proliferation, survival and migration. Specifically, FAK and Src (Proto-oncogene tyrosine-protein kinase) play important roles in the transmission of the signals from FAs into the cell through phosphorylating integrin (Nagano et al., 2012).

FAs initiate through the binding of talin with the β -subunit of integrin. Talin has two domains, the head domain interacts with integrin and the rod domain has several binding sites which recruit and interact with many intracellular proteins, such as vinculin and α -actinin to form nascent FAs. The nascent structure then grows and becomes larger via the recruitment of additional proteins and kinases to form mature FAs. This stage needs extra tension of actin that is regulated by the Rho small GTPase (Nagano et al., 2012).

FAs sometimes grow to mature FAs and sometimes remain nascent due to components of FA proteins that respond to the mechanical force generated from actomyosin and the ECM (Ballestrem et al., 2001, Holt et al., 2008, Rid et al., 2005, Zamir et al., 2000).

The actin-talin-integrin complex stabilizes FAs and stress fibres via the recruitment of extra FA components, such as FAK (Ren et al., 2000, Shi and Boettiger, 2003), paxillin (Brown et al., 1996, Mofrad et al., 2004) and Src-family kinases (SFKs) to the integrin tail (Arias-Salgado et al., 2003, Reddy et al., 2008). SFKs are activated by tyrosine phosphatase α (RPTP- α) to enhance α V β 3-cytoskeletal linkage (Jiang et al., 2006, von Wichert et al., 2003). Talin activates FAK (Ling et al., 2002, Kong et al., 2006), FAK enhances the recruitment of talin to form a cluster which is pushed outwards by Src-dependent actin polymerization (Lawson et al., 2012). Actomyosin contractility extends the binding sites of talin to other FA components, such as vinculin (Margadant et al., 2011, Lee et al., 2007, Ziegler et al., 2008, del Rio et al., 2009).

1.3. II. Actin polymerisation

Actin polymerisation plays a role in driving cancer cell migration by actin monomers polymerisation into filaments (F-actin) and also helps maintain the structure and integrity of the cell (Olson and Sahai, 2009). Single actin molecules are known as G actin which has a pointed end and a barbed end. Actin filaments are formed by polymerisation of G actin monomers at the barbed end and deformed by depolymerisation of G actin monomers at the pointed end (Olson and Sahai, 2009). The actin polymerisation process undergoes many stages, including the nucleation stage in which three G actin monomers are nucleated to form a trimer (Figure 1.6 A). Then, the actin polymerisation process starts from both ends to add monomers called F actin (Le Clainche and Carlier, 2008).

In the treadmilling stage, the barbed end increases in length continually, while the pointed end decreases in length (Le Clainche and Carlier, 2008). So, the treadmilling process acts as a cycle in which net gain of individual actin monomer on the barbed end and net loss on the pointed end (Figure 1.6 B) (Le Clainche and Carlier, 2008).

There are different proteins which interact with actin in this process to remodel the filament conformation (Le Clainche and Carlier, 2008, Olson and Sahai, 2009). ADF or Cofilin binds with actin filaments and acts as an enhancer for the dissociation of ADP-actin monomers from the pointed end. Profilin acts as stimulator through binding with ADP-actin and converts it to ATP-actin allowing assembly again at the barbed end (Figure 1.6C). Formin interacts with actin monomers to enhance the nucleation process and form actin polymerisation quickly. Actin-Related Proteins_{2/3} (Arp_{2/3}) interact near the barbed end of filaments and forms a new branch of actin filaments. Arp_{2/3} also help

modifying of the actin cytoskeleton at the front edge of migrating cells (Figure 1.6 C) (Le Clainche and Carlier, 2008, Olson and Sahai, 2009).

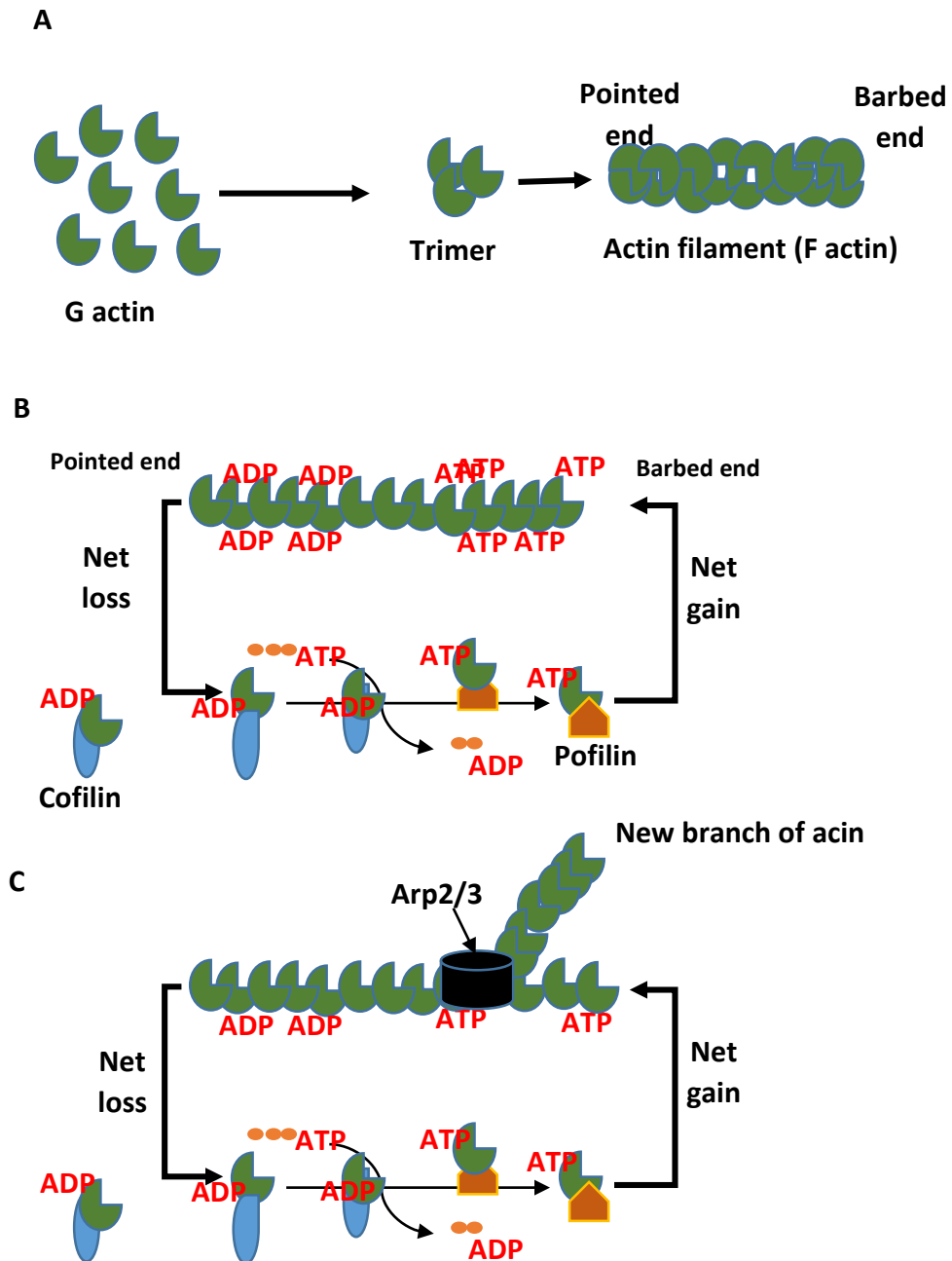


Figure (1.6): Actin polymerisation. A) Actin filaments are formed by polymerisation of G actin monomers at the barbed end and deformed by depolymerisation of G actin monomers at the pointed end. **B)** Treadmilling process acts as a cycle in which net gain of individual actin monomer on the barbed end and net loss on the pointed end. **C)** Arp 2/3 generates a branch of actin filaments at the barbed end.

Actin filaments assembly play an important role in the formation of protrusion at the front edge of cell. Actin filaments are also involved in cell migration and direction through determination of the shape of the cell and provision of the mechanical stiffness of protrusion (Yamaguchi and Condeelis, 2007)

1.3. III. Myosin

Myosin II plays a role in cell migration by regulation of adhesion. Myosin binds with the actin cytoskeleton and affects actin polymerisation and remodels the dynamic of the actin cytoskeleton. Myosin II enhances adhesion maturation and controls retrograde flow in the lamellum. Myosin II contributes in FA disassembly at the trailing edge of the cell. Myosin also plays a role in cell migration through pushing actin forward FA via generating force through converts chemical energy to mechanical energy (Vicente-Manzanares et al., 2009b).

Eventually, FA assembly forms as a molecular clutch to link between ECM and actin. This molecular clutch transmits chemical force to mechanical force to push cell on ECM forward during cell migration (Vicente-Manzanares et al., 2009a). This mechanical force is generated by myosin II at the front edge of cell as mentioned in Figure 1.7 (Vicente-Manzanares et al., 2009b).

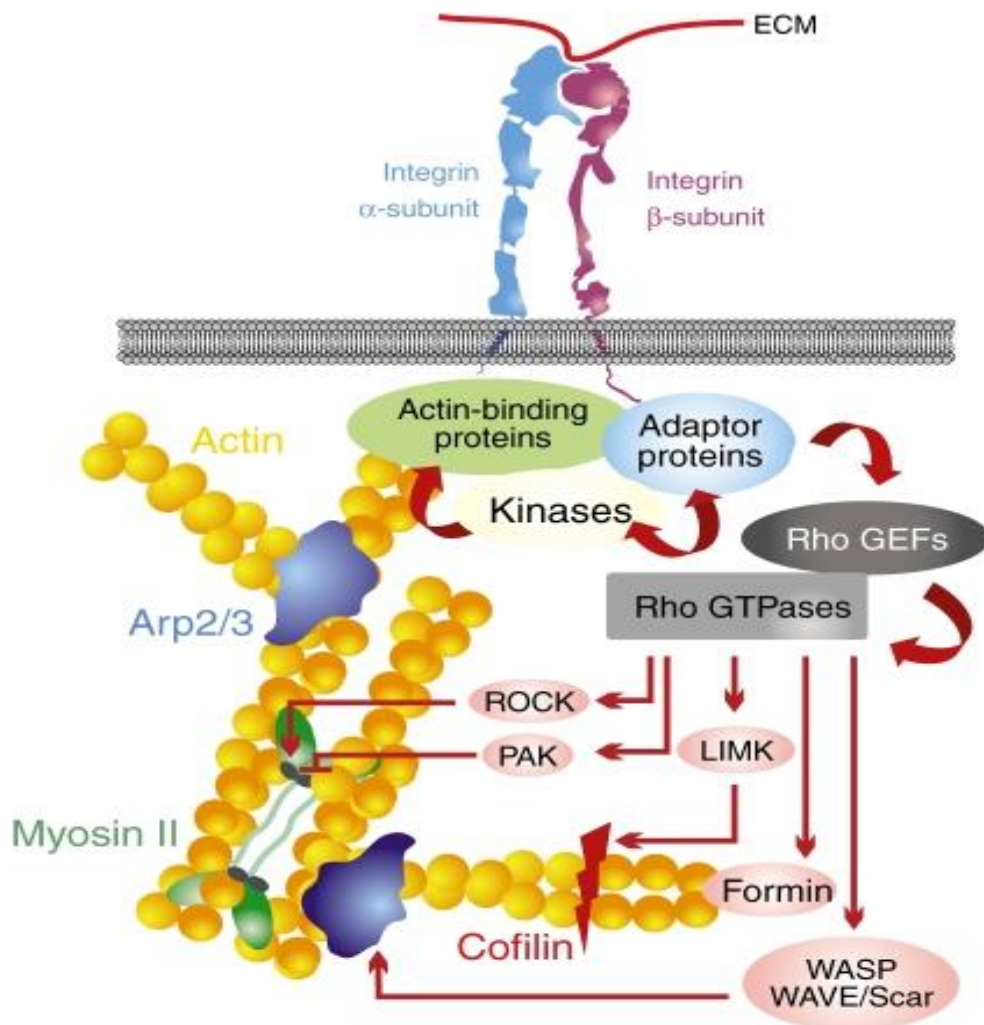


Figure (1.7): Adhesive signalling in cell migration. Integrin is involved in the stimulation of different signalling, such as kinases, non-catalytic adaptor proteins and actin-binding proteins. These proteins can affect the recruitment and activation of other signalling of adhesions, such as Rho GEFs, Rho GTPases, formin and cofilin which regulate polymerisation of actin (Vicente-Manzanares et al., 2009a).

1.3. IIII. FA disassembly

The life cycle of FAs ends by detachment of FAs from the ECM (Partridge and Marcantonio, 2006). Calpain and microtubules play an important role in FA disassembly through regulation of tyrosine phosphorylation and cytoskeletal tension events (Crowley and Horwitz, 1995, Franco and Huttenlocher, 2005). Microtubules extend to FAs and stimulate the cell to detach at the trailing edge (Nagano et al., 2012). Calpain cleaves FA components, such as talin, FAK and integrin to enhance FAs disassembly (Figure 1.9) (Franco et al., 2004b, Flevaris et al., 2007, Chan et al., 2010). FA disassembly can also be enhanced via deactivation of Rho activity by FAK (Schober et al., 2007). FA disassembly is regulated by FAK-Src signalling pathway at the trailing edge of the cell (Owen et al., 2007, Webb et al., 2004).

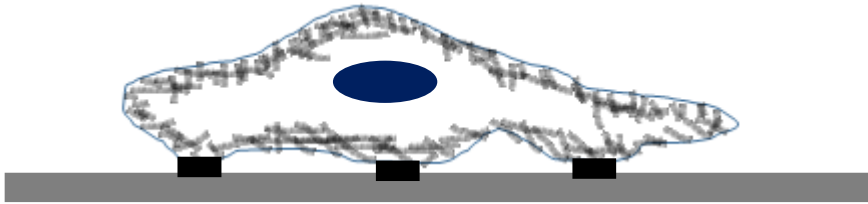
It has been shown that autophagy plays a role in FA disassembly. Inhibition of autophagy decreases cancer cell migration and there is an accumulation of a large number of FAs in cancer cells which are deficient in autophagy (Sharifi et al., 2016). It has also been shown that 3-phosphoinositide-dependent protein kinase 1 (PDK1) enhances FA disassembly by regulation of endocytosis of integrin $\alpha\beta3$. PDK1 is involved in this process through association and phosphorylation of integrin $\alpha\beta3$. The size of FAs is increased and their disassembly is reduced by downregulation of PDK1 (di Blasio et al., 2015). Ubiquitination is also involved in FA disassembly at the leading edge of cell migration. Phosphorylation of Cas (Crk-associated substrate/p130Cas/BCAR1) induces FA disassembly. FAs at the leading edge contain phospho-Cas which recruits suppressor

of cytokine signalling 6 (SOCS6). SOCS6 leads to inhibition of Cas-dependent FA disassembly at the leading edge of cell migration (Teckchandani and Cooper, 2016).

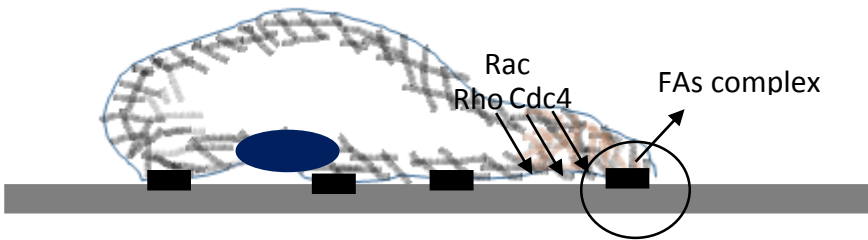
Mendoza et al. (2017) hypothesised that Rab5 plays a role in FA disassembly by stimulation of calpain2. They found that Rab5 and EEA1 co-localise with calpain2, and knock-down or silencing of Rab5 leads to reduction of calpain 2 activity and FA disassembly. However, the molecular events of FAs disassembly are not well understood (Nagano et al., 2012, di Blasio et al., 2015, Mendoza et al., 2017). So, Figure 1.8 shows the traditional view of cell migration, but in fact FA disassembly also occur at the leading edge of cell as shown in our results.

In summary, the turnover (assembly and disassembly) of the FA components occurs throughout life cycle of adhesion, with conservation of balance between removal and recruitment rate during different stages. The FAs at the end each step passing in stationary phase for a certain period of time before embarking on the next step (Gardel et al., 2010). However, each single component of FAs has a different rate of turnover during the life cycle time of FAs (Laukaitis et al., 2001, Ballestrem et al., 2001, Digman et al., 2008, Ji et al., 2008). The difference rate of assembly and disassembly between individual FA components may act to transform the mechanical signal to chemical signals inside cells (Guo and Wang, 2007).

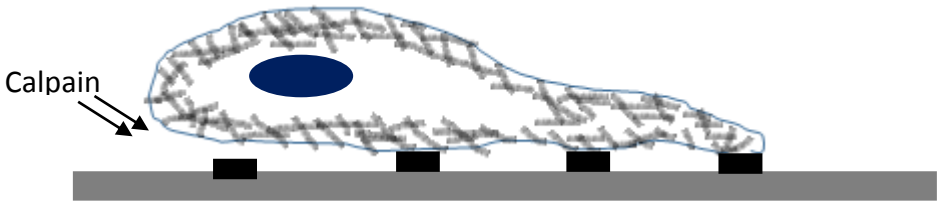
1) First contact with ECM (protrusion at the leading edge)



2) Assembly, Maturation and Signalling



3) Disassembly at trailing edge and assembly at leading edge



4) Direction of cell migration

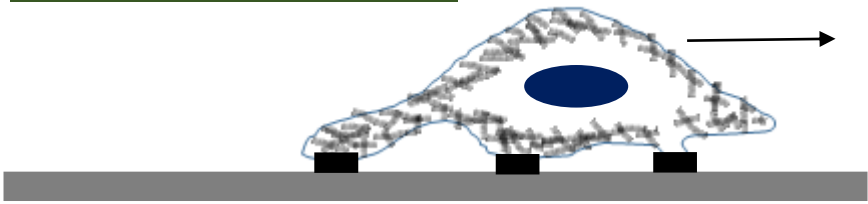


Figure (1.8): Traditional view of cell migration. Cells adhere to the ECM via integrins, the FAs are activated and grow from nascent to mature to form FA complexes through binding with the actin cytoskeleton and recruitment of many kinases.

1.5. Phospholipids

Phospholipids are the main constituent of all cell membranes and form lipid bilayers due to their amphiphilic compound (Mashaghi et al., 2013). The phospholipid molecule contains two hydrophobic fatty acid “tails” and a hydrophilic “head” containing of a phosphate group. The two constituents are combined together by a glycerol molecule. The phosphate groups can be amended with simple organic molecules such as choline or inositol (Mashaghi et al., 2013).

Phospholipid signalling plays a key role in the regulation of a substantial number of cellular processes, such as migration, cell proliferation, apoptosis and metabolism (Santos and Schulze, 2012). Phosphatidylinositols (PtdIns) are a type of phospholipids that exist in the cytoplasmic layer of cell (Balla, 2013). They consist of a glycerol group which is esterified to two fatty acid chains and a phosphate group that binds to a polar inositol head group and extends into the cytoplasm (Figure1.9). Phosphorylated forms of PIs are phosphoinositides (Figure1.9) and constitute a small percentage of the lipid in the plasma membrane (Balla, 2013). The amount of PtdIns has been evaluated and found that PI forms ~10–20% (mol%) of total cellular phospholipids, Phosphatidylinositol 4-phosphate (PI4P), Phosphatidylinositol 4,5-bisphosphate (PtdIns(4,5)P₂) form ~0.2–1%, and Phosphatidylinositol 3,4,5-trisphosphate (PtdIns(3,4,5)P₃) constitutes approximately 2–5% of the PtdIns(4,5)P₂(Balla, 2013).

PIs play a very important role in many cellular processes, such as cell migration, vesicle trafficking and ion channels due to its inositol rings head group which have free hydroxyl groups (D₃, D₄ and D₅) and can be phosphorylated or dephosphorylated by lipid kinases and phosphatases (Figure1.9) (Balla, 2013).

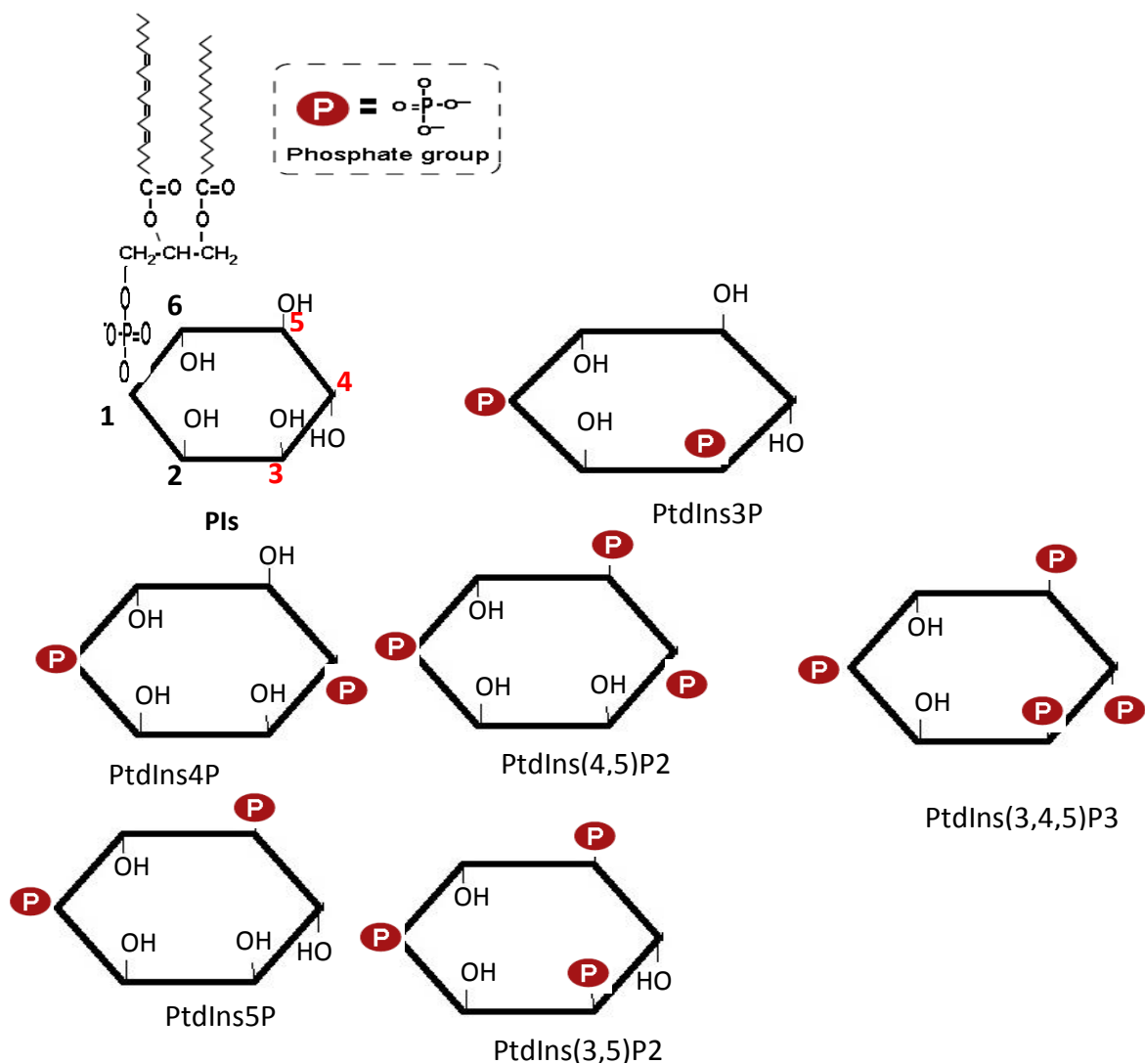


Figure (1.9): Structure of PI and its phosphoinositide derivatives. PI has a glycerol backbone (two fatty acids interact with D-1 inositol ring via phosphate). PI can be phosphorylated and dephosphorylated via their hydroxyl group at the D3, 4 and 5 positions to produce phosphoinositide derivatives.

1.6. Lipid kinases and phosphatases in PtdIns cycle

There are many molecules that associate with phosphoinositides, such as scaffold proteins, cytoskeletal proteins, protein kinases, phospholipases and ion channel proteins. These proteins perform their function through production or degradation of certain types of phosphoinositides in the cell membrane (Sasaki et al., 2009).

Phosphoinositides are produced and controlled by kinases and phosphatases as summarised in Figures 1.12 and 1.13, which are crucial for the function, biological effects and localisation of phosphoinositides (Sasaki et al., 2009). There are around 50 genes that encode phosphoinositide kinases and phosphatases which enable the cell to respond to surrounding environmental changes quickly and effectively by the regulation of phosphoinositides metabolism (Sasaki et al., 2009).

1.6. I. Types of kinases and phosphatase involved in PIs cycle;

Phosphoinositides 3-kinases (PI3Ks) are classified into three classes depending on its structure as shown in Figure 1.10. Class I PI3Ks are heterodimeric enzymes that generate PtdIns(3,4,5)P₃ from PtdIns(4,5)P₂, class II PI3Ks are monomeric enzymes that generate PtdIns3P from PtdIns and class III PI3Ks are vacuolar protein sorting 34 (Vps34) that generate PtdIns3P from PtdIns (Sasaki et al., 2009). PtdIns(4,5)P₂ can recruit phospholipases C (PLCs) which are phosphodiesterases and are encoded by different genes and classified into six families as mentioned in Figure 1.11 (Zheng et al., 2015).

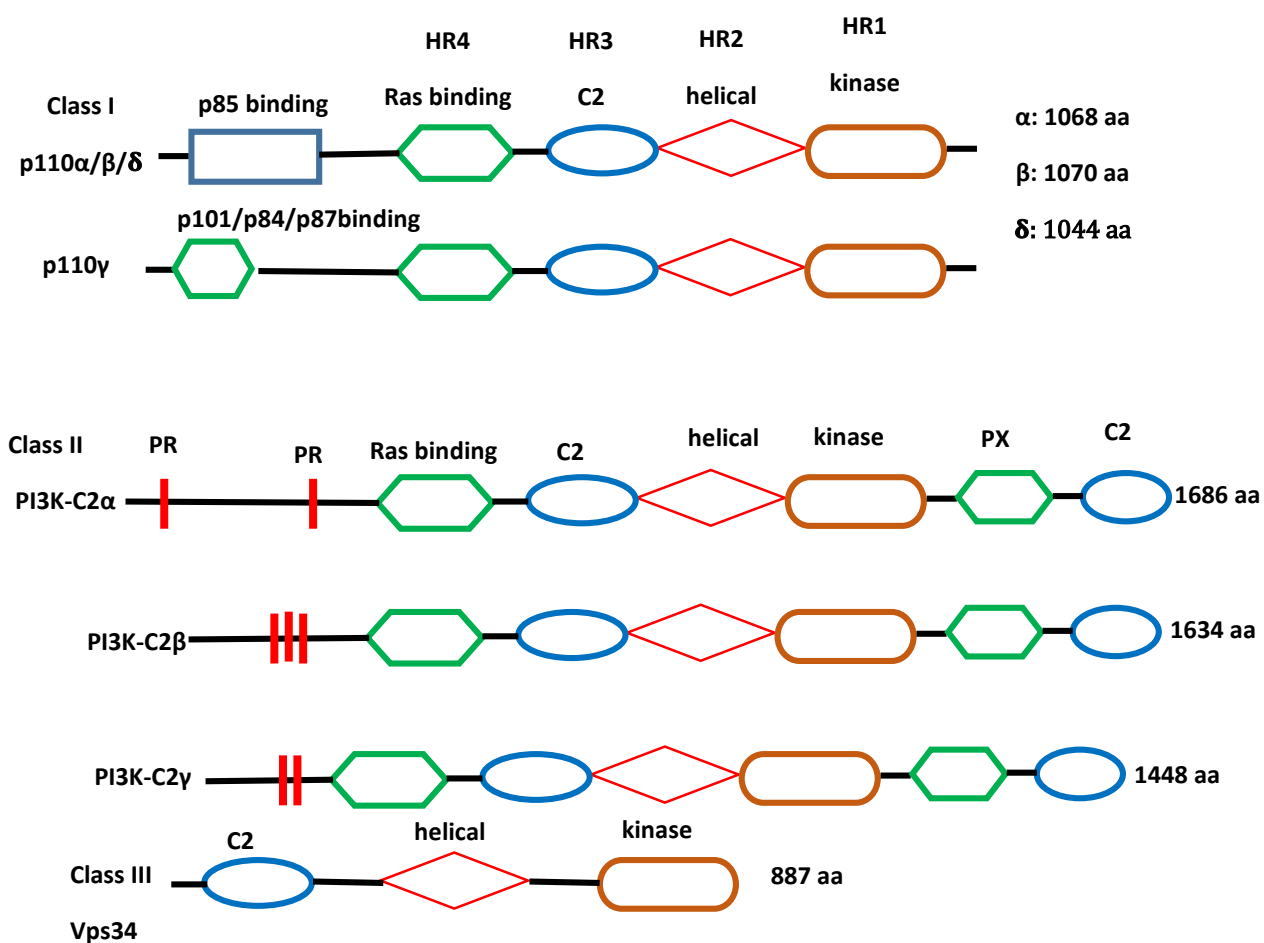


Figure (1.10): molecular structure of mammalian PI3K isoforms. Mammalian PI3K catalytic subunits are shown, but regulatory subunits are not shown. HR 1-4 refers to homology regions of class I and II PI3Ks which have Ras- HR4 interaction, a protein kinase C homology domain 2 (C2)- HR3 interaction, a helical domain (HR2), and a kinase domain (HR1). The p85 binding and p101/p84/p87 binding domains facilitate interaction with the PI3K regulatory subunits. Class II contains a proline-rich region (PR) and a phox homology domain (PX). The sole class III enzyme, Vps34, contains the C2, helical and kinase domains, but lacks a Ras-binding domain. Numbers of amino acids in the human proteins are mentioned, modified: from Sasaki et al. (2009).

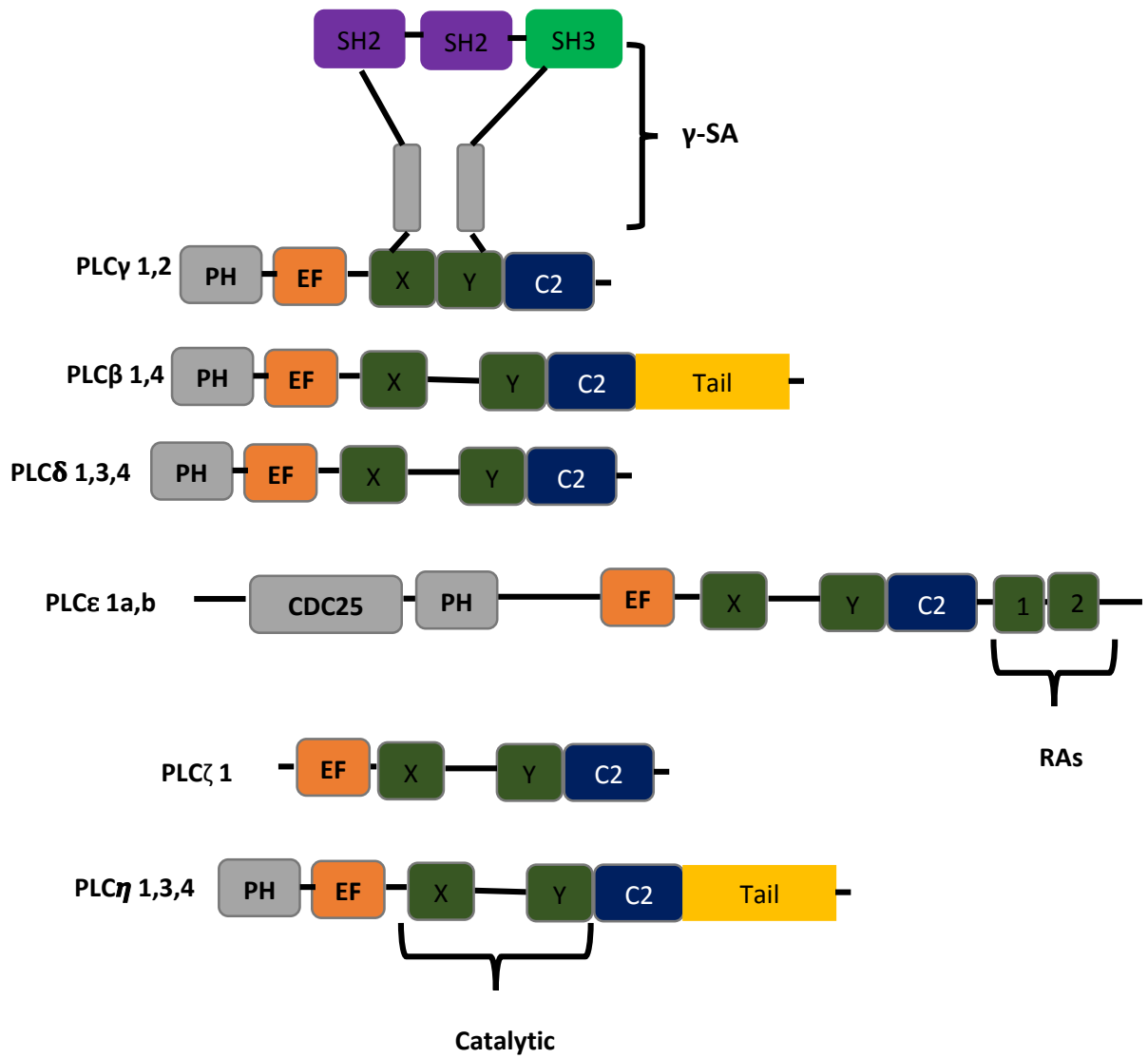


Figure (1.11): Structure of mammalian of PLC isoforms. PLC isoforms have an N-terminal pleckstrin homology (PH) domain (Grey colour), EF hands (orange), split catalytic X and Y domain (green colour) and a C-terminal C2 domain (blue colour). PLC γ isoforms have a γ -specific array (γ -SA) that includes a split PH domain, two Src homology (SH) (purple colour), one SH3 domain (green colour) and an activating tyrosine (Y) phosphorylation site. PLC β and PLC η family members have unique C-terminal tails (yellow colour). PLC ϵ has a unique N-terminal CDC25 domain (grey colour) and two Ras-association (RA) domains (green colour) at the C-terminus, Modified: from Zheng et al. (2015).

Phosphatidylinositol-4 kinases (PI4Ks) are classified into PI4KI, PI4KII and PI4KIII. Class II and III contain PI4K enzymes. They produce PtdIns4P through phosphorylation of the D4-inositol ring of PtdIns. This reaction is considered the first important step for synthesising other derivatives, such as PtdIns(4,5)P₂ and PtdIns(3,4,5)P₃ (Figures 1.12) (Sasaki et al., 2009).

Phosphatidylinositol phosphate kinases (PIPKs) are classified into Class I, II and III. Class I PIPKs are PI4P5 kinase that phosphorylates PtdIns4P at the D5-inositol ring to generate PtdIns(4,5)P₂. Class II PIPKs are PI5P4-kinases that phosphorylate PtdIns5P at the D4-inositol ring to generate PtdIns(4,5)P₂. Class III phosphorylate PtdInsP and PtdIns3P at the D5-inositol ring to generate PtdIns5P and PtdIns(3,4,5)P₃ (Figures 1.12) (Sasaki et al., 2009).

Phosphoinositide 3-phosphatases include PTEN, TPIP (TPTE and PTEN homologous inositol lipid phosphatase), and multiple members of the myotubularin family. PTEN dephosphorylates PtdIns(3,4,5)P₃ at the D3-inositol ring, TPIP dephosphorylates PtdIns(3,4,5)P₃ and myotubularin dephosphorylates PI3P (Figures 1.13) (Sasaki et al., 2009).

Phosphoinositide 4-phosphatases are inositol polyphosphate 4-phosphatases called INPP4A and INPP4B which dephosphorylate PtdIns(3,4,5)P₃ at the D4-inositol ring (Sasaki et al., 2009). Phosphoinositide 5-phosphatases (INPP5s) have four classes. Class II enzymes include the synaptojanins, OCRL1, INPP5B, INPP5J and SKIP. Class III INPP5 enzymes include SHIP1 and SHIP2 and sole class IV enzyme includes INPP5E (Figures 1.13) (Sasaki et al., 2009). The function of kinases and phosphatases which generate these phosphoinositides are summarised in Table 1.1 and 1.2.

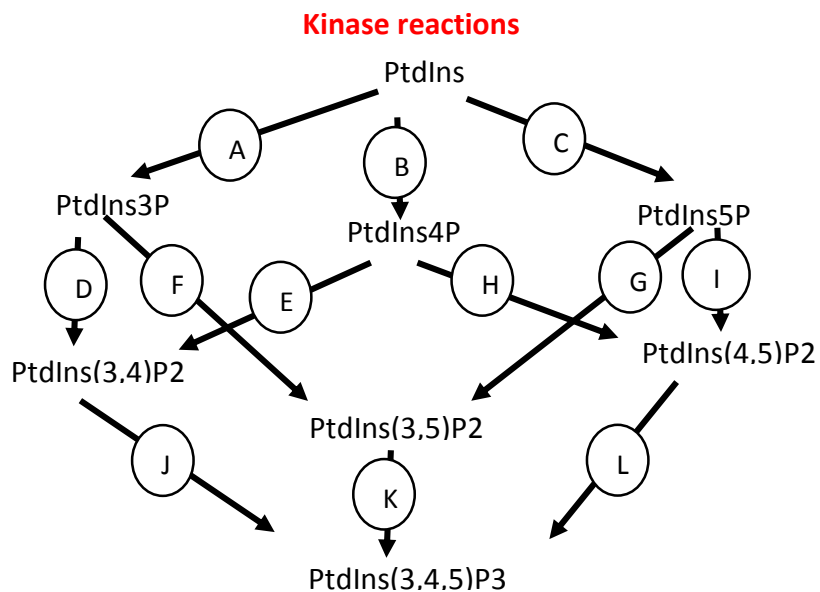


Figure (1.12): PtdIns cycle. Phosphoinositides are catalysed by kinases and each reaction arrow labelled with capital letter as mentioned in table 1.1. (Sasaki et al., 2009).

Table 1.1: Mammalian phosphoinositide kinases.

Class	Protein	Reaction
Phosphoinositide 3-kinases		
Class IA PI3K	p110 α p110 β p110 δ	L (A, E) L(A, E) L(A, E)
Class IB PI3K	p110 γ	L(A, E)
Class II PI3K	PI3K-C2 α PI3K-C2 β PI3K-C2 δ	A(E) A(E) A(E)
Class III PI3K	Vps34	A
Phosphatidylinositol 4-kinases		
Type II PI4Ks	PI4K II α PI4K II β	B B
Type III PI4Ks	PI4KIII α PI4KIII β	B B
Phosphatidylinositol phosphate kinases		
Type I PIPKs	PIPK I α PIPK I β PIPK I γ	H H H
Type II PIPKs	PIPKII α PIPKII β PIPKII γ	I I I
Type III PIP	PIPK III	F (C)

Phosphatase reactions

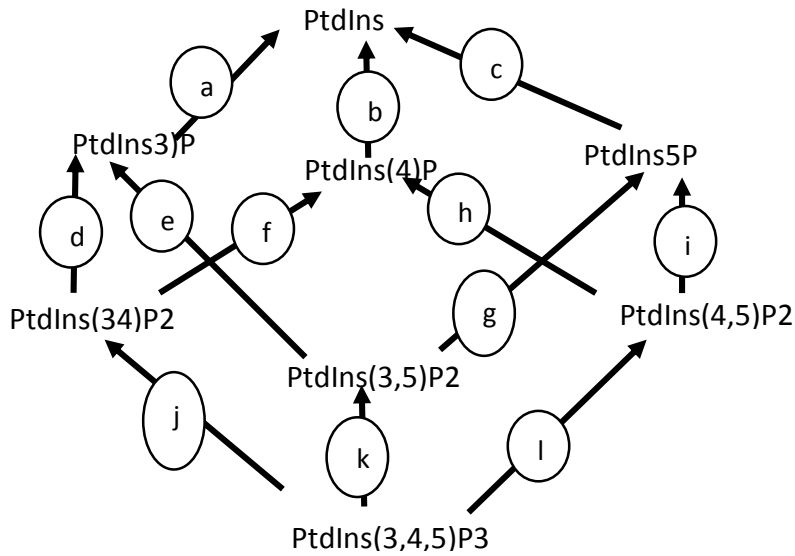


Figure (1.13): PtdIns cycle. Phosphoinositides are catalysed by phosphatases and each reaction arrow labelled with small letter as mentioned in table 1.2. (Sasaki et al., 2009).

Table 1.2: Mammalian phosphoinositide phosphatases.

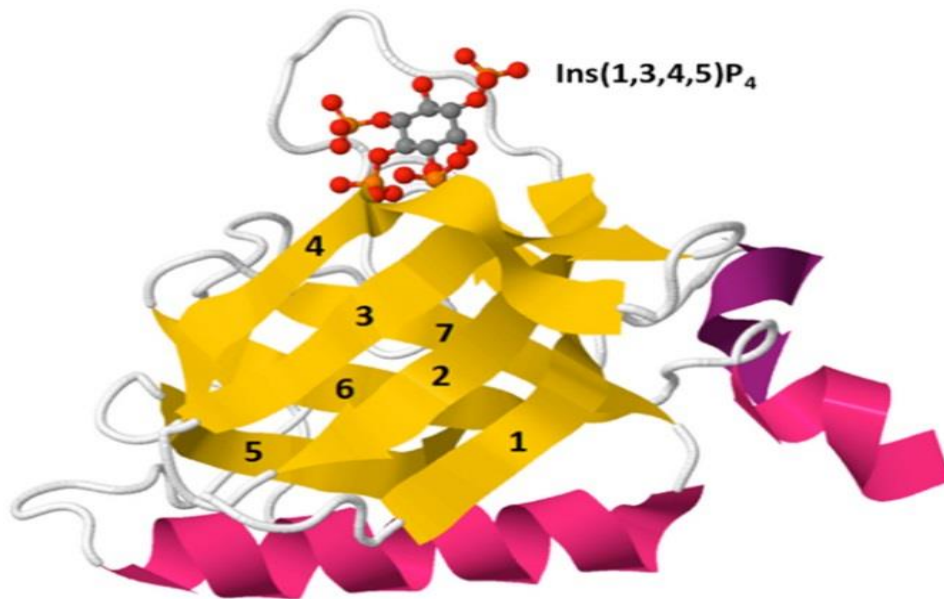
Class	Protein	Reaction
Phosphoinositide 3-phosphatases		
PTEN	PTEN	L (a)
TPIP	TPIP	g, l
Myotubularins	MTM1 MTMR1 MTMR2 MTMR3 MTMR4 MTMR6 MTMR7 MTMR8 MTMR14	a, g a, g a, g a, g a, g a, (g) a (a) a, g
Phosphoinositide 4-phosphatases		
INPP4	INPP4A INPP4B	d d
TMEM55	TMEM55A TMEM55B	i i
Phosphoinositide 5-phosphatases		
Type II INPP5s	SYNJ1 SYNJ2 OCRL1 INPP5B INPP5J SKIP	a, b, f, h, l, j a, b, f, h, l, j h, j h, j h, j j, (h)
Type III INPP5s	SHIP1 SHIP2	j j
Type IV INPP5	INPP5E	f, h, j
Other		
PLIP	PLIP	c
Sac	SAC1 SAC2 SAC3	a, b, (f) h, j f

1.7. PH domains and phosphoinositide

Pleckstrin Homology (PH) domains consist of around 120 amino acids and have a seven-strand β -barrel which forms of two anti-parallel β sheets and a C-terminal α helix (Figure 1.14). The β 1, β 2, β 3 and β 4 loops form specific sites to bind with the inositol ring of phosphoinositide (Wang et al., 2015). Approximately 10% of all PH domains have high affinity and specificity to bind with phosphoinositide (Lemmon, 2007). PtdIns(4,5)P₂ has high affinity and specificity to bind with phospholipase C delta (PLC δ) PH domain and PtdIns(3,4,5)P₃ also has high affinity and specificity to bind with Bruton's tyrosine kinase (Btk) PH domain due to neighbouring phosphates in their inositol ring. However, other types of phosphoinositide, such as PtdIns3P, PtdIns5P and PtdIns(3,5)P₂ bind with another type of domains, such as FYVE domains, PHD finger and PX (Lemmon, 2007).

This diversity in the specificity of phosphoinositide to associate with different types of PH domain containing proteins is important due to the recruitment of a variety of proteins to the cell membrane to perform their function and interact with other signalling pathways (Lemmon, 2007). Some of these proteins phosphorylate the inositol ring to generate a new phosphoinositide or produce new second messengers, such PI3K phosphorylate PtdIns(4,5)P₂ to PtdIns(3,4,5)P₃ and PLC cleaves PtdIns(4,5)P₂ to Inositol trisphosphate (IP₃) and diacylglycerol (DAG). Other proteins dephosphorylate sites on the inositol ring, such as PTEN dephosphorylates PtdIns(3,4,5)P₃ to PtdIns(4,5)P₂ (Lemmon, 2007, Wang et al., 2015).

A) Btk-PH



B) PLC δ 1-PH

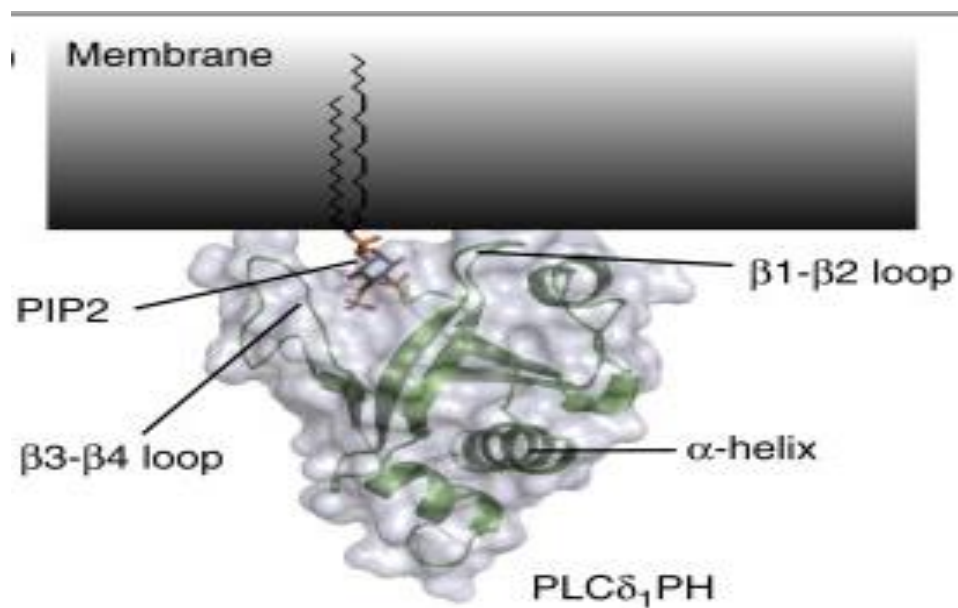


Figure (1.14): Structure of PH domain in complex with PtdIns. PH domain consists of a β -barrel composed by seven β -strands (yellow colour) coated by α -helix (pink colour). PI binds with PH domain through its loops of the β -barrel. **A)** Btk-PH-Ins(1,3,4,5)P₄ interaction, **B)** PLC δ -PH PtdIns(4,5)P₂ interaction (Wang et al., 2015, Bunney and Katan, 2011).

1.8. Role of the PtdIns cycle in cancer

Phosphoinositides and their downstream signalling molecules have been shown to be involved in several processes linked with cancer including adhesion, proliferation and invasion (Baenke et al., 2013).

The PI3K family plays a crucial role in several cellular functions including cell growth, motility, proliferation, differentiation and survival. There are several stimuli including growth factors, extracellular matrix and cytokines that activate class I PI3K and serine/threonine-specific protein kinase Akt signalling complexes (Thapa et al., 2015). Then, PI3K produces PtdIns(3,4,5)P₃ which in turns activate Akt, PDK1 and cytosolic proteins that implicated in the regulation of cancer cell migration (Thapa et al., 2015). The PI3K–Akt–mTOR (Mammalian target of rapamycin) pathway is often activated in cancer. PDK1 activates Akt and then Akt activates mTOR (Figure 1.16) (Zhou and Huang, 2011).

PLCs are stimulated by extracellular stimuli including neurotransmitters, growth factors and hormones (Lattanzio et al., 2013). Lysophosphatidic acid (LPA) induces the generation of PI3P through activation of a class II PI3K (PI3K-C2 β). Both PI3P and PI3K-C2 β are implicated in LPA-mediated cell migration (Maffucci et al., 2005). The PI3K Class IB isoform p110 γ is overexpressed in human pancreatic cancer tissues (Edling et al., 2010) and p110 α is also overexpressed in breast, ovarian and colon cancer (Bader et al., 2006, Bader et al., 2005, Kang et al., 2005, Shayesteh et al., 1999). PTEN is frequently mutated in cancer and participates in oncogenesis through changing the level of PtdIns(3,4,5)P₃ (Li et al., 1997, Majerus and York, 2009).

1.9. Role of the PtdIns in FAs

Spatial and temporal organisation of PtdIns(4,5)P₂ and PtdIns(3,4,5)P₃ are involved in the activation of many proteins (Hilpela et al., 2004). PtdIns(4,5)P₂ and PtdIns(3,4,5)P₃ have the ability to participate in the regulation of dynamic functions of the membrane and cell shape through the control of FAs between cytoskeleton and plasma membrane (Sun et al., 2007, Raucher et al., 2000, Hilpela et al., 2004, Thapa et al., 2015). During FA formation many kinases are recruited to FA sites, such as PIP5K γ 90 which generates PtdIns(4,5)P₂ pools in cell membranes (Legate et al., 2011, Di Paolo et al., 2002, Izard and Brown, 2016, Wu et al., 2011). PtdIns(4,5)P₂ synthesis in the cell membrane recruits many kinases to the cell membrane which are implicated in the regulation of FA turnover (Izard and Brown, 2016). PtdIns(4,5)P₂ also increases in the binding between FAs and integrin during the assembly process (Figure 1.15) (Izard and Brown, 2016, Chandrasekar et al., 2005, Wang, 2012, Yuan et al., 2017). PtdIns(3,4,5)P₃ also plays a role in the regulation of FA turnover through restructuring of FAs via association with α -actinin and deactivation of the interaction between α -actinin and β -integrin (Rubashkin et al., 2014, Greenwood et al., 2000).

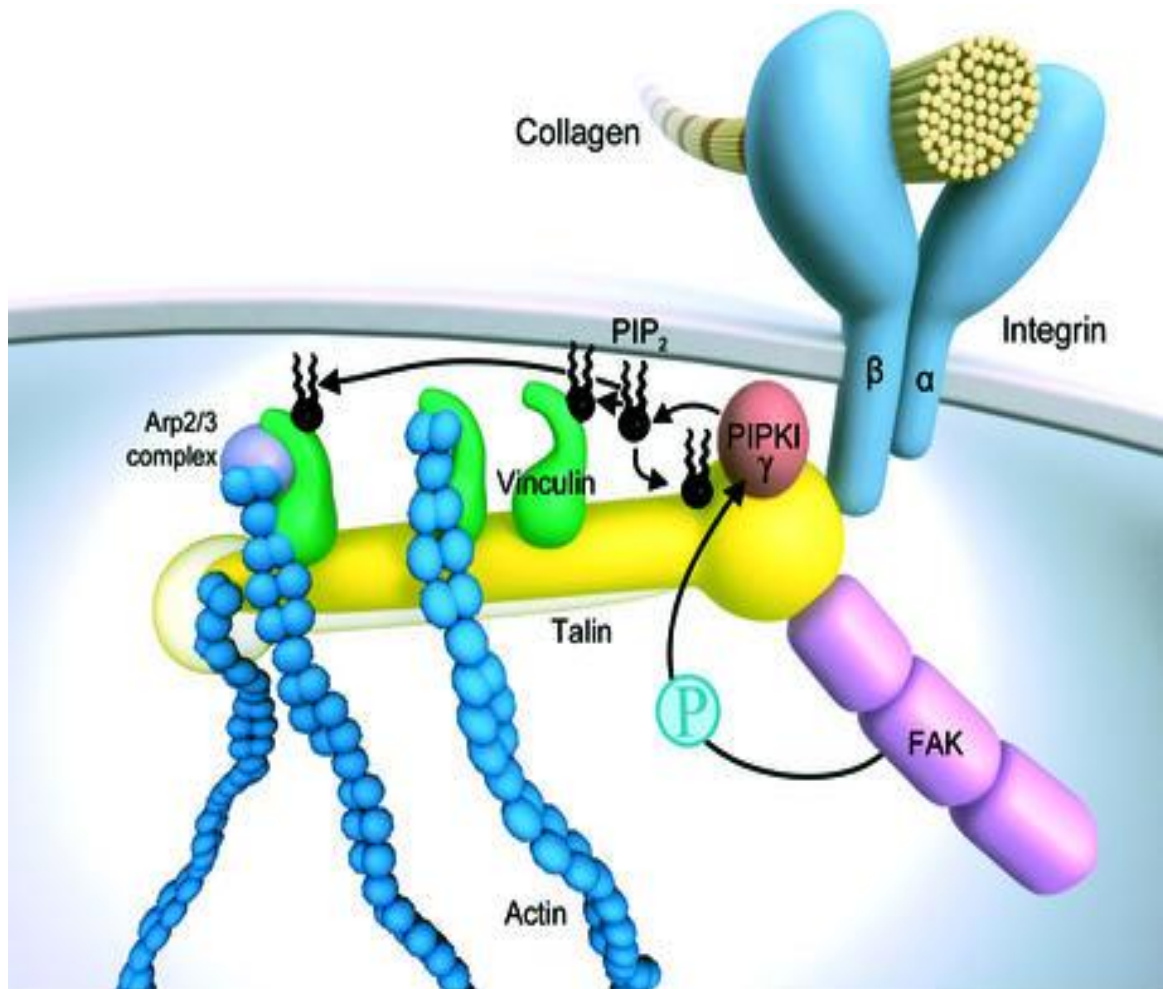


Figure (1.15): PtdIns(4,5)P₂ may enhance talin-integrin interaction. PIPK γ generates PtdIns(4,5)P₂ then PtdIns(4,5)P₂ interacts with talin and vinculin. PtdIns(4,5)P₂-FA interaction associates with actin filaments-Arp2/3 complex which involves in nucleation of actin polymerization. PtdIns(4,5)P₂ also enhances the strength of the interaction between FA-actin complex and integrin (Brakebusch and Fassler, 2003).

PLCs are recruited by PtdIns(4,5)P₂ during FA formation and cleave it into IP₃ and DAG messengers (Izard and Brown, 2016, van den Bout and Divecha, 2009). These second messengers are implicated in the regulation of FA turnover through activation of protein kinase C (PKC) and Ca²⁺ signalling (Fogh et al., 2014, Chen et al., 2013). IP₃ diffuses away to the cytoplasm and interacts with the IP₃ receptor to open a ligand gated ion channel and release of Ca²⁺ from the endoplasmic reticulum (ER) to the cytoplasm (Wuttke, 2015, Tsai et al., 2015) (Figure 1.17). Whereas, DAG remains in the membrane and activates PKC (Wuttke, 2015, Tsai et al., 2015). The Ca²⁺ participates in FA disassembly, but not in FA formation (Giannone et al., 2002) through activation of calpain, proline-rich tyrosine kinase 2 (Pyk2) and PKC (Chen et al., 2013, Fogh et al., 2014). Calpain is involved in FA disassembly through cleavage of vinculin, FAK, talin and FAK (Figure 1.16), while Pyk2 acts as a biochemical bridge between FAs and Ca²⁺ (Chen et al., 2013). PKCs also participate in FA turnover and forward migration. PKC α binds directly with Integrin β 1 during FAs formation and may be able to mediate the signal transformation from inside-outside of α 4 β 1 integrin (Figure 1.16) (Tsai et al., 2014, Fogh et al., 2014).

Given the importance of the effective contribution of lipid signalling in particular Phosphoinositides signalling in cancer metabolism and tumour progression (Baenke et al., 2013), many pharmacological inhibitors have been designed, such as wortmannin and LY294002 to inhibit the PI3K-Akt pathway, as potential treatment for cancer (Kong and Yamori, 2008).

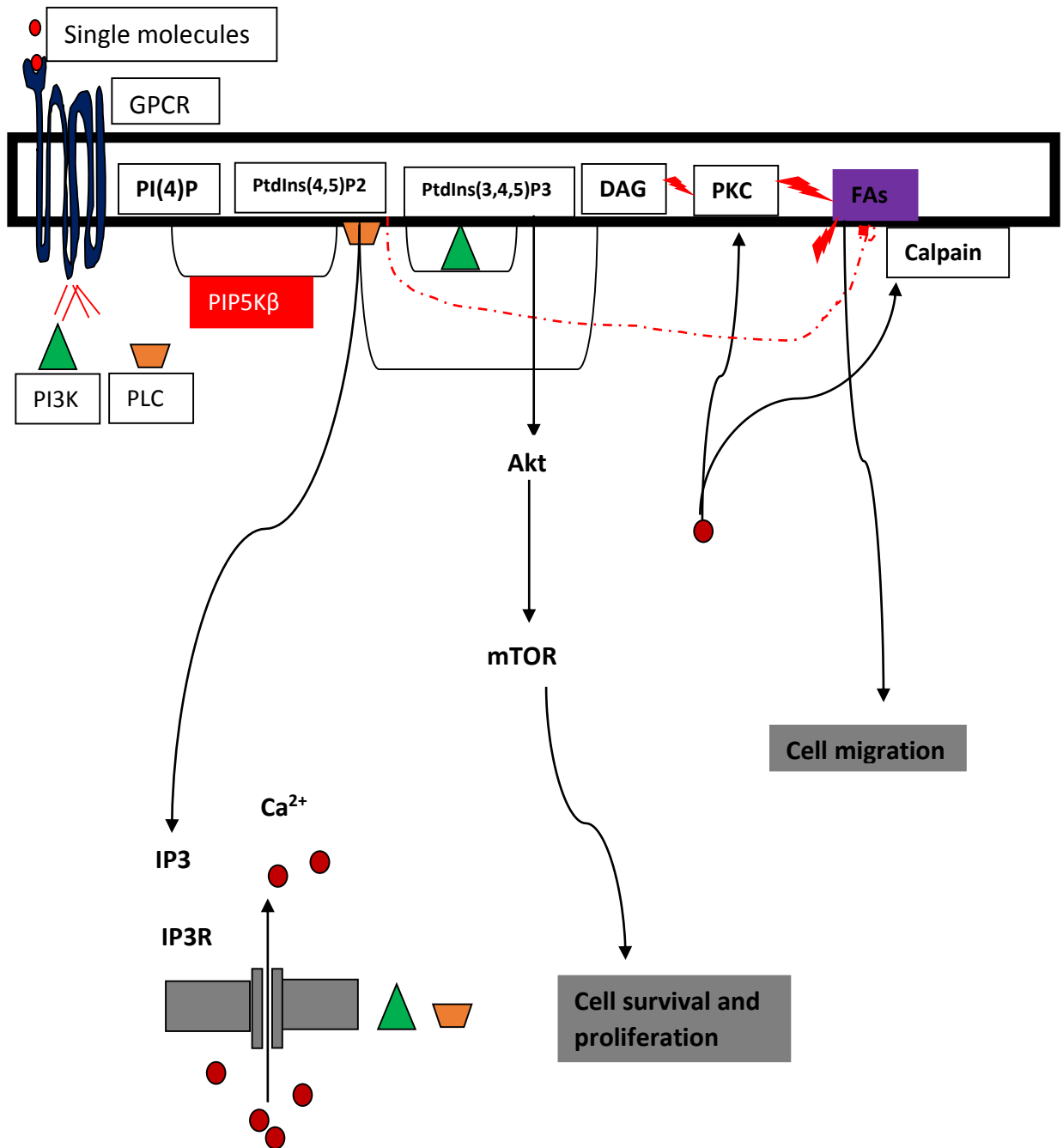


Figure (1.16): A model showing a possible role of PI3K and PLC signalling in cancer cell migration. PLC cleaves PtdIns(4,5)P2 into DAG and IP3 and PI3K converts PtdIns(4,5)P2 to PtdIns(3,4,5)P3. IP3-dependent Ca^{2+} and DAG activates PKC and calpain. Activated calpain and PKC promote FAs. PI3K-dependent PtdIns(3,4,5)P3 activates Akt/mTOR pathway.

Phosphoinositides are thought to modulate the conformation and activity of FA proteins. The interaction of PtdIns(4,5)P₂ with FA proteins plays a role in the regulation and activation of talin, vinculin and integrins. It has been suggested that vinculin might be activated and recruited into FA sites through interaction with PtdIns(4,5)P₂. It has been proposed that vinculin interacts with PtdIns(4,5)P₂ after activation by talin. However, it has also been observed that tail and head binding of vinculin blocks PtdIns(4,5)P₂ from interacting with it (Thompson et al., 2017, Izard and Brown, 2016).

Since talin is a main activator for vinculin it must be activated before recruitment of vinculin as it would otherwise be in an auto-inhibited state. It has been proposed that recruitment of an auto-inhibited talin into FAs may occur via interaction of its C-terminal with actin or via binding of its N-terminal with integrin, PtdIns(4,5)P₂ or other FAs components (Atherton et al., 2016, Wehrle-Haller and Imhof, 2002). Possibly, its head-rod binding is disrupted by PtdIns(4,5)P₂ which permits the N-terminal domain of talin to activate integrins and therefore link talin to cell membrane. Activation of vinculin by PtdIns(4,5)P₂ may allow interaction of vinculin with actin directly as well as its interaction with talin. This may play a crucial role in the formation of FAs. (Atherton et al., 2016, Wehrle-Haller and Imhof, 2002).

It has been shown that actin-vinculin interaction increased 3-fold in the presence of PtdIns(4,5)P₂, so this proposes that PtdIns(4,5)P₂ interaction enhances FA sites targeting vinculin (Gilmore and Burridge, 1996). However, another study showed that the interaction of PtdIns(4,5)P₂ with vinculin prevents its binding with F-actin (Steimle et al., 1999), suggesting that more work needs to be done to fully understand the role

of PtdIns(4,5)P2 in vinculin activation and FA formation (Thompson et al., 2017, Izzard and Brown, 2016)

Even though the interaction of PtdIns(4,5)P2 with FAs plays an auxiliary role in the activation of vinculin, it might be crucial for modulation (Thompson et al., 2017, Izzard and Brown, 2016). It has been suggested that local levels of PtdIns(4,5)P2 in FA sites modulate talin-1 affinity for vinculin and other FA proteins. The molecular mechanism of activation of auto-inhibited talin is poorly understood (Ye et al., 2016b). FRET based binding assays shows that the R9 and R12R13 segments of the talin rod domain block the interaction of the talin head domain to lipids (Ye et al., 2016b). However, other studies show that the interaction of talin head domain to PtdIns(4,5)P2 is insensitive to the existence of the inhibitor domains (Ye et al., 2016a). Possibly, PtdIns(4,5)P2 directly activate talin via interaction with the F2F3 domain of the talin head. So, PtdIns(4,5)P2 might play an important role in the regulation and recruitment of the auto-inhibited of talin to the cell membrane, which is crucial for integrin inside-out signalling (Ye et al., 2016a, Ye et al., 2016b).

It has been suggested that the conformation of integrin α IIb β 3 could be directly altered by PtdIns(4,5)P2-talin interaction (Martel et al., 2001, Orłowski et al., 2015) It has also been shown that PtdIns(4,5)P2 is involved in the activation of integrin via the charged head group of PtdIns(4,5)P2 which can perturb a clasp of the integrin at the cytoplasmic face (Orłowski et al., 2015).

Inactive vinculin is characterised by a closed state of head–tail interactions in which its N-terminal helix domain of the head is bundled with the tail. It can be altered to an active state through binding with talin which disrupt these interactions, and allows an open conformation of its tail domain which then interacts with PtdIns(4,5)P2 and F-actin (Figure 1.17)(Short, 2014) (Thompson et al., 2017, Izard and Brown, 2016).

Probably, actin and PtdIns(4,5)P2 bind with vinculin simultaneously when PtdIns(4,5)P2 remains in the membrane. This could be a temporary event that happens in the integrin signalling layer to activate vinculin (Figure). So, local levels of PtdIns(4,5)P2 may temporally activate vinculin in the distal tip of FAs. While binding of vinculin with actin might promote release of PtdIns(4,5)P2 from vinculin to enhance full activation and transfer of vinculin to the actin regulatory layer(Izard and Brown, 2016). However, another study showed that actin interacting-deficient vinculin mutants still concentrate to the actin regulatory layer(Izard and Brown, 2016). So, actin interacting might participate to activate vinculin and transport to the actin regulatory layer but not be fully required (Thompson et al., 2017, Izard and Brown, 2016).

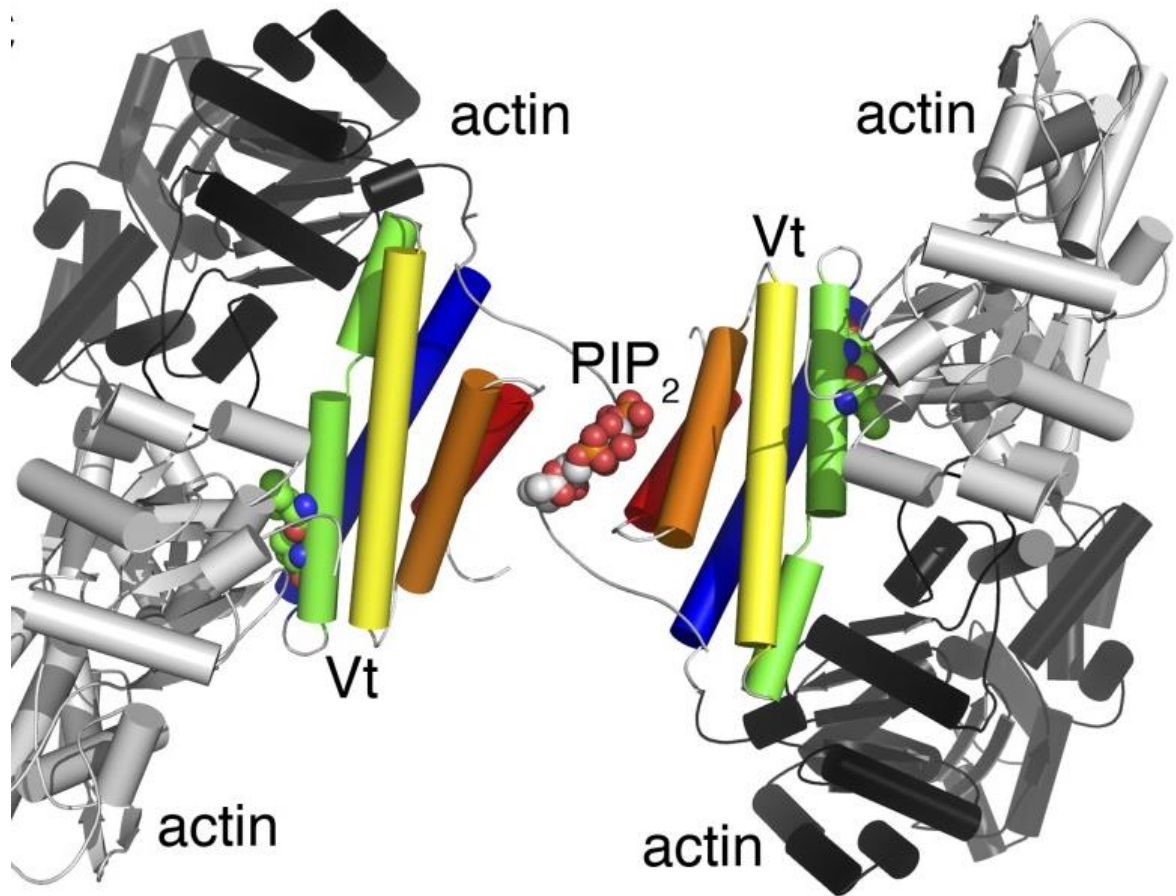


Figure (1.17): The Vinculin tail–F-actin structure: F-actin subunits (gray or black) onto the PtdIns(4,5)P₂-interacted vinculin tail dimer α -helices H1(red)–H5(blue) and PtdIns(4,5)P₂ are shown as sphere, which propose that vinculin has distinct F-actin-lipid interaction sites. (Ile-997 and Val-1001) residing on α -helices H3 (green) that show a significant decreased affinity for F-actin (Thompson et al., 2017, Izard and Brown, 2016).

The interaction of PtdIns(4,5)P₂ with vinculin might be important for release of vinculin from FAs, and the binding of vinculin with actin and talin might be important for forming the molecular clutch (Dumbauld et al., 2013, Izzard and Brown, 2016). Possibly, the binding of PtdIns(4,5)P₂ and actin with vinculin will be antagonistic, then FA tension might be detached and PtdIns(4,5)P₂ released. So, PtdIns(4,5)P₂ binding is a transient but necessary event in the recruitment and activation of vinculin in FAs (Thompson et al., 2017, Izzard and Brown, 2016).

The identification of the PtdIns(4,5)P₂ binding sites by crystallography permitted design of mutants for vinculin that specifically block interaction with PtdIns(4,5)P₂ (Thompson et al., 2017, Izzard and Brown, 2016). It has been shown through studying the crystal structure between vinculin- PtdIns(4,5)P₂ complex that PtdIns(4,5)P₂ directs the structure of vinculin to oligomerisation (Chinthalapudi et al., 2014) (Figure 1.18). The turnover of vinculin is required for direct oligomerisation which directly affects vinculin dynamic at FAs. It has also been shown using mutants of the binding site between vinculin and PtdIns(4,5)P₂ in vinculin-null mouse embryonic fibroblasts that PtdIns(4,5)P₂ is still essential for maintaining FAs, actin organisation and cell migration (Thompson et al., 2017, Izzard and Brown, 2016).

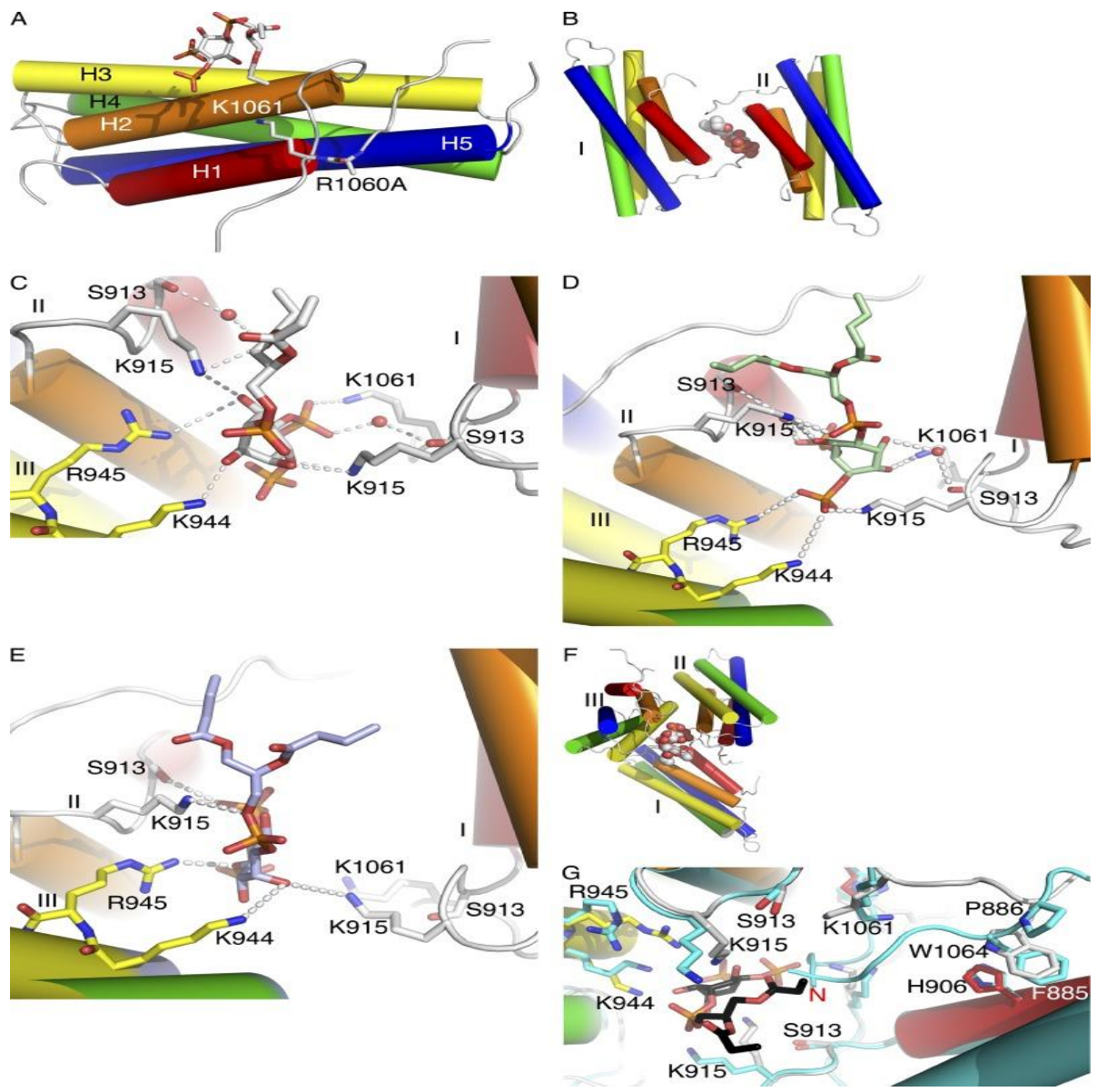


Figure (1.18): PtdIns(4,5)P2 leads to vinculin oligomerisation by unfolding the N terminus of the vinculin tail (Vt). (A) shows (R1060A mutation) used for crystallization does not impact PtdIns(4,5)P2 where oxygen (red), phosphor (orange), and carbon atoms (white sticks) interaction. Vt α -helices contain H1 (red) to H5 (blue). 1,060 and 1,061 residues are showed. (B) PtdIns(4,5)P2 directed dimerization of the vinculin α -helices tail domain to monomers which are (I and II) by interacting to the loops (α 1- α 2) and the C terminus of Vt. (C–E) PtdIns(4,5)P2-directed oligomerisation of Vt. (Lys-944 and Arg-945 residues) from a third (III) monomer. (D and E) PtdIns(4,5)P2 in the asymmetric unit in the same orientation as in C, which shows the specificity. (F) The PtdIns(4,5)P2-directed Vt trimer, Vt α -helices PtdIns(4,5)P2 is exposed as domains, and the three Vt molecules (I–III) (Izard and Brown, 2016)

It has been shown that phosphoinositide metabolism is essential for cell growth and proliferation and involved in tumour progression (Baenke et al., 2013). Phosphoinositides play a key role in the regulation of FA turnover during adhesion and migration (Legate et al., 2011, Di Paolo et al., 2002, Izzard and Brown, 2016, Wu et al., 2011). However, their potential role within a single FA during cancer cell migration, and also their role in FA turnover at leading edge of cell are not yet fully understood. These studies have focused on their role in FAs turnover through kinases which generate or phosphatases that degrade them (Wu et al., 2011, Durand et al., 2016). In the present study, PtdIns(4,5)P2 and PtdIns(3,4,5)P3 have been studied directly through studying the temporal and spatial organisation of PtdIns(4,5)P2 and PtdIns(3,4,5)P3 within a single FA turnover. Additionally, the molecular interaction events between FA composition and PI3K and PLC has been studied.

1.7. Hypothesis and aims

The hypothesis of this thesis is that the local generation of lipid signalling molecules including PtdIns(4,5)P2 and PtdIns(3,4,5)P3 are essential for the regulation of FAs turnover in cancer cell migration.

This project aims to visualise the spatial regulation between FAs and PtdIns(4,5)P2 or PtdIns(3,4,5)P3, using biosensors (Btk-PH and PLC δ -PH) for detecting PtdIns(4,5)P2 and PtdIns(3,4,5)P3 directly in live cells.

A further aim is to understand the possible role of PtdIns(4,5)P2 and PtdIns(3,4,5)P3 through studying their temporal regulation by measuring the local levels of PtdIns(4,5)P2 and PtdIns(3,4,5)P3 within and around single FAs during the assembly and disassembly process.

Finally this project aims to determine the reasons for temporal changes in PtdIns(4,5)P2 levels during FA disassembly. The role of PLC and PI3K on the molecular composition of FAs will also be investigated.

Chapter two: Materials and methods

2.1. Reagents

Table 2.1. Cell culture reagents

Reagents	Source
Dimethyl sulphoxide (DMSO)	Sigma Aldrich
Fetal Bovine Serum (FBS)	Gibco
20mM (100X)L-Glutamine	Gibco
10,000µg/ml Penicillin/Streptomycin	Gibco
Dulbecco's Modified Eagle's Media (DMEM X1)	Gibco
Trypsin/EDTA	Gibco
Polyethylenimine	Sigma Aldrich
Phosphate Buffered Saline (PBS)	Gibco
Fibronectin	BD Bioscience
Collagen	BD Bioscience
Gelatine	Sigma Aldrich
Recombinant human- epidermal growth factor (EGF)	Tocris Bioscience
Wortmannin	Tocris Bioscience
LY 294002	Tocris Bioscience
U73122	Tocris Bioscience

Table 2.2. Molecular Biology Reagents

Reagent	Source
Agarose	Sigma Aldrich
Ampicillin	Sigma Aldrich
Kanamycin	Sigma Aldrich
Midiprep Kit	Qiagen
Miniprep Kit	Qiagen
Maxprep Kit	Qiagen
Luria Bertani Agar and Broth	Sigma Aldrich
Restriction Enzymes	Thermo scientific
Competent E.coli I	Gift from <u>Dr Andrew Bicknell</u> lab
pmCherry N1	TAKARA (632523)
mCherry C1	Addgene (632524)
GFP-C1-PLCdelta-PH	Addgene (Plasmid #21179)
Btk-GFP-PH	Addgene (Plasmid #51463)
Primers	Thermo scientific
Ethidium bromide	Sigma Aldrich

Table 2.3. Biochemical assay reagents

Reagent	Source
Acrylamide	Sigma Aldrich
Ammonium persulphate (APS)	Sigma Aldrich
Bromophenol Blue	Sigma Aldrich
ECL Plus western blotting detection system	GE Healthcare
Glycine	Sigma Aldrich
Glycerol	Sigma Aldrich
Hybond ECL Nitrocellulose Membrane	Amersham Biosciences
Medical X-Ray Film	Fuji
Paraformaldehyde (PFA)	Sigma Aldrich
PBS Tablets	Sigma Aldrich
Pierce ECL Western Blotting Substrate	Thermo Scientific
Pierce™ Protein A/G Agarose	Thermo Scientific
Sodium Chloride	Sigma Aldrich
Sodium Dodecyl Sulphate	Sigma Aldrich
Sodium Fluoride	Sigma Aldrich
Tetramethylethylenediamine (TEMED)	Sigma Aldrich
Tris-Base	Sigma Aldrich
Tris-HCl	Sigma Aldrich
Triton X-100	Sigma Aldrich
Tween-20	Sigma Aldrich
Protease Inhibitor Cocktail set I	Calbiochem
Skimmed Milk Powder	Supermarket

Table 2.4. Materials and solutions for biochemical assays

Buffer/Solution	Composition
10X Sodium dodecyl sulphate (SDS)	500 ml: 50g of SDS (Sodium dodecyl sulphate), 450ml of ddH ₂ O
5X Tris –Glycine electrophoresis (Running Buffer)	1 Liter: 15.1g Tris base, 94g Glycine (in 900ml ddH ₂ O), Then add 50ml of 10%SDS, Complete to 1 liter by ddH ₂ O
1X Tris –Glycine electrophoresis (Running Buffer)	1 Liter: 200ml of 5X Tris –Glycine electrophoresis (Running Buffer), Add 800ml of ddH ₂ O Check the pH and adjust to <u>pH 8.3</u>
Transfer Buffer	1 Liter: 1. 2.9g Glycine 2. 2.8g Tris base 3. 200ml Methanol 4. Complete to 1 liter by ddH ₂ O Check the pH and adjust to <u>pH 8.3</u>
1. 10X Tris Buffer Saline (TBS)	1 Liter: 1. 80g of NaCl 2. 2g KCl 3. 30g Tris base 4. Add 800ml of ddH ₂ O 5. Adjust to the pH to <u>7.4</u> using concentrated HCl 6. Complete to 1 liter by ddH ₂ O
2. 1X Tris Buffer Saline Tween (TBST)	1 Liter: 1. 100ml of 10X TBS 2. 900ml of ddH ₂ O 3. 1ml of Tween 20
10% Stacking Acrylamide Gel (15ml)	4.9 H ₂ O, (6ml)30% acrylamide mix, (3.8 ml)1.5 M Tris (pH 8.8), (0.15ml)10% SDS, (0.15ml)10% ammonium persulfate , 0.006mlTEMED

12% Stacking Acrylamide Gel (15ml)	5.9 H ₂ O, (5ml)30% acrylamide mix, (3.8 ml)1.5 M Tris (pH 8.8), (0.15ml)10% SDS, (0.15ml)10% ammonium persulfate , 0.006mlTEMED SDS, 0.1% APS, 0.05% TEMED
RIPA Lysis Buffer	10 mM Tris, 150 mM NaCl, 1 mM EDTA, 1% TritonX-100, Protease inhibitor cocktail set 1
PBS-Tween	10 tablets of Phosphate buffered saline dissolved in 1L water, 0.1% Tween-20
SDS Sample Buffer 5x	312.5 mM Tris base (1.514g), 10% v/v SDS (4g), 50% v/v glycerol (20g), 25% v/v mercaptoethanol (10g), 0.0125% v/v bromophenol blue (5mg).

Table 2.5 Antibodies

Reagent	Species	Dilution	Source	Catalogue Number
Anti-PtdIns(4,5)P2	Mouse	1:100 (IF)	Echelon Biosciences	(Z-P045)
Anti-PtdIns(3,4,5)P3	Mouse	1:100 (IF)	Echelon Biosciences	(Z-P345)
Anti-Vinculin	Rabbit	1:200 (IF) 1:50 (IP) 1:1000 (WB)	Abcam	(EPR8185)
Anti-Vinculin	Mouse	1:200 (IF) 1:50 (IP) 1:1000 (WB)	Abcam	(ab130007)
Anti-Talin1	Rabbit	1:200 (IF) 1:50 (IP) 1:1000 (WB)	Abcam	(ab71333)
Anti-Talin1	Mouse	1:200 (IF) 1:50 (IP) 1:1000 (WB)	Abcam	(ab157808)
Anti-FAK	Mouse	1:200 (IF) 1:50 (IP) 1:1000 (WB)	Abcam	(ab28152)
Anti-FAK	Rabbit	1:200 (IF) 1:50 (IP) 1:1000 (WB)	Abcam	(ab76496)
Anti-Actin	Rabbit	1:200 (IF) 1:50 (IP) 1:1000 (WB)	Abcam	(ab179467)
Anti-Paxillin	Mouse	1:200 (IF) 1:50 (IP) 1:1000 (WB)	Abcam	(ab23510)
Anti-Paxillin	Rabbit	1:200 (IF) 1:50 (IP) 1:1000 (WB)	Abcam	(ab32084)
Anti-PI3Kp85	Rabbit	1:200 (IF) 1:50 (IP) 1:1000 (WB)	Cell Signalling	(4292S)
Anti-p100 α	Rabbit		Cell Signalling	(4255S)
Anti-PLC β 1	Rabbit	1:200 (IF) 1:50 (IP) 1:1000 (WB)	Abcam	(ab182368)
Anti-Mouse HRP	Goat	1:1000-2000 (WB)	Cell Signalling	7076
Anti-Rabbit HRP	Goat	1:1000-2000 (WB)	Cell Signalling	7074

Anti-mouse Alexa Flour 488	Goat	1:200-1:400	Cell Signalling	4408
Anti-rabbit Alexa Flour 488	Goat	1:200-1:400	Cell Signalling	4412
Anti-mouse Alexa Flour 594	Goat	1:200-1:400	Cell Signalling	8890
Anti-Rabbit Alexa Flour 594	Goat	1:200-1:400	Cell Signalling	8889

2.2. Methods

2.2.1. Molecular biology and cloning

2.2.1.I. Ampicillin (100 mg/ml) and kanamycin (50 mg/ml)

Stocks were prepared by weighing 1g of ampicillin and 0.5g of kanamycin powder into two tubes containing 10 ml dH₂O. Then, solutions were completely dissolved by vortexing and filtered through a 0.22µm sterilised syringe filter in a tissue culture hood. The stocks were aliquoted into sterile eppendorf tubes and kept at -20°C. The working concentration of ampicillin is 100µg/ml and kanamycin is 50µg/ml (recommended by Addgene).

2.2.1. II. LB Agar

Luria-Bertani (LB) media was made by adding tryptone (10g), yeast extract (5g), NaCl (10g) into 1 litre deionized H₂O. The solution was then shaken until completely dissolved. The pH was adjusted to 7.0 using a pH monitor with 5M NaOH. The bacto agar was prepared by adding 15g agar into LB media. LB-agar was then transferred into a suitably sized bottle for autoclaving. The cap of the bottle was covered with aluminium foil and autoclaved for 15 minutes at 120°C. The LB solution was cooled at room temperature to about 50°C. The antibiotic which was prepared in section 2.2.1.I was added into 1L of the solution and then swirled to ensure the antibiotic was evenly dissolved and distributed throughout the agar.

2.2.1. III. Agar Plates

The required amount of LB agar which was made in section 2.2.1.II was directly poured into a petri dish and evenly distributed to cover the bottom of the petri dish. The lids of plates were replaced and then left to solidify at room temperature for 30 minutes. The plates were inverted and sealed with parafilm and labelled with a selected antibiotic. Plates were placed in plastic bags and stored at 4°C. The bench was sterilised before preparation of agar plates and flame was used throughout the pouring the LB media into plates.

2.2.1. IV. Plasmid DNA Purification

The bench was sterilised by using 70% ethanol then wiped with a paper towel and a Bunsen burner was used to maintain sterility. The E.coli bacteria stabs which contain inserted GFP/mCherry plasmid construct were taken out from a 4°C fridge. A freshly sterilised loop was used and a colony was picked from the bacteria stabs into labelled falcon tubes. The tubes were incubated in a shaker at 285 rpm for 8 h at 37°C until the mixture becomes cloudy. The labelled agar plates were taken out from cold room and placed on a bench until warm. 10µl of the bacterial growth was taken from each labelled tube and gently spread over labelled selective plates. The plates were incubated overnight at 37°C to obtain single colonies. A single colony was picked from each plate and transferred into a sterilised falcon tube containing 5ml of LB media plus appropriate antibiotic. Labelled tubes were incubated in the shaker at 285 rpm for 10 h at 37° C until the mixture becomes cloudy. 400µl of the suspension was taken into a sterilized flasks containing 200 ml LB media with appropriate antibiotic then shaken at 285 rpm for 16 h at 37° C. Each culture was transferred into 250 ml tube and centrifuged at 6000 x g for

20 min at 4°C. The supernatant was removed and the pellet was either frozen at -80°C or used immediately for plasmid amplification and purification using Qiagen HiSpeed Plasmid Maxi kit.

Briefly, RNase A was added to buffer P1 and then 10 ml of buffer P1 was transferred into the bacterial pellet to resuspend the pellet. Then, 10 ml of buffer P2 was added and the tube was inverted 4-6 times and incubated at room temperature for 5 min. 10 ml of chilled buffer P3 was added and immediately mixed by inverting 4-6 times until the suspension becomes colourless. The lysate was poured into QIAfilter Cartridge and incubated for 10 min. HiSpeed Maxi was equilibrated by adding 10ml of QBT buffer. The cap of QIAfilter Cartridge was removed and lysate was inserted into equilibrated Hispeed Tip to allow all lysate enter the resin at room temperature. 60 ml buffer QC was added to HiSpeed Tip for washing and DNA was then eluted by adding 15 ml of buffer QF and then precipitated by incubation for 5 min with 10.5 ml isopropanol. The plunger was removed from the syringe and an elute-isopropanol mixture was transfer into a QIAprecipitator for filtration. 2ml of 70% ethanol was added through QIAprecipitator for washing. QIAprecipitators were dried and DNA was finally eluted with 1 ml buffer TE into a 1.5 ml sterilised tube for each plasmid.

2.2.1. V. Determination of DNA concentration and Purity

A NanoDrop spectrophotometer (Thermo Scientific, NanoDrop 200) was used to determine the concentration of plasmid. The nanoDrop spectrophotometer measures at wavelengths of 260nm and 280nm and determines absorption spectrum from 220-350nm. Briefly, 1µl of buffer TE was added on the bottom pedestal in order to read a blank. The blank was gently cleaned and 1µl of DNA sample was added and the concentration was measured. These steps were repeated three times to take three values in (µg/ml) for each plasmid. All plasmid purities were above 1.8.

2.2.2. Construction of fluorescent biosensors

2.2.2. I. Digestion of Plasmid

After purification and extraction of GFP or mCherry tagged-Plasmids in section 2.2.1. III were then cloned to create new mCherry-Biosensors. Btk-PH-GFP biosensor was digested by BamH1 + EcoR1 and mCherry-N1 vector was digested with the same restriction enzymes BamH1 + EcoR1. Double digestion reaction was prepared as following;

- 1 µg Btk-PH-GFP biosensor/ mCherry-N1 vector
- 1 µL of BamH1 + 1 µL of EcoR1
- 3 µL 10x fast digest buffer (digestion buffer uses for cutting DNA in short time (5 minutes) with high efficiency and supports 100% activity of all FastDigest restriction enzymes).
- 24 µL dH₂O

This reaction was prepared on ice. The mixture was placed into two labelled 1.5ml tubes gently pipetted and then incubated at 37°C for 1 hour.

2.2.2. II. Separation of digested plasmid

Gel electrophoresis was used to detect digested DNA bands according to their size s. The

Gel electrophoresis was prepared as following;

- 1% agarose (1g of agarose mix with 100 ml 1x TAE in microwave flask)
- Microwave was used to dissolve agarose completely in TAE (The flask was swirled during the process).
- The flask was put on the bench for 5 minutes until the solution cools to 50°C.
- 2-3 µL of ethidium bromide (EtBr) was added to solution and mixed well.
- Agarose was transferred into a gel tray after putting comb in appropriate place.
- Poured gel was left about 20-30 minutes at room temperature until solidified.
- Gel tray was placed into the gel box.

The gel box was filled and covered with 1x TAE and loading buffer was added to each digested sample. Samples were loaded into wells and the first lane was loaded with a ladder (Thermo Scientific, GeneRuler 1kb plus DNA ladder 50 µg). The gel was run at 150 V for about 45 minutes until the dye reaches about 75% of the edge of the gel. UV light was used to visualise DNA fragments to show there were had two bands vector (4722 bp) and PH domain (531bp). The mCherry-N1 vector fragments had two bands mCherry-N1 vector (4691 bp) and (31bp) as in figure 2.2.

2.2.2. III. Agarose gel purification and gel extraction

PH domain (531bp) and mCherry-N1 (4691 bp) vector were extracted and purified from the gel. QIAquick Gel Extraction Kit was used throughout these purification steps. Briefly, the gel was moved to a UV box and the PH domain (531bp) and mCherry-N1 vector fragments were carefully sliced from gel and put in labelled tubes. The isolated fragments were weighed to determine the amount of buffer that be should added throughout the DNA purification steps. The required amount of QG buffer was added to isolated fragments (each 100 mg=100 μ L). Labelled tubes were incubated at 50°C for 10 minutes and the tubes were vortexed every 3 minutes to dissolve the sliced gel completely. The colour of the mixture was checked and should be yellow similar to QG buffer. 1 volume isopropanol was then added to samples and mixed well. QIAquick column was placed in 2ml collection tubes and the samples were transferred into QIAquick column and centrifuged for 1 minute. After passing all samples into the QIAquick column the flow was discarded and the QIAquick column was placed back into the same tube. 500 μ L of QG buffer was added to the QIAquick column and centrifuged for 1 minute and the flow was discarded and the QIAquick column was placed back into the same tube. 750 μ L of PE buffer was added into the QIAquick column for washing. The QIAquick column was then placed into a new 1.5 micro centrifuge tube and 30 μ L of EB buffer was added and incubated for 5 minutes to increase the concentration of DNA. This was then centrifuged for 1 minute to elute the DNA. The concentration of Eluted DNA was measured as in section 2.2.1. V. Likewise with PLC δ 1-PH-GFP, mCherry-C1 was digested by Bgl11 + EcoR1 domain and gave the correct size (4680bp and 20bp). PLC δ 1-PH was cloned by PCR through designing forward and reverse primers to add restriction sites for restriction enzymes (Bgl11 + EcoR1) as in figure 2.1.

2.2.2. IV. Construction of primers

In order to add restriction sites for PLC δ 1-PH it is important to design primers. The restriction sites of Bgl11 + EcoR1 enzymes were placed to the end of both primers.

ACAACAACAATTGCATTCATTTTATGTTTCAGGTTTCAGGGGGAGGTGTGGGAGGTTTTTTTAA
AGCAAGTAAAACCTCTACAAATGTGGTATGGCTGATTATGATCAGTTATCTAGATTACTGGA
TGTTGAGCTCCTTCAGGAAGTTCTGCAGCTCCTTGAAGCTCATCTTGTTGTCCTTGTTTTTGTG
AGCTTTTCGCAAGCAGGAGTGAATCCAGTGCTGTAGCTTCTGACGCTGGTCCATGGAGCCTG
AGTGGTGGATGATCTTGTGCAGCCCCAGCACCCAGTGCTGGGCATCAGCTGGCGATGGGGC
GATGAGGTCTAGTGTATTGCGCTGGTCCTTGAAGACAATGGAGAAGCAGCGGTCCCTCGGGC
ACATCACGGGGCAACTTCTCCAGACCCTCCGTGCGGTGCCCATTCGCACCTCCTGAATGTC
CTCGATGGAGAACAGCTGGGACTCCGGGGTCCGCATGACCTTGCGGGACTCCTGCCAGATG
GTCTTGCACTCCTGCAACTTGTAGAAGCGCTCTCCTCCATGAGCTGGACTTCACCTTC
AGGAGCTGGCTGCCCTTCAGCAGCGCCTGTAGATCCTCATCATCCTGTAGGCCGTGCAGGGT
CAGGAAGTCCCGGCCCGAGTCCATGGATCCCGGGCCCGCGGTACCGTGCAGTGCAGAATTC
GAAGCTTGAGCTCGAGATCTGAGTCCGGACTTGTACAGCTCGTCCATGCCGAGAGTGATCCC
GGCGGCGGTACGAACTCCAGCAGGACCATGTGATCGCGCTTCTCGTTGGGGTCTTTGCTCA
GGGCGGACTGGGTGCTCAGGTAGTGGTTGTCGGGCAGCAGCACGGGGCCGTCCCGATGGG
GGTGTCTGCTGGTAGTGGTCCGGCAGCTGCACG

Forward Primer: AGCTAGATCTTTACTGGATGTTGAGCTCCT

Reverse Primer: AAGTCCCGGCCCGAGTCCATGGATCCAGCT

Restriction enzymes	Restriction sites
EcoR1	5' G ↓ A A T T C 3' 3' C T T A A ↑ G 5'
BglII	5' A ↓ G A T C T 3' 3' T C T A G ↑ A 5'
BamHI	5' G ↓ G A T C C 3' 3' C C T A G ↑ G 5'

2.2.2. V. Amplification of PH domain-PCR conditions

PCR mixture was made on the ice as following;

- 10 μ L Master mix
- 0.5 μ L Template PH domain (1 μ g)
- 1 μ L Forward Primer (10 μ M stock)
- 1 μ L Reverse Primer (10 μ M stock)
- 7 μ L Sterile dH₂O

The PCR amplified PLC δ 1-PH after the PCR was adjusted according to the primers melting temperature. The denaturation, annealing and elongation conditions were 94, 57 and 72 respectively.

The PLC δ 1-PH was digested by Bgl11 + EcoR1 then isolated and purified from gel as in section 2.3.1.5.III. The concentration of PLC δ 1-PH was measured (30ng/ml) and then ligated with mCherry-C1. The ligation reactions for both Btk-PH and PLC δ 1-PH were prepared as following;

- | | |
|---|--|
| • 25ng (0.5 μ L) of mCherry-N1 | 25ng (0.5 μ L) of mCherry-C1 |
| • 75ng (3 μ L) of Bk-PH | 75ng (3 μ L) of PLC δ 1-PH |
| • 1 μ L of ligase buffer (10x buffer) | 1 μ L of ligase buffer (10x buffer) |
| • 1 μ L T4 DNA ligase | 1 μ L T4 DNA ligase |
| • 4 μ L of H ₂ O to a total of 10 μ L | 4 μ L of H ₂ O to a total of 20 μ L |
| • The reaction was incubated for 1 hour at room temperature | |

4 tubes were prepared, 1 and 2 tubes contained uncut and cut vector respectively without ligase, while 3 and 4 contained cut vector and insert respectively with ligase. The purpose for doing these controls was to check as following;

- Viability of competent cells.

- Resistance of plasmid for antibiotic.
- Vector re-circularization.
- Contamination of plasmid in ligation reaction or transformation reagents.
- Background due to uncut vector.

2.2.2. VI. Transformation

After ligation of the PH domains into mCherry-vector competent cells were taken out of -80 and thawed on ice for 20-30 minutes. 4 μ L (usually 100ng) of Btk-PH or PLC δ 1-PH-mChery was added into labelled tubes containing 30 μ L of competent cells then were gently mixed by flicking the bottom of the tube a few times. The competent cells were then placed on ice for 25 minutes. The bottom of transformation tubes were placed into 42°C water for heat shocking for around 45 second. Transformation tubes were placed back on ice for 2 minutes. 400 μ L of LB media without antibiotic were added to transformation tubes and incubated with shaking for 45 minutes. After that 50 μ L of transformed bacterial growth was added onto plates which contain an appropriate antibiotic and then incubated at 37°C overnight.

2.2.2. VII. Miniprep

After incubation overnight a single colony was picked and transferred into labelled tubes containing 5 ml LB media with an appropriate antibiotic. Labelled tubes were incubated at 37°C for 8 hours until the growth become cloudy. 4 mL of bacteria were added into centrifugation tube and centrifuged at 8000 rpm for 3 minutes at room temperature. 250 μ L of P1 was added to the bacteria pellet for resuspending and then 250 μ L of P2 was added and mixed by inverting the tubes 4-6 times. 350 μ L of buffer N3 was added

and mixed immediately by inverting the tube 4-6 times and then centrifuged for 10 minutes at 13,000 rpm. The supernatant was transferred into QIAprep spin column and centrifuged for 1 minute and the flow was discarded. QIAprep spin column was washed by adding 750 μ L of PE buffer and centrifuged for 1 minute and flow was discarded. QIAprep spin column was centrifuged for 1 minute to discard residual buffer. QIAprep spin columns were placed into labelled micro centrifuge tube and 50 EB buffer was added and incubated for 1 minute then centrifuged for 1 minute to elute Btk-PH /PLC δ 1-PH-mChery. After purification and extraction the concentration of Btk-PH/PLC δ 1-PH-mChery was measured to take an appropriate amount to digest them again for confirmation of the ligation as in section 2.2.2.VI. New Btk-PH /PLC δ 1-PH-mChery was transfected into MDA-MB-231 cells and compared with Btk -PH-GFP/ Btk-PH-GFP biosensor to make ensure the cloning was successful (Figure 2.1& 2.2).

C

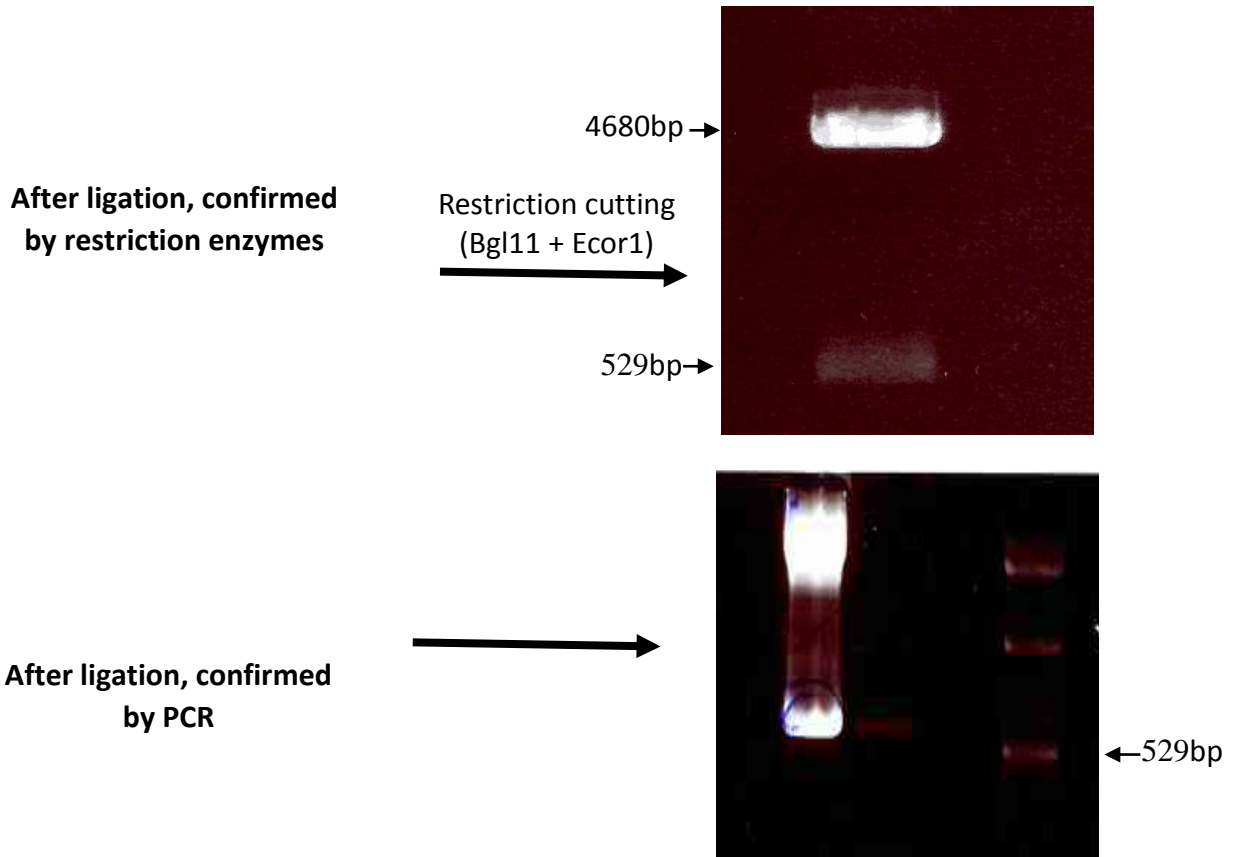
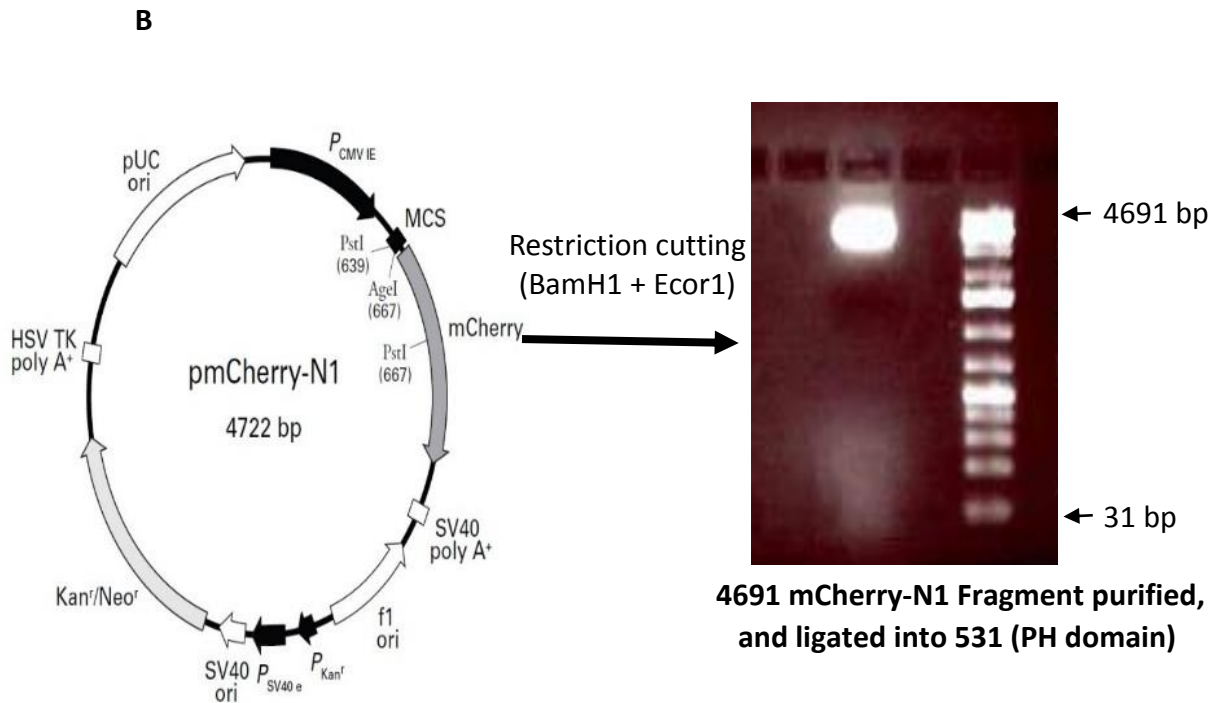
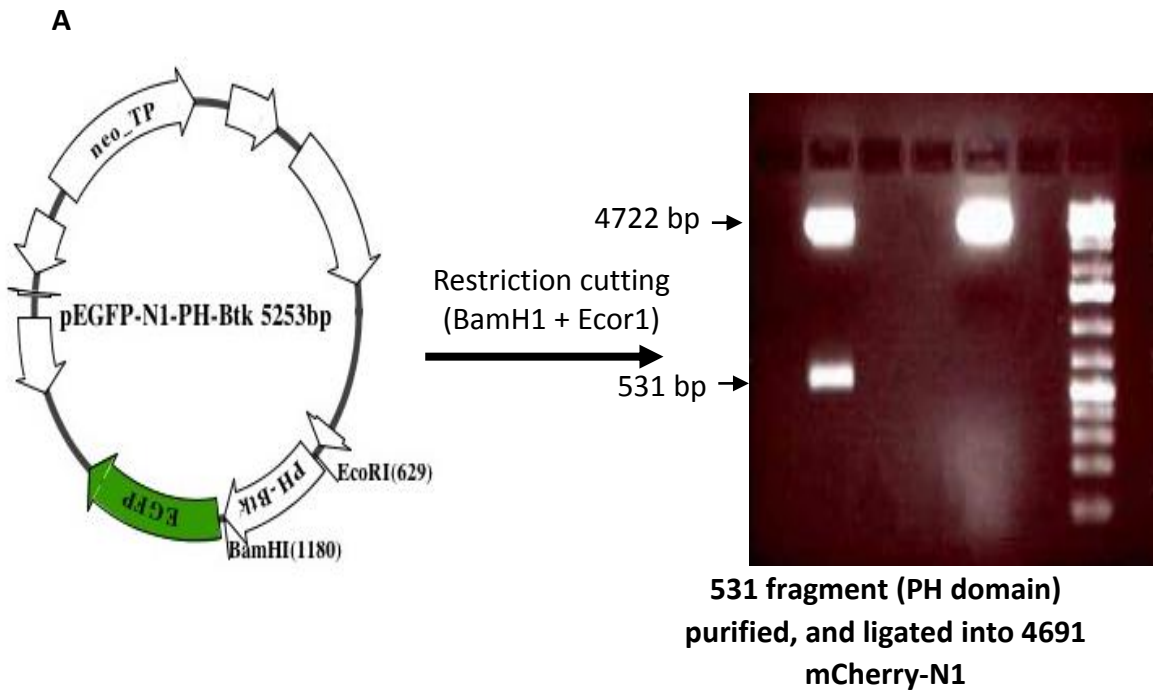


Figure (2.1): Construction of PLC δ 1-PH-mCherry: A) PH domain of PLC δ 1 was cloned by PCR to add restriction sites to PLC δ 1-PH, then digested by Bgl11 + EcoR1. Agarose gel showed band 529bp which is PLC δ 1-PH. **B)** mCherry-C1 was digested by same restriction enzymes Bgl11 + EcoR1. Agarose gel showed two bands 4680 which is mCherry vector and another band fragment of vector is 20bp. **C)** Ligation between PLC δ 1-PH and mCherry-C1 was digested by Bgl11 + EcoR1 into C1-PLC δ -PH (529bp) and mCherry-C1 (4680bp) and then ligation was confirmed by PCR to amplify the segment which was cloned with vector.



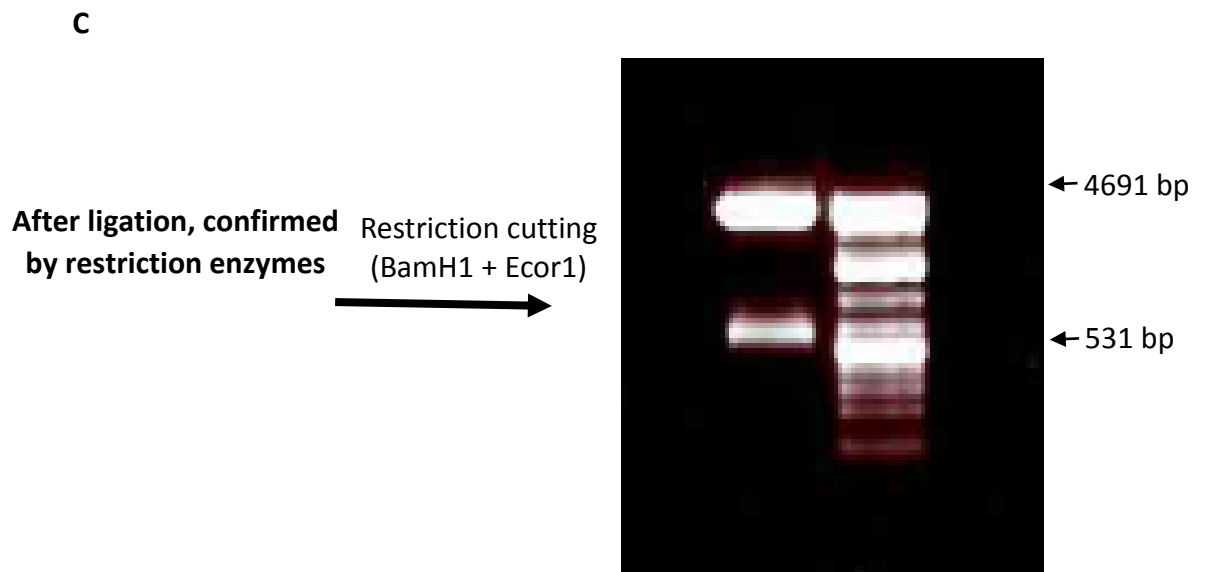


Figure (2.2): Construction of Btk-PH-mCherry: A) Btk –PH-GFP was digested by BamH1 + EcoR1 and agarose gel showed two bands (4722bp) vector and Btk-PH (551bp). **B)** mCherry-C1 was digested by BamH1 + EcoR1 and agarose gel showed two bands which are mCherry (4691bp) vector and another band (31bp). **C)** Ligation between Btk-PH and mCherry-N1 was digested by BamH1 + EcoR1 into Btk-PH (531bp) and mCherry-N1 (4691bp).

2.2.3. Cell culture

MDA-MB-231 cells aliquot was taken out from liquid nitrogen and defrosted gently in water bath at 37°C. Thawed cells were transferred into 10ml of DMEM and spun at 200g for 5 minutes. The pellet was taken and suspended in 5ml of fresh DMEM then added into a 75 cm² flask. The flask was incubated at 37°C, 5% CO₂ and 95% humidity until the cells become confluent. The media was changed every 2 days. 1 week was required for the cells to grow and reach confluence.

The growth of MDA-MB-231 cells was maintained in DMEM (Dulbecco's Modified Eagle's Medium 1x) containing 1g/L D-glucose, L-glutamine and pyruvate. 500 ml of media was supplemented with 10% (v/v) fetal bovine serum (FBS, Gibco), 5ml of 20 mM L-glutamine (100X, Gibco) and 5 ml of 1% v/v Penicillin/ Streptomycin (10,000 units/ml, 10,000µg/ml, Gibco). Serum free DMEM was also prepared without FBS, L-Glutamine and Penicillin/Streptomycin. The tools and equipment were used in tissue culture were sterilised.⁸⁸

2.2.3. I. Routine cell Passaging

The MDA-MB-231 cells were grown in T75 flasks and cell passaging was used to maintain growth of cells. For routine cell passage, MDA-MB-231 cells were passaged each for three days and sometimes longer depending on the confluence of the cells and the type of experiment. After disposal of old media the cells were washed with 10ml of Dulbecco's phosphate buffered saline (PBS, without calcium chloride and magnesium chloride, Sigma) once. The cells were then trypsinized with 2 ml of 0.05% Trypsin-EDTA (1X, Gibco) in the humidified environment of 5% CO₂ /95 % air at 37 °C for 3-5 minutes. After detaching the cells 5ml of fresh culture media was added and suspended to quickly

inactivate the trypsin. The cell suspension was mixed well to ensure single cell separation. The cells were seeded at 1:4 or 1:6 splitting ratio with $1-5 \times 10^5$ cells. New flasks were labelled with name and date and incubated in 5 % CO₂ /95% humidified air environment at 37°C for 3 days until 80% confluent.

To count cells a haemocytometer was used after cells were washed and suspended. A clean glass cover-slip was fixed on top of haemocytometer. 25µl of cell suspension was pipetted and placed at one edge of the coverslip and flow through the empty chamber. The cells were then counted in four large corners squares under microscope. The average number was recorded and multiplied by 10^4 . To determine the number of cells required for each experiments a formula was used:

No. Cells/ml= (average No. of cells counted/No. of cells wanted) $\times 10^4$ x dilution factor

2.2.4. Co-localisation Assay

2.2.4. I. Coating wells plated with ECM

In order to study the co-localisation between PtdIns(4,5)P₂ or PtdIns(3,4,5)P₃ and FAs it is important to coat the coverslip with ECM (collagen, fibronectin and gelatine) and grow the MDA-MB-231 cells on coverslips. Coverslips were put in each well of the plate then were sterilised by adding 1ml of 100% methanol for 1 hour in a culture hood. After aspiration of ethanol, the coverslips were left to dry.

Then, 1ml of 0.2% w/v gelatine was added on coverslips for coating for 20 minutes then removed and left to dry about 2 hours. Fibronectin was diluted with cold sterilised PBS to prepare stock solution on the ice at a culture hood. 1ml of 10µg/ml v/v fibronectin was added for coating then left for 1 hour in the culture hood. After 1 hour the fibronectin was aspirated off and a thin layer was left in each well for the cells to adhere. The thin layer was washed gently with PBS three times and PBS was swirled gently during washing. The plate can be immediately used or sealed in the fridge until needed. Collagen was prepared by using 4.41 mg/ml v/v chilled rat tail type 1 non-pepsinized collagen and mixed with DMEM (100 µL/ML) in the sterilised tube at culture hood. 15-20 µL of NaOH was added (pH normalized to 7.0) drop by drop on collagen/DMEM mixture until the colour changed to pink. The chilled culture media was added into collagen/DMEM mixture to make the final required amount. These steps were prepared on the ice in the culture hood and bubbles in solution were avoided. All the ingredients were mixed thoroughly on the ice and care was taken to avoid bubble formation in the mixture solution. 100µl of the mixture was poured for each well and then spread to cover the well. The plate was incubated at 5 % CO₂ /95% humidified air environment at 37C° initially for 30 minutes.

2.2.4. II. Transfection

After coating the coverslips in wells of the plate. The 6-well plate was seeded with 1×10^5 MDA-MB-231 cells for 24 hours at 70% confluence before transfection. Next day, 3 μg of PLC δ 1-PH-GFP or Btk-PH- GFP was added in 100 μl of serum-free media in labelled eppendorf tubes. 6 μl Polyethylenimine (PEI) transfection reagent was added to each labelled tube and then immediately mixed by vortex for 10 seconds. The labelled tubes were incubated for 15 minutes in the culture hood. The Plasmid/PEI mixture was added into each well which contains 2ml of complete media. The plate was gently swirled and incubated overnight.

2.2.4. III. Immunofluorescence Staining

After transfection of MDA-MB-231 cells with Btk-PH- GFP or PLC δ 1-PH-GFP, the media was aspirated and washed with pre-warmed PBS once. Then, 1ml of 4% PFA was added to each well for 20 minutes to fix cells at room temperature. 1ml of PBS was added for washing (three times each wash 10 minutes). 1ml of 0.5 % Triton-X 100 was added for permeabilisation of cells for 10 minutes at room temperature. The cells were then washed with PBS three times (each wash 10 minutes). 1ml of 10 % goat serum was added around 30 minutes for blocking. The cells were incubated with anti-rabbit-talin, vinculin, FAK and paxillin antibody (1:10, 2 μl antibody, 200 μl PBS, 4 μl 2% goat serum) for each well around 1 hour. The cells were washed three times with PBS for 10 minutes and then incubated with 546 Alexa Fluor anti-mouse solution (1:10, 2 μl antibody, 200 μl PBS, 4 μl 2% goat serum) for 1 hour in the dark. The cells were washed with PBS three times for 10 minutes and then stained with DAPI (4',6-diamidino-2-phenylindole is a fluorescent stain that interacts with DNA which mix with fluoroshield Mounting

Medium) on the glass slide. Nail polish was used to brush the borders of the coverslips to fix them onto the slides.

The immunostaining on collagen was similar to the steps on fibronectin and gelatine but after fixation by 2ml 4% PFA the cells were washed in 5% sucrose in PBS for 15-20 minutes or in 0.15 M glycine in PBS for 15 minutes.

2.2.4. III. Confocal microscopy

After MDA-MB-231 cells were transfected with Btk-PH- GFP or PLC δ 1-PH-GFP and stained with anti-FA proteins antibodies confocal microscopy (Nikon) (Nikon camera software was used to visualise the co-localisation of PtdIns(4,5)P2 or PtdIns(3,4,5)P3 with FA proteins. Fixed MDA-MB-231 cells were taken to the confocal microscopy for visualisation. One drop of oil was put on 100x lens to allow detection of FAs and lipids on cell membrane. To make sure the light was transmitted from the lasers the GALVANO was selected and interlock was removed (The galvano scanner was used to enable high-resolution imaging of up to 4096 x 4096 pixels). The E100 was altered to L100 confocal and lamp shutter was turned off (the light path can be used either through E100 which is dependent 100% to the eyepieces to observe image or through L100: confocal which uses to record or capture image). The format (1024*1024) was used for imaging in the xyz axis. Then Z-Stacking or single slice confocal images were acquired to determine an accurate co-localisation point between a single FA and PtdIns(4,5)P2 or PtdIns(3,4,5)P3 in the live and fixed cells. The 488 green channel (PtdIns(4,5)P2) or (PtdIns(3,4,5)P3) and 546 red channel (FAs). Likewise, MDA-MB-231 cells were plated on (fibronectin 20 μ g/ml and collagen 2mg/ml) and co-transfected with PLC δ 1-PH- mCherry (red) or GFP (green) & paxillin-GFP (green), or zyxin-RFP (red), then the z-stacking was scanned from top to

bottom of the cell membrane and the laser was switched on and the pinhole size was 1.2.

2.2.4. IV. Co-localisation analysis

In order to measure the co-localisation value between PtdIns(4,5)P2 or PtdIns(3,4,5)P3 and FAs the images were taken using the same objectives and laser settings. ImageJ was used to adjust the images to 8-bit colour and choose the single slice which contains an accurate co-localisation point between PtdIns(4,5)P2 or PtdIns(3,4,5)P3 and FAs of Z-stack images. The image was split into two channels the first channel contains RFP-FA and the second channel contains GFP- PtdIns(4,5)P2 or PtdIns(3,4,5)P3. The first channel image was zoomed and FA was selected closely around individual FA after subtracting background. Then through choosing the options as following;



Spearman's rank correlation value was taken between PtdIns(4,5)P2 or PtdIns(3,4,5)P3. Spearman's rank correlation value refers to statistical co-localisation which estimates the amount of co-localisation between two of the fluorescent intensity in the images. Then, it gives the value of co-localisation to each fluorescent intensity between green and red channels of confocal microscopy to express the correlation of co-localisation between signal intensities. The reverse co-localisation value was measured between PtdIns(4,5)P2 or PtdIns(3,4,5)P3 and FA with the same steps but the first channel was PtdIns(4,5)P2 or PtdIns(3,4,5)P3 and the second was FA as mentioned in figure 2.3.

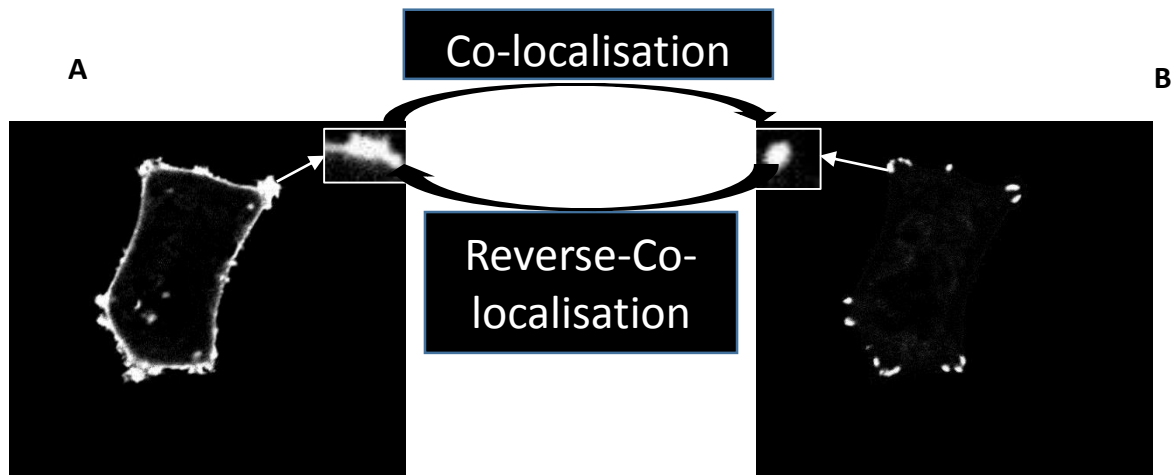


Figure (2.3): showing **A)** spatial co-localisation between PtdIns(4,5)P2 and paxillin. **B)** Reverse spatial co-localisation measurement between paxillin and PtdIns(4,5)P2.

2.3.5. Local levels of lipids within FA turnover assay.

2.3.5. I. Co-transfection

Collagen was prepared using 4.41 mg/ml chilled rat tail type 1 non-pepsinized collagen and mixed with DMEM (100 μ L/mL) in the sterilised tube in the culture hood. 15-20 μ L of NaOH was added (pH normalized to 7.0) drop by drop on collagen/DMEM mixture until the colour changed to pink. The chilled culture media was added into the collagen/DMEM mixture to make the final required amount. These steps were prepared on ice in the culture hood and bubbles in solution were avoided. 100 μ L of the mixture

was poured into ibidi glass bottom dishes then spread to cover the dish. The dishes were incubated at 5 % CO₂ /95% humidified air environment at 37°C initially for 30 minutes. The dishes were seeded with 1 x 10⁵ MDA-MB-231 cells for 24 hour at 70% confluence before transfection. The next day, 3 µg of PLCδ1-PH-GFP and RFP-zyxin or Btk-PH- GFP and RFP-zyxin were added in 100 µl of serum-free media in labelled eppendorf tubes. 6 µl Polyethylenimine (PEI) transfection reagent was then added to each labelled tube then immediately mixed by vortex for 10 seconds. The labelled tubes were incubated for 15 minutes in the culture hood. The Plasmid/PEI mixture was added into each dish containing 2ml of complete media. The dishes were swirled gently and incubated overnight.

2.3.5. II. Confocal microscopy and live cell imaging

The ibidi dish was put in the confocal chamber and the chamber was connected to CO₂ supply needle and warmed at 37°C 1 hour prior to use. The 488nm and 568nm channels of confocal microscopy were used to visualise GFP and RFP or mCherry respectively. Z-Stacks were taken with time-lapse series acquired over a 10 minute period with an interval of 15 seconds to be able to determine an accurate co-localisation between PtdIns(4,5)P₂ or PtdIns(3,4,5)P₃ and FA proteins over time. Laser intensity and exposure time were adjusted to rid of noise background.

The local levels of PtdIns(4,5)P₂ or PtdIns(3,4,5)P₃ were measured at different time points and different focal planes within and around a single FA during the assembly and disassembly process. Quantitative measurement of these live images was performed by ImageJ. In the channel of FA-RFP the region of interest (ROI) was selected closely around individual FA, then the same selection applied via restore the selection to the GFP

channel of PtdIns(4,5)P₂ or PtdIns(3,4,5)P₃ to determine the specific localisation of PtdIns(4,5)P₂ or PtdIns(3,4,5)P₃ within a single FA during turnover after subtracting background. In order to measure the intensity of PtdIns(4,5)P₂ or PtdIns(3,4,5)P₃ within FA turnover, the complete lifetimes of FA turnover cycle was observed. In other words, individual FA should be absent both in the beginning and the end of time-lapse series. So, a single FA was selected for measuring the intensity from its appearance to its disappearance. Meanwhile, the intensity of PtdIns(4,5)P₂ or PtdIns(3,4,5)P₃ was measured from the same time frame that the FA was measured and until the last frame when it disappeared. Likewise, the local levels of PtdIns(4,5)P₂ or PtdIns(3,4,5)P₃ were measured around a single FA. The local levels of PtdIns(4,5)P₂ or PtdIns(3,4,5)P₃ were measured at different time points and different focal planes within and around a single FA during assembly and disassembly.

2.2.6. Inhibitor treatment

The PLC inhibitor U73122 was dissolved in DMSO. To prepare a 5mM stock (2.15 ml) the DMSO was added to the 5mg of U73122. 10 µl of inhibitor U73122 was aliquoted into labelled sterile eppendorf tubes in a culture hood then stored at -20°C.

The PI3K inhibitor LY294002 was dissolved in DMSO. To prepare a 5mM stock (2.91 ml) DMSO was added to 5mg of LY294002. 10 µl of inhibitor LY294002 was aliquoted into labelled sterile eppendorf tubes in culture hood then stored at -20°C.

The PI3K inhibitor Wortmannin was dissolved in DMSO. To prepare 5mM stock (2.33 mL) the DMSO was added to 5mg of Wortmannin. 10 µl of inhibitor Wortmannin was aliquoted into labelled sterile eppendorf tubes in a culture hood then stored at -20°C.

DMSO control was used as the same as the inhibitors, i.e. if 4 μ l was added from inhibitor the same amount of DMSO will be added.

2.2.6. I. Co-Transfection

Ibidi dishes were co-transfected with PLC δ 1-PH-GFP and RFF-zyxin as in section 2.3.4. I. The next day, dishes were treated with PLC inhibitor U73122 (1 μ m) or PI3K inhibitor LY294002 (25 μ m) and DMSO was used as control. Live images were immediately taken for each dish by confocal microscopy as in section 2.3.4.II over 10 and 30 min. The effect of inhibitors on the decline of PtdIns(4,5)P₂ during disassembly of FA was measured .

The effect of inhibitors on FA turnover was measured. Image J was used to analysis the FA turnover by measuring the lifetime of individual FA. The time period between appearing and disappearing of FA was accounted. The mean of time for FA was taken and compared with non-treated cells.

2.2.6. II. Live-cell time-lapse microscopy

After coating a 6 well-plate with fibronectin (20 μ g/ml) v/v as in section 2.3.3. I the plate was seeded with MDA-MB-231 cells. The next day, new media was used with different concentrations of U73122 (0.5 μ M, 1 μ M, 2 μ M and 3 μ M) or Wortmannin (0.1 μ M, 0.2 μ M, 1 μ M and 2 μ M) or LY294002 (7 μ M, 14 μ M, 24 μ M and 50 μ M). DMSO was used as control for each inhibitor. Old media was aspirated and 2ml of media in each well of plate was added with appropriate concentration of inhibitor. The plate was sealed with parafilm and a hole was then made at the edge of plate to insert the CO₂ supply needle. The heater was set at 37°C 2 hours before using time-lapse. The plate was placed on the stage of the Nikon Tie time-lapse microscope and a 10x objective was used. The ND

setting of images was set up (ND acquisition was used to setup the experiment through adding a time phase, interval and duration and number of loops if its require) and the camera was chosen as live-fast(use to capture live images with normal high quality). X/Y was selected (to add XY position for move stage to selected point which enable freely move between the points through clicking on them in the XY box) and perfect focus system (PFS) was used (which is used to extremely reduce axial focus change during long-term imaging) and E100 was changed to L100, then 5 spots were taken for each well. The images were taken over 24 hours with intervals of 15 minutes. ImageJ was used to analyse the cell migration in non-treated and treated cells. The speed of cell migration was measured by using the ImageJ-MTrackJ plugin. 30 cells of each well was measured by using equation: Speed of cell= Total length of cell (μm).

2.2.6. III. Wound Healing Assay

A 6-well plate was coated with fibronectin as in section 2.2.4. I then seeded with MDA-MB-231 cells. After the cell became 90 % confluent the cell monolayer was gently and slowly scratched in the culture hood using a sterile 500 μl tip to create a gap across the well. The next day, new media was used with different concentrations of U73122 (0.5 μM , 1 μM , 2 μM and 3 μM) or Wortmannin (0.1 μM , 0.2 μM , 1 μM and 2 μM) or LY294002 (7 μM , 14 μM , 24 μM and 50 μM). DMSO was used as control for each inhibitor. Old media was aspirated and 2ml of media in each well of plate was added with appropriate concentration of inhibitors. The image was taken in 0 time and 24 hours by an inverted microscope (AXIO, ZEISS). ImageJ was used to measure the wound healing by using equation: % wound closure = Average area at 0time- average area of 24h time/ average area at 0 time x 100.

2.2.7. Immunoprecipitation and western blotting (IP and WB)

2.2.7. I. Cell lysate preparation

MDA-MB-231 cells were grown in a 75 cm² flask until they became confluent (90%). The old media was removed and 5ml of chilled PBS was added into the flask to wash cells. After adding 5ml of chilled PBS the cells were scraped and then transferred into the labelled 50ml tube. The labelled tube was centrifuged at 4°C 1500g for 15 minutes. After discarding supernatant the protease inhibitor cocktail (PIC) +RIPA (1:100) was added to the pellet. A 21 gauge needle was used to shear DNA through passing the lysate several times. The suspension was left on ice for 30 minutes then was transferred into 1.5 ml eppendorf tube and centrifuged at 4°C 13000g for 15 minutes. The supernatant was transferred into a new 1.5 ml eppendorf tube and stored in a freezer.

2.2.7. II. Bradford protein assay

The cell lysate was collected, the Bradford protein assay was used to measure the concentration of proteins. A 96 well plate was used and 195µl of Bradford reagent was added to the first column and used as blank (A 1 - H 1). 195 µl of Bradford reagent plus 5µl of BSA with different concentrations (25-2000 µg/ml) were added in duplicate wells. The concentration of a standard protein was measured through reading the absorption curve and R² was (0.95-0.99). Then, 195 µl Bradford reagent plus 5µl of lysate were added to triplicate wells. The plate was shaken for 30 seconds and then placed to the plate reader (Emax molecular devices) to read the concentration of proteins in µg/ml by reading the absorbency at 595nm.

2.2.7. III. Immunoprecipitation

After measuring the concentration of proteins by using Bradford reagent assay. 400 μ l of the lysate were incubated with primary antibody using mouse anti-talin or anti-vinculin or anti-paxillin or anti-actin antibodies. Then, the labelled eppendorf tubes were rotated at 4°C overnight to precipitate specific FA proteins. Protein A/G agarose beads were prepared according to the manufacturers instructions. 100 μ l of re-suspension beads was added each sample and incubated in cold room for 2 hours. After incubation, the samples were centrifuged at 2000 rcf for 1 minute then washed three times with 0.3ml RIPA buffer. After washing the pellets were seen in the bottom of tubes and the supernatant was discarded. 100 μ l of 5x SDS buffer was added to the pellet and boiled at 95°C. The samples were centrifuged for 1 minute at 4°C and the supernatant was collected and transferred into new labelled tubes. The collected supernatant either use immediately for western blotting or keep at -20°C.

2.2.7. IIII. Western blotting

After IP, western blotting was used to detect the binding of PI3K or PLC. 100 μ l of samples were mixed with 25 μ l 5x v/v of loading buffer and 5 μ l of β -mercaptoethanol v/v and then boiled for 3-4 minutes at 90 °C. 12 % and 10% SDS-PAGE gels were prepared and the running buffer was added to the tank. The samples were loaded in the stacking gel. 0.06 A and 180 V were used for 2 gels for around 1 hour. After separation of proteins, the gels were transferred to transfer buffer for 20 minutes. Meanwhile, PVDF (polyvinylidene difluoride) membrane was cut in (8* 8 cm) and submerged in methanol for 30 seconds then washed in distilled water. Filter paper was cut in (8* 8 cm) and then submerged in transfer buffer. The semi-dry transfer machine (Bio Rad) was used and

three filter papers were placed on the machine and transfer membrane was put on the top of filter papers then the gel was put on the top of the membrane. An extra three filter papers were placed on the top of the gel and the gel was transferred for 1.5 hour at 250V and 0.1A. After transferring the proteins, the membrane was blocked using 5%BSA for 1 hour with gentle shaking. After blocking the membrane was washed three times with 1x TBST, each wash 10 minutes. The membrane was incubated with primary antibody rabbit anti-PI3K110 α , anti-Kinase p85 or PLC β 1 (1: 1000) in 2% BSA then incubated overnight in the cold room. The next day, the membrane was washed three times with 1x TBST, each wash 10 minutes. HRP secondary antibodies were added 1:2000 in 2% BSA to the membrane in the bag and incubated with shaking for 1 hour. Then, the membrane was washed with 1x TBST each wash 10 minutes. 2ml of ECL prime detection (1ml of the solution and 1 ml of solution B) was used for 1 minute and kept in the dark. The bands were detected by Image Quant LAS 4000 minim (GE Healthcare) to see the protein-protein interaction. Reverse IP was also used to confirm the interaction. The steps of reverse IP are similar to IP but the antibodies are inverse.

2.3. Statistical analysis

Statistical significance was determined by one-way analysis of variance after Tukey's or Dunn's multiple comparisons for three or more variables. GraphPad Prism 5 software (GraphPad Software, San Diego, CA) was used to accomplish all comparisons. All results were made from at least three independent experiments in triplicate (n=3), and P values < 0.05 were considered statistically significant.

Chapter 3. Spatial organisation between PtdIns(4,5)P₂ or PtdIns(3,4,5)P₃ and FAs

3.1. Introduction

In order to understand the possible role of PtdIns(4,5)P₂ and PtdIns(3,4,5)P₃ within a single FA during cell migration it is important to study their spatial co-localisation.

All molecules of cells are systematically organised and highly spatially distributed. Many of these molecules are responsible for the organising of cellular signalling functions (Ruth, 2013). The distribution of lipids and proteins in various forms and certain areas gives their spatial organisation more efficiency and specificity to perform their interactions (Susann et al., 2016, Spira et al., 2012). Therefore, it is essential to study the spatial organisation between proteins in order to understand how they regulate cellular functions, such as FA turnover (Ruth, 2013).

Fluorescence microscopy is an important technique that is used to understand spatial organisation (Pageon et al., 2016, Ruth, 2013) through quantifying the co-localisation between protein interactions in defined regions of the cell, such as FAs and lipid compositions (Ruth, 2013, Wu et al., 2010, Dunn et al., 2011, van Zanten and Mayor, 2015).

It has been shown that FAs are extremely spatially organised to perform their function and interact with other signals in the PM (Kanchanawong et al., 2010, Giannone, 2015). The FAs region consists of many proteins distributed in the form of layers depending on their nanoscale spatial organisation. The first layer is the integrin signalling layer which is the nearest to the ECM containing paxillin, FAK and integrin cytoplasmic tails and

forms around 0-30 nm from the PM. The second layer is the force transduction layer that transmits the signals from actin to integrin and containing vinculin and talin and forms around 30-60 nm of PM. The third layer is the actin regulatory layer containing zyxin and α -actinin and forms around 60nm of PM. Integrin and actin are separated by FA core region which forms around 40-60nm in depth (Morimatsu et al., 2015, Kanchanawong et al., 2010). The spatial interaction of FAs plays roles, including a signal transduction (Morimatsu et al., 2015), anchoring the cell to the ECM and responding to mechanical and physical forces (Butcher et al., 2009, Geiger et al., 2009, Hoffman et al., 2011, Jaalouk and Lammerding, 2009).

Although PtdIns(4,5)P₂ and PtdIns(3,4,5)P₃ form only a small fraction of the membrane, they are responsible for temporal and spatial regulation of many signalling pathways. van den Bogaart et al. (2011) showed that PtdIns(4,5)P₂ localised in distinct nanoscale regions within the cell membrane of Pheochromocytoma (PC12) cells which had a size around 73nm. Wang and Richards (2012) also showed that PtdIns(4,5)P₂ localised in distinct nanoscale regions with a size around 64.5 ± 28 nm, whereas PtdIns(3,4,5)P₃ localised in regions with a size around 125.6 ± 22 nm in membrane domains of PC12 cells. This may mean that an enrichment of PtdIns(4,5)P₂ and PtdIns(3,4,5)P₃ are restricted to specific regions. Possibly, many signalling pathways in these distinct regions are regulated by PtdIns(4,5)P₂ and PtdIns(3,4,5)P₃ through recruitment many kinases by PtdIns(4,5)P₂ and PtdIns(3,4,5)P₃ to these specific sites to perform their functions (Wang and Richards, 2012).

PIP1 and PI3K isoforms play a role in the regulation of FAs by recruiting proteins to FA sites through the production of PtdIns(4,5)P₂ and PtdIns(3,4,5)P₃ in the cell membrane

(Chao et al., 2010, Legate et al., 2011, Wu et al., 2011, Nader et al., 2016, Rubashkin et al., 2014). It has also been shown that PIPK1 and PI3K localise at the leading edge of the cell and play an important role in cell migration (Bae et al., 2010, Sharma et al., 2008, Thapa and Anderson, 2012, Falke and Ziemba, 2014). However, these studies did not directly examine the role of PtdIns(4,5)P2 and PtdIns(3,4,5)P3 but instead are examined indirectly their role through the enzymes that make them.

MDA-MB-231 cells were used in this thesis as it is a metastatic cancer cell line and highly motile (Cailleau et al., 1974). In this chapter, PLC δ 1-PH and Btk-PH GFP or mCherry were used as biosensors to monitor changes or differences in the local generation of PtdIns(4,5)P2 and PtdIns(3,4,5)P3 in the cell membranes. PLC δ 1-PH and Btk-PH GFP or mCherry bind specifically with PtdIns(4,5)P2 and PtdIns(3,4,5)P3 respectively (Manna et al., 2007, Varnai et al., 1999, Stauffer et al., 1998). In order to know whether PtdIns(4,5)P2 and PtdIns(3,4,5)P3 are interacting with FAs, the spatial organisation of PtdIns(4,5)P2 and PtdIns(3,4,5)P3 has been directly investigated within single FAs. The aim of the experiments is to analyse the spatial co-localisation between PtdIns(4,5)P2 or PtdIns(3,4,5)P3 and single FAs. This study has been performed by observing the spatial interaction between PtdIns(4,5)P2 or PtdIns(3,4,5)P3 and FA proteins using confocal microscopy and quantitative co-localisation analysis. This chapter aimed to study this as well as studying the effect of PI3K and PLC inhibitors on co-localisation between PtdIns(4,5)P2 or PtdIns(3,4,5)P3 and FA proteins.

3.2 Results

3.2.1 Visualisation of PtdIns(4,5)P₂ and PtdIns(3,4,5)P₃ by PLC δ 1-PH-GFP or mCherry and Btk-PH-GFP or mCherry biosensors respectively in fixed and live cells.

In order to be able to further investigate the role of PI(PtdIns(4,5)P₂ and PtdIns(3,4,5)P₃) directly in MDA-MB-231 cells, PLC δ 1- PH-GFP or mCherry and Btk-PH-GFP or mCherry were used as biosensors to monitor changes or differences in the local generation of PI(PtdIns(4,5)P₂ and PtdIns(3,4,5)P₃) in the cell membranes.

MDA-MB-231 cells were seeded on a variety of surfaces (gelatine 0.2%, fibronectin 20 μ g/ml and collagen 2mg/ml), then transfected with Btk-PH-GFP or mCherry and PLC δ 1-PH-GFP or mCherry biosensors. Later, the cells were fixed with paraformaldehyde after stimulating PtdIns(3,4,5)P₃ production with epidermal growth factor (EGF) (100 ng/ml) for 5 minutes, then images were visualised by confocal laser scanning microscopy. Our results showed that PLC δ 1-PH-GFP or mCherry was localised at the cell membrane when transiently expressed in MDA-MB-231 cells (Figure 3.1). Btk-PH-GFP or mCherry was sometimes localised at the cell membrane but there was also a large amount of fluorescence present in the cytosol and nucleus (Figure 3.1). Likewise, in live images the results were similar (Figure 3.2).

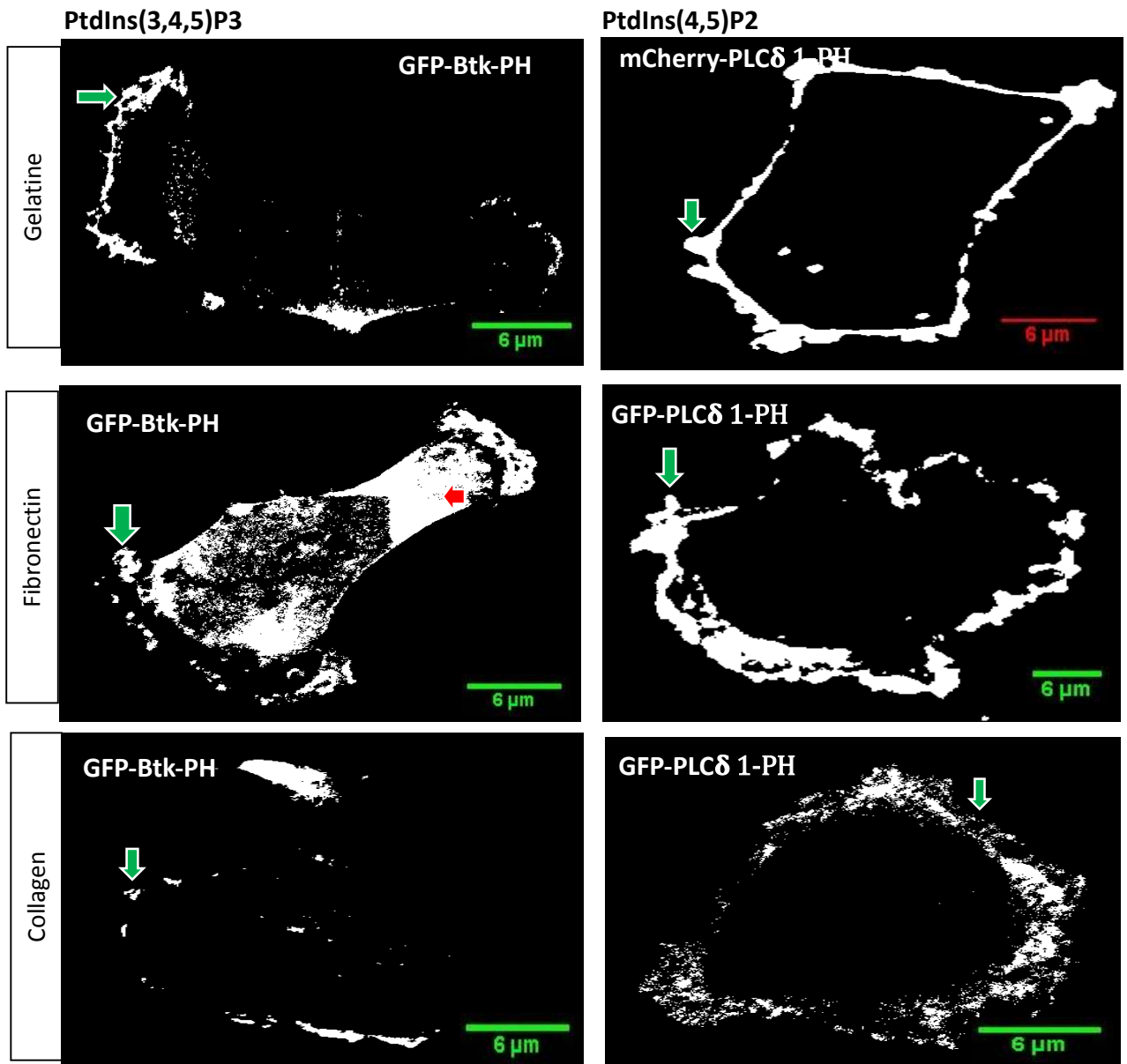


Figure (3.1): visualisation of PtdIns(4,5)P2 and PtdIns(3,4,5)P3 on the variety of surfaces in fixed cells : Confocal images of MDA-MB-231 cells expressing the PLC δ 1-GFP or mCherry and Btk-PH-GFP were used as biosensors to identify PtdIns(4,5)P2 and PtdIns(3,4,5)P3 lipids in the plasma membrane of MDA-MB-321 cells respectively. MDA-MB-321 cells were seeded on the variety of surfaces (gelatine 0.2%, fibronectin 20 μ g/ml and collagen 2mg/ml). Then, cells were transfected with PLC δ 1-GFP or mCherry and Btk-PH-GFP or mCherry after stimulating PtdIns(3,4,5)P3 production with EGF (100 ng/ml) for 5 minutes. Then, cells were fixed with paraformaldehyde to visualise PtdIns(4,5)P2 and PtdIns(3,4,5)P3. The green arrow indicates the localisation of PtdIns(4,5)P2 and PtdIns(3,4,5)P3 on the cell membrane and the red arrow indicates the localisation of PtdIns(3,4,5)P3 in the cytosol. Three independent experiments were performed, representative pictures are shown.

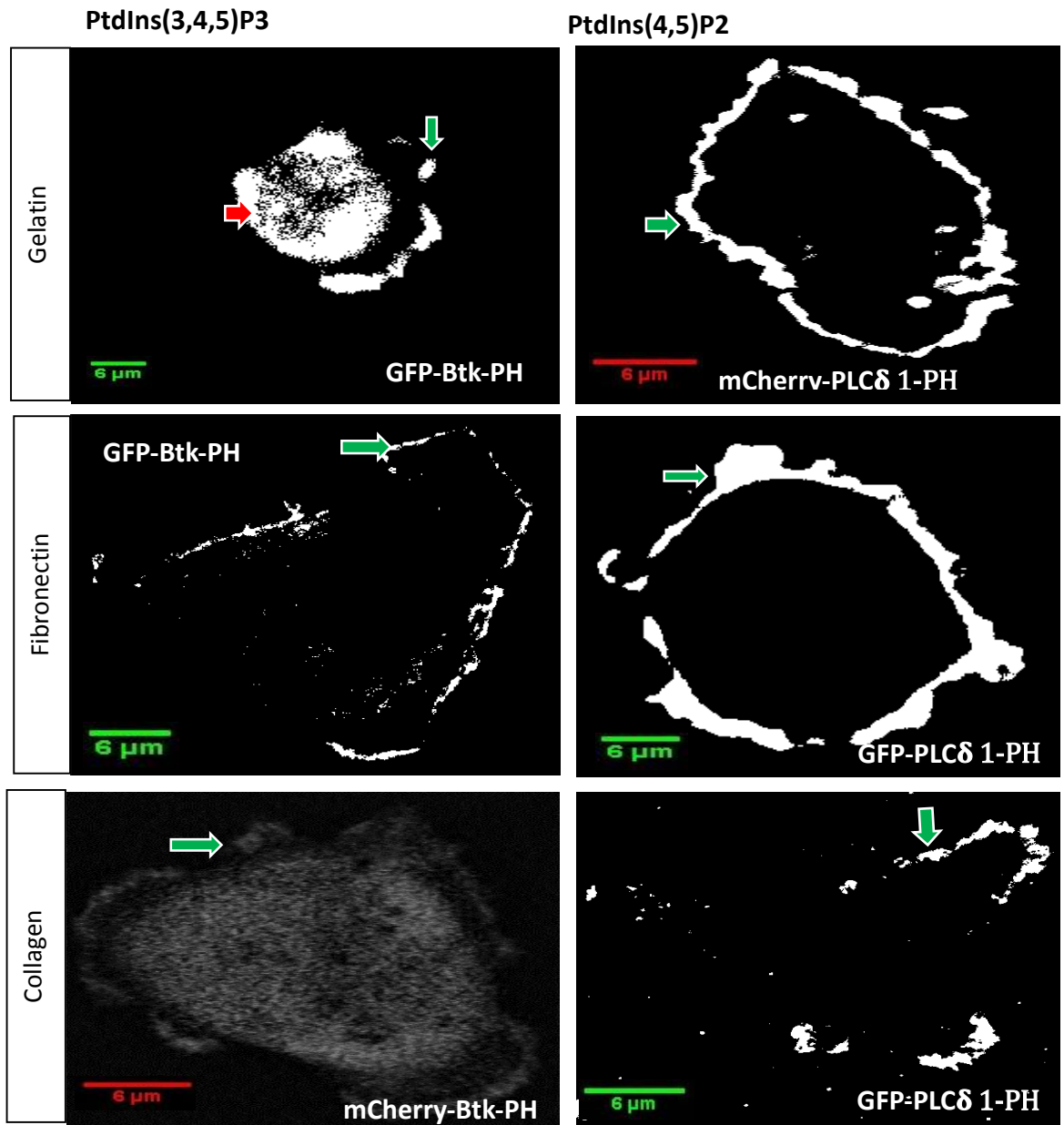


Figure (3.2): Visualisation of PtdIns(4,5)P2 and PtdIns(3,4,5)P3 on the variety of surfaces in live cells : Confocal images of MDA-MB-231 cells expressing the PLCδ1-GFP or mCherry and Btk-GFP or mCherry were used as biosensors to identify PtdIns(4,5)P2 and PtdIns(3,4,5)P3 lipids in the plasma membrane of MDA-MB-321 cells respectively. MDA-MB-231 cells were seeded on the variety of surfaces (gelatine 0.2%, fibronectin 20μg/ml and collagen 2mg/ml). Then, cells were transfected with PLCδ1-GFP or mCherry and Btk-PH-GFP or mCherry after stimulating PtdIns(3,4,5)P3 production with EGF (100 ng/ml) for 5 minutes. Confocal live images were maintained at 37°C and CO₂. The green arrow indicates the localisation of PtdIns(4,5)P2 and PtdIns(3,4,5)P3 on the cell membrane and the red arrow indicates the localisation of PtdIns(3,4,5)P3 in the cytosol. Three independent experiments were performed, representative pictures are shown.

3.2.2 Effect of Btk-PH-GFP overexpression

MDA-MB-231 cells were seeded and transfected as in Section 3.2.1. Our results showed that the cells that expressed low levels of Btk-PH-GFP the fluorescence was predominantly localised to the cell membrane (Figures 3.3A & 3.4A). While the cells that expressed high levels of Btk-PH-GFP there was localisation in the cytosol and cell membrane (Figures 3.3C and 3.4C). The fluorescence intensity in the cell membrane and cytosol were measured to compare the fluorescence intensity between them. In cells that expressed low levels of Btk-PH-GFP the peak of fluorescence intensity in the cell membrane was around (150 levels of pixel intensity), while in the cytosol was around (10 levels of pixel intensity). This refers that localisation of Btk-PH-GFP in cell membrane higher than in the cytosol (Figures 3.3B & 3.4B). In cells that expressed high levels of Btk-PH-GFP the peak of intensity in the cell membrane was around (100 levels of pixel intensity), while in the cytosol was around (125 levels of pixel intensity). This also refers that localisation of Btk-PH-GFP in the cytosol higher than in the cell membrane (Figures 3.3D & 3.4D).

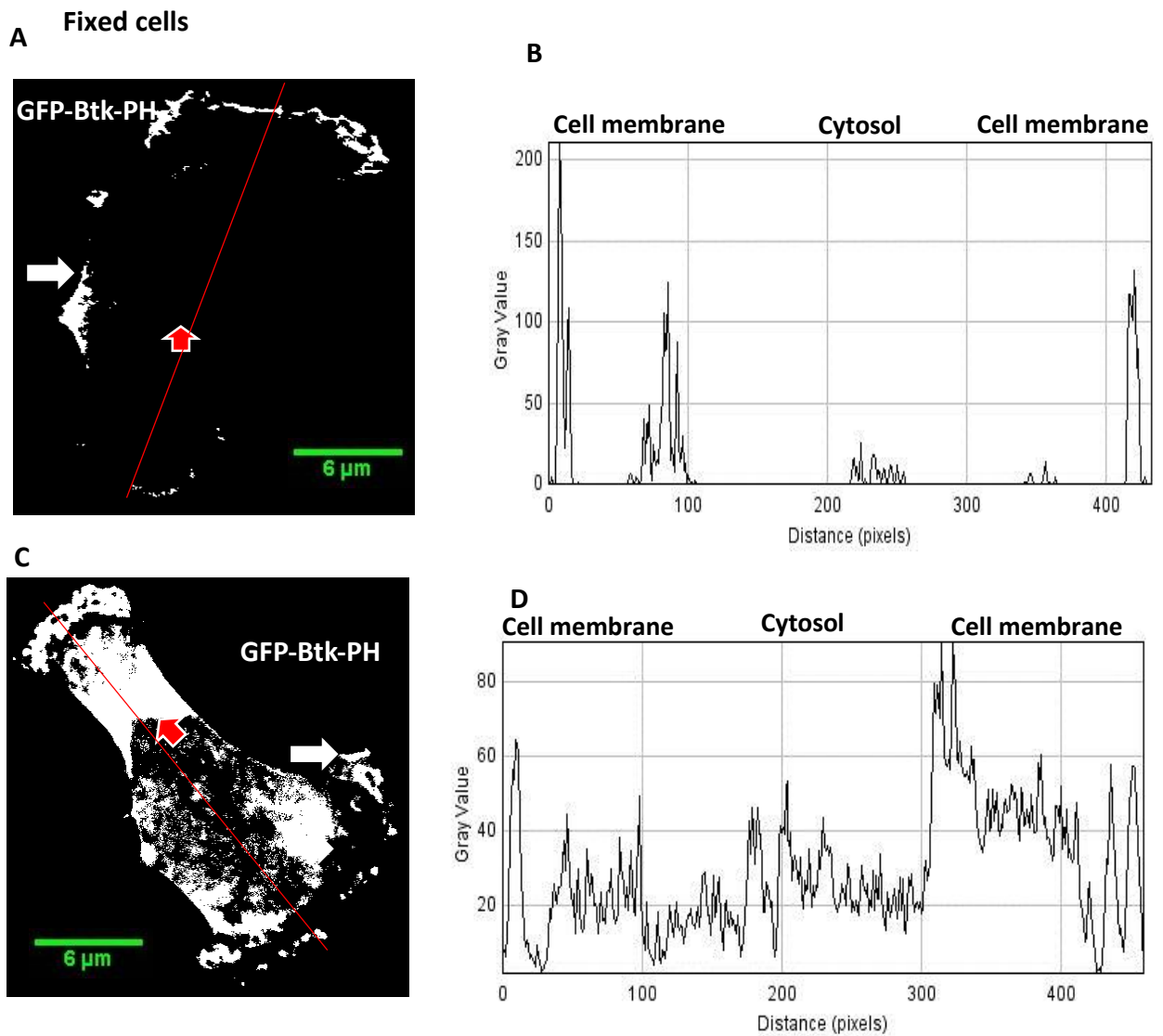


Figure (3.3): Effect of Btk-PH-GFP overexpression in the fixed cell. Confocal images of MDA-MB-231 cells that were transfected with Btk-PH-GFP for 24 hour, A&B) At low expression levels, the peak of intensity in the cell membrane was higher than in the cytosol. C&D) At high expression levels, the peak of intensity in the cell membrane and cytosol was similar. The white arrow indicates the localisation of PtdIns(3,4,5)P3 in the cell membrane and the red arrow indicates the localisation of PtdIns(3,4,5)P3 in the cytosol. The red line across cell refers to the measurement of intensity in the cell membrane and cytosol of the cell. Data are a representative of three independent experiments in which 10 cells were measured.

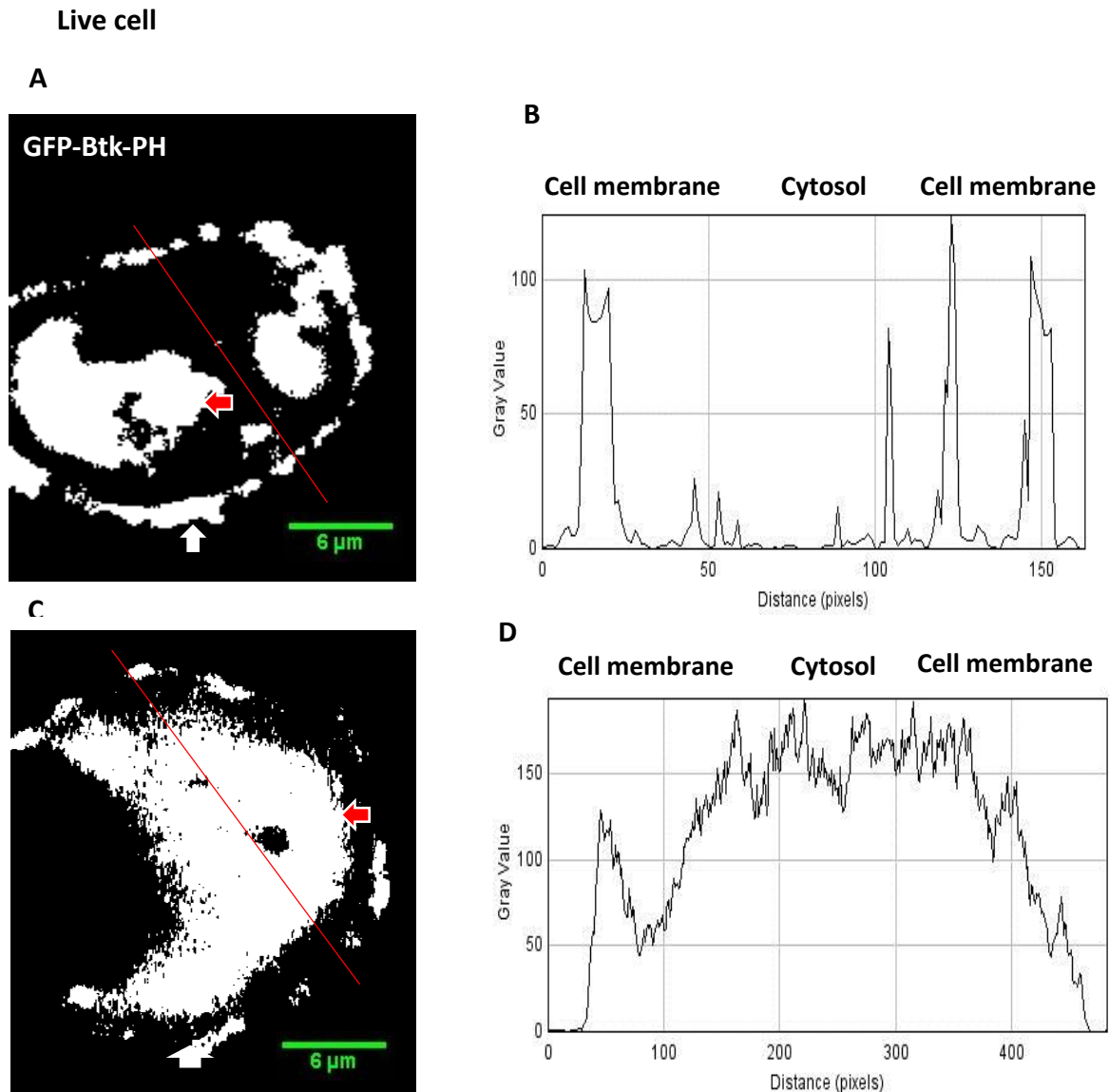


Figure (3.4): Effect of Btk-PH-GFP overexpression in live cells. Confocal images of MDA-MB-231 cells that were transfected with Btk-PH-GFP for 24 hour. **A&B)** At low expression levels, the peak of intensity in the cell membrane was higher than in the cytosol. **C&D)** At high expression levels, the peak of intensity in the cell membrane and cytosol was similar. The white arrow indicates the localisation of PtdIns(3,4,5)P3 on the cell membrane and the red arrow indicates the localisation of PtdIns(3,4,5)P3 in the cytosol. Confocal live images were maintained at 37°C and CO₂. The red line across cell refers to the measurement of intensity in the cell membrane and cytosol of the cell. Data are a representative of three independent experiments in which 10 cells were measured.

3.2.3. Comparison between antibodies and PH-domains to detect PtdIns(3,4,5)P3 and PtdIns(4,5)P2

MDA-MB-231 cells were transfected with PLC δ 1-PH-GFP or mCherry and Btk-PH-GFP or mCherry biosensors to visualise PtdIns(4,5)P2 and PtdIns(3,4,5)P3 respectively. Later, the PtdIns(3,4,5)P3 production was stimulated by EGF (100 ng/ml) for 5 minutes then fixed with paraformaldehyde. The results showed that PLC δ 1-PH-GFP or mCherry and Btk-PH-GFP or mCherry were localised in the cell membrane when transiently expressed in MDA-MB-231 cells (Figures 3.5A & 3.6A). Likewise, MDA-MB-231 cells were seeded on fibronectin 20 μ g/ml, then fixed with paraformaldehyde and stained with anti-PtdIns(4,5)P2 and anti-PtdIns(3,4,5)P3 antibodies. The results showed that both anti-PtdIns(4,5)P2 and anti-PtdIns(3,4,5)P3 antibodies were localised in the cytosol and cell membrane (Figure 3.5C & 3.6C).

The fluorescence intensity in the cell membrane and cytosol of cell were measured to compare between them. The data showed that the peak of fluorescence intensity of PLC δ 1-PH-GFP in the cell membrane was around (300 levels of pixel intensity) and in the cytosol which was (0 levels of pixel intensity) (Figure 3.6 B). While, the peak of fluorescence intensity of anti-PtdIns(4,5)P2 antibody in both cell membrane and cytosol was around (250 levels of pixel intensity) (Figure 3.6 D). This refers that PLC δ 1-PH-GFP has more specificity to bind with and detect PtdIns(4,5)P2.

The peak of intensity of Btk-PH-GFP in the cell membrane was around (170 levels of pixel intensity) and in the cytosol which was around (20 levels of pixel intensity) (Figure 3.7 B). While the peak of intensity of anti-PtdIns(3,4,5)P3 antibody in both cell membrane and cytosol was around (60 levels of pixel intensity) (Figure 3.5 D). This also refers that Btk-PH-GFP has more specificity to bind with and detect PtdIns(3,4,5)P3.

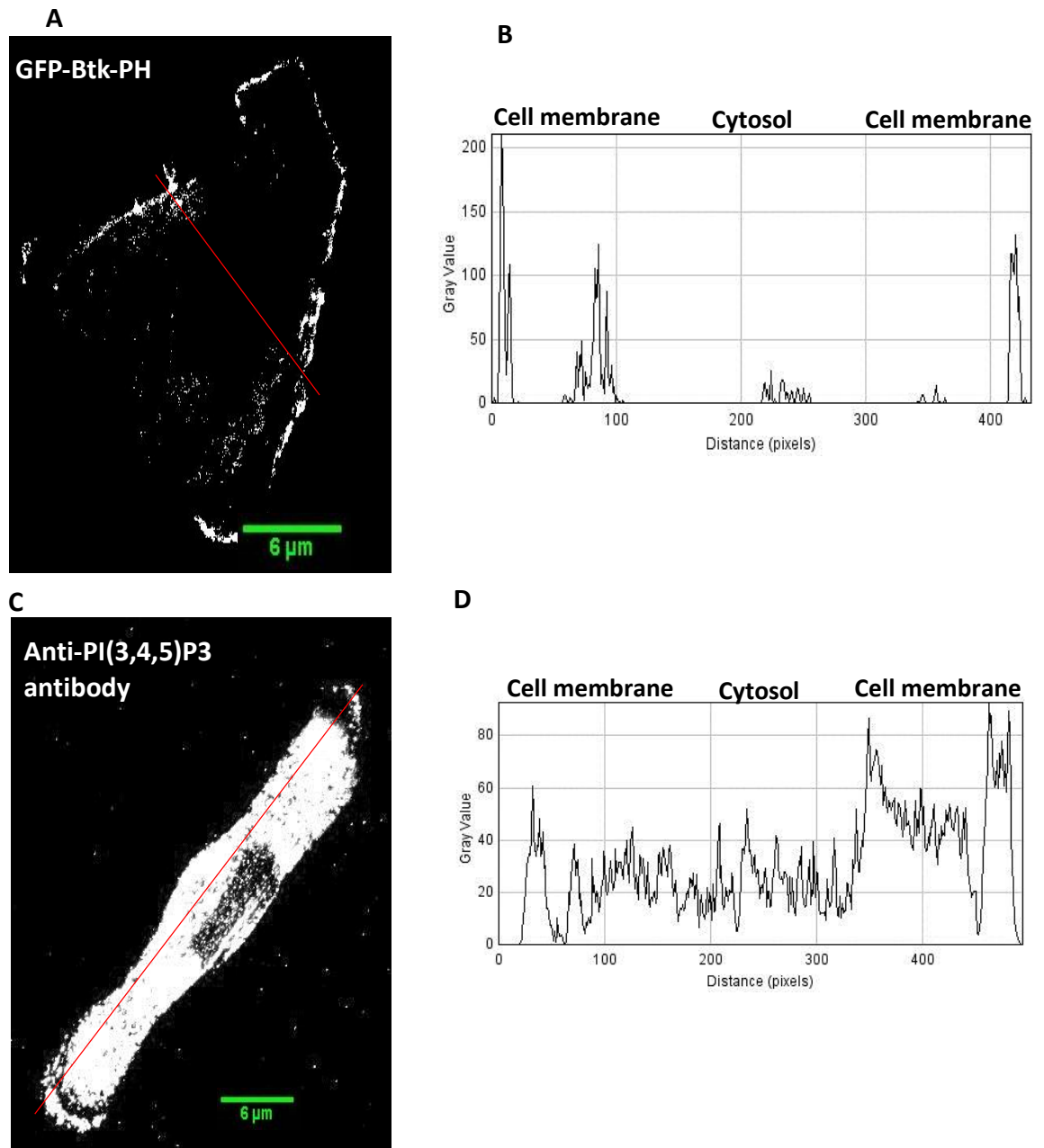


Figure (3.5): Quantification of PtdIns(3,4,5)P3 localisation. A) MDA-MB-231 cells were transfected with Btk-PH-GFP and fixed with paraformaldehyde. **B)** Quantification of the intensity in the cell membrane and cytosol. The peak of intensity in the cell membrane was higher than in the cytosol. **C)** MDA-MB-231 cells were stained with anti-PtdIns(3,4,5)P3 antibody and then fixed with paraformaldehyde. **D)** Quantification of the intensity in the cell membrane and cytosol of the cell. The peak of intensity in the cell membrane and cytosol was similar. Data are representative of three independent experiments in which 10 cells were measured.

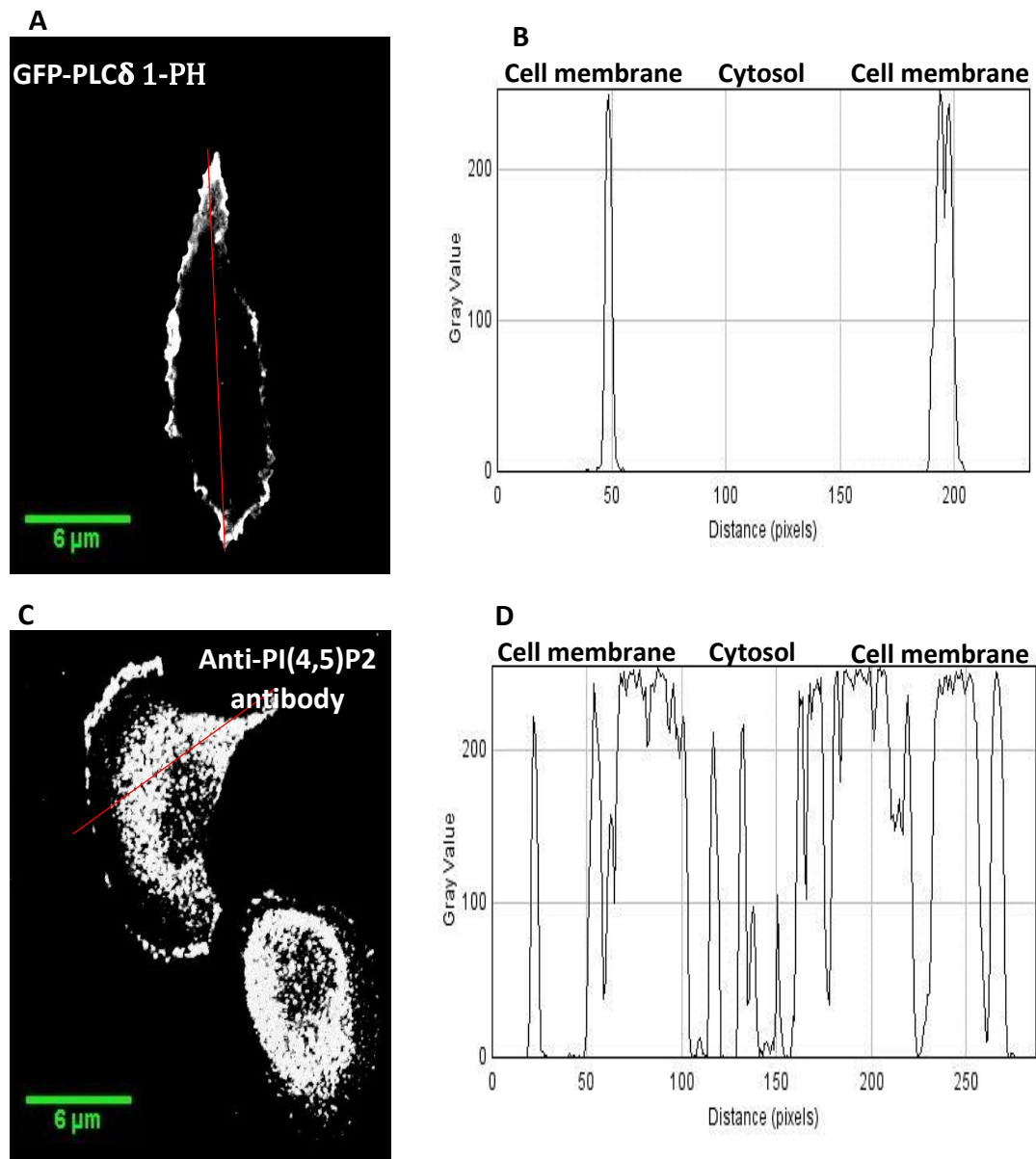


Figure (3.6): Quantification of PtdIns(4,5)P2 localisation. **A)** MDA-MB-231 cells were transfected with PLC δ 1-PH-GFP and fixed with paraformaldehyde. **B)** Quantification of intensity in the cell membrane and cytosol of the cell. The peak of intensity was only in the cell membrane. **C)** MDA-MB-231 cells were stained with anti-PtdIns(4,5)P2 antibody and fixed with paraformaldehyde. **D)** Quantification of intensity in the cell membrane and cytosol of the cell. The peak of intensity in the cell membrane and cytosol was similar. Data are representative of three independent experiments in which 10 cells were measured.

3.2.4. Spatial regulation of PtdIns(4,5)P2 within a single FA in live and fixed cells.

MDA-MB-231 cells were plated on gelatine 0.2%, and transfected with PLC δ 1-PH-GFP. The cells were fixed with paraformaldehyde and immunostained for anti-paxillin, talin, vinculin and FAK antibody and then stained with Alexa Fluor secondary antibody (Figure 3.7) to visualise the spatial interaction between PtdIns(4,5)P2 and FAs. In live cells, MDA-MB-231 cells were plated on (fibronectin 20 μ g/ml and collagen 2mg/ml) and then co-transfected with PLC δ 1-PH- mCherry (red) & paxillin-GFP (green), or PLC δ 1-PH-GFP & zyxin-RFP (red) (Figure 3.7). The Z-Stacking-single slice was performed through taking different slices to record the entire cell membrane from the bottom to the top. Then, single slice was selected to determine an accurate co-localisation point between a single FA and PtdIns(4,5)P2. Spatial co-localization was measured between PtdIns(4,5)P2 and FAs. Our results showed that co-localisation values were moderate in live and fixed cells (Figures 3.8 & 3.9). In fixed cell, the co-localisation values of PtdIns(4,5)P2 with talin, vinculin and paxillin were 0.60 ± 0.05 , 0.56 ± 0.04 and 0.58 ± 0.037 respectively. In live cell, The co-localisation values of PtdIns(4,5)P2 with FAK, paxillin and zyxin were 0.55 ± 0.04 , 0.57 ± 0.06 and 0.54 ± 0.07 respectively as summarised in table3.1.

The co-localisation values of PtdIns(4,5)P2 with paxillin on collagen, fibronectin and gelatine were 0.61 ± 0.05 , 0.55 ± 0.04 and 0.61 ± 0.03 respectively as summarised in table 3.2.

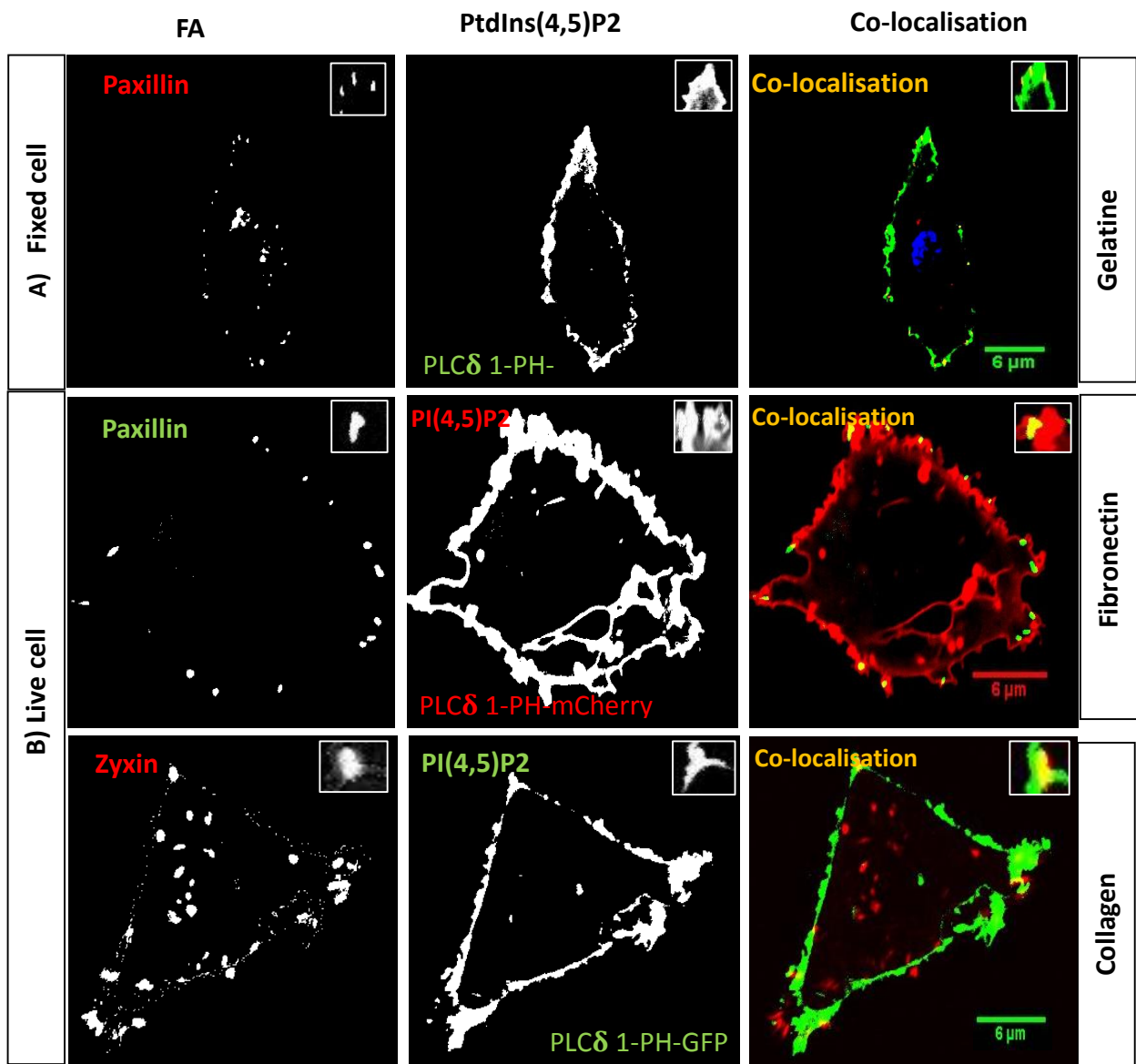


Figure (3.7): Spatial co-localisation between PtdIns(4,5)P2 and a single FA in MDA-MB-231 cells on the variety of surfaces . A) MDA-MB-231 cells were plated on gelatine 0.2%, and transfected with PLC δ 1-PH-GFP, then fixed and immunostained for paxillin, talin, vinculin and FAK (red) to visualise the spatial interaction between PtdIns(4,5)P2 and FAs . **B)** MDA-MB-231 cells were plated on (fibronectin 20 μ g/ml and collagen 2mg/ml) and co-transfected with PLC δ 1-PH-mCherry (red) & paxillin-GFP(green), or PLC δ 1-PH-GFP(green) & zyxin-RFP(red). The highlighted areas show a magnification of the spatial co-localisation region between PtdIns(4,5)P2 and a single FA. Three independent experiments were performed, Representative pictures are shown. Scale bars = 6 μ m.

Table 3.1: Data showing co-localisation values \pm standard deviation (SD) between PtdIns(4,5)P2 and FAs.

	Talin	Vinculin	Paxillin	FAK	Paxillin	Zyxin
PtdIns(4,5)P2	0.60 \pm 0.05	0.56 \pm 0.04	0.58 \pm 0.037	0.55 \pm 0.04	0.57 \pm 0.06	0.54 \pm 0.07

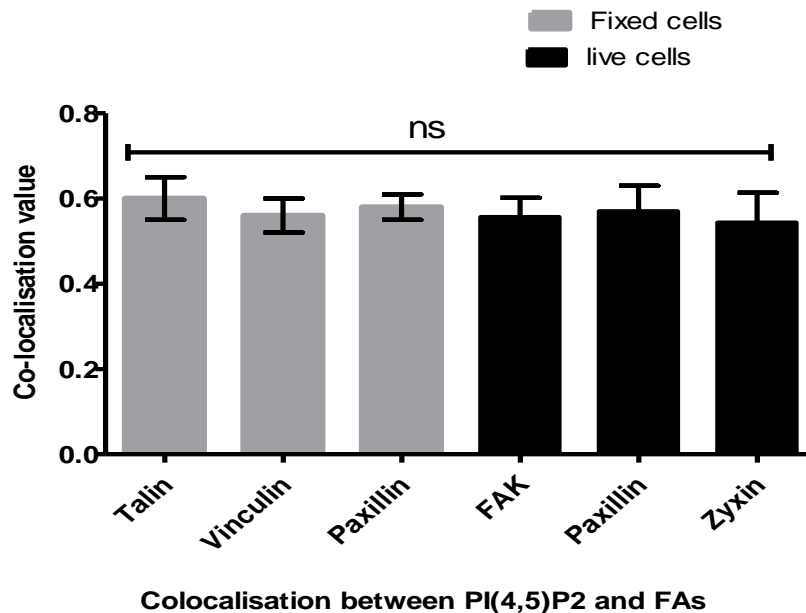
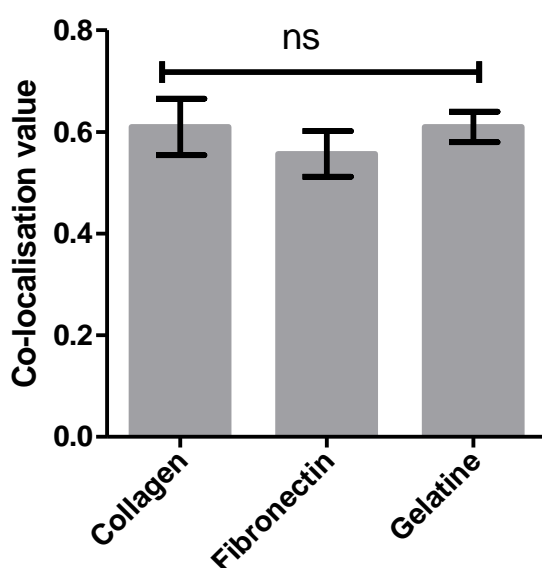


Figure (3.8). Quantification of the spatial co-localisation of PtdIns(4,5)P2 within single FA. Spearman's (rho) correlation coefficient analysis was used to measure co-localisation value between PtdIns(4,5)P2 and FAs. **Fixed cells**, the co-localisation values of (talin, vinculin and paxillin) and PtdIns(4,5)P2 were moderate co-localisation. **Live cells**, co-localisation values of FAK or Zyxin or paxillin and PtdIns(4,5)P2 were also a moderate co-localisation. Statistical analysis was performed by One-way ANOVA with Tukey's Multiple Comparison Test. Non-significant differences between co-localisation values at $P \leq 0.05$. Data is a representative of the means \pm SD of three independent experiments in which $n = 30$ cells were measured, and number of a single FA= 10 for each cell.

Table 3.2: Data showing co-localisation values \pm SD between PtdIns(4,5)P2 and paxillin on collagen, fibronectin and gelatine

	PI(4,5)P2 + Paxillin
Collagen	0.61 \pm 0.05
Fibronectin	0.55 \pm 0.04
Gelatine	0.61 \pm 0.03



Co-localisation between PI(4,5)P2 and paxillin

Figure (3.9). Quantification of spatial co-localisation between PtdIns(4,5)P2 and paxillin. Spearman's (ρ) correlation coefficient analysis was used to measure co-localisation value between PtdIns(4,5)P2 and paxillin. Pooled data show co-localisation values between PtdIns(4,5)P2 and paxillin on different surfaces. Statistical analysis was performed by One-way ANOVA with Tukey's Multiple Comparison Test. Non-significant differences between co-localisation values at $P \leq 0.05$. Data is a representative of the means \pm SD of three independent experiments in which $n = 20$ cells were measured, and number of a single FA = 10 for each cell.

3.2.5. Spatial regulation of PtdIns(3,4,5)P3 within a single FA in live and fixed cells.

MDA-MB-231 cells were plated on gelatine 0.2%, and transfected with Btk-PH-GFP. The cells were fixed with paraformaldehyde and immunostained for anti-paxillin, talin, vinculin and FAK antibody and then stained with Alexa Fluor secondary antibody (Figure 3.10) to visualise the spatial interaction between PtdIns(3,4,5)P3 and FAs. In live cells, MDA-MB-231 cells were plated on (fibronectin 20µg/ml and collagen 2mg/ml) and then co-transfected with Btk-PH- mCherry (red) & paxillin-GFP (green), or Btk-PH- GFP (green) & zyxin-RFP (red) (Figure 3.10). The Z-Stacking-single slice was performed through taking different slices to record the entire cell membrane from the bottom to the top. Then, single slice was selected to determine an accurate co-localisation point between a single FA and PtdIns(3,4,5)P3. Spatial co-localization was measured between PtdIns(3,4,5)P3 and FAs. Our results showed co-localisation values were moderate (Figures 3.11 &12). In fixed cell, the co-localisation values of PtdIns(3,4,5)P3 with talin, vinculin and paxillin were 0.52 ± 0.04 , 0.51 ± 0.03 and 0.50 ± 0.01 respectively. In live cell, the co-localisation values of PtdIns(3,4,5)P3 with FAK, paxillin and zyxin were 0.49 ± 0.03 , 0.44 ± 0.04 and 0.48 ± 0.07 respectively as summarised in tables 3.3.

The co-localisation values of PtdIns(3,4,5)P3 with paxillin on collagen, fibronectin and gelatine were 0.52 ± 0.08 , 0.49 ± 0.07 and 0.48 ± 0.08 respectively as summarised in tables 3.4.

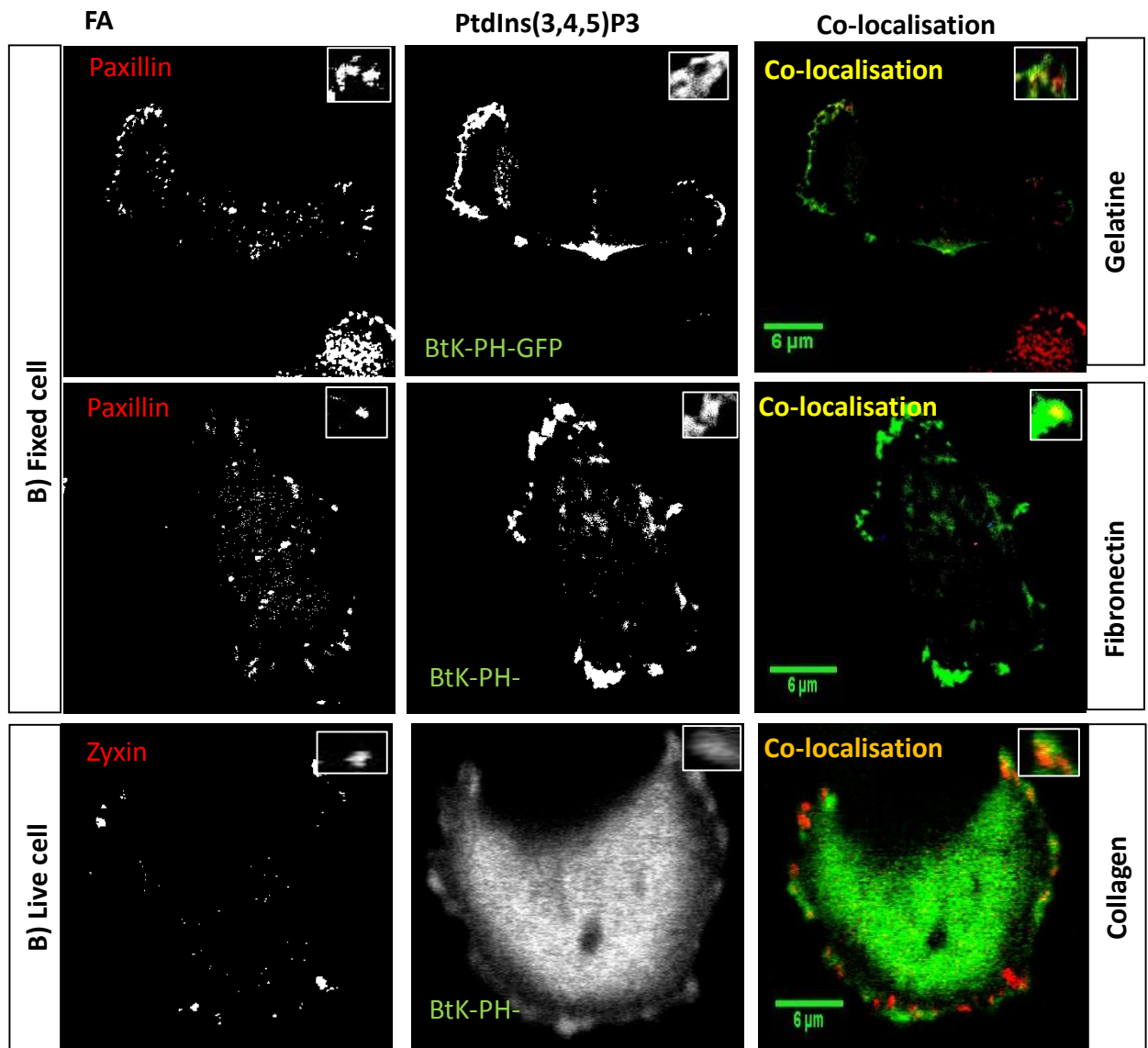


Figure (3.10): Spatial co-localisation between PtdIns(3,4,5)P3 and a single FAs in MDA-MB-231 cells on variety of surfaces . A) MDA-MB-231 cells were plated on gelatine 0.2%, and transfected with Bk-PH-GFP, then fixed and immunostained for paxillin, talin and vinculin to visualise the spatial interaction between PtdIns(3,4,5)P3 and FAs . **B)** MDA-MB-231 cells were plated on (fibronectin 20μg/ml and collagen 2mg/ml) and co-transfected with Btk-PH-mCherry (red) & paxillin-GFP (green), or Btk-PH-GFP (green) & zyxin-RFP(red). The highlighted areas show a magnification of the spatial co-localisation region between PtdIns(3,4,5)P3 and a single FA. Three independent experiments were performed, representative pictures are shown. Scale bars = 6μm.

Table 3. 3: Data show co-localisation values \pm SD between PtdIns(3,4,5)P3 and FAs.

	Talin	Vinculin	Paxillin	FAK	Paxillin	Zyxin
PI(3,4,5)P3	0.52 \pm 0.04	0.51 \pm 0.032	0.50 \pm 0.01	0.49 \pm 0.03	0.44 \pm 0.04	0.48 \pm 0.07

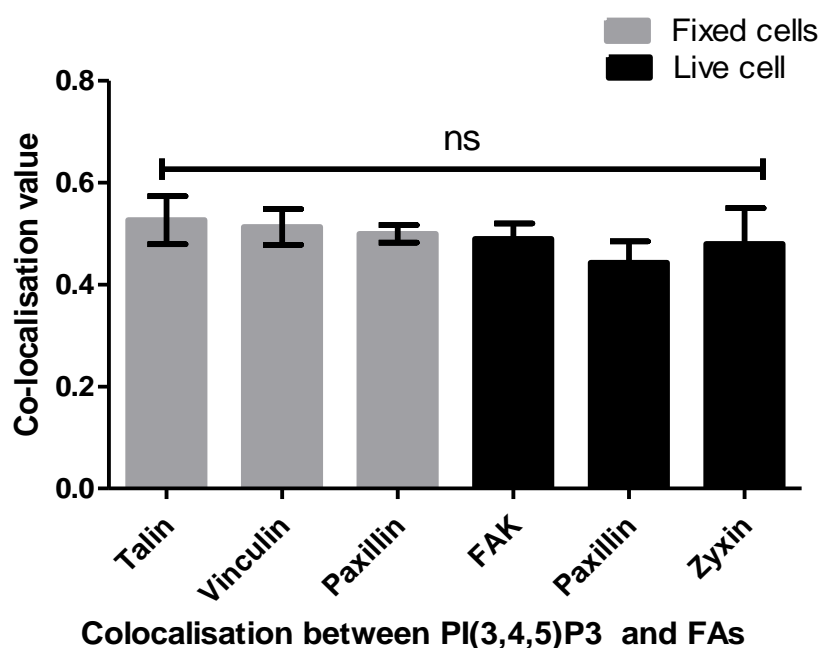


Figure (3.11). Quantification of spatial co-localisation between PtdIns(3,4,5)P3 and a single FA. Spearman's (ρ) correlation coefficient analysis was used to measure co-localisation value between PtdIns(3,4,5)P3 and FAs. **In fixed cells**, Co-localisation values of (talin, vinculin, FAK and paxillin) and PtdIns(3,4,5)P3 were moderate co-localisation. **In live cells**, co-localisation values between FAK or zyxin or paxillin and PtdIns(3,4,5)P3 were moderate co-localisation. Statistical analysis was performed by One-way ANOVA with Tukey's Multiple Comparison Test, non-significant differences between co-localisation values at $P \leq 0.05$. Data is a representative of the means \pm SD of three independent experiments in which $n = 20$ cells were measured, and number of a single FA= 10 for each cell.

Table 3.4: Data showing co-localisation values \pm SD between PtdIns(3,4,5)P3 and paxillin on collagen, fibronectin and gelatine.

	PI(3,4,5)P3 + Paxillin
Collagen	0.52 \pm 0.08
Fibronectin	0.49 \pm 0.07
Gelatine	0.48 \pm 0.08

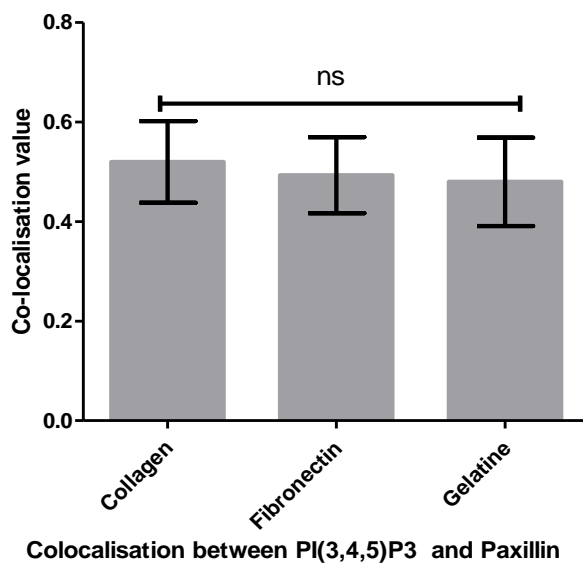


Figure (3.12). Quantification of spatial co-localisation between PtdIns(3,4,5)P3 and paxillin. Spearman's (ρ) correlation coefficient analysis was used to measure co-localisation value between PtdIns(3,4,5)P3 and paxillin. Pooled data showing co-localisation value between PtdIns(3,4,5)P3 and paxillin on different surfaces. Statistical analysis was performed by One-way ANOVA with Tukey's Multiple Comparison Test, non-significant differences between co-localisation values at $P \leq 0.05$. Data is a representative of the means \pm SD of three independent experiments in which $n = 20$ cells were measured, and number of a single FA= 10 for each cell.

3.2.6. Spatial regulation of PtdIns(4,5)P2 and PtdIns(3,4,5)P3 within a single FA at the leading and trailing edges of the cell

MDA-MB-231 cells were seeded on different surfaces (fibronectin 20 μ g/ml and collagen 2mg/ml) and transfected with Btk-PH-GFP or mCherry and PLC δ 1-PH-GFP or mCherry, then fixed with paraformaldehyde. Later, the cells were incubated with an anti-paxillin monoclonal antibody, and then stained with Alexa Fluor secondary antibody. The co-localisation values between PtdIns(4,5)P2 or PtdIns(3,4,5)P3 and paxillin were measured by ImageJ at both the leading and trailing edges, through selecting the regions of interest (ROI) of PtdIns(4,5)P2 or PtdIns(3,4,5)P3. The reverse co-localisation value between paxillin and PtdIns(4,5)P2 or PtdIns(3,4,5)P3 was also measured by ImageJ at the leading and trailing edges, through selecting the ROI of paxillin (Figures 3.13 & 3.15). Co-localisation value at the leading edge was slightly higher than trailing edges but not significantly and reverse co-localisation was similar to regular co-localisation (Figures 3.14A-B & 3.16A-B). The co-localisation values of PtdIns(4,5)P2 with paxillin on collagen at the leading and trailing edge were 0.60 ± 0.05 and 0.56 ± 0.02 respectively and reverse co-localisation values at the leading and trailing edge were 0.64 ± 0.03 and 0.62 ± 0.02 respectively. The co-localisation values of PtdIns(4,5)P2 with paxillin on fibronectin at the leading and trailing edge were 0.57 ± 0.06 and 0.51 ± 0.05 respectively and reverse co-localisation values at the leading and trailing edge were 0.60 ± 0.05 and 0.56 ± 0.03 respectively as summarised in tables 3.5.

The co-localisation values of PtdIns(3,4,5)P3 with paxillin on collagen at the leading and trailing edge were 0.49 ± 0.16 and 0.43 ± 0.05 respectively and reverse co-localisation values at the leading and trailing edge were 0.52 ± 0.13 and 0.46 ± 0.08 respectively. The co-localisation values of PtdIns(3,4,5)P3 with paxillin on fibronectin at the leading and trailing edge were 0.56 ± 0.10 and 0.56 ± 0.16 respectively and reverse co-localisation values at the leading and trailing edge were 0.61 ± 0.08 and 0.44 ± 0.15 respectively as summarised in tables 3.6.

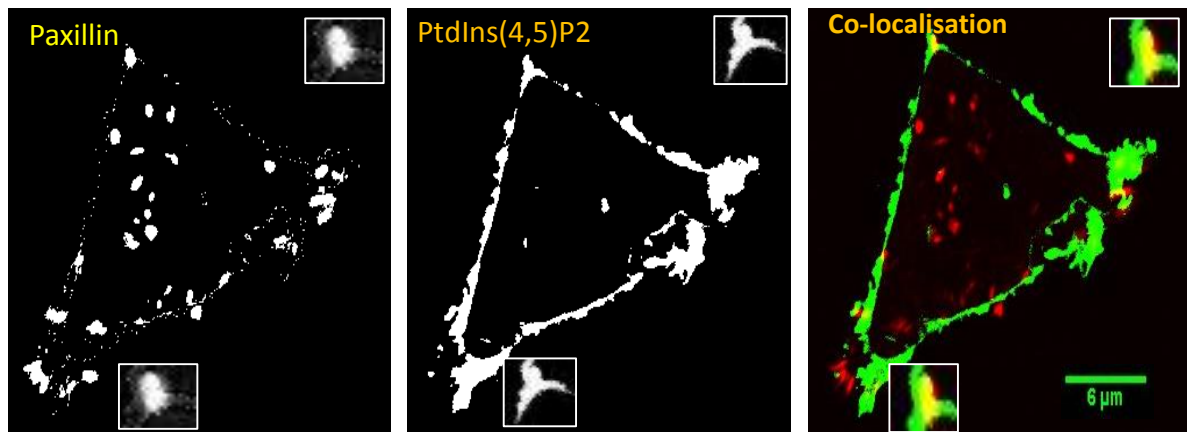


Figure (3.13) : Spatial co-localisation between PtdIns(4,5)P2 and paxillin at the leading and trailing edges of MDA-MB-231 cells on variety of surfaces . Cells were plated on collagen 2mg/ml and co-transfected with PLC δ 1-PH-GFP (green) then fixed and immunostained for paxillin (red). The spatial interaction between PtdIns(4,5)P2 and paxillin was measured through selection ROI at the leading and trailing edges of the cell. The highlighted areas show a magnification of spatial co-localisation region between PtdIns(4,5)P2 and a single FA at the leading and trailing edges. Representative picture is shown.

Table 3.5: Data show co-localisation values \pm SD between PtdIns(4,5)P2 and paxillin at the leading and trailing edge on collagen and fibronectin.

	PIP2/paxillin (leading edge)	PIP2/paxillin (trailing edge)	Paxillin/PIP2 (leading edge)	Paxillin/PIP2 (Trailing edge)
Collagen	0.60 ± 0.05	0.56 ± 0.02	0.64 ± 0.03	0.62 ± 0.02
Fibronectin	0.57 ± 0.06	0.51 ± 0.05	0.60 ± 0.05	0.56 ± 0.03

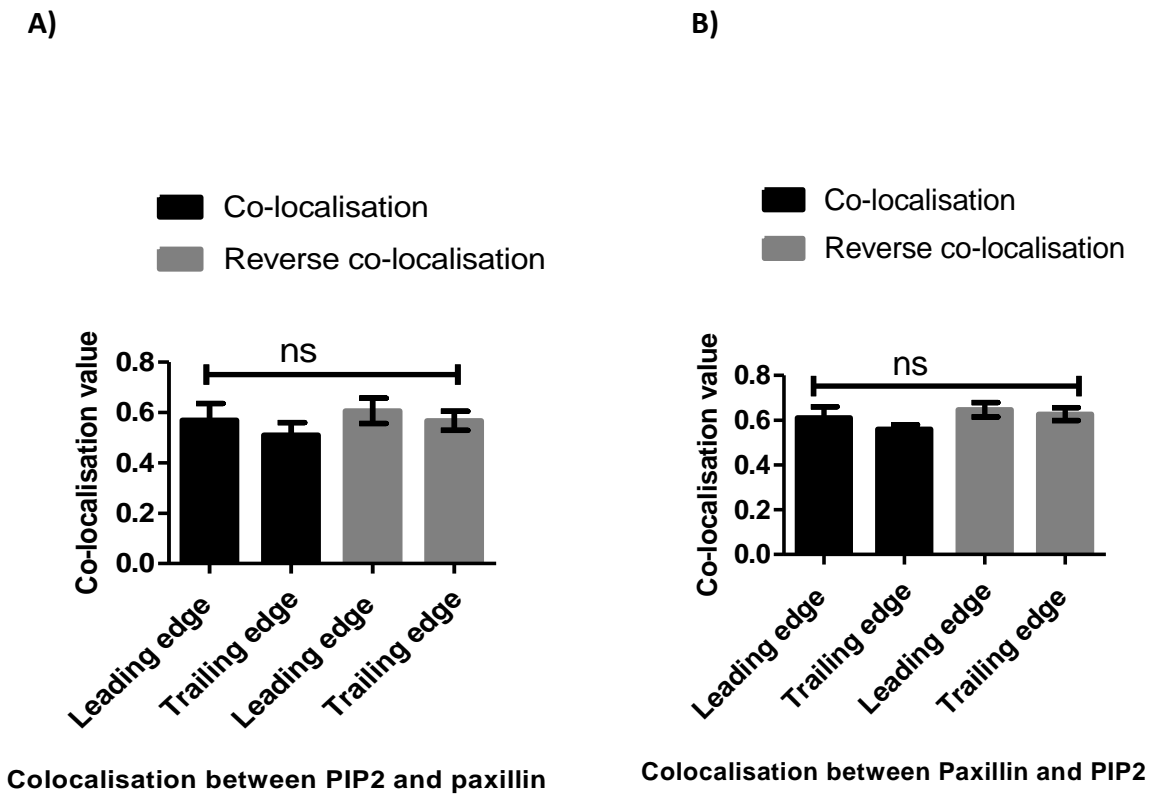


Figure (3.14): Quantification of spatial co-localisation between PtdIns(4,5)P2 and paxillin at the leading and trailing edges. Spearman's (ρ) correlation coefficient analysis was used to measure a co-localisation value between PtdIns(4,5)P2 and paxillin at the leading and trailing edges. **A) On fibronectin:** Co-localisation and reverse co-localisation values between PtdIns(4,5)P2 and paxillin were moderate co-localisation. **A) On collagen:** Co-localisation and reverse co-localisation values between PtdIns(4,5)P2 and paxillin were moderate co-localisation. Statistical analysis was performed by One-way ANOVA with Tukey's Multiple Comparison Test, non-significant differences between co-localisation values at $P \leq 0.05$. Data are a representative of the means \pm SD of three independent experiments in which $n = 10$ cells were measured, and number of a single FA = 10 for each cell.

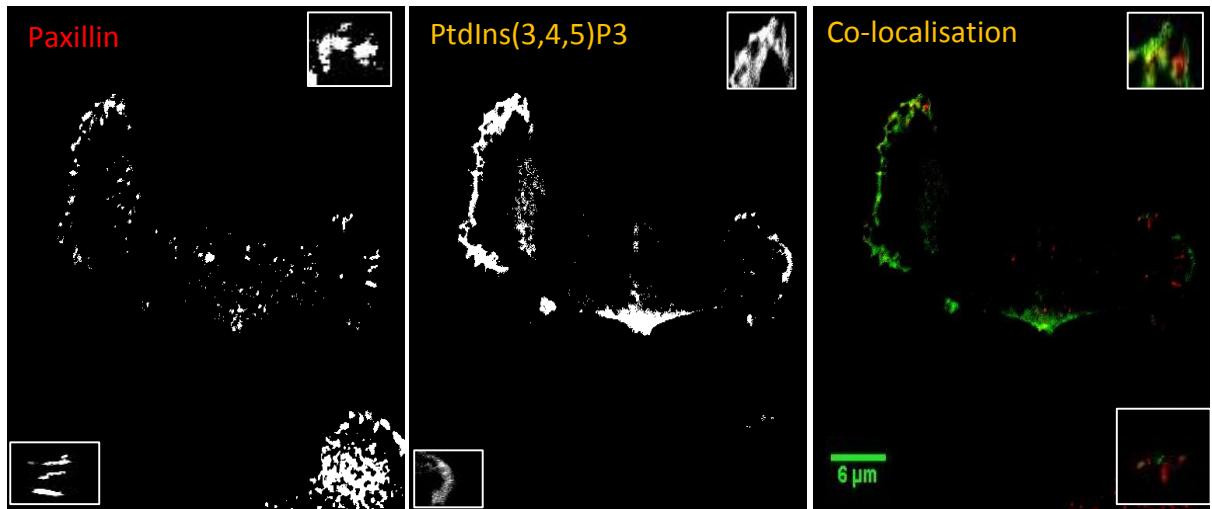


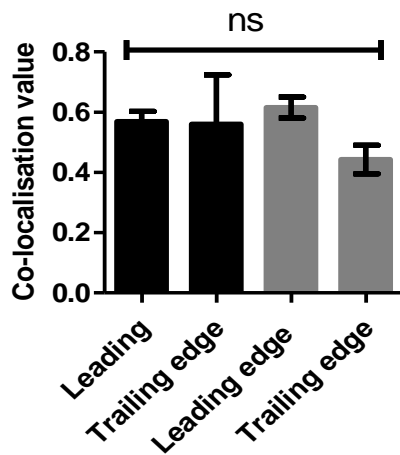
Figure (3.15): Spatial co-localisation between PtdIns(3,4,5)P3 and paxillin at the leading and trailing edges of MDA-MB-231 cells on a variety of surfaces . MDA-MB-231 cells were plated on collagen 2mg/ml and transfected with Btk-PH-GFP (green) then fixed and immunostained for paxillin (red). The spatial co-localisation between PtdIns(3,4,5)P3 and paxillin was measured through selection ROI at the leading and trailing edges of the cell. The highlighted areas show magnification of the spatial co-localisation region between PtdIns(3,4,5)P3 and a single FA at the leading and trailing edges. Representative picture is shown.

Table 3.6: Data shows Co-localisation values \pm SD between PtdIns(3,4,5)P3 and paxillin at the leading and trailing edge on collagen and fibronectin

	PIP3/paxillin (leading edge)	PIP3/paxillin (trailing edge)	Paxillin/PIP3 (leading edge)	Paxillin/PIP3 (Trailing edge)
Collagen	0.49 \pm 0.16	0.43 \pm 0.05	0.52 \pm 0.13	0.46 \pm 0.08
Fibronectin	0.56 \pm 0.10	0.56 \pm 0.16	0.61 \pm 0.08	0.44 \pm 0.15

A)

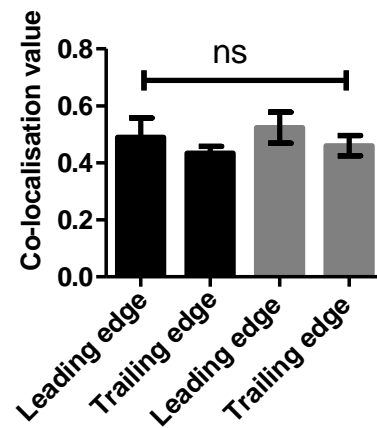
Co-localisation
 Reverse co-localisation



Colocalisation between PIP3 and Paxillin

B)

Co-localisation
 Reverse co-localisation



Colocalisation between paxillin and PIP3

Figure (3.16): Quantification of spatial co-localisation between PtdIns(3,4,5)P3 and paxillin at the leading and trailing edges. Spearman's (ρ) correlation coefficient analysis was used to measure co-localisation value between PtdIns(3,4,5)P3 and paxillin at the leading and trailing edges **A) On fibronectin:** Co-localisation and Reverse co-localisation values between PtdIns(3,4,5)P3 and paxillin were moderate co-localisation. **B) On collagen:** Co-localisation and Reverse co-localisation values between PtdIns(3,4,5)P3 and paxillin were moderate co-localisation. Statistical analysis was performed by One-way ANOVA with Tukey's Multiple Comparison Test, non-significant difference between co-localisation values at $P \leq 0.05$. Data are a representative of the means \pm SD of three independent experiments in which $n = 10$ cells were measured, and number of a single FA= 10 for each cell.

3.2.7. Effect of PI3K and PLC inhibitors on co-localisation of PtdIns(4,5)P2 and PtdIns(3,4,5)P3 within FAs.

MDA-MB-231 cells were plated on fibronectin (20µg/ml) and transfected with PLCδ1-PH-GFP and RFP-zyxin and then treated with PI3K inhibitors Wortmannin (1 µm) or LY 2940 02 (25µm) or PLC inhibitor U733122 (1 µm) for 30 minutes, and then fixed with paraformaldehyde (Figure 3.17). Our results showed that co-localisation value between PtdIns(4,5)P2 and zyxin was significantly increased by PLC inhibitor U733122 (1 µm) treatment during 30 minutes compared with the control. While, PI3K inhibitors Wortmannin (1 µm) or LY 2940 02 (25µm) had no effect (Figure 3.18). In tables 3.7, compared with DMSO control, the mean of the co-localisation value was significantly increased after PLC U73122 treatment from 0.37 ± 0.02 to 0.50 ± 0.05 and PI3K LY294002 and Wortmannin treatment had no effect from 0.37 ± 0.02 to 0.43 ± 0.03 , 0.42 ± 0.0 respectively.

Similarly, MDA-MB-231 cells were transfected Btk-PH-GFP and RFP-zyxin plasmid after PtdIns(3,4,5)P3 production was stimulated by EGF (100ng/ml) for 5 minutes. Then, cell were treated with Wortmannin (1 µm) or LY 294002 (25µm) for 30 minute (Figure 3.19). The co-localisation value between PtdIns(3,4,5)P3 and zyxin was slightly reduced but not significantly (Figure 3.20). In tables 3.8, compared with DMSO control, the mean of the co-localisation value was slightly reduced after LY294002+EGF and Wortmannin+EGF from 0.43 ± 0.05 to 0.35 ± 0.05 and 0.36 ± 0.04 respectively.

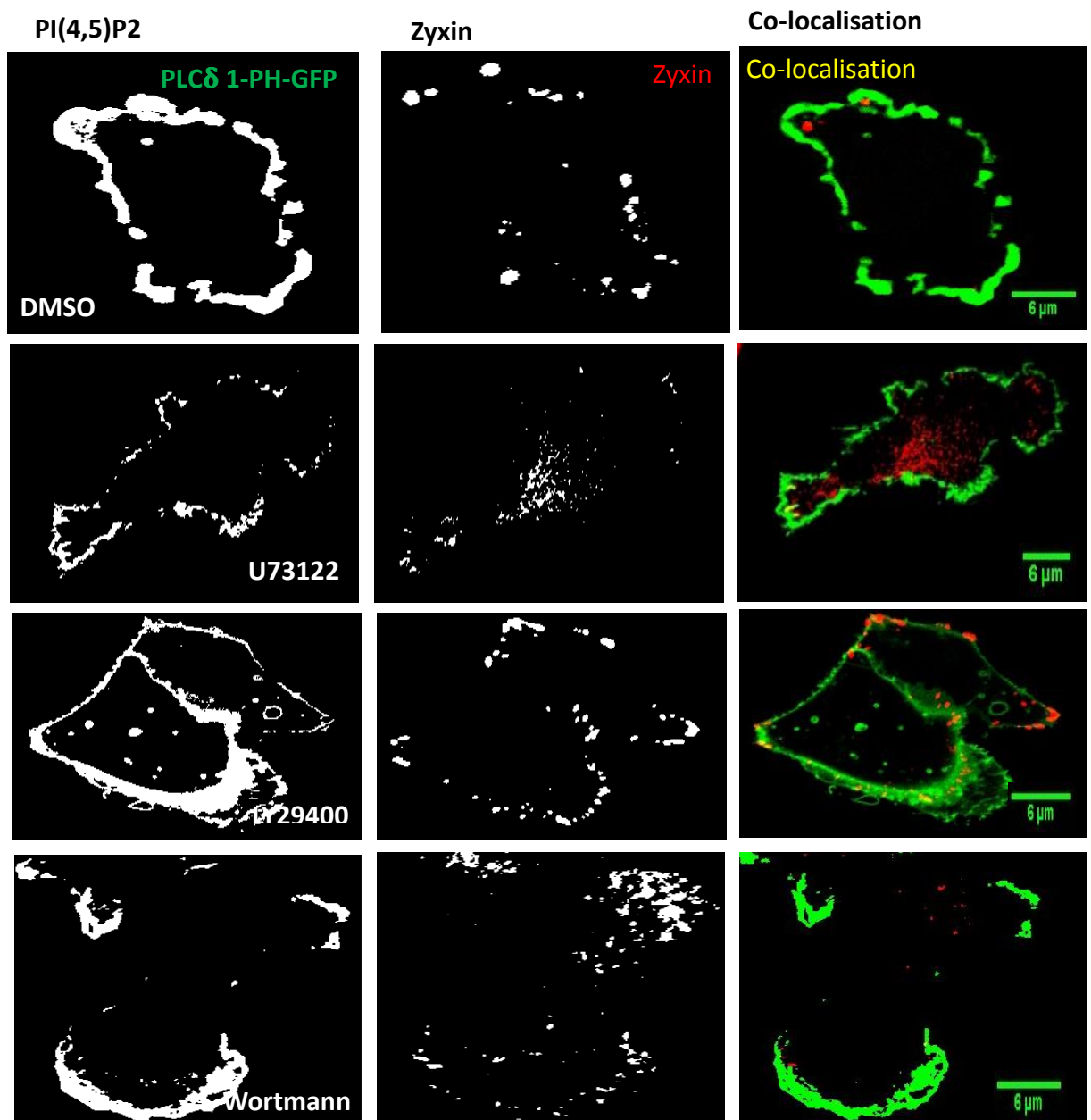


Figure (3.17): Effect of PI3K and PLC inhibitors on the spatial co-localisation between PtdIns(4,5)P2 and zyxin. **A)** MDA-MB-231 cells were grown on fibronectin and co-transfected with PLC δ 1-PH-GFP(green) & Zyxin-RFP (red), and treated with PI3K and PLC inhibitors during 30 minutes, then fixed with paraformaldehyde. **A)** Cells were treated with DMSO used as a control. **B)** Cells were treated with PLC inhibitor U73122 (1 μ m) for 30 minutes. **C)** Cells were treated with PI3K inhibitor LY294002 (25 μ m) for 30 minutes. **D)** Cells were treated with PI3K inhibitor Wortmaninn (1 μ m) for 30 minutes.

Table 3.7: Data showing Co-localisation values \pm SD between PtdIns(4,5)P2 and zyxin

	PIP2 \pm Zyxin
DMSO	0.37 \pm 0.02
LY294002	0.43 \pm 0.03
Wortmannin	0.42 \pm 0.01
U73122	0.50 \pm 0.05

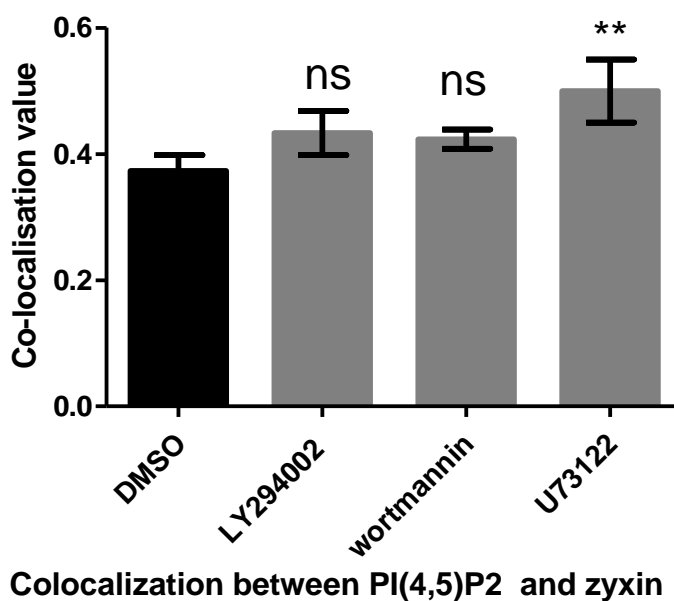


Figure (3.18): PI3K and PLC inhibitors increase spatial co-localisation between PtdIns(4,5)P2 and Zyxin. Spearman's (rho) correlation coefficient analysis was used to measure co-localisation value between ROI of PtdIns(4,5)P2 and Zyxin . Co-localisation values between Zyxin and PtdIns(4,5)P2 were moderate co-localisation. Statistical analysis was performed by One-way ANOVA with Dunnett's Multiple Comparison Test. Statistical significance differences were accepted at $**P \leq 0.005$. Data are a representative of the means \pm SD of three independent experiments in which n =20 cells were measured, and number of a single FA= 10 for each cell.

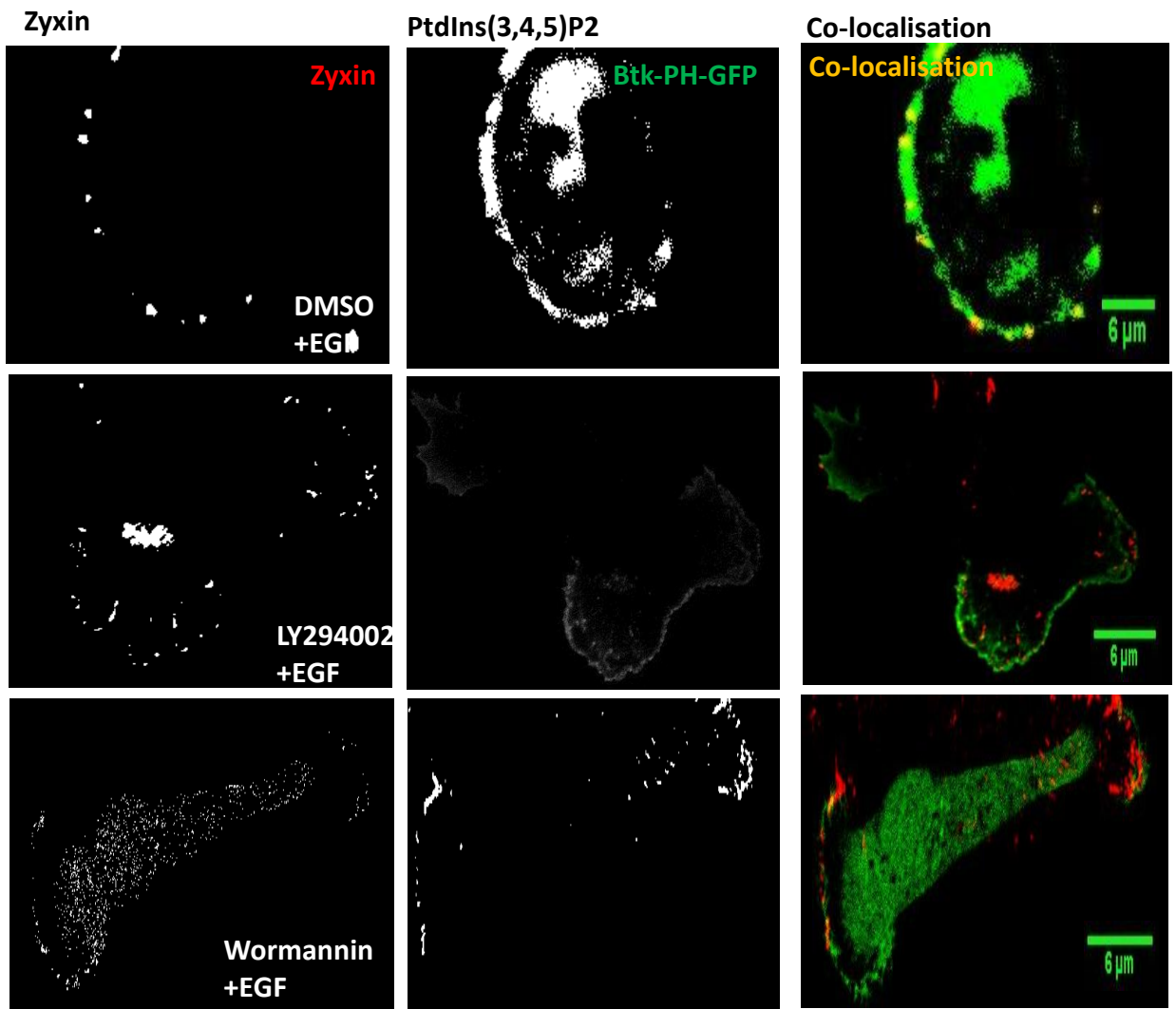
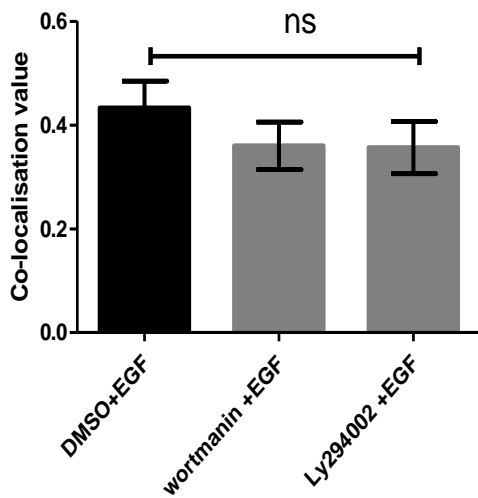


Figure (3.19): Effect PI3K inhibitors on spatial co-localisation between PtdIns(3,4,5)P3 and zyxin. **A)** MDA-MB-231 cells were grown on fibronectin and co-transfected with Btk-PH-GFP(green) & Zyxin-RFP, and treated with PI3K and PLC inhibitors during 30 minutes after stimulating PtdIns(3,4,5)P3 production by EGF (10ng/ml) for 5 minute. Then cells were fixed with paraformaldehyde. **A)** Cells were treated with DMSO used as a control. **B)** Cells were treated with PI3K inhibitor LY294002 (25 μ m) for 30 minutes. **C)** Cells were treated with PI3K inhibitor Wortmaninn (1 μ m) for 30 minutes.



Colocalization between PI(3,4,5)P3 and zyxin

Table 3.8: Data showing Co-localisation values \pm SD between PtdIns(3,4,5)P3 and zyxin

	PIP3 \pm Zyxin
DMSO+EGF	0.43 \pm 0.05
LY294002+EGF	0.35 \pm 0.05
Wortmannin +EGF	0.36 \pm 0.04

Figure (3.20): PI3K inhibitors reduce spatial co-localisation between PtdIns(3,4,5)P3 and Zyxin. Spearman's (ρ) correlation coefficient analysis was used to measure co-localisation value between ROI of PtdIns(3,4,5)P3 and Zyxin. Co-localisation values were moderate co-localisation. Statistical analysis was performed by One-way ANOVA with Dunnett's Multiple Comparison Test. Statistical significance was accepted at $P \leq 0.05$. Data are a representative of the means \pm SD of three independent experiments in which $n = 20$ cells were measured, and number of a single FA= 10 for each cell.

3.3. Discussion

The aim of this chapter was to visualise PtdIns(4,5)P2 and PtdIns(3,4,5)P3 directly within single FAs in MDA-MB-231 cells. Furthermore, their interactions with FA proteins are determined through a quantitative analysis of their co-localisation within single FAs in live and fixed cells.

Our data showed that PLC δ 1-PH-GFP which binds PtdIns(4,5)P2 (Figure 3.21) was almost entirely recruited to the cell membrane in both fixed and live cells (Figures 3.1 & 3.2), while an anti- PtdIns(4,5)P2 antibody was localised throughout the cells, not just in the membrane (Figure 3.6) as has been previously shown (Matsuda et al., 2001, Várnai and Balla, 1998, Stauffer et al., 1998). The probe Btk-PH-GFP for PtdIns(3,4,5)P3 (Figure 3.21) was sometimes localised at the cell membrane, but in other cells there was a large amount of fluorescence present in the cytosol and nucleus in both fixed and live cells (Figures 3.1 & 3.2). The anti-PtdIns(3,4,5)P3 antibody was localised throughout the cell (Figure 3.5) as has been previously shown (Manna et al., 2007, Varnai et al., 1999).

Many biosensors have been designed to detect PtdIns(3,4,5)P3, such as the cytosolic regulator of adenylyl cyclase (CRAC) protein (Huang et al., 2003, Dormann et al., 2002) and Akt-PH domain. Although Akt-PH domain considered to be a good reporter, it also binds with PtdIns(4,5)P2 (Servant et al., 2000). Btk-PH domain is considered to be the best biosensor to visualise PtdIns(3,4,5)P3 as it has more affinity with, and specificity for PtdIns(3,4,5)P3 (Manna et al., 2007, Varnai et al., 1999, Balla and Varnai, 2009). Our results also showed in transfected cells that expressed only a small amount of Btk-PH-GFP, the majority of the biosensor was recruited to cell membrane (Figures 3.3 A & 3.4 A). MDA-MB-231 cells were transfected with Btk-PH-GFP for 24 hour then the

fluorescence intensity was measured in both transfected cells that expressed a small amount and more of Btk-PH-GFP .

Our results showed that transfected cells that expressed a small amount the peak of fluorescence intensity in the cell membrane was higher than cytosol in live and fixed cells (Figures 3.3 B & 3.4 B). While transfected cells that expressed more Btk-PH-GFP showed localisation of the probe throughout the cell (Figures 3. C, 3.4 C), and the peak of fluorescence intensity in the cell membrane and cytosol was similar in live and fixed cells (Figure 3.3 D, 3.4 D). This may mean that Btk-PH-GFP interacts with PtdIns(3,4,5)P3 but it depends on the availability of PtdIns(3,4,5)P3 in the cell membrane to recruit Btk-PH-GFP to the cell membrane (Figure 3.22). Therefore, in transfected cells that expressed more Btk-PH is likely to saturate the available amount of PtdIns(3,4,5)P3 pools in the cell membrane and the rest either binds with other types of inositides or remains in the cytoplasm (Balla and Varnai, 2009).

There are many possible reasons why PLC δ 1-PH and Btk-PH were recruited to the cell membrane differently. First, the abundance of PtdIns(3,4,5)P3 is much less than PtdIns(4,5)P2 in the cell membrane (Ji et al., 2015). PI(4,5)P2 forms around 5,000-20,000 molecules/ μm^2 , while PtdIns(3,4,5)P3 forms only 2-5% of PtdIns(4,5)P2 (Balla, 2013, Falkenburger et al., 2010). Therefore, our results showed that PLC δ 1-PH-GFP was almost entirely recruited to the cell membrane in both fixed and live cells due to an enrichment of PtdIns(4,5)P2 in the cell membrane.

Second, Balla and Varnai (2009) supposed that there is the compensatory increase in the PtdIns(4,5)P2 amount in the cells expressing large amount of proteins. This compensatory increase occurs rarely with PtdIns(3,4,5)P3 due to its dependence on certain stimuli, including PtdIns(3,4,5)P3 synthesis mainly relies on the presence of PI3K

activity; therefore, whenever PI3Ks are recruited to the cell membrane, the synthesis of PtdIns(3,4,5)P3 increases after stimulating PI3K activity by EGF (Thapa et al., 2015). However, the synthesis of PtdIns(3,4,5)P3 is decreased whenever PTEN is recruited to the cell membrane because PTEN dephosphorylates PtdIns(3,4,5)P3 to PtdIns(4,5)P2 (Nguyen et al., 2014).

Third, the overexpression of PH domain might affect the specificity and affinity of binding between inositides and kinases (Balla and Varnai, 2009). The excess amount of PH-GFP either interacts with other types of inositides or remains in the cytosol and thus affect the cellular metabolism of the cell (Figure 3.22) (Balla and Varnai, 2009).

It can be concluded that PLC δ 1-PH is likely to be entirely recruited by PtdIns(4,5)P2 in the cell membrane. In transfected cells that expressed only a small amount of Btk-PH is likely to be recruited by PtdIns(3,4,5)P3, while in transfected cells that expressed more Btk-PH is likely to saturate the available amount of PtdIns(3,4,5)P3 pools in the cell membrane and the rest either binds with other types of inositides or remains in the cytoplasm.

It has been shown that PH-domains more suitable, reliable and accurate than antibodies for visualising and studying the molecular dynamics of phospholipids in live cells (Balla and Varnai, 2009, Idevall-Hagren and De Camilli, 2015). Indeed, our results showed that PH domains have more specificity and affinity than antibodies (Figure 3.7 A-D, 3.8 A-D). However, there are some side-effects, the overexpression of the PH domain fused with GFP sometimes affects the physiological nature of the cell. It also can affect the binding of PH-domain with inositols. The overexpression of PH domain might block other kinases or proteins through interfering or interaction with their inositols which assigned to interact with these proteins, this could affect their downstream signalling (Idevall-

Hagren and De Camilli, 2015, Balla and Varnai, 2009). Even though PH domain is the best option to visualise PtdIns(4,5)P2, not all of the lipids could be visualised using these methods. For instance, PtdIns(4,5)P2 and PtdIns(3,4,5)P3 might bind with other proteins, thus rendering them incapable of binding with PH probes or antibodies, which could lead to inaccurate detection (Ji and Lou, 2016).

It is necessary to use PH domain in both fixed and live cells as both approaches have advantages and disadvantages. For example, in fixed cell can be used with high power lasers and kept in a convenient location. However, the materials that are used for fixation and permeabilization may affect the physiological and morphological nature of the cell. Might also affect the dynamic nature of PH domain-proteins interaction. Therefore, to get more accurate results, both fixed and live cells should be used (Balla and Varnai, 2009).

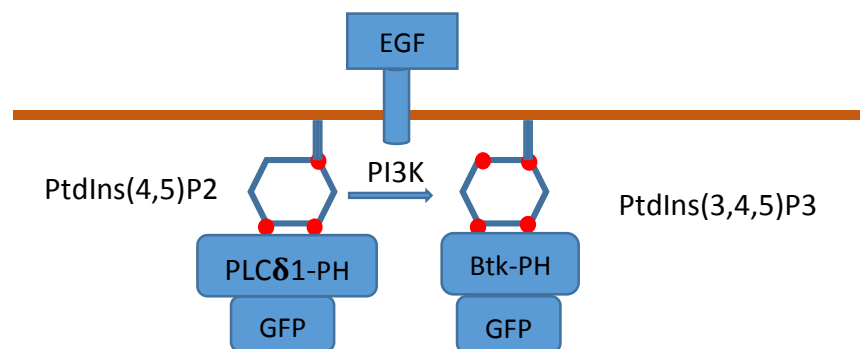


Figure (3.21): Showing Btk-PH and PLC δ 1-PH domains which are recruited by PtdIns(4,5)P2 and PtdIns(3,4,5)P3 respectively.

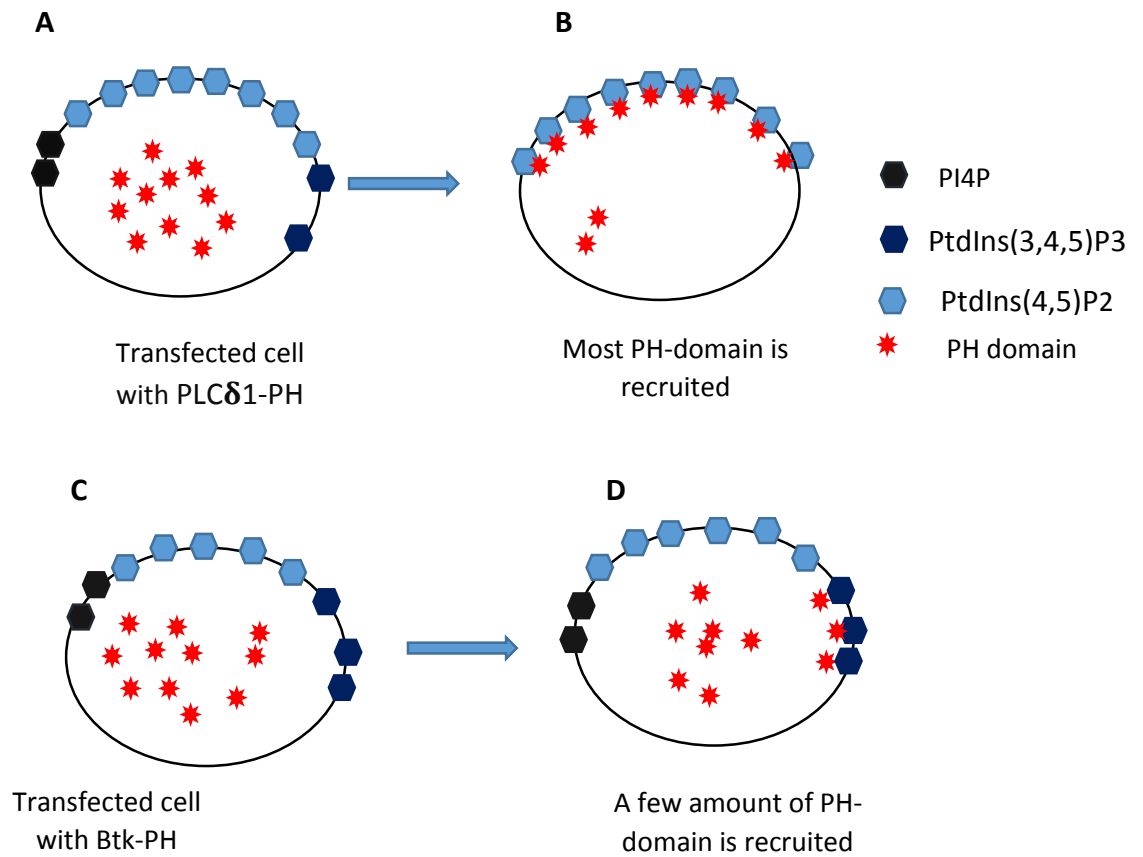


Figure (3.22): Illustrating the effect of overexpression of PH domain and the abundance of lipids. A&B) Showing MDA-MB-231 cells transfected with PLC δ 1-PH-GFP or mCherry and most of PH-domain is recruited due to abundance of PtdIns(4,5)P2. **C&D)** Showing MDA-MB-231 cells transfected with Btk-PH-GFP or mCherry and a few of PH-domain is recruited due to inadequacy of PtdIns(3,4,5)P3.

In order to study the spatial organisation between PtdIns(4,5)P₂ or PtdIns(3,4,5)P₃ and FAs it is important to use co-transfection experiments. Our data showed that PtdIns(4,5)P₂ and PtdIns(3,4,5)P₃ co-localised with several types of FA proteins. The co-localisation values were moderate in both fixed and live cells on different surfaces (Figure 3.11 & table1). This spatial co-localisation reveals several potential implications. First, PtdIns(4,5)P₂ and PtdIns(3,4,5)P₃ signalling may interact with FAs and play a role in FAs-integrin signalling pathways (Figure3.28) (Goni et al., 2014, Thapa et al., 2015, Orłowski et al., 2015, Chinthalapudi et al., 2014). Second, PtdIns(4,5)P₂ and PtdIns(3,4,5)P₃ could be implicated in the regulation of FA dynamics through recruitment of FAs and strengthening the link between FAs and integrin (Le et al., 2015, Gilmore and Burridge, 1996). The following chapters will address these possibilities.

The measurement of strength of spatial co-localisation between two molecules ranged from 1 to -1. The co-localisation values can express the strength degree of co-localisation between proteins, such as if the value range from 0.1-0.19 very weak, 0.20-0.39 weak, 0.40-0.59 moderate, 0.60-0.79 strong and 0.80-1 very strong (Zinchuk et al., 2013, Dunn et al., 2011, Hauke and Kossowski, 2011).

Different surfaces were used to determine what surface would be the best to study the co-localisation between FAs and PtdIns(4,5)P₂ and PtdIns(3,4,5)P₃. Previous studies have shown that the initiation of the formation of FAs depends on the association between integrins and ECM. Each type of ECM responds to different types of integrins, which affect the behaviour of FA turnover (Calderwood, 2004, Harburger and Calderwood, 2009). Integrins play an important role in the cell migration through the link of FA proteins to ECM. The specificity of this binding mainly relies on a type of ECM

and the extracellular domain of integrins (Hynes, 2002), such as ($\alpha5\beta1$, $\alpha v\beta1$, $\alpha4\beta1$) recognise fibronectin and ($\alpha1\beta1$, $\alpha2\beta1$) recognise collagen.

These various isoforms of integrins, which recognise different surfaces have different effect on FA dynamics and cell motility (Huveneers and Danen, 2009, Truong and Danen, 2009, Huttenlocher and Horwitz, 2011). Our results showed that co-localisation values were similar on various surfaces (Figures 3.12 & 3.16). This refers that different types of ECM have no effect on co-localisation of PtdIns(4,5)P2 or PtdIns(3,4,5)P3 with FAs.

Previous studies have shown that FAs and PtdIns(4,5)P2 or PtdIns(3,4,5)P3 were distributed at different nanoscale distances on the cell membrane (Giannone, 2015, Kanchanawong et al., 2010, Ji et al., 2015). It has also been shown that paxillin is the closest to the cell membrane while zyxin is the furthest from the cell membrane (figure 3.17) (Kanchanawong et al., 2010). Therefore, Z-Stacking-single slice was performed through taking different slices to record the entire FAs and cell membrane from the bottom to the top. Then, one of these single slices was selected which contains an accurate co-localisation point between a single FA and PtdIns(4,5)P2 or PtdIns(3,4,5)P3.

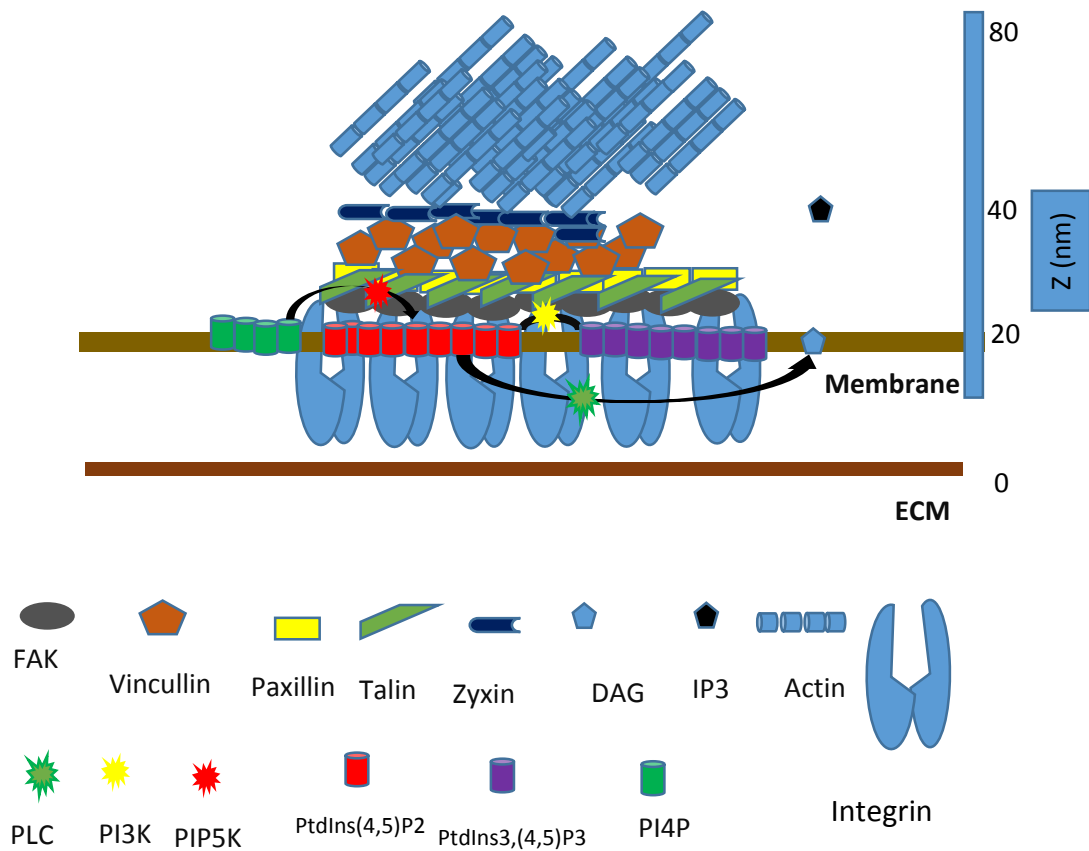


Figure (3.23): Schematic model of the spatial organisation of FA-Phosphatidylinositol interactions within cell membrane. PtdIns(4,5)P2 and PtdIns(3,4,5)P3 spatially localised with FAs in cell membrane.

Previous studies have shown that spatio-temporal distribution of FAs and both PtdIns(4,5)P2 and PtdIns(3,4,5)P3 and their second messengers at the leading edge play roles in recruiting many proteins to leading edge. The enzymes responsible for the production of these lipids are different in terms of their concentrations at the front and rear of the cell; therefore, they are distributed unequally in the cell membrane (Falke and Ziemba, 2014, Thapa and Anderson, 2012, Nishioka et al., 2008, Sharma et al., 2008). However, our data showed that PtdIns(4,5)P2 and PtdIns(3,4,5)P3 were equally

distributed at leading and trailing edges of MDA-MB-231 cells (Figures 3.113 & 3.15). The co-localisation and reverse co-localisation between PtdIns(4,5)P2 and PtdIns(3,4,5)P3 and FA were measured at the leading and trailing edges of the cell by selecting the region of interest (ROI) for PtdIns(4,5)P2 or PtdIns(3,4,5)P3 and FA. In other words, the ROI of PtdIns(4,5)P2 or PtdIns(3,4,5)P3 was selected and its localisation with FA was measured which is called regular localisation analysis. The ROI of a single FA was selected and its localisation with PtdIns(4,5)P2 or PtdIns(3,4,5)P3 was measured which is called reverse localisation analysis. Our Data showed moderate co-localisation, but the co-localisation value at the leading edge was slightly higher than trailing edge but was not significant (figure3.13 & 3.16). The reverse co-localisation was similar to regular co-localisation (figure3.11 & 3.13). The implications of these results that PtdIns(4,5)P2 and PtdIns(3,4,5)P3 are equally distributed at the leading and trailing edge of the cell. It can be said that PtdIns(4,5)P2 and PtdIns(3,4,5)P3 are interacted and involved within FAs at the leading and trailing edge of the cell.

There are several reasons why the reverse co-localisation was measured. First, FAs and PtdIns(4,5)P2 and PtdIns(3,4,5)P3 might have different distribution areas at the leading and trailing edge of cell, which could have given them different roles. Second, a single FA is very small in size compared to the PtdIns(4,5)P2 and PtdIns(3,4,5)P3 domains in the cell membrane. So, a single FA can entirely be localised within PtdIns(4,5)P2 or PtdIns(3,4,5)P3 domains in the cell membrane, this might have a different localization value. Third, the Spearman correlation requires a measurement of the co-localisation and reverse co-localisation between two variables using fluorescence microscope images.

The advantages of Spearman's rank correlation are as follows: it is monotonic association and does not require assumptions. It uses when the data makes Pearson coefficient correlation (PCC) unwanted or misleading. It uses ranks data, and measures the strength degree of co-localisation between two molecules. So, this statistical method is more understandable in measuring fluorescence intensity when compared to others(Hauke and Kossowski, 2011).

MDA-MB-231 cells were treated with PI3K and PLC inhibitors (Figure3.30) to examine their effects on the spatial co-localisation between PtdIns(4,5)P₂ or PtdIns(3,4,5)P₃ and FA. Our results showed that co-localisation value between PtdIns(4,5)P₂ and zyxin was significantly increased by PLC U733122 treatment compared with the control. While, PI3K LY 294002 and Wortmannin treatment had no effect (Figure 3.18). The co-localisation value between PtdIns(3,4,5)P₃ and zyxin was slightly reduced but not significantly by PI3K LY294002 and Wortmannin treatment (Figure 3.20). These results are in agreement with previous studies were showed that PLC inhibitor reduced the PtdIns(4,5)P₂ level in the cell membrane, while PI3K inhibitors had no effect (Stauffer et al., 1998). Finally, our data gave us good insight into the spatial co-localisation between PtdIns(4,5)P₂ or PtdIns(3,4,5)P₃ and FA proteins.

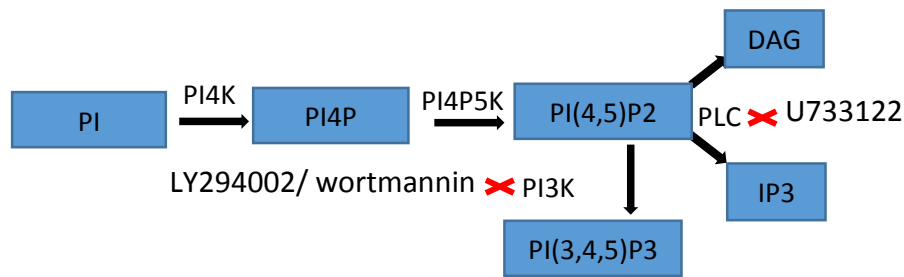


Figure (3.24): Illustrating of PtdIns(3,4,5)P3 and PtdIns(4,5)P2 metabolic pathways on plasma membrane and the effect PLC and PI3K inhibitors on local levels of PtdIns(3,4,5)P3 and PtdIns(4,5)P2.

Confocal microscopy is the most commonly used method to detect the interaction between PH-domain and PtdIns(3,4,5)P3 and PtdIns(4,5)P2. Although confocal microscopy provides a very high quality images and has high resolution to monitor intracellular molecules, there are some limitations, such as inability to visualise the fine details of PtdIns(3,4,5)P3 and PtdIns(4,5)P2 due to diffraction limit (Idevall-Hagren and De Camilli, 2015). These resolution limitations are also known as the diffraction barrier, which limits the ability of optical resolution to visualise or distinguish between smallest details which around 200nm by a lateral distance around half of the wavelength of light to image the specimen (Patterson, 2009).

Recent studies have investigated PtdIns(3,4,5)P3 and PtdIns(4,5)P2 in more details due to the availability of modern techniques that can surpass the diffraction limit, which is around 200nm (Ji et al., 2015, Wang and Richards, 2012). For example, the single-molecule super resolution microscopy (PALM and STORM) and FRET have been designed to overcome these problems and measure the spatial co-localisation more precisely (Patterson, 2009, Warren et al., 2015). These methods have very high sensitivity to visualise the fine details of PtdIns(3,4,5)P3 and PtdIns(4,5)P2, and can even reach 10 nm

in resolution. However, these methods have limitations, such as STORM can only be used in fixed cells and needs very efficient antibodies to detect PtdIns(3,4,5)P3 and PtdIns(4,5)P2 clearly (Idevall-Hagren and De Camilli, 2015, Ji et al., 2015, Balla and Varnai, 2009, Warren et al., 2015, Wang and Richards, 2012). Due to difficulties in direct visualisation of PtdIns(3,4,5)P3 and PtdIns(4,5)P2 at cell surface by antibodies PH domains were used as effective tools that bind selectively to PtdIns(3,4,5)P3 and PtdIns(4,5)P2 (Czech, 2000).

Although PALM and FRET can be used in live cells and can detect with a resolution of around 10nm, the measurement of distances is still limited to 10nm. The efficiency of FRET is not very high at low expression levels of lipids and even at high probe concentrations there could be low FRET signal if the concentration of the lipids is underneath a certain level (Balla and Varnai, 2009). Therefore, they might not confirm the interaction between PtdIns(3,4,5)P3 or PtdIns(4,5)P2 and FAs precisely. Furthermore, the membrane sheets that are used in these methods need detergent, which often affects phospholipid signals. The fixation steps that are used in these methods were at a lower temperatures, which could deform the PtdIns(3,4,5)P3 and PtdIns(4,5)P2 localisations (Ji and Lou, 2016). Thus, it is difficult to detect them in live cells under these physiological conditions (Ji and Lou, 2016).

Chapter 4. Temporal organisation of PtdIns(3,4,5)P3 and PtdIns(4,5)P2 within FAs

4.1. Introduction

To investigate the dynamic role of PtdIns(3,4,5)P3 and PtdIns(4,5)P2 within the assembly and disassembly process of FAs it is important to study how this interaction is temporally organised at single FA sites.

FAs are highly temporally organised and play a crucial role in cell migration through undergoing dynamic changes involving many temporal stages (Zaidel-Bar et al., 2004, Fogh et al., 2014). The first stage, the life cycle of FA turnover starts once the cell attaches to ECM, then integrin receptors are activated and associate with the ECM. Activated integrin recruits many proteins to FA sites, such as talin, vinculin and paxillin to form nascent FAs at the leading edge known as a nascent assembly stage (Shen et al., 2012, Zaidel-Bar et al., 2004, Fogh et al., 2014). In the second stage, additional proteins are recruited, such as FAK, α -actinin, zyxin, VASP and tensin to form mature FAs known as a mature assembly stage (Zaidel-Bar et al., 2004, Fogh et al., 2014). In the final stage, mature FAs are detached to enable the cell to migrate forward known as a disassembly stage which is poorly understood (Fogh et al., 2014, Kirfel et al., 2004).

Previous studies have shown that PtdIns(4,5)P2 is implicated in the recruitment of FA proteins over time during the FA cycle. PtdIns(4,5)P2 interacts with talin and vinculin and alters them from an inactive form to an active state during the assembly process (Izard and Brown, 2016, Chandrasekar et al., 2005, Wang, 2012, Yuan et al., 2017).

Activated talin and vinculin interact with integrins (Izard and Brown, 2016, Chandrasekar et al., 2005, Wang, 2012, Yuan et al., 2017).

In terms of the temporal recruitment of proteins into FA sites. talin is first recruited to the FA sites after activation by PtdIns(4,5)P₂ then vinculin is recruited by talin (Carisey et al., 2013, Zhang et al., 2008, Carisey and Ballestrem, 2011). Later, paxillin is recruited independently by vinculin and talin (Humphries et al., 2007), activated paxillin recruits FAK to form mature FAs (Lawson et al., 2012, Hu et al., 2014, Scheswohl et al., 2008, Wozniak et al., 2004). In later stages, VASP is recruited by vinculin and then activated VASP recruits zyxin into mature FA sites (Garvalov et al., 2003), this interaction is highly supported by PtdIns(4,5)P₂ (Huttelmaier et al., 1998, Carisey and Ballestrem, 2011, Garvalov et al., 2003). Ultimately, FA proteins activate each other to make a bridge between the actin cytoskeleton and integrins. PtdIns(4,5)P₂ pools increase the strength of binding between FAs and integrin during the assembly process (Izard and Brown, 2016).

It has also been shown that during these temporal stages of FA proteins that many kinases are activated and recruited into FA sites, such as PIP5K γ 90, PLC and PI3K. Talin recruits PIP5K γ 90 which generates PtdIns(4,5)P₂ pools in cell membranes (Legate et al., 2011, Di Paolo et al., 2002, Izard and Brown, 2016, Wu et al., 2011). PLC is recruited by PtdIns(4,5)P₂ and then cleaves PtdIns(4,5)P₂ to IP₃ and DAG (Izard and Brown, 2016, van den Bout and Divecha, 2009). IP₃ and DAG activate many kinases, such as PKC and Ca²⁺ which play a role in the regulation of FA turnover (Fogh et al., 2014, Chen et al., 2013). PI3K is recruited by PtdIns(4,5)P₂ and converts it to PtdIns(3,4,5)P₃ which plays

a role in the regulation of FAs turnover through deactivation of interaction between α -actinin and β integrin (Rubashkin et al., 2014, Greenwood et al., 2000).

In addition, Izard and Brown (2016) reviewed that PtdIns(4,5)P₂ synthesis is temporally organised in the cell membrane and probably plays a possible role in the regulation of FAs through changes the conformation of talin and oligomerizaion of vinculin. Thus, allow them to interact with both integrin and actin which in turn work as a main regulator for FAs turnover (Nayal et al., 2004, Chinthalapudi et al., 2014).

While the dynamic role of FA proteins and PtdIns(4,5)P₂ or PtdIns(3,4,5)P₃ activities has been investigated, little attention has been given to examining the local generation change of PtdIns(4,5)P₂ or PtdIns(3,4,5)P₃ within and around a single FA during the assembly and disassembly process in MDA-MB-231 cells.

The aim of this chapter is to study the temporal organisation of the local generation of PtdIns(4,5)P₂ and PtdIns(3,4,5)P₃ within and around a single FA directly during an assembly and disassembly process to examine whether PtdIns(4,5)P₂ or PtdIns(3,4,5)P₃ enhances and regulates the temporal organisation of single FA turnover at the leading and trailing edge. This study has been performed by observing the temporal organisation between PtdIns(4,5)P₂ or PtdIns(3,4,5)P₃ and FA protein using confocal microscopy. This would provide a novel insight concerning temporal organisation of PtdIns(4,5)P₂ and PtdIns(3,4,5)P₃.

4.2. Results

4.2.1. Temporal regulation of PtdIns(4,5)P₂ during assembly and disassembly of a single FA.

MDA-MB-231 cells were seeded on collagen (2mg/ml), then co-transfected with PLC δ 1-PH-GFP and RFP-zyxin or PLC δ 1-PH-mCherry and GFP-paxillin. The 488nm and 568nm channels were used to visualise GFP and RFP or mCherry respectively in live cell imaging (Figure 4.1). Z-Stacks were at 0.150 μ m distance with time-lapse series acquired over a 10 minute period with an interval of 15 second to be able to determine an accurate co-localisation between PtdIns(4,5)P₂ and zyxin or paxillin over time. The local levels of PtdIns(4,5)P₂ were measured at different time points and different focal planes within and around a single FA during assembly and disassembly. Quantitative measurement of these live images was performed by ImageJ. In the channel of zyxin-RFP or paxillin-GFP the region of interest (ROI) was selected closely around individual zyxin or paxillin, then the same selection applied to the GFP or mCherry channel of PtdIns(4,5)P₂ to determine the specific localisation of PtdIns(4,5)P₂ within a single FA during turnover after subtracting background (Figure 4.1)

In order to measure the fluorescence intensity of PtdIns(4,5)P₂ within zyxin or paxillin, the complete lifetimes of zyxin or paxillin turnover cycle was observed. In other words, individual zyxin and paxillin should be absent both in the beginning and the end of time-lapse series. So, single FA was selected for measuring the intensity from its appearance to the disappearance. Meanwhile, the intensity of PtdIns(4,5)P₂ was measured from the same time frame that FA was measured and until the last frame when was disappeared (Figure 4.1). Likewise, the local levels of PtdIns(4,5)P₂ were measured around a single FA .

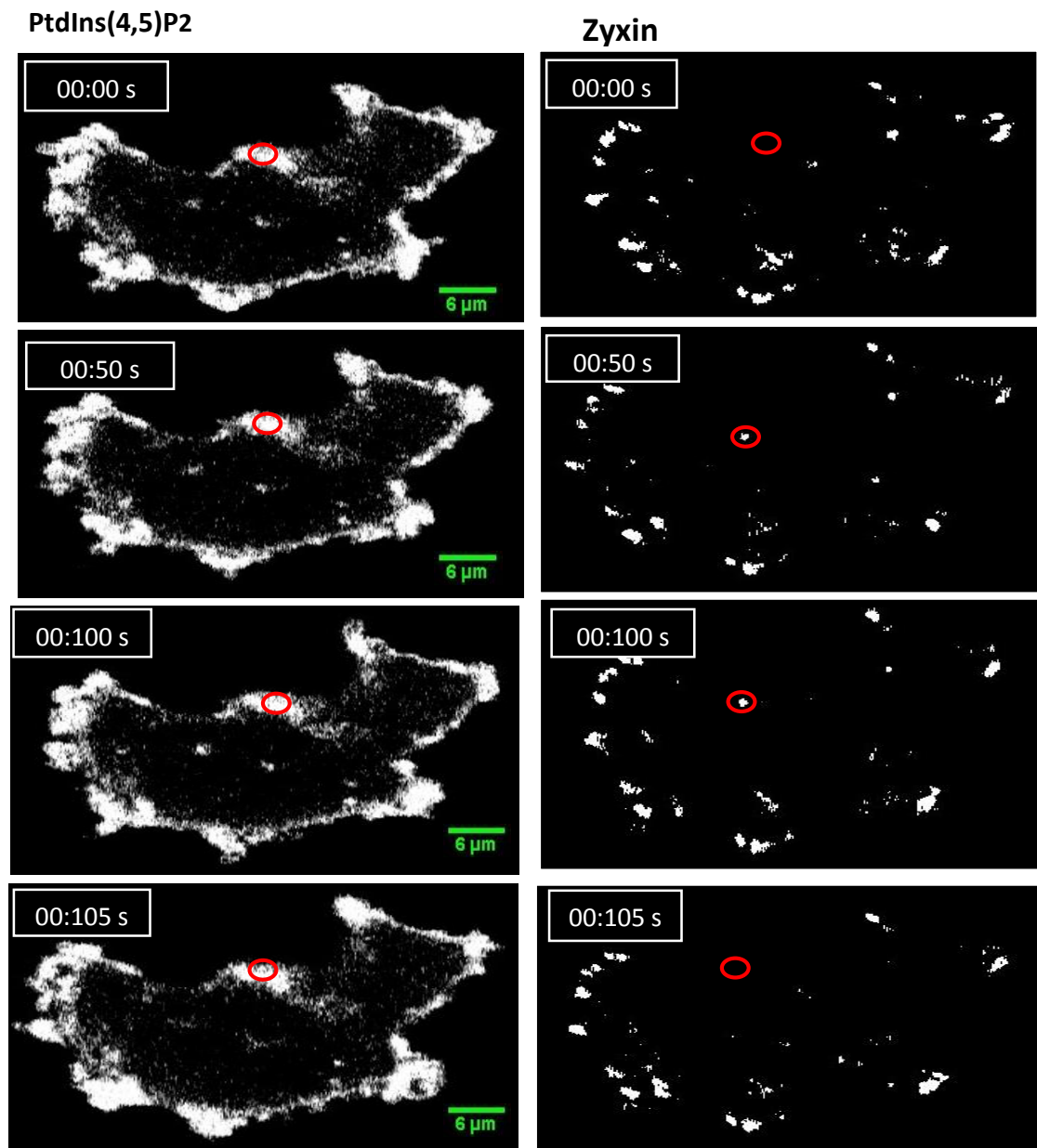


Figure (4.1): Quantification of the local levels of PtdIns(4,5)P2 within a single FA. Confocal live imaging showing the local levels of PtdIns(4,5)P2 during zyxin turnover over time. The MDA-MB-231 cells were plated on collagen 2mg/ml and co-transfected with PLC δ 1-PH-GFP & zyxin-RFP. Z-Stacks were taken at (0.15 μ m) distance with time-lapse series acquired over a 10 minute period with an interval of 15 second. The first column refers to local levels of PtdIns(4,5)P2 and the second column refers to zyxin assembly and disassembly. The highlighted areas show the ROI that was drawn closely around the zyxin and the PtdIns(4,5)P2 to measure the specific localisation of local levels of PtdIns(4,5)P2 within a single zyxin. The zyxin selected for measuring should be absent both in the beginning and the end of time-lapse series.

Our results showed that dynamic changes of local levels of PtdIns(4,5)P2 within zyxin and paxillin complexes increased gradually during assembly of zyxin or paxillin containing FAs, and declined gradually during disassembly of these FAs (Figures 4.2A & 4.3A). Around a single FA the dynamic changes of local levels of PtdIns(4,5)P2 during assembly and disassembly of zyxin and paxillin were slightly changed (Figures 4.2B & 4.3B). The percentage change of PtdIns(4,5)P2 within and around zyxin or paxillin was measured and found that local levels of PtdIns(4,5)P2 within zyxin or paxillin significantly higher than around zyxin or paxillin (Figures 4.2C & 4.3C).

In table 4.1, the mean of the percentage change of PtdIns(4,5)P2 during assembly with zyxin was (182 % \pm 14.77) while around zyxin was (21% \pm 4.7). The mean of the percentage change during disassembly within zyxin was (-55% \pm 4.45) while around zyxin was (-15% \pm 6.7).

In table 4.2, the mean of the percentage change of PtdIns(4,5)P2 during assembly with paxillin was (113 % \pm 6.6) while around paxillin was (23% \pm 6.9). The mean of the percentage change during disassembly within paxillin was (-55% \pm 4.9) while around paxillin was (-17% \pm 2.7)

The local levels of PtdIns(4,5)P2 were also measured at different focal planes. Our results showed the that local levels of PtdIns(4,5)P2 increased gradually during assembly of zyxin or paxillin containing FAs, and declined gradually during disassembly of these FAs (Figures 4.2D&4.3D).

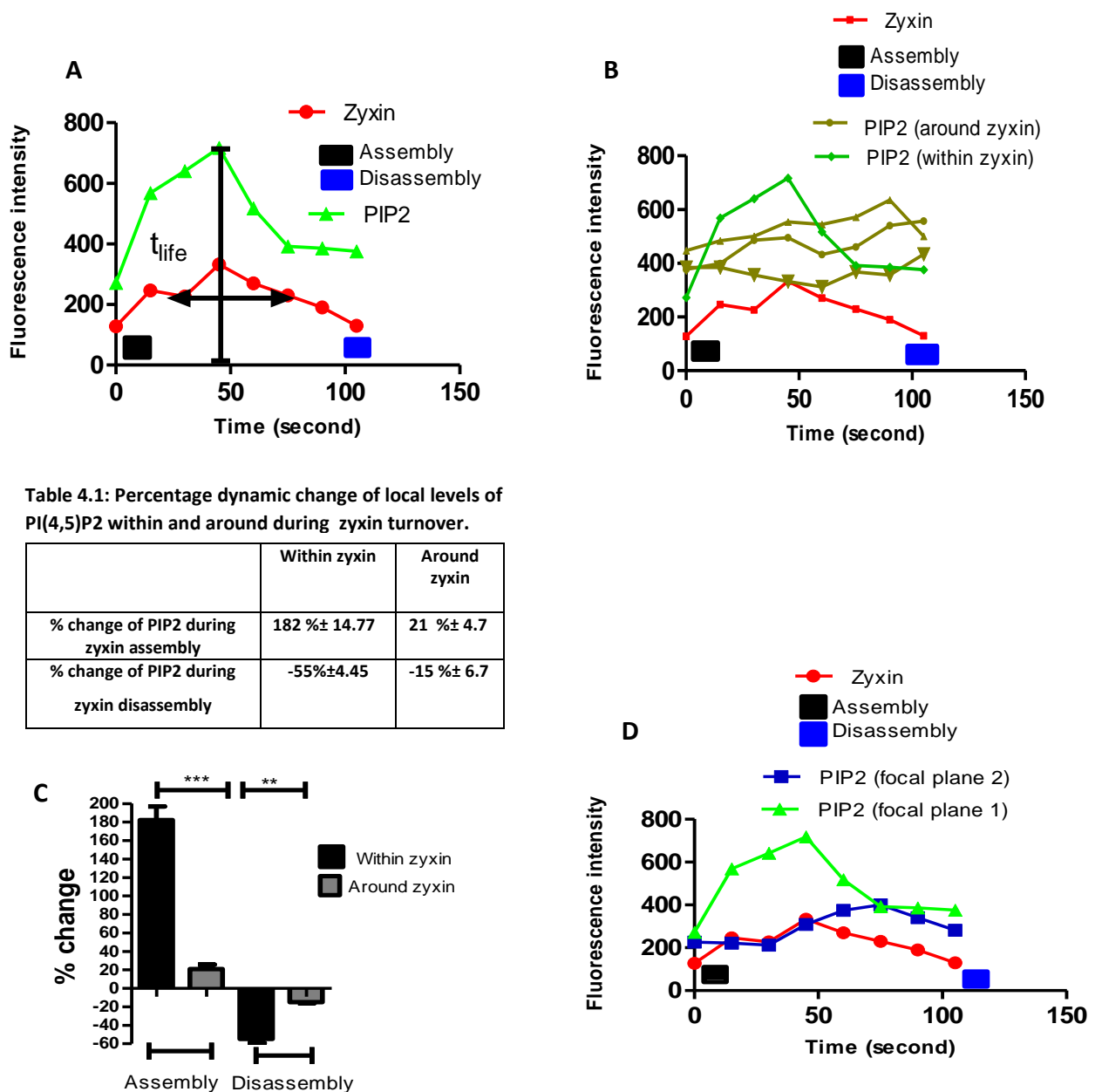


Figure (4.2): Quantification of the local levels of PtdIns(4,5)P2 within and around a single FA. A&B) The dynamic change of PtdIns(4,5)P2 within and around of zyxin during assembly and disassembly. The green curve refers to measurement the intensity level of PtdIns(4,5)P2 over time course (105 second). The red curve refers to measurement the intensity of zyxin turnover over time course (105 second). The local levels of PtdIns(4,5)P2 were increased gradually within zyxin during assembly and declined during disassembly, while around zyxin the local levels of PtdIns(4,5)P2 were slightly changed. **C)** During assembly and disassembly the percentage change of local levels of PtdIns(4,5)P2 within zyxin was significantly higher than around zyxin. **D)** Quantification of the dynamic change of PtdIns(4,5)P2 at different focal plane within zyxin during assembly and disassembly. Data are representative of n=30 FA in 10 migrating MDA-MB-231 cells. Statistical analysis was performed by one way ANOVA with Tukey's multiple comparison test. Statistical significance was accepted at *** P < 0.0005. Data represents mean ± SEM of the three independent experiments.

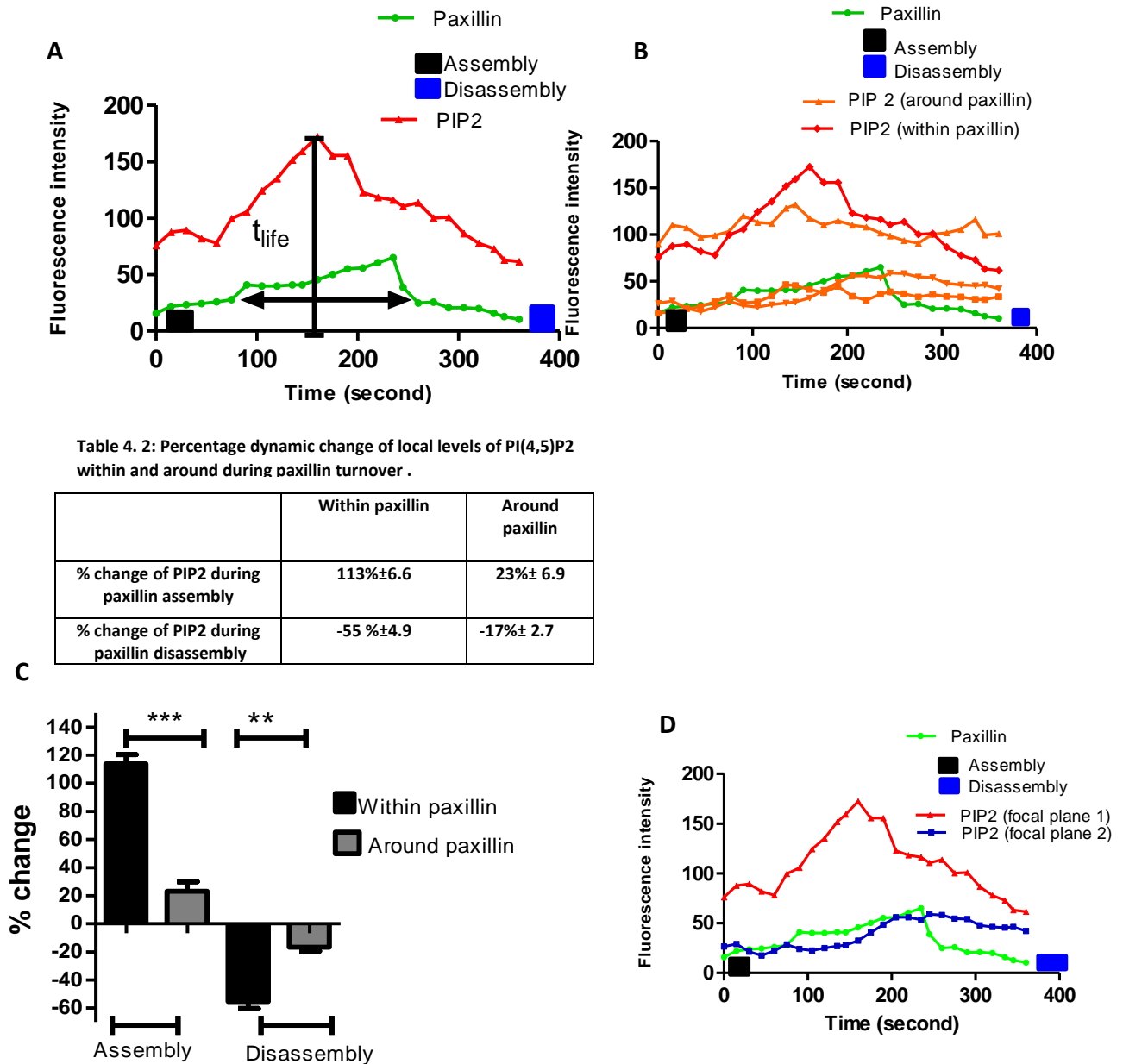


Figure (4.3): Quantification of the local levels of PtdIns(4,5)P2 within and around a single FA. A&B) The dynamic change of PtdIns(4,5)P2 within and around of paxillin during assembly and disassembly. The red curve refers to measurement the intensity level of PI(4,5)P2 over time course (105 second). The green curve refers to measurement the intensity of paxillin turnover over time course (105 second). The local levels of PtdIns(4,5)P2 were increased gradually within paxillin during assembly and declined during disassembly, while around zyxin the local level of PtdIns(4,5)P2 was slightly changed. **C)** During assembly and disassembly the percentage change of local level of PtdIns(4,5)P2 within paxillin was significantly higher than around zyxin. **D)** Quantification of the dynamic change of PtdIns(4,5)P2 at different focal plane within paxillin during assembly and disassembly. Data are representative of n=6 FA in 3 migrating MDA-MB-231 cells. Statistical analysis was performed by one way ANOVA with Tukey's multiple comparison test. Statistical significance was accepted at *** P < 0.0005. Data represents mean ± SEM of the three independent experiments.

Our results also showed that the local levels of PtdIns(4,5)P2 within n=8 FA of total number n=30 FA were at constant level during FA disassembly (Figure 4.4 A-D). 74% of FA disassembly-dependent on the PtdIns(4,5)P2 decline, while 26% of FA disassembly-independent on the PtdIns(4,5)P2 decline (Figure 4.4 C).

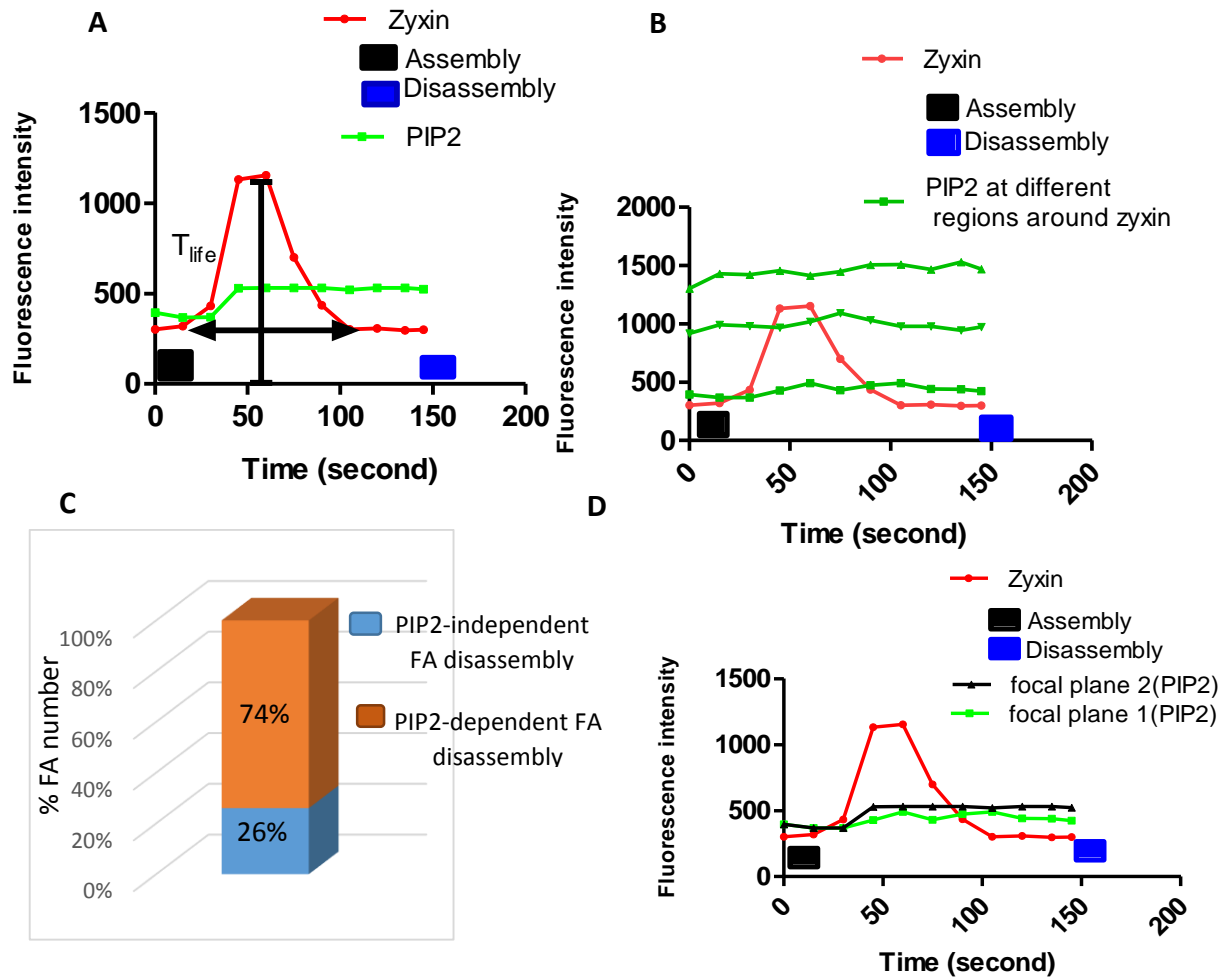


Figure (4.4): The dynamic change of local levels of PtdIns(4,5)P2 during zyxin turnover: A&B) Quantification the dynamic change of PtdIns(4,5)P2 within and around zyxin during assembly and disassembly. The green curve refers to measurement the intensity levels of PtdIns(4,5)P2 over time course (150 second). The red curve refers to measurement the intensity zyxin turnover over time course (150 second). The local levels of PtdIns(4,5)P2 were at constant level during assembly and disassembly process. **C)** 74% of FA turnover-dependent on the decline of PtdIns(4,5)P2 and 26% FA turnover-independent on the decline of PI(4,5)P2. **D)** The dynamic change of PtdIns(4,5)P2 within zyxin at different focal plane. Data are representative of n=8 FA intensity profiles in 10 migrating MDA-MB-231 cells.

4.2.2. Temporal regulation of PtdIns(3,4,5)P3 during assembly and disassembly of a single FA.

MDA-MB-231 cells were seeded on collagen (2mg/ml), then co-transfected with Btk-PH-GFP and RFP-zyxin or Btk-PH-mCherry and GFP-paxillin. The 488nm and 568nm channels were used to visualise GFP and RFP or mCherry respectively in live cell imaging (Figure 4.5). Z-Stacks were at 0.15 μ m distance with time-lapse series acquired over a 10 minute period with an interval of 15 seconds to be able to determine an accurate co-localisation between PtdIns(3,4,5)P3 and zyxin or paxillin over time. The local levels of PtdIns(3,4,5)P3 were measured at different time points and at different focal planes within and around assembly and disassembly of FAs.

Quantitative measurement of these live images was performed by ImageJ. In channel of zyxin-RFP or paxillin-GFP the region of interest was selected closely around individual zyxin or paxillin, then the same selection applied to GFP or mCherry channel of PtdIns(3,4,5)P3 to determine the specific localisation of PtdIns(3,4,5)P3 within a single FA during turnover after subtracting background. In order to measure the intensity of PtdIns(3,4,5)P3, the complete lifetimes of zyxin or paxillin turnover cycle was observed. In other words, individual zyxin and paxillin should be absent both in the beginning and the end of time-lapse series. So, single FA was selected for measuring the intensity from its appearance to the disappearance. Meanwhile, the intensity of PtdIns(3,4,5)P3 was measured from the same time frame that FA was measured and until the last frame when was disappeared (Figure 4.5). Likewise, the local levels of PtdIns(3,4,5)P3 were measured around a single FA .

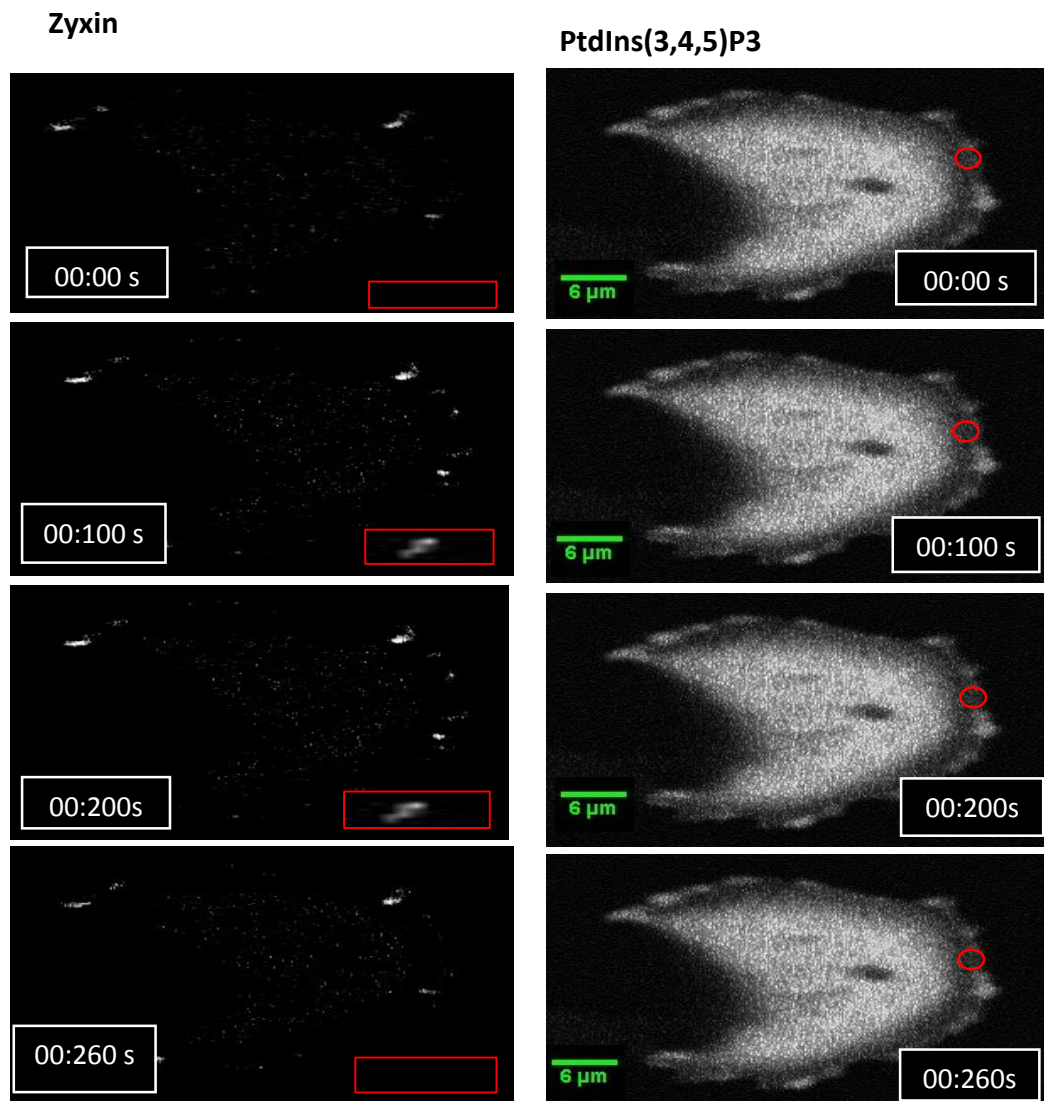


Figure (4.5): Quantification of the local levels of PtdIns(3,4,5)P3 within a single FA. Confocal live imaging showing the local level of PtdIns(3,4,5)P3 during zyxin turnover over time. The MDA-MB-231 cells were plated on (collagen 2mg/ml) and co-transfected with Btk-PH-GFP & zyxin-RFP. Z-Stacks were taken at (0.15 μ m) distance with time-lapse series acquired over a 10 minute period with an interval of 15 second. The first column refers to zyxin assembly and disassembly and the second column refers to local level of PI(3,4,5)P3. The highlighted areas show the ROI that was drawn closely around the FA and the mCherry channel of PtdIns(3,4,5)P3 to measure the specific localisation of local level of PtdIns(3,4,5)P3 within a single zyxin. The zyxin selected and for measuring should be absent both in the beginning and the end of time-lapse series.

Our results showed that dynamic changes of local levels PtdIns(3,4,5)P3 within and around zyxin and paxillin complexes were in constant level or a little fluctuation during assembly and disassembly of zyxin or paxillin containing FAs (Figures 4.6A-B & 4.7A-B). The percentage change of local level of PtdIns(3,4,5)P3 within and around zyxin and paxillin was measured during assembly and disassembly was no significant differences between them (Figures 4.6C & 4.7C).

In table 4.3, the mean of the percentage change of PtdIns(3,4,5)P3 during assembly with zyxin was (26 % \pm 4.5) while and around zyxin was (20% \pm 5.9). The mean of the percentage change during disassembly within zyxin was (-16% \pm 2.15) while around zyxin was (-15.8% \pm 1.9)

In table 4.4, the mean of the percentage change of PtdIns(3,4,5)P3 during assembly with paxillin was (25 % \pm 10.37) while and around paxillin was (28% \pm 17.76). The mean of the percentage change during disassembly within paxillin was (-24% \pm 13.20) while around paxillin was (-36% \pm 5.8).

The local levels of PtdIns(3,4,5)P3 were also measured at different focal planes and were in constant level during assembly and disassembly of zyxin or paxillin (Figures 4.6D and 4.7D).

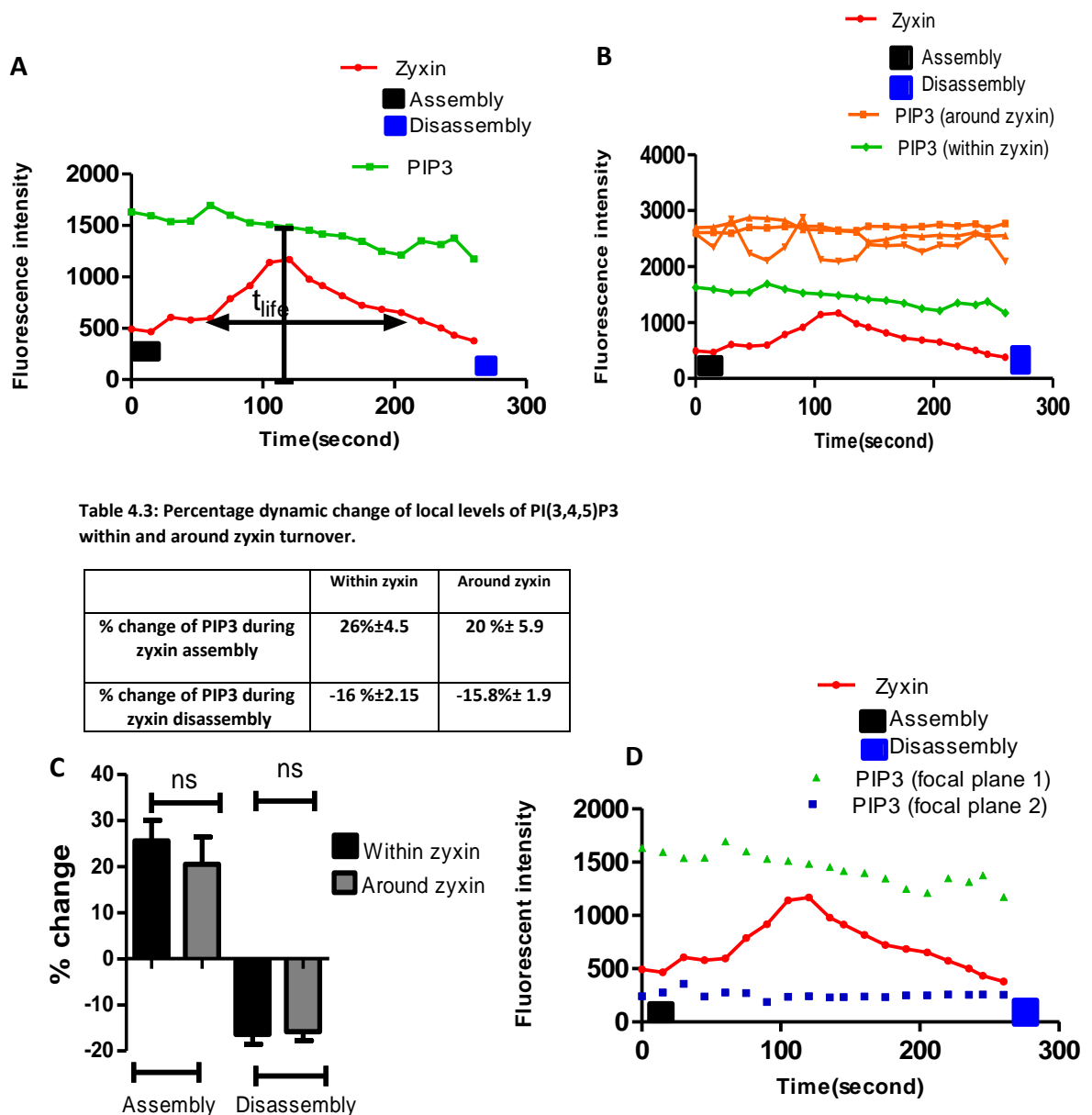


Figure (4.6): The dynamic change of local levels of PtdIns(3,4,5)P3 during zyxin turnover: A&B) Quantification the dynamic change of PtdIns(3,4,5)P3 within and around zyxin assembly and disassembly. The green curve refers to measurement the intensity level of PtdIns(3,4,5)P3 over time course (260 second). Red curve refers to measurement the intensity zyxin turnover over time course (260 second). PtdIns(3,4,5)P3 was in constant level during assembly and disassembly process. **C)** During assembly and disassembly the percentage change of local levels of PtdIns(3,4,5)P3 within zyxin and around zyxin was not significantly different. **D)** The dynamic change of PtdIns(3,4,5)P3 within zyxin at different focal plane. Data are representative of n=30 FA intensity profiles in 10 migrating MDA-MB-231 cells. Statistical analysis was performed by one way ANOVA with Tukey's multiple comparison test. Statistical significance was accepted at $P < 0.05$. Data represents mean \pm SEM of the three independent experiments.

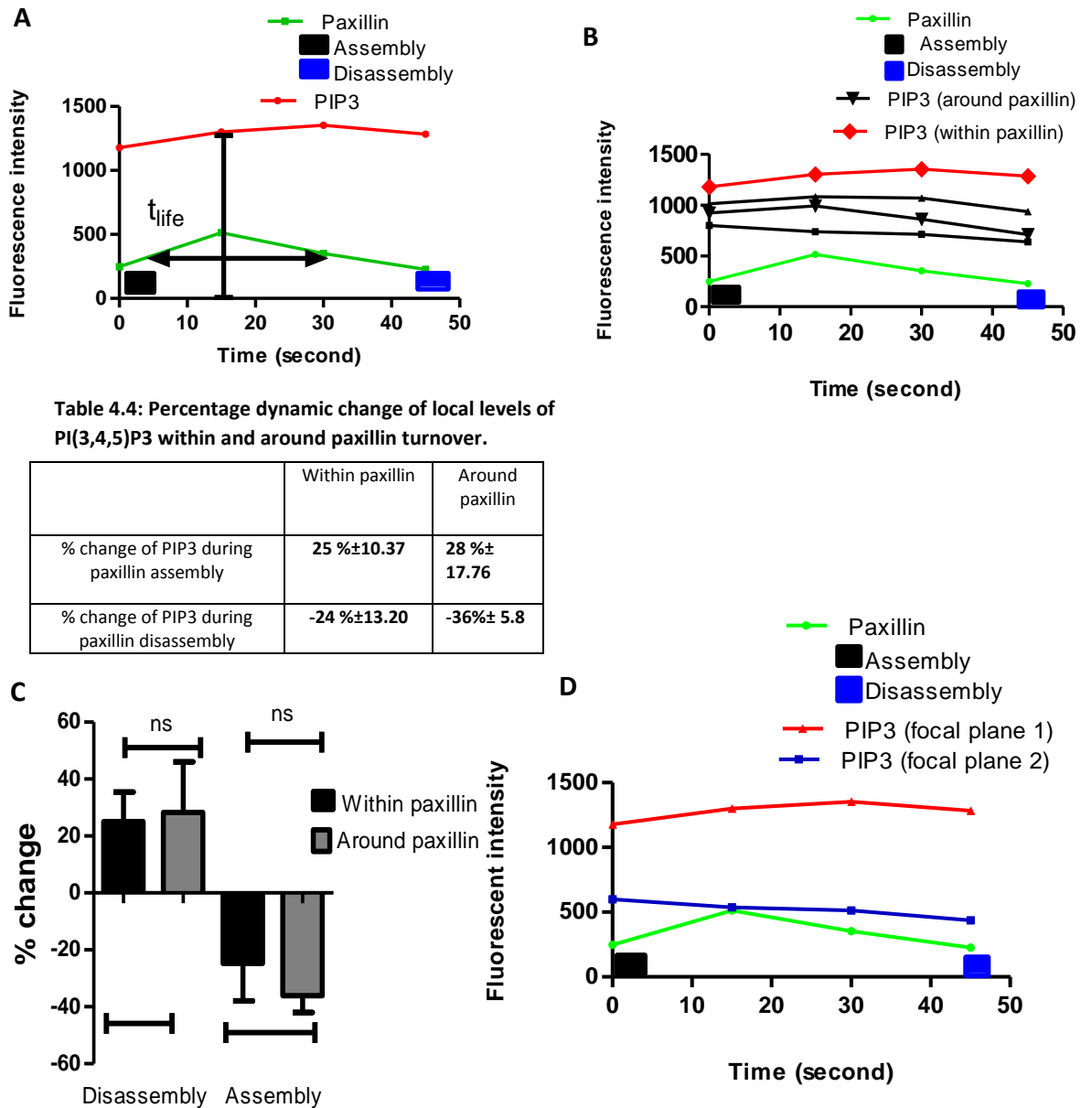


Figure (4.7): The dynamic change of local levels of PtdIns(3,4,5)P3 during paxillin turnover: A&B) Quantification the dynamic change of PtdIns(3,4,5)P3 within and around paxillin assembly and disassembly. The red curve refers to measurement the intensity level of PtdIns(3,4,5)P3 over time course (45 second). Green curve refers to measurement the intensity paxillin turnover over time course (45second). PtdIns(3,4,5)P3 was in constant level during assembly and disassembly process. **C)** During assembly and disassembly the percentage change of local levels of PtdIns(3,4,5)P3 within and around zyxin was not significantly different. **D)** The dynamic change of PI(3,4,5)P3 within paxillin at different focal plane. Data are representative of n=6 FA intensity profiles in 3migrating MDA-MB-231 cells. Statistical analysis was performed by one way ANOVA with Tukey's multiple comparison test. Statistical significance was accepted at $P < 0.05$. Data represents mean \pm SEM of the three independent experiments.

4.2.3. Discussion

The aim of this chapter was to investigate the temporal organisation of PtdIns(4,5)P₂ and PtdIns(3,4,5)P₃ within and around a single FA. These experiments were carried out by using co-transfection of biosensors-GFP or mCherry which detect PtdIns(4,5)P₂ and PtdIns(3,4,5)P₃ with GFP or RFP tagged FA proteins in live cells.

Our results showed that of local levels of PtdIns(4,5)P₂ within a single FA increased gradually during assembly and declined gradually during the disassembly process (Figures 4.2A & 4.3A). This may have a number of possible interpretations. One possibility is due to PIP5K recruitment by talin to the cell membrane during FA assembly. Activated PIP5K phosphorylates PtdIns4P to produce and increase a local enrichment of PtdIns(4,5)P₂ (Figure 4.9) (Wu et al., 2011, Izard and Brown, 2016, Legate et al., 2011). PIP5K promotes FA formation and regulates FA dynamics, so probably PtdIns(4,5)P₂ plays a role in FA dynamics through localisation or interaction with FA proteins (Wu et al., 2011, Izard and Brown, 2016, Legate et al., 2011). Izard and Brown (2016) reviewed that PtdIns(4,5)P₂ binds with talin and vinculin and alters them from an inactive form to an active state (Figure 4.8). Thus, enables talin to recruit to FA sites which in turn interacts and activates vinculin during the early stages (Figure 4.9).

It has been shown that vinculin-talin interaction might be enhanced by PtdIns(4,5)P₂ (Izard and Brown, 2016, Chandrasekar et al., 2005, Wang, 2012, Yuan et al., 2017), so possibly PtdIns(4,5)P₂ involves the regulation of the FA through associating with the tail domain of vinculin (Chinthalapudi et al., 2014). It has also been shown the enzymes that generate PtdIns(4,5)P₂ accumulated at the leading edge due to FAs assembly at the leading edge (Bae et al., 2010, Sharma et al., 2008, Thapa and Anderson, 2012, Falke and Ziemba, 2014).

In the later stages of the FA cycle activated vinculin recruits additional FA proteins, such as VASP and zyxin to the FA site (Garvalov et al., 2003) and this interaction is supported by PtdIns(4,5)P2 (Huttelmaier et al., 1998, Carisey and Ballestrem, 2011, Garvalov et al., 2003). Thus, PtdIns(4,5)P2 might increase the strength of binding between FAs and integrin during the assembly process (Saltel et al., 2009).

During FA disassembly, however, our results showed that the local levels of PtdIns(4,5)P2 declined gradually (Figure 4.2A & 4.3A). There are several possible reasons behind that. One possibility could be due to PIP5K γ loss during detachment of FAs from the ECM. Loss of PIP5K γ could be caused by deactivation of talin and which would no longer have the ability to activate and recruit PIP5K γ which is the main enzyme that generates PtdIns(4,5)P2 in cell membrane (Figure 4.9) (Wu et al., 2011, Izard and Brown, 2016, Legate et al., 2011). It has been shown that decline of PtdIns(4,5)P2 might be implicated in the FA disassembly. Mutating the vinculin- PtdIns(4,5)P2 interaction site in B16-F1 mouse melanoma cells led to the reduction of FA turnover (Chandrasekar et al., 2005, Saunders et al., 2006). It has also been shown the increase in PtdIns(4,5)P2 level by PIP5K overexpression stimulated the release of vinculin from FA in B16-F1 mouse melanoma cells (Chandrasekar et al., 2005, Saunders et al., 2006). Izard and Brown (2016) reviewed that actin interacts with the vinculin tail and breaks down the interaction between PtdIns(4,5)P2 and vinculin to complete activation during FA formation (Figure 4.8). The second possibility could be that PI3K and PLC recruitment by PtdIns(4,5)P2, where PLC converts it to DAG and IP3 while PI3K converts it to PtdIns(3,4,5)P3 (Figure 4.9) (Gericke et al., 2013). Thereby, the local levels of PtdIns(4,5)P2 can be reduced during FA disassembly (Izard and Brown, 2016, van den Bout and Divecha, 2009, Raucher et al., 2000).

The dynamic activation of PLC and PI3K and FA turnover are important events to investigate the reasons why local levels of PtdIns(4,5)P₂ declined during the disassembly process of FAs and this will be discussed further in chapter 5.

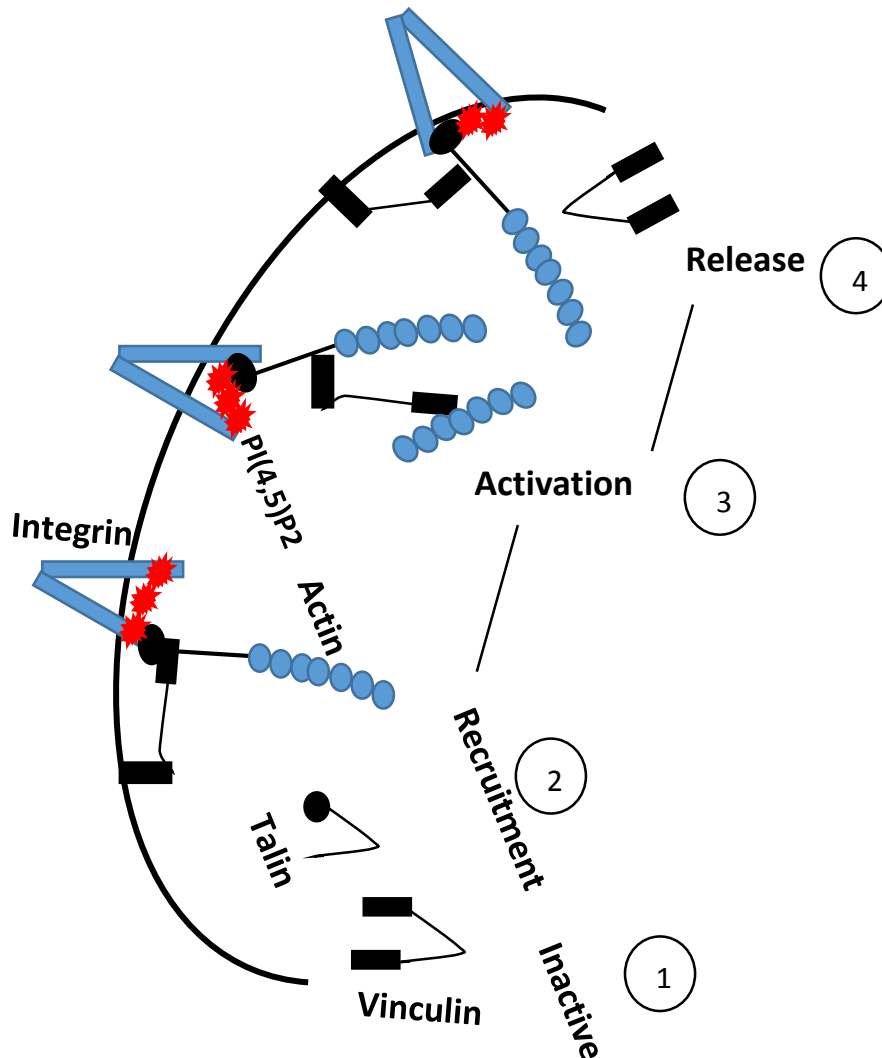


Figure (4.8): Schematic of the recruitment and release of talin and vinculin by PtdIns(4,5)P₂ during FA assembly and disassembly: 1) PtdIns(4,5)P₂ activates and recruits talin to FA complex which in turn binds with integrin. 2) During early stages vinculin is recruited by talin then interacts with PtdIns(4,5)P₂. 3) Vinculin-talin interaction might be enhanced by a local enrichment of PI(4,5)P₂. 4) Actin binds with vinculin tail and blocks the PtdIns(4,5)P₂ -vinculin interaction to complete activation this stage might be reverse to enhance the release of vinculin during the disassembly

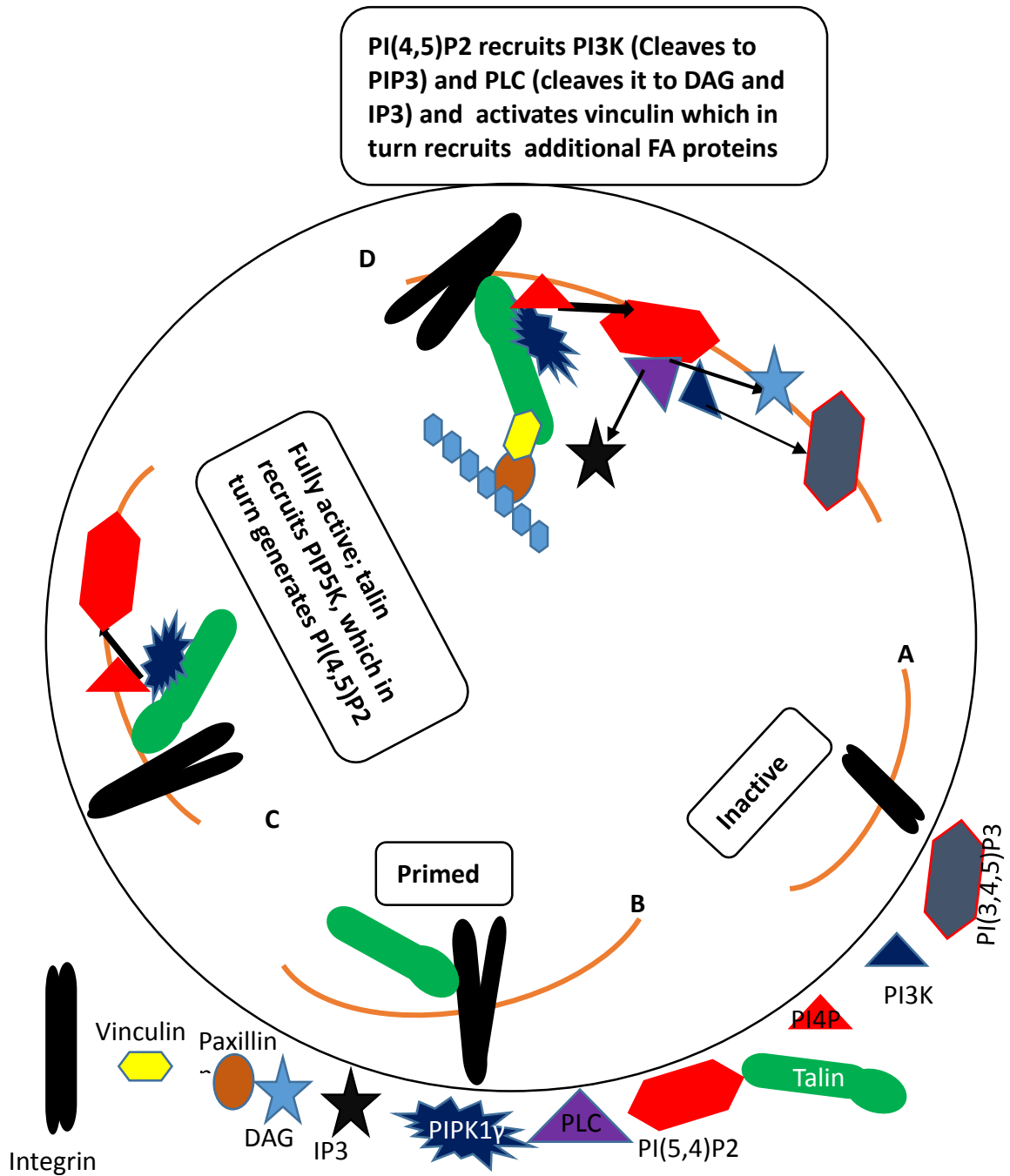


Figure (4.9): Proposed model of the interaction between PtdIns(4,5)P2 and FA proteins during assembly and disassembly process: A model showing (A) Inactive state during disassembly process where FA proteins and other kinases in the cytoplasm. (B) Integrins bind with ECM and recruit talin. (C) PIP5K is recruited by talin which in turn generates PtdIns(4,5)P2 via phosphorylating PI4P. (D) PI(4,5)P2 activates additional FA proteins such as vinculin which in turn recruits extra proteins to FA sites. PI(4,5)P2 recruits many enzymes such as PLC which cleave it to DAG and IP3 and recruits PI3K which converts to PtdIns(3,4,5)P3.

Collectively, these molecular events are in agreement with our results which show that FA activation and turnover are dependent on a local availability of PtdIns(4,5)P₂. It can be said that the decline of PtdIns(4,5)P₂ during a disassembly process might enhance the release of FAs.

However, there has long been a debate about the sequence of events leading to talin and vinculin activation. Some studies have shown that vinculin in the cytosolic environment is inactive due to its closed conformation between head-tail interaction (Johnson and Craig, 1995). This blocks the interaction of vinculin with PtdIns(4,5)P₂ (Johnson and Craig, 1995) but it can interact with PtdIns(4,5)P₂ after activation by talin (Chinthalapudi et al., 2014). It has also been shown that vinculin can be recruited to FA sites without need for activation of PtdIns(4,5)P₂ but in an inactive state (Chinthalapudi et al., 2015, Chandrasekar et al., 2005, Saunders et al., 2006). Phosphorylated paxillin recruits inactive vinculin to FA sites (Case et al., 2015, Pasapera et al., 2010). In the absence of PtdIns(4,5)P₂ or in the inability of vinculin to interact with PtdIns(4,5)P₂ the FA turnover becomes stable or inactive (Izard and Brown, 2016).

It has also been shown that talin interacts with and activates integrin. This interaction can be enhanced by PtdIns(4,5)P₂ which can change the conformation of talin. This leads exposure of its head-domain to the β -tail of integrin. PtdIns(4,5)P₂ also interacts with integrins and changes their conformation through its charged head group which can perturb the integrin at the opposite direction of the cytoplasm and promote its interaction with ECM. Thus, PtdIns(4,5)P₂ is involved in the transmission of mechanical and physical force from outside to inside the cell membrane (Orłowski et al., 2015, Ye et

al., 2016a). These studies suggest that PtdIns(4,5)P2 might play an auxiliary role in the activation of vinculin and talin (Izard and Brown, 2016).

The data in this chapter showed that the local levels of PtdIns(4,5)P2 surrounding a single FA at different regions is almost at a constant level during assembly and disassembly of FAs (Figures 4.2B & 4.3B). The percentage change of local levels of PtdIns(4,5)P2 within FAs was significantly higher than around FAs (Figure 4.2C & 4.3C) as summarised in table 4.1 & 4.2. This may mean that an enrichment of PtdIns(4,5)P2 is restricted to specific regions. So, possibly many signalling pathways in these distinct regions require PtdIns(4,5)P2 in order to recruit some kinases to these specific sites to perform their functions (Wang and Richards, 2012). Some studies have also revealed that an enrichment of PtdIns(4,5)P2 is different in concentration from one region to another (Ji et al., 2015, Wang and Richards, 2012).

Our results showed that the local levels of PtdIns(4,5)P2 were at a constant level during FA disassembly in n=8 FA of total number n=30 FA (Figure 4.4 A-D). This result may suggest there are two different mechanisms for FA disassembly; PtdIns(4,5)P2-dependent FA disassembly and PtdIns(4,5)P2-independent FA disassembly. This means that 74% of FA turnover is caused by the decline of PtdIns(4,5)P2 within FA and 26% of FA turnover probably depend on other signalling pathways or kinases involved in FA disassembly (Figure 4.4 C). So, probably provide a novel insight concerning other mechanisms which may involve in the temporal organisation of a single FA. It is important to be investigated to know other mechanisms which involved in FA turnover. This will be discussed in chapter 5.

Our data also showed that PtdIns(3,4,5)P3 within and around FAs was almost at a constant level during FA assembly and disassembly process (Figure 4.5A-B & 4.6A-B). The Percentage change within and around FA was not significantly different between them (Figure 4.5C & 4.6C) as summarised in table 4.3& 4.4. This may indicate that PtdIns(3,4,5)P3 plays a role in other aspects in cancer migration but is not fundamental in FA turnover (Qin et al., 2009). However, other studies suggest that PtdIns(3,4,5)P3 plays a role in the restructuring of FAs via association with α -actinin and deactivation of the interaction between α -actinin and β integrin (Rubashkin et al., 2014, Greenwood et al., 2000). PtdIns(4,5)P2 is essential for FA turnover, but not PtdIns(3,4,5)P3 (Wu et al., 2011).

It has been shown that PtdIns(4,5)P2 and PtdIns(3,4,5)P3 may differ in their temporal and spatial organisation (Insall and Weiner, 2001). This may suggest they perform different roles in the cell (Insall and Weiner, 2001). So, PtdIns(3,4,5)P3 might play an indirect role in cell migration through activation of signalling pathways which involve in cell migration (Insall and Weiner, 2001). This will be discussed in chapter 5.

Balla and Varnai (2009) reviewed that there are different kinases affect PtdIns(3,4,5)P3 levels, including the presence of PI3K and PTEN activity. PtdIns(3,4,5)P3 synthesis mainly relies on the presence of PI3K activity; therefore, whenever PI3Ks is recruited to the cell membrane, the synthesis of PtdIns(3,4,5)P3 increases (Thapa et al., 2015). However, it is decreased whenever PTEN is recruited to the cell membrane because PTEN dephosphorylates PtdIns(3,4,5)P3 to PtdIns(4,5)P2 (Nguyen et al., 2014). This might affect local levels of PtdIns(3,4,5)P3 and PtdIns(4,5)P2 in the cell membrane.

Previous studies have shown that the local level of PtdIns(4,5)P₂ is declined to ~40% of control through PIPK1 γ depletion, while local level PtdIns(3,4,5)P₃ is undetectable (Wu et al., 2011). This might be due to the fact that PtdIns(3,4,5)P₃ is not abundant in the cell membrane. The abundance of PtdIns(3,4,5)P₃ is much less than PtdIns(4,5)P₂ in the cell membranes (Ji et al., 2015a), PI(4,5)P₂ forms 5,000-20,000 molecules/ μm^2 of PI(4,5)P₂, but PtdIns(3,4,5)P₃ form only 2-5% of PtdIns(4,5)P₂ (Balla, 2013, Falkenburger et al., 2010). Therefore, even if there is a dynamic change in the local level of PtdIns(3,4,5)P₃ but might be undetectable during the assembly and disassembly of FA.

Z-stacks were used in live cells to record the entire cell membrane volume at different focal planes. So, PtdIns(4,5)P₂ and PtdIns(3,4,5)P₃ within a FA can be visualised precisely. The main reason for measuring PtdIns(4,5)P₂ and PtdIns(3,4,5)P₃ levels within FAs at different focal planes was to determine an accurate co-localisation between them. Paxillin is the nearest FA molecule to the cell membrane, while zyxin is the furthest away from cell membrane (Kanchanawong et al., 2010). FA complexes form around 60nm in size (Kanchanawong et al., 2010). PtdIns(4,5)P₂ and PtdIns(3,4,5)P₃ are located on the cell membrane, while FAs locate underneath the cell membrane which constitute around 60nm in size (Kanchanawong et al., 2010) as discussed in more details in chapter 3. Our data showed that local levels of PtdIns(4,5)P₂ increased and decreased gradually during an assembly and disassembly process at different focal plane (Figure 4.2D & 4.3D) . Whereas, local levels of PtdIns(3,4,5)P₃ were almost constant (Figure 4.5D & 4.6D).

The experiments in this chapter would benefit from the use of control. The binding-deficient mutant versions of the probe which can be used as a negative control, such as PLC δ -GFP PH domain mutant (R40L) which is a negative control of PLC δ -PH domain (wild type)(Várnai and Balla, 1998). R40L mutation blocks the cytosol translocation of PLC δ -PH domain (wild type) even if PLC δ is activated. Mutant domains that are unable to bind with phosphoinositides (Várnai and Balla, 1998). They can be used to define specificity of the biosensors and to ensure that any changes that are observed in PtdIns(4,5)P₂ are not a consequence of changes in the shape or amount of membrane within and around a single FA turnover(Várnai and Balla, 1998, Balla and Várnai, 2009).

Furthermore, due to the PLC δ -GFP PH domain mutant (R40L) stops the PH domain binding to PtdIns(4,5)P₂ but would not stop it binding to membrane proteins, it is important to use a myristoylated/palmitoylated GFP (PM-GFP) or GFP-CAAX are preferentially targeted to and serve as markers of the membrane proteins (Botelho et al., 2000, Madugula and Lu, 2016). Then, quantify the amount of PM-GFP and PLC δ -PH-GFP within and around FA turnover. This quantitation confirms PLC δ -PH-GFP mutant does not bind to membrane proteins and the changes within FA turnover due to PtdIns(4,5)P₂ levels as Grinstein laboratory describing similar changes in lipid levels at the site of phagocytosis (Botelho et al., 2000).

In order to maintain the increase in local levels of PtdIns(4,5)P₂ which occur within FA assembly it is possible to block the enzymes which hydrolyse PtdIns(4,5)P₂, such as PLC and PI3K using inhibitors or siRNA/shRNA. Alternatively PIP5K could be targeted by these approaches as this is the main enzyme that generates PtdIns(4,5)P₂.

Utilising PH domains as genetically encoded probes for phosphoinositides have advantages and limitations. Some PH domains have affinity and specificity to bind with particular lipids. As they are genetically encoded PH domains fused with GFP are more suitable for detecting and studying the dynamics of phospholipid-binding proteins in live cells (Balla and Varnai, 2009, Idevall-Hagren and De Camilli, 2015).

Lipid changes can be quantified as a ratio of fluorescence intensity by using approaches including single-particle tracking (SPT), fluorescence recovery after photobleaching (FRAP) and fluorescence correlation spectroscopy (FCS) (Maekawa and Fairn, 2014, Balla and Varnai, 2009). Many signal-transduction pathways and protein-protein interactions can be studied using PH domains as genetically encoded fluorescent probes by direct binding with phosphoinositide. The spatiotemporal of these signalling and membrane trafficking can also be investigated at the single-cell level.

However, there are limitations to the use of GFP/mCherry-tagged domains for studying phosphoinositide signalling in living cells. One limitation is overexpressed phosphoinositide-proteins binding could sequester phosphoinositide from its endogenous interaction partners (Halet, 2005). The overexpression of GFP/mCherry-tagged domain might also influence the specificity of interaction between phosphoinositides and kinases, and interfere with other cell signalling functions (Balla

and Varnai, 2009). This could affect their downstream signalling (Idevall-Hagren and De Camilli, 2015, Balla and Varnai, 2009).

A further limitation is that measurement of change of fluorescent probe intensity might be caused by cell movement or membrane shrinkage and uneven illumination between taking two images will create artificial gradients in ratio images. Thus, fluorescent probe intensity may give rise to misinterpretation and photobleaching over time of live imaging may also affect the change in intensity ratio during total laser exposure time (Halet, 2005).

It has been shown that PH domains can bind to phosphoinositides with varying degrees of specificity as some phosphoinositide have approximately similar structure of inositol ring. So, PH domains might bind with more than one phosphoinositide (Halet, 2005).

In conclusion, there are many crucial factors that should be considered when using fluorescent proteins including physical and biological parameters each of which can significantly effect on experiment, including protein expression, folding efficiency, stability and environmental sensitivity. Controlling these factors can facilitate monitoring protein dynamics and expression in living cells, measuring protein turnover, tracking protein localization, monitoring biochemical changes within the cellular environment and measuring protein-protein interactions (Newman et al., 2011).

Taken together, our results suggest that PtdIns(4,5)P2 might regulate FA dynamic turnover during an assembly and disassembly process to facilitate cell migration. The temporal change of PtdIns(4,5)P2 within a single FA turnover reflects the role PtdIns(4,5)P2 in cancer cell migration. This will be discussed further in chapter 5.

Chapter five: The role of the PLC and PI3K signalling in FA turnover and cell migration.

5.1. Introduction

In order to determine the reasons for the changes in PtdIns(4,5)P₂ within single FA disassembly it is important to study the effect of PLC and PI3K signalling on PtdIns(4,5)P₂ and FA turnover.

PI3K isoforms use PtdIns(4,5)P₂ as a major substrate after activation by different signalling, such as p110 α , p110 δ , and p110 γ are activated by RAS signalling, p110 β is activated by Rho signalling (Thorpe et al., 2015) and p85 is activated by RTKs to produce PtdIns(3,4,5)P₃ which in turn activates Akt/mTOR signalling. The PI3Ks are involved in the regulation of cell growth, cell survive and proliferation (Laplante and Sabatini, 2009, Slomovitz and Coleman, 2012), either via the direct interaction with proteins, or the indirect interaction with other signalling pathways (Cain and Ridley, 2009). They also play a role in cancer through the occurrence of mutations in the p110 α which is frequently mutated, and p110 β , p110 δ , and p110 γ which are rarely mutated (Thorpe et al., 2015).

Beside that PI3Ks signalling participates in the regulation of integrin signalling and FAs complexes (Wegener et al., 2007, Somanath et al., 2007, Tadokoro et al., 2003), via interaction with Src, Ras signalling (Cote and Vuori, 2007, Cain and Ridley, 2009), RhoA signalling (Tadokoro et al., 2003, Graupera et al., 2008) and activate myosin II (Tadokoro et al., 2003, Graupera et al., 2008). The PI3K p110 β and p85 α are also involved in the disassembly process through interaction with Rab5 that activates endocytosis (Zerial and McBride, 2001, Chamberlain et al., 2004). This lead to internalisation and recycling of integrin and FAs by endocytosis from trailing edge to leading edge (Jones et al., 2006).

This process is regulated by Akt which is one of the main downstream targets for PI3K signalling (Roberts et al., 2004, Chamberlain et al., 2004).

The PLC family (β , γ , δ , ϵ , ζ , η) consists of pleckstrin homology (PH) domain, catalytic X and Y domain, Ca^{2+} -dependent phospholipid binding domain (C2) and EF-hand motif (EF) (Rebecchi and Pentylala, 2000). They have also been shown to use $\text{PtdIns}(4,5)\text{P}_2$ as a substrate. They are involved in the regulation of cell migration and FAs through their second messengers, such as Ca^{2+} and DAG, which interact with other signalling pathways and FA proteins to enhance FAs turnover (Tsai et al., 2015, Tsai et al., 2014).

At the molecular level it has been found that PI3Kp85 is able to interact with vinculin in OCUM-2MD3 cells (Matsuoka et al., 2012), with paxillin in NMuMG cells (Tsubouchi et al., 2002) and binds to FAK (Tyr-397) in vitro and in vivo and then activates PI3K during cell adhesion (Chen et al., 1996, Guinebault et al., 1995, Chen and Guan, 1994). PLC- γ 1(C-terminal SH2 domain) is identified to be able to interact with the FAK Tyr-397 site in COS-7 cells (Zhang et al., 1999), and also identified to be able to bind to the actin-cytoskeleton (Pei et al., 1996).

These studies have demonstrated a role for a PLC and PI3K signalling in cell migration. However, it is not clear whether these kinases work together in concert to enhance FAs disassembly process via hydrolysis of $\text{PI}(4,5)\text{P}_2$. It is also not clear whether PLC and PI3K isoforms interact with FA proteins in breast cancer cells.

The aims of this chapter are to determine the causes of the temporal change of $\text{PtdIns}(4,5)\text{P}_2$ during single FA disassembly, by investigating the interaction of PLC and PI3K within the molecular composition of FAs, and their effect on FA turnover, cell migration and wound healing will be investigated.

5.2. Results

5.2.1. PLC and PI3K inhibitors reduce the decline of PtdIns(4,5)P2 during FA disassembly:

In order to determine the reasons for the temporal decline in PtdIns(4,5)P2 levels within FAs during their disassembly it is important to inhibit PLC and PI3K signalling, to determine what role they play in this process.

MDA-MB-231 cells were seeded on collagen (2mg/ml), and co-transfected with PLC δ 1-PH-GFP and RFP-zyxin for 24 hour, then treated with PLC U73122 inhibitor (1 μ m), PI3K LY294002 inhibitor (25 μ m) and DMSO used as control and incubated over 10 and 30 min. The 488nm and 568nm channels of confocal microscopy were used to visualise GFP and RFP or mCherry respectively in live cell imaging. Quantitative measurement of these live images was performed by ImageJ after subtracting background. In the channel of zyxin-RFP the region of interest (ROI) was selected closely around individual zyxin regions, then ROI was applied to the GFP-channel of PtdIns(4,5)P2 to determine the specific localisation of PtdIns(4,5)P2 within zyxin regions. In order to measure the intensity of lifetimes of zyxin the complete zyxin turnover cycle was observed. The individual zyxin regions selected for measuring were absent both in the beginning and the end of time-lapse series. The intensity of PtdIns(4,5)P2 was measured from the same time frame that zyxin was measured until the last frame in which zyxin disappeared. The percentage decline of PtdIns(4,5)P2 level during zyxin disassembly was measured in both untreated cells and treated cells (Figures 5.1 A-C and 5.3 A-C). Our results showed that the percentage decline is significantly reduced during the disassembly of zyxin

following incubation with the PLC inhibitor, while the PI3K inhibitor had little effect (Figures 5.2 & 5.4).

In tables 5.1 & 5.2, compared with DMSO control, the mean of the percentage decline of PtdIns(4,5)P₂ during disassembly of zyxin was significantly reduced after PLC U73122 treatment from 43 %± 0.98 to 24. %± 1.1, while PI3K LY294002 treatment had only a small effect which was from 43 %± 0.98 to 38%± 1.6.

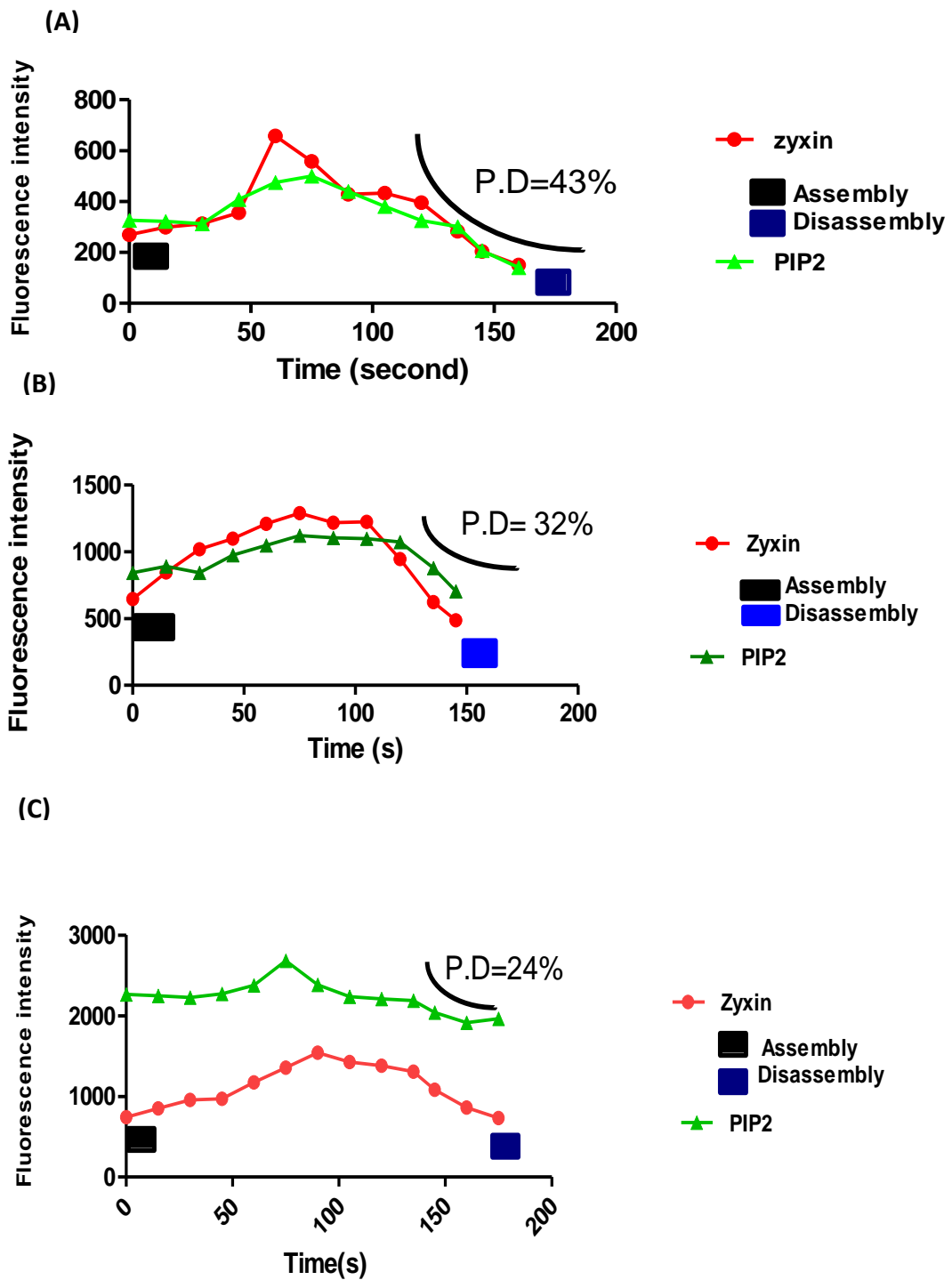


Figure (5.1): Effect of PLC on the decline of PtdIns(4,5)P2 during FA disassembly. MDA-MB-231 cells were plated on (collagen 2mg/ml) and co-transfected with PLC δ 1-PH-GFP & zyxin-RFP. **A)** Cells were treated with DMSO and incubated 10 and 30 min. **B)** Cells were treated with PLC (U73122) inhibitor (1 μ m) and incubated 10 min. **C)** Cells were treated with PLC (U73122) inhibitor (1 μ m) and incubated 30 min. Graphs representative three independent experiments. PD (Percentage Decrease).

Table 5.1: Percentage decrease of local levels of PtdIns(4,5) within zyxin disassembly.

	DMSO	10 min	30 min
Percentage decrease of PIP2 during zyxin disassembly	43 %± 0.98	32. %± 1.2	24. %± 1.1

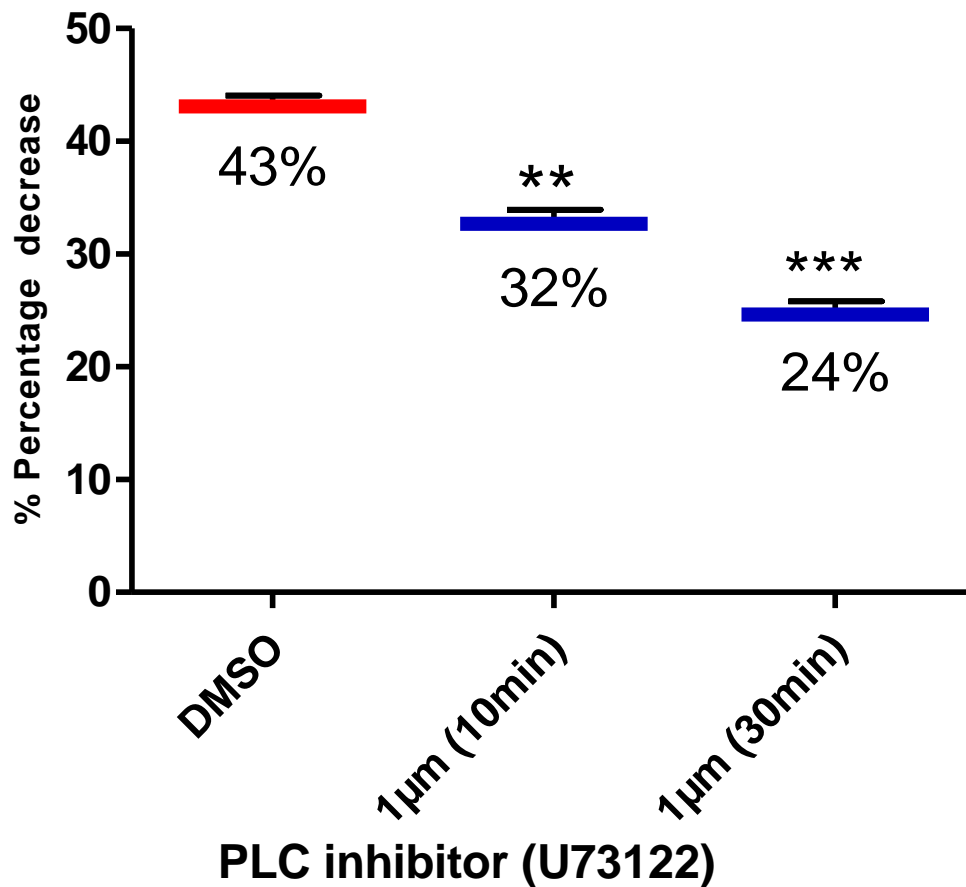


Figure (5.2): PLC (U73122) inhibitor reduces the decline of PtdIns(4,5)P2 during FA disassembly. Statistical analysis of percentage decline of PtdIns(4,5)P2 within a single FA this graph is representative of n=10 FA intensity profiles in 4 migrating MDA-MB-231 cells. The decline of PtdIns(4,5)P2 was significantly reduced when incubated during 30 min. Statistical analysis was performed by one way ANOVA with Dunnett's test for multiple comparison. Statistical significance was accepted at *** P < 0.0005. Data represents mean ± SEM of the three independent experiments.

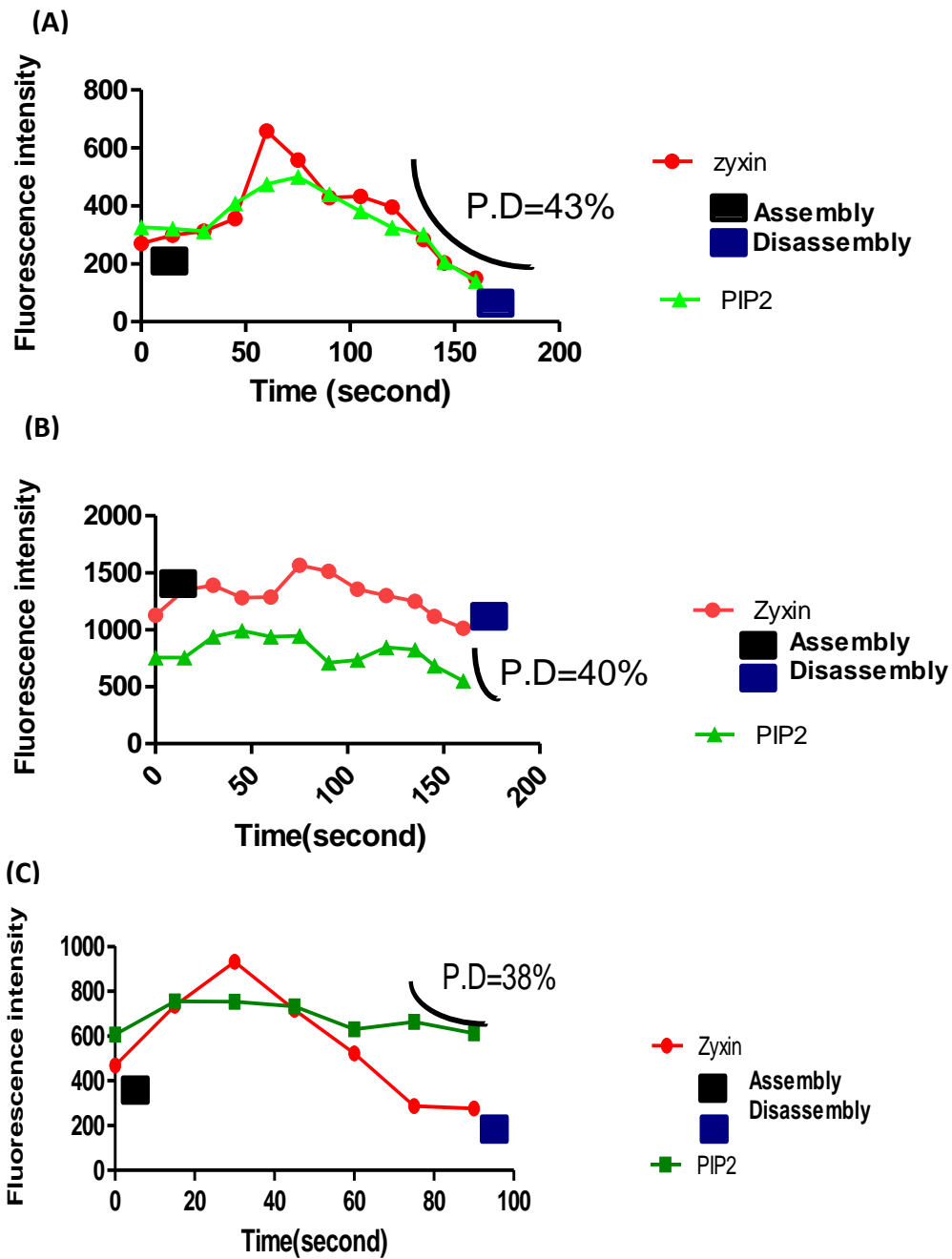


Figure (5.3): Effect of PI3K on the decline of PtdIns(4,5)P2 during FA disassembly. MDA-MB-231 cells were plated on (collagen 2mg/ml) and co-transfected with PLC δ 1-PH-GFP & zyxin-R FP. **A)** Cells were treated with DMSO and incubated 30 min. **B)** Cells were treated with PI3K (LY294002) inhibitor (25 μ m) and incubated 10 min. **C)** Cells were treated with PI3K (LY294002) inhibitor (25 μ m) and incubated 30 min. Graphs representative three independent experiments. PD (Percentage Decrease).

Table 5.2: Percentage decrease of local levels of PtdIns(4,5)P2 within zyxin disassembly.

	DMSO	10 min	30 min
Percentage decrease of PIP2 during zyxin disassembly	43 %± 0.98	40 %± 0.72	38%± 1.6

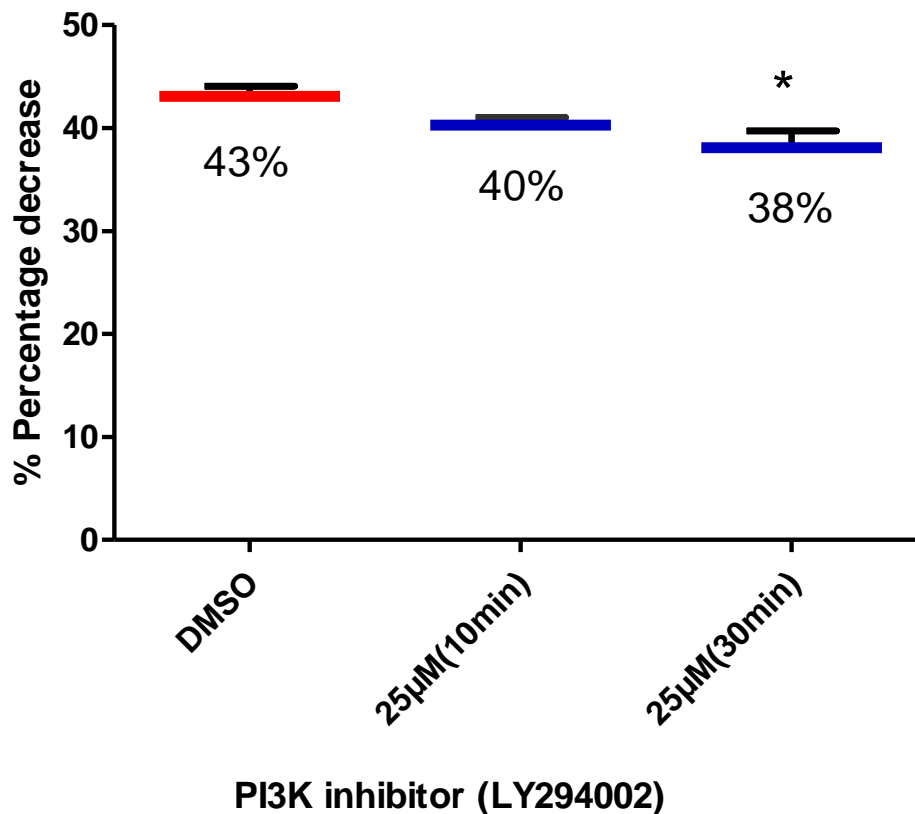


Figure (5.4): PI3K (LY294002) inhibitor reduces the decline of PtdIns(4,5)P2 during FA disassembly. Statistical analysis of percentage decline of PtdIns(4,5)P2 within a single FA during disassembly this graph is representative of n=10 FA intensity profiles in 4 migrating MDA-MB-231 cells. The decline of PtdIns(4,5)P2 was reduced significantly when incubated during 30 min. Statistical analysis was performed by one way ANOVA with Dunnett's test for multiple comparison. Statistical significance was accepted at at * P < 0.05. Data represents mean ± SEM of the three independent experiments.

5.2.2. Effect of PLC and PI3K inhibition on FA turnover:

Experiments were carried out to study the effect of PLC and PI3K signalling pathways on FA turnover rates. MDA-MB-231 cells were seeded on collagen (2mg/ml), and transfected with RFP-zyxin for 24 hours, then treated with PLC (U73122) inhibitor (1 μ m), PI3K (LY294002) inhibitor (25 μ m) and DMSO used as a control and incubated over 10 and 30 min (Figures 5.5 & 5.7). The 568nm channel of confocal microscopy was used to visualise RFP-zyxin in live cell imaging. Quantitative measurement of zyxin turnover was performed by ImageJ after subtracting background. Our data showed that PLC and PI3K inhibitor slow zyxin turnover during 30 minute (Figures 5.6 & 5.8). In tables 5.3 & 5.4, compared with DMSO control, the mean of the turnover time of zyxin was significantly decreased after PLC U73122 treatment from $32 \pm 0.88s$ to $42 \pm 1.3s$ and PI3K LY294002 treatment from $32 \pm 0.88s$ to $41 \pm 2.5s$.

5.2.3. Effect PLC and PI3K inhibition on cell migration and wound healing:

Experiments were carried out to study the effect of PLC and PI3K signalling pathway on cell migration and wound healing. MDA-MB-231 cells were seeded on fibronectin (20 μ g/ml) for 24 hours then treated with PI3K (LY294002 & Wortmannin) inhibitor and PLC (U73122) inhibitor with different concentrations and incubated for 24 hours. Speed of cell migration and wound closure were measured by using ImageJ. In Figures 5.9, 5.10 & 5.11, our data showed that MDA-MB-231 cells were significantly inhibited by PI3K and PLC inhibitor.

In figures 5.9 A, 5.10A & 5.11A, compared with DMSO control, the mean speed of cell migration was inhibited significantly after 3 μ M PLC U73122 24 hrs treatment from 22 \pm 2.9 to 5 \pm 0.6 μ m/hr⁻¹, 50 μ M PI3K LY294002 24 hrs treatment was from 15 \pm 0.9 to 4.5 \pm 0.7 μ m/hr⁻¹ and 50 μ M PI3K Wortmannin 24 hrs treatment was from 14.7 \pm 0.9 to 5 \pm 0.4 μ m/hr⁻¹.

MDA-MB-231 cells were also seeded on fibronectin (20 μ g/ml) and left to grow until they become 100% confluent then a wound was made (Figure 5.10A & 5.12A). Then cell were treated with PI3K inhibitor (LY294002 & Wortmannin) and PLC inhibitor (U73122) with different concentrations and incubated for 24 hours. Wound healing assay data showed both PI3K inhibitor and PLC inhibitor reduced wound healing significantly.

In figures 5.9 B& 5.10B & 5.11B, compared with DMSO control, the mean of wound closure was significantly decreased after 3 μ M PLC U73122 24 hrs treatment from 58% \pm 1.4 to 12% \pm 1.2, 50 μ M PI3K LY294002 24 hrs treatment was from 62.6% \pm 1.5 to 3.9% \pm 2.9 and 50 μ M PI3K Wortmannin 24 hrs treatment was from 57% \pm 8.0 to 22.6% \pm 4.6.

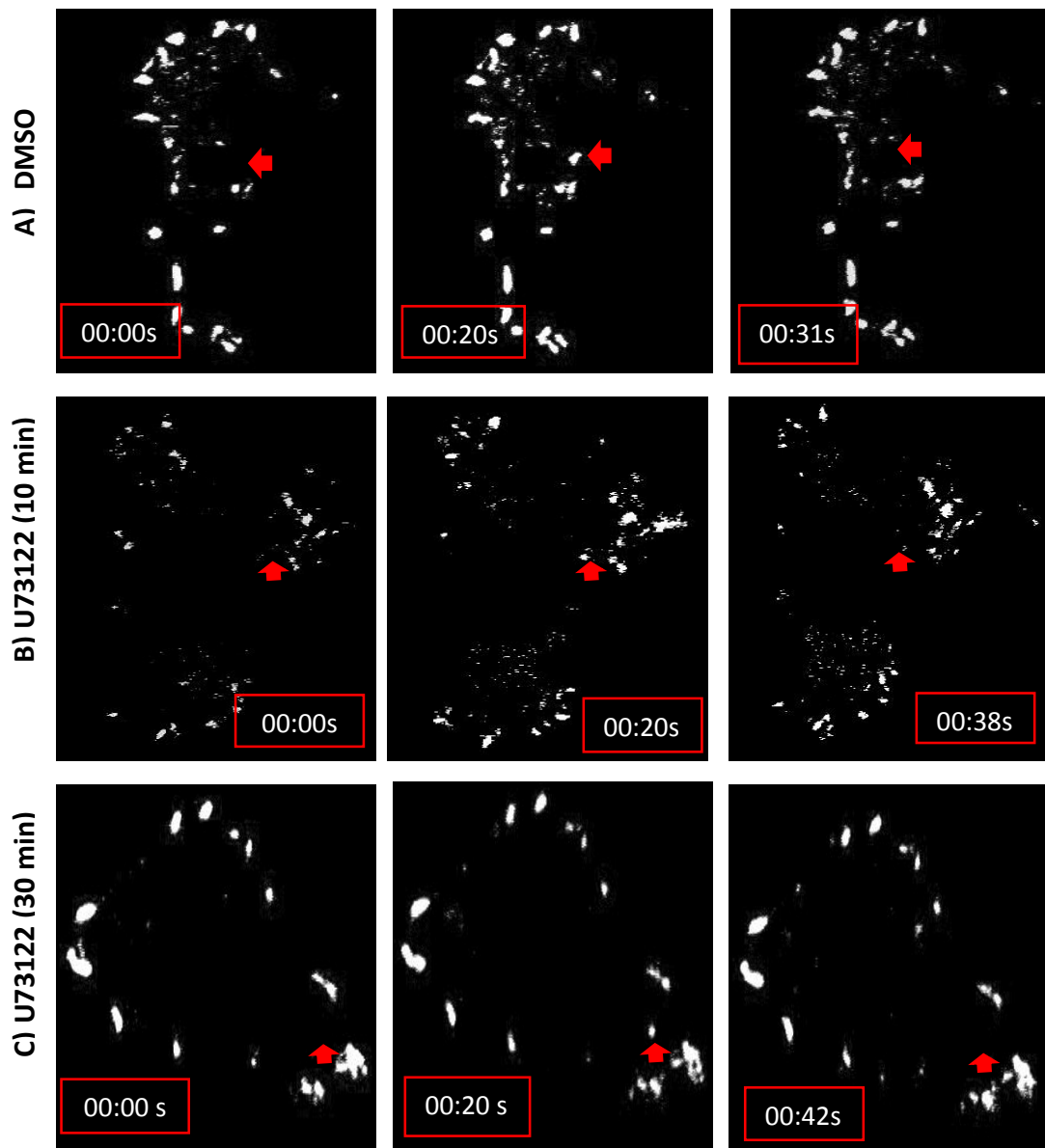


Figure (5.5): Effect of PLC inhibitor (U73122) on FA turnover: Confocal live imaging showing zyxin turnover over time. MDA-MB-231 cells were plated on collagen (2mg/ml), and transfected with RFP-zyxin for 24 h. **A)** The Cells were treated with DMSO and incubated 10 and 30 min. **B)** The Cells were treated with PLC (U73122) inhibitor (1 μ m) and incubated 10 min. **C)** The Cells were treated with PLC (U73122) inhibitor (1 μ m) and incubated 30 min. The red arrow refers to zyxin turnover during time.

Table 5.3: Effect of PLC inhibitor on FA turnover time

	DMSO	10 min	30 min
Turnover time of Zyxin	32 ± 0.88s	39 ± 1.8s	42 ± 1.3s

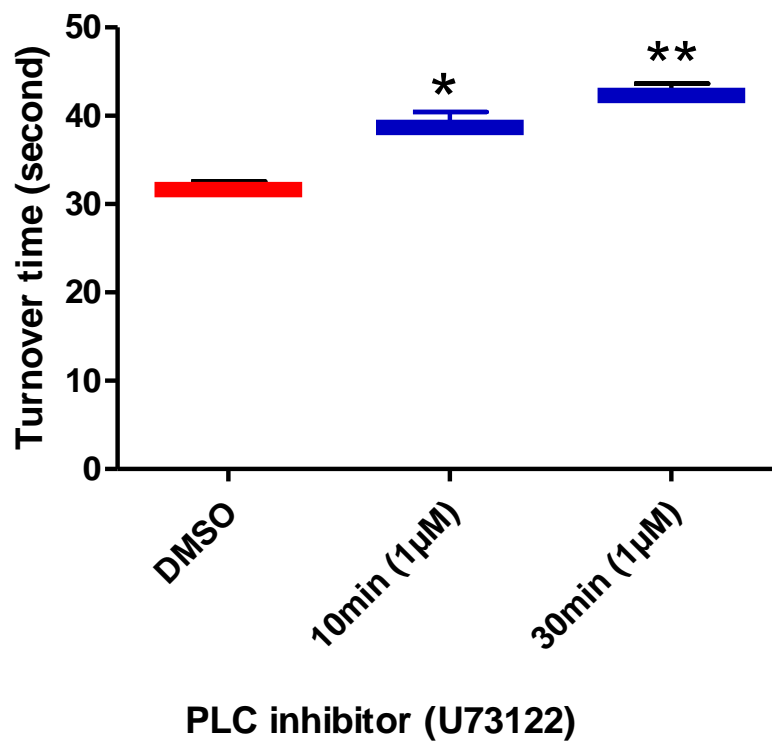


Figure (5.6): Effect of PLC inhibitor (U73122) on FA turnover: Statistical analysis of turnover of zyxin rates from n=40 FA intensity profiles in 10 migrating MDA-MB-231 cells. The turnover of zyxin rate decreased significantly when incubated with U73122 for during 30 min. Statistical analysis was performed by one way ANOVA with Dunnett's test for multiple comparison. Statistical significance was accepted at ** P < 0.05. Data represents mean ± SEM of the three independent experiments.

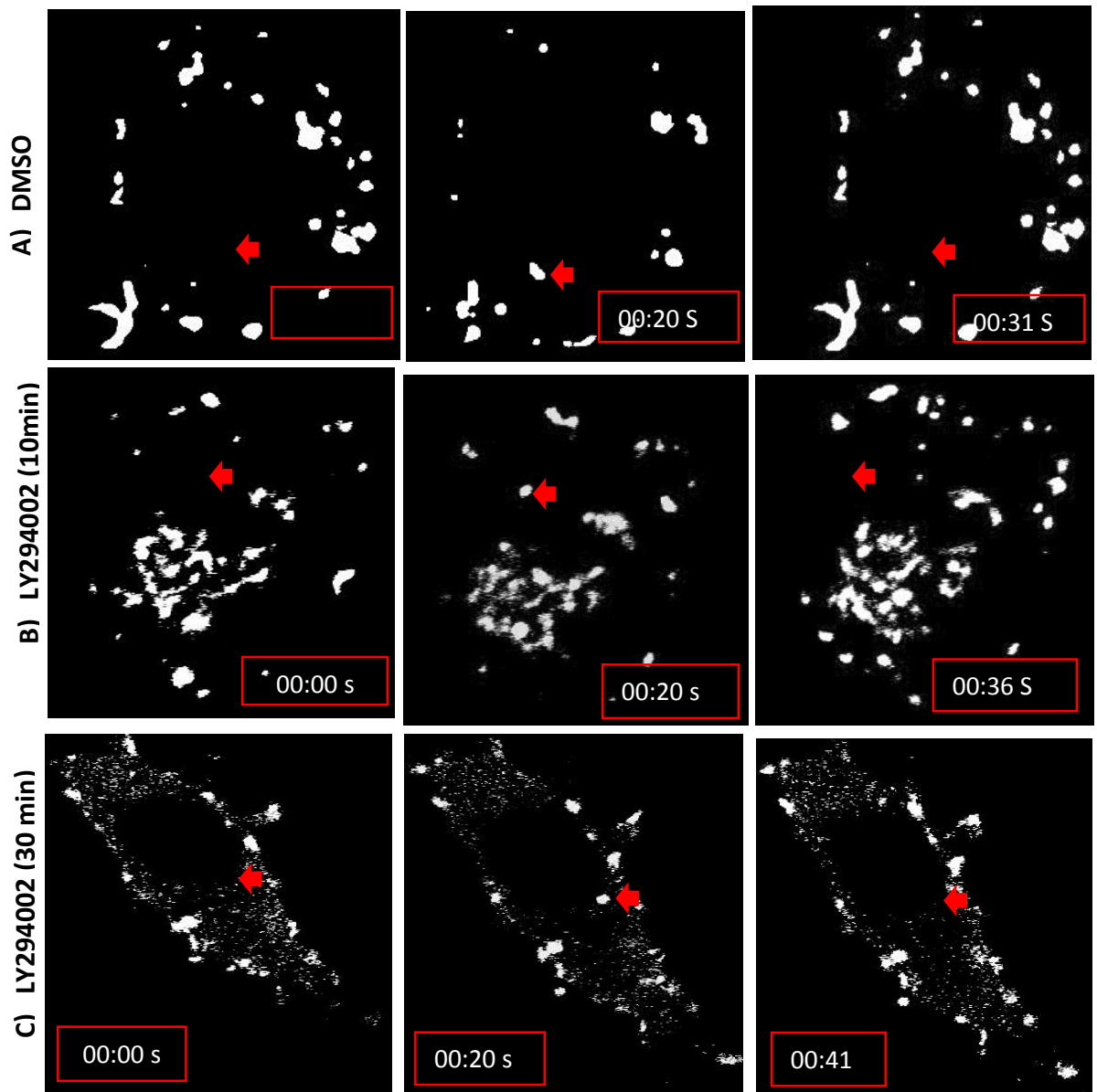


Figure (5.7): Effect of PI3K inhibitor (LY294002) on FA turnover: A) Confocal live imaging showing zyxin turnover time. MDA-MB-231 cells were plated on collagen (2mg/ml), and transfected with RFP-zyxin for 24 h. **A)** The Cells were treated with DMSO and incubated 10 and 30 min. **B)** The Cells were treated with PI3K (LY294002) inhibitor (25 μ m) and incubated 10 min. **C)** The Cells were treated with PLC (LY294002) inhibitor (25 μ m) and incubated 30 min. Red arrow refers to zyxin turnover over time.

Table (5:4): Effect of PI3K (LY294002) inhibitor on FA turnover time

	DMSO	10 min	30 min
Turnover time of zyxin	32 ± 0.88 s	36 ± 2.9s	41± 2.5s

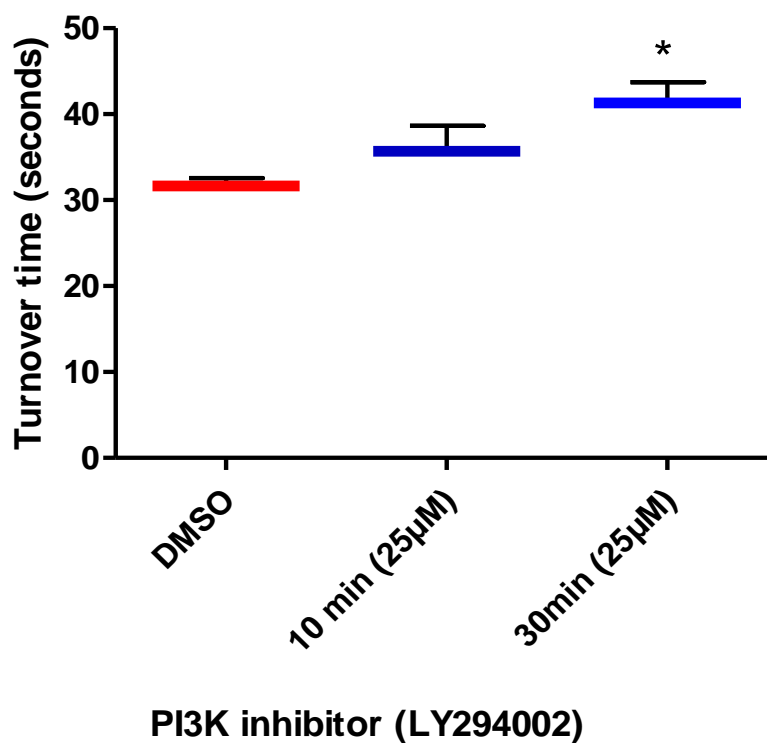


Figure (5.8): Effect of PI3K inhibitor (LY294002) on FA turnover. Statistical analysis of turnover of zyxin rates from n=40 FA intensity profiles in 10 migrating MDA-MB-231 cells. The turnover of zyxin rate decreased significantly when incubated with LY294002 for 30 min. Statistical analysis was performed by one way ANOVA with Dunnett's test for multiple comparison. Statistical significance was accepted at *P < 0.05. Data represents mean ± SEM of the three independent experiments.

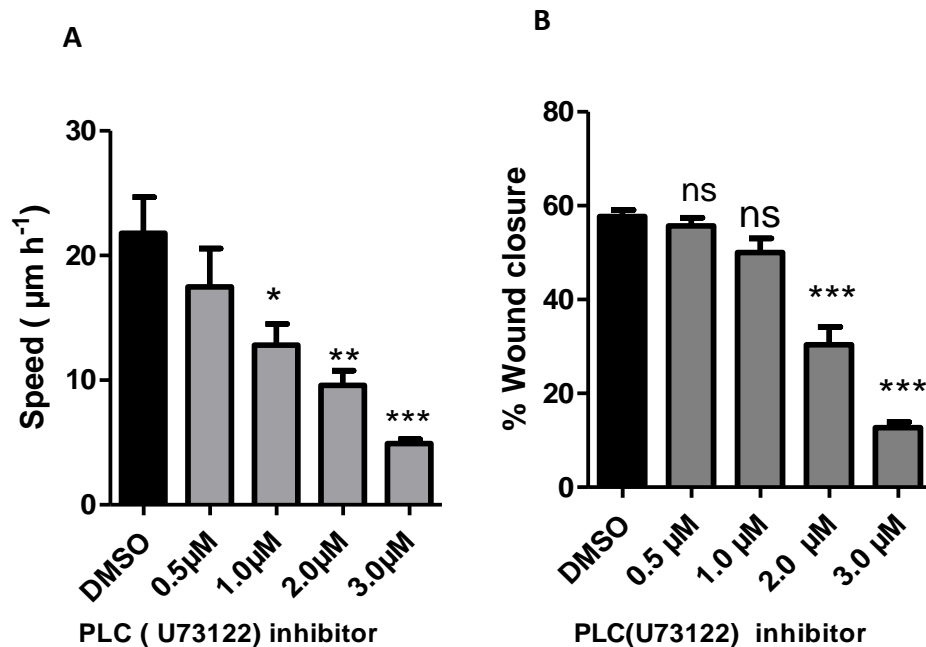


Figure (5.9): Effect of PLC U73122 inhibitor on cell migration and wound healing in MDA-MB-231 cells on a fibronectin surface. A) Control: treated with DMSO, and others wells were treated with U73122 at (0.5 μM , 1 μM , 2 μM and 3 μM). Time-lapse microscopy was used to track cell migration for 24 hours and MTrackJ was used to measure cell migration the mean total distance inhibited significantly compared with control. **B)** Control: treated with DMSO, and others wells were treated with U73122 at (0.5 μM , 1 μM , 2 μM and 3 μM). An inverted microscopy was used to capture wound healing in 0 time and after 24 hours and ImageJ was used to measure wound closure at 0 and 24 hours the mean total wound closure was inhibited significantly compared with control. Statistical analysis was performed by one way ANOVA with Dunnett's test for multiple comparison. Statistical significance was accepted at *** P < 0.0005. Data represent mean \pm SEM of the three independent experiments.

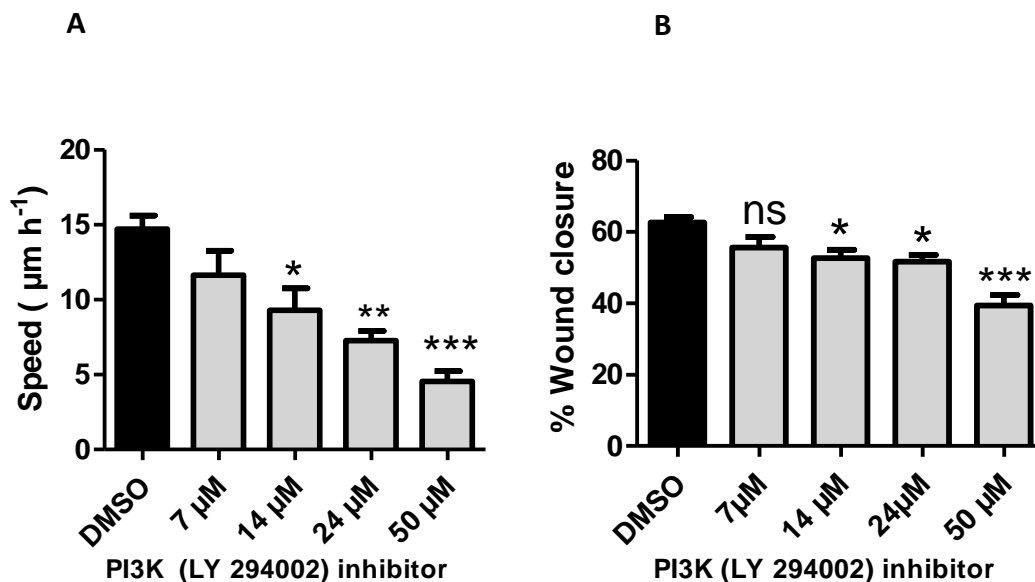


Figure (5.10): Effect of PLC LY294002 inhibitor on cell migration and wound healing in MDA-MB-231 cells on a fibronectin surface. A) Control: treated with DMSO, and others wells were treated with LY294002 at (7 μM , 14 μM , 24 μM and 50 μM). Time-lapse microscopy was used to track cell migration for 24 hours and MTrackJ was used to measure cell migration the mean total distance inhibited significantly compared with control. **B)** Control: treated with DMSO, and others wells were treated with LY294002 at (7 μM , 14 μM , 24 μM and 50 μM). An inverted microscopy was used to capture wound healing in 0 time and after 24 hours and Image was used to measure wound closure at 0 and 24 hours the mean total wound closure was inhibited significantly compared with control. Statistical analysis was performed by one way ANOVA with Dunnett's test for multiple comparison. Statistical significance was accepted at *** $P < 0.0005$. Data represent mean \pm SEM of the three independent experiments.

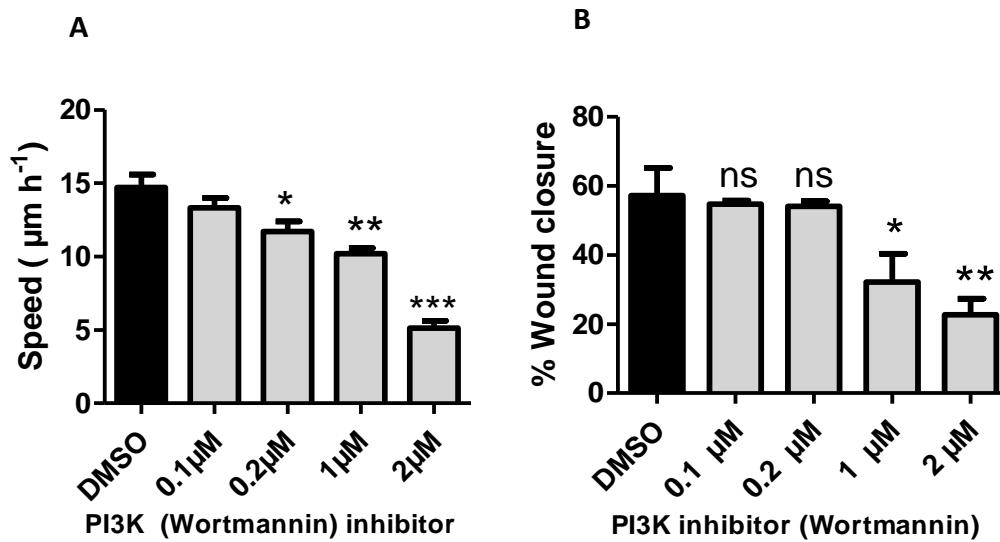


Figure (5.11): Effect of PLC Wortmannin inhibitor on cell migration and wound healing in MDA-MB-231 cells on a fibronectin surface. A) Control: treated with DMSO, and others wells were treated with Wortmannin at (0.1 µM, 0.2 µM, 1 µM and 2 µM)). Time-lapse microscopy was used to track cell migration for 24 hours and MTrackJ was used to measure cell migration the mean total distance inhibited significantly compared with control. **B)** Control: treated with DMSO, and others wells were treated with Wortmannin at (0.1 µM, 0.2 µM, 1 µM and 2 µM). An inverted microscopy was used to capture wound healing in 0 time and after 24 hours and ImageJ was used to measure wound closure at 0 and 24 hours the mean total wound closure was inhibited significantly compared with control. Statistical analysis was performed by one way ANOVA with Dunnett's test for multiple comparison. Statistical significance was accepted at *** P < 0.0005. Data represent mean ± SEM of the three independent experiments.

5.2.4. Interaction of PLC and PI3K with FAs.

MDA-MB-231 cell lysates were prepared and measured by Bradford assay. Lysates were incubated with primary antibody using mouse anti-talin, vinculin, paxillin and actin antibodies and rotated in the cold room at 4°C overnight to precipitate specific FA proteins, then were detected by western blotting using rabbit anti-talin, vinculin, paxillin and actin antibodies. Meanwhile, reverse-IP was used for same antibodies. Our data showed that vinculin was bound with talin and actin, while paxillin was not bound with vinculin but bound with actin (Figure 5.12 A-E).

Later, specific FA proteins were immunoprecipitated, then were detected by western blotting using rabbit anti-PI3K110 α , Kinase p85 and PLC β 1 antibodies. Reverse-IP lysates were incubated with primary antibody using rabbit anti-PI3K110 α , p85 and PLC β 1 and rotated in the cold room at 4°C overnight to precipitate specific kinase, then were detected by western blotting using mouse anti-talin, vinculin, paxillin and actin antibodies. Our data showed that PLC β 1 and PI3K110 α were bound with talin and vinculin, whereas PI3K p85 was not bound with FAs (Figure 5.13 A-C, 5.15 A-B & 5.17A-C).

MDA-MB-231 cells were seeded on fibronectin and fixed then co-stained with anti-PI3K110 α (red) and vinculin (green) or Kinase p85 (red) and vinculin (green) antibodies and nuclei was stained by DAPI (Blue). Co-localisation analysis between these proteins was visualised by using confocal microscopy. Our data showed that PI3K110 α was localised with vinculin and co-localisation value 0.58 ± 0.10 . While Kinase p85 was not localised with vinculin and the co-localisation value was -0.25 ± 0.28 (Figures 5.14 and 5.16).

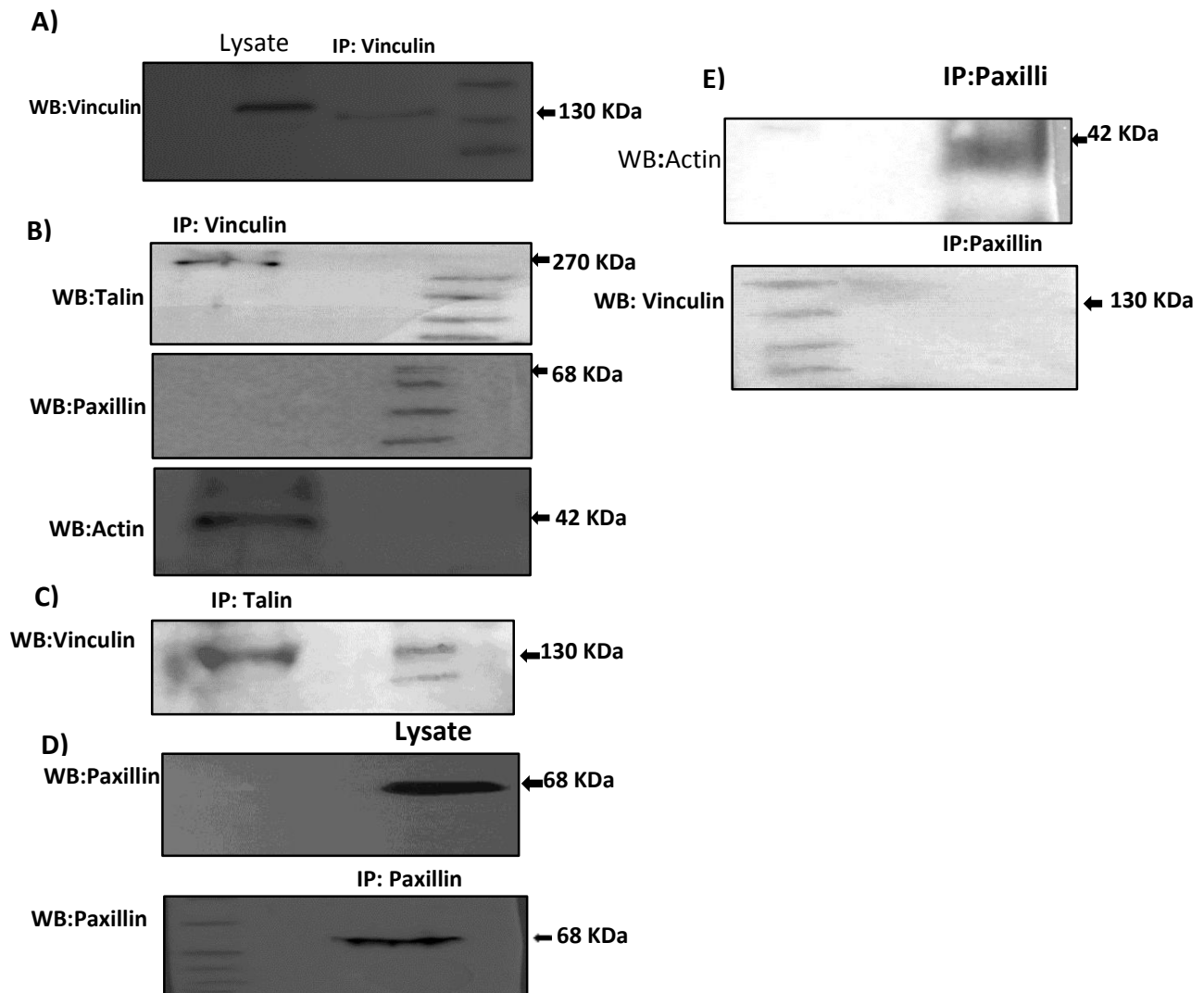


Figure (5.12): Co-immunoprecipitates(IP) of FA complex. Proteins were extracted from MDA-MB-231 cells then incubated overnight with primary antibodies. **A)** Vinculin was precipitated from lysate using mouse anti-vinculin antibody and detected by western blotting using rabbit anti-vinculin was used as a control. **B)** Vinculin was precipitated from lysate using mouse anti-vinculin antibody and detected by western blotting using rabbit anti-talin, actin and paxillin and found that vinculin bound with talin and actin, but not bound with paxillin. **C)** Reverse-IP, talin was precipitated from lysate using rabbit anti- talin antibody and detected by western blotting using mouse anti-vinculin antibody and found it is bound with vinculin. **D)** paxillin was precipitated from lysate using mouse anti-paxillin antibody and was detected by western blotting using rabbit anti-paxillin was used as a control. **E)** Paxillin was precipitated from lysate using mouse paxillin antibody and detected by western blotting using rabbit anti-vinculin and actin and found that bound with actin but not bound with vinculin. These experiments were performed four times independently.

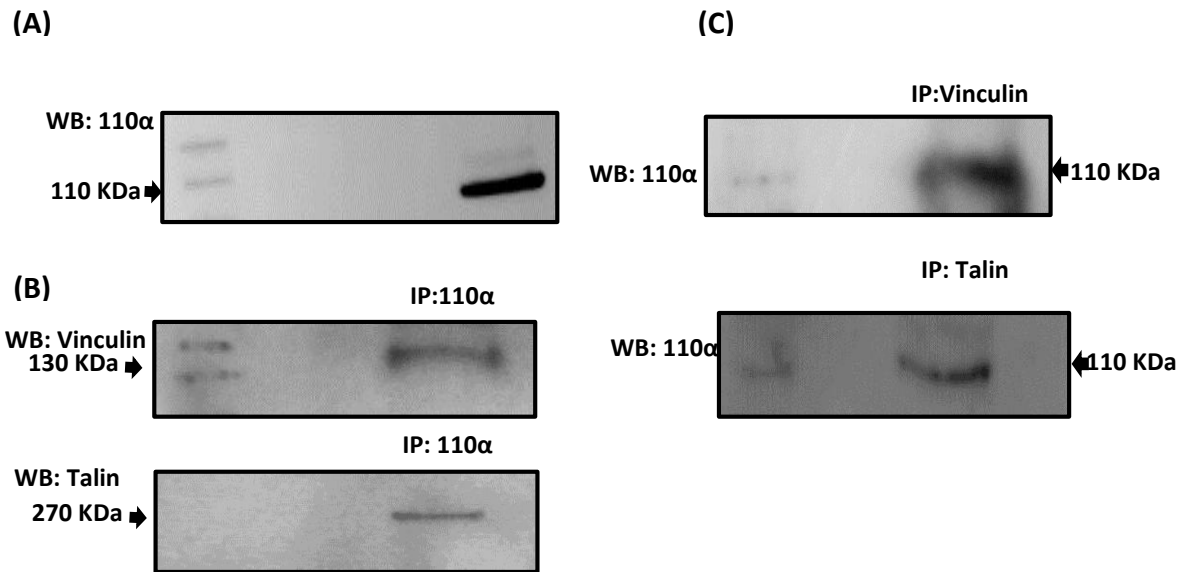


Figure (5.13): co-immunoprecipitates(IP) of PI3K110α and FAs. A) Proteins were extracted from MDA-MB-231 cells then incubated overnight with primary anti- PI3K110α and used as a control. **B)** PI3K110α was precipitated from lysate using rabbit anti-PI3K110α antibody and detected by western blotting using mouse anti-vinculin antibody. Reverse-IP, vinculin was precipitated from lysate using mouse anti-vinculin antibody and detected by western blotting using rabbit anti-PI3K110α antibody. **C)** PI3K110α was precipitated from lysate using rabbit anti-PI3K110α antibody and detected by western blotting using mouse anti-talin-1 antibody. Reverse-IP, talin-1 was precipitated from lysate using mouse anti-talin antibody and detected by western blotting using rabbit anti-PI3K110α antibody and found that PI3K110α bound with talin-1 and vinculin. These experiments were performed four times independently.

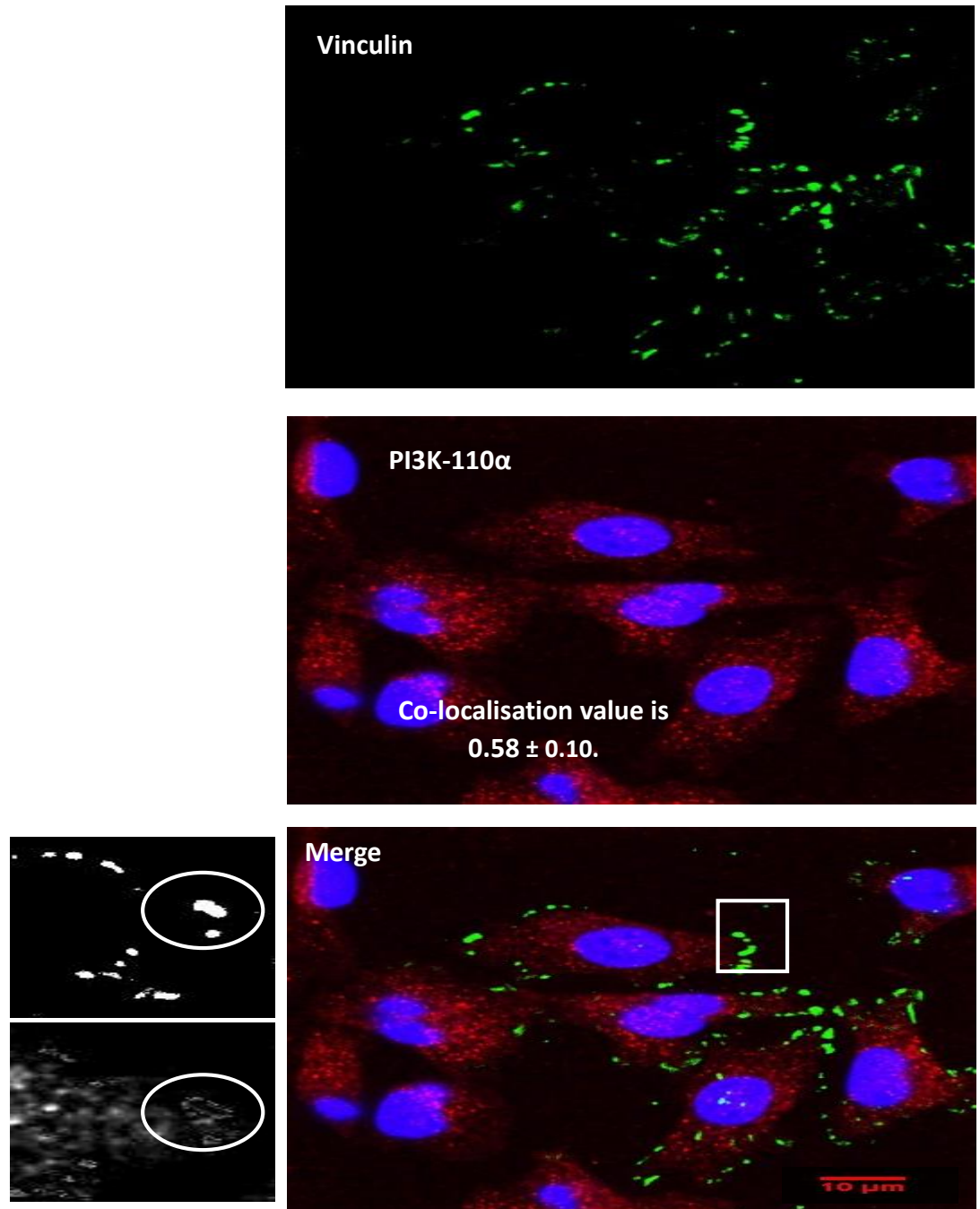


Figure (3.14): Spatial co-localisation between anti-PI3K110 α and vinculin MDA-MB-231 cells on the fibronectin. A) MDA-MB-231 cells were plated on fibronectin 20 μ g/ml, then fixed and co-stain with anti-PI3K110 α (red) and vinculin (green) antibodies and nuclei was stained by DAPI (Blue) to visualise the spatial interaction between vinculin and PI3K110 α . Z-Stacking was taken with confocal microscopy. The highlighted areas are shown the magnification of spatial co-localisation region between vinculin and PI3K110 α and found that the co-localisation value between them was 0.58 ± 0.10 . These experiments were performed four times independently.

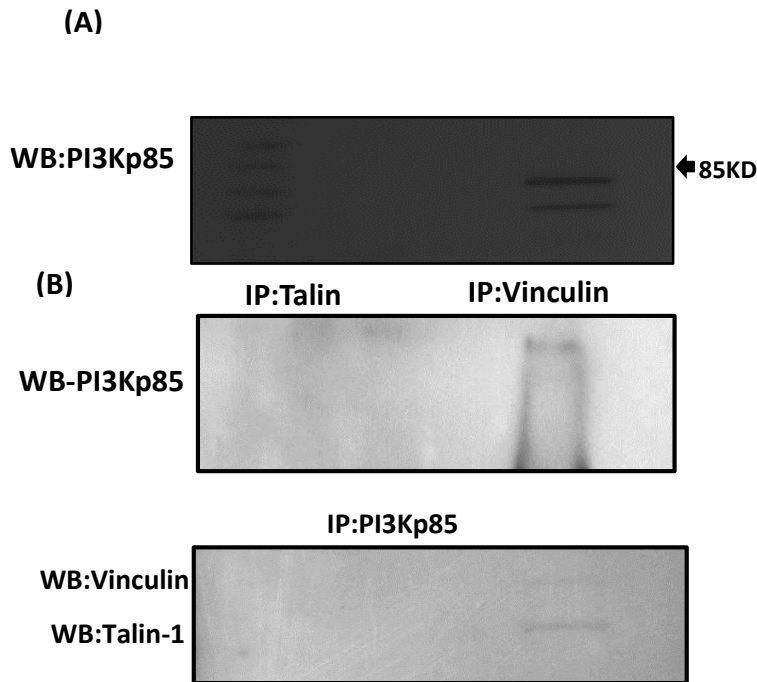


Figure (5.15): Co-localisation and co-immunoprecipitates(IP) of PI3K85 and FAs. A) Proteins were extracted from MDA-MB-231 cells then incubated overnight with primary anti- PI3K85. **B)** PI3K85 was precipitated from lysate using rabbit anti-PI3K85 antibody and detected by western blotting using mouse anti-vinculin&talin-1 antibody. Revers-IP, talin-1 & vinculin were precipitated from lysate using mouse anti-vinculin&talin-1 antibody and detected by western blotting using rabbit anti-PI3K85 antibody and found that PI3K85 was not bound with talin-1 and vinculin. These experiments were performed four times independently.

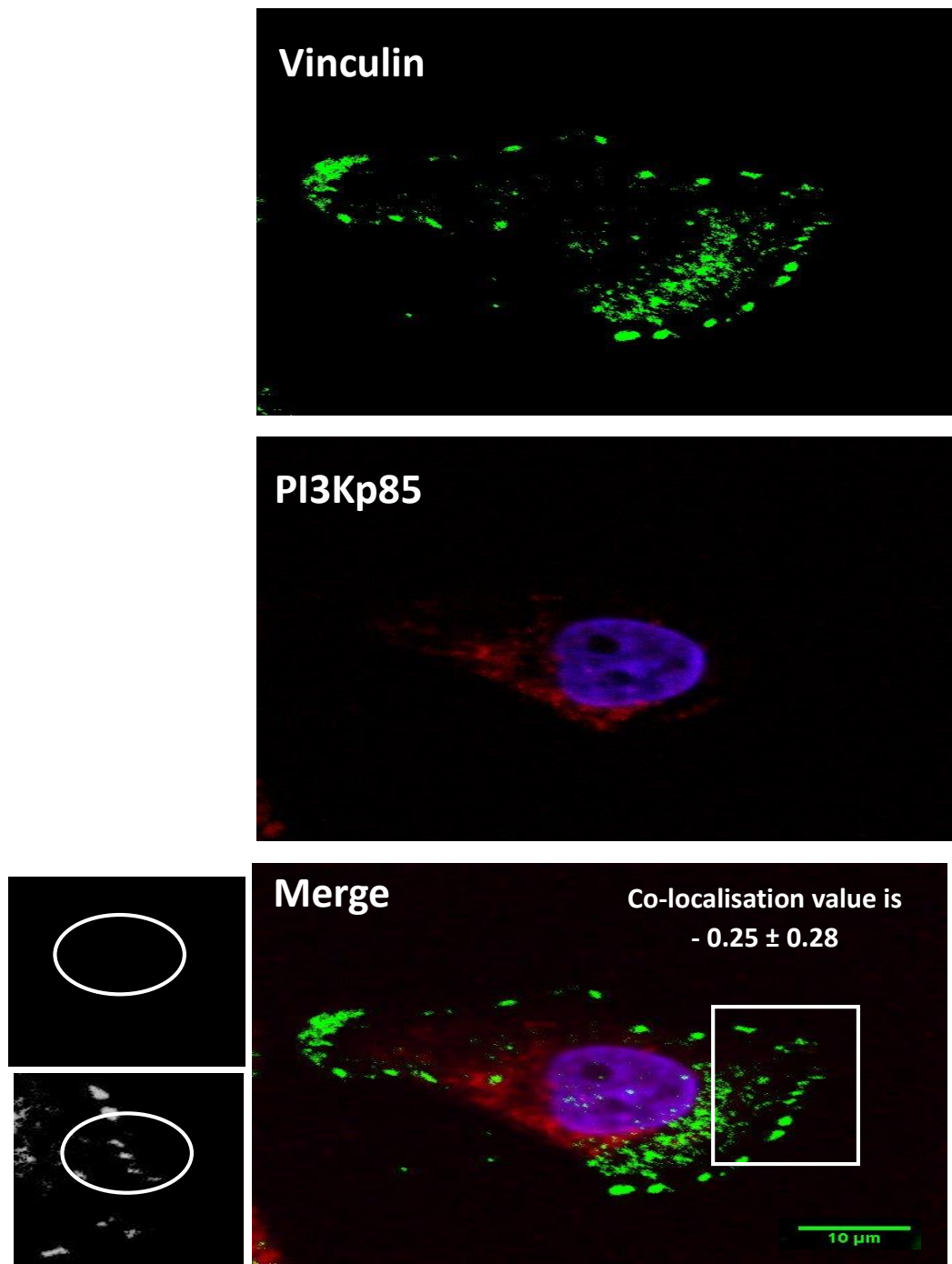


Figure (5.16): Spatial co-localisation between anti-PI3Kp85 and vinculin MDA-MB-231 cells on the fibronectin. A) MDA-MB-231 cells were plated on fibronectin 20µg/ml, then fixed and co-stain with anti-PI3Kp85 (red) and vinculin (green) antibodies and nuclei was stained by DAPI (Blue) to visualise the spatial interaction between vinculin and PI3Kp85. Z-Stacking was taken with confocal microscopy. The highlighted areas are shown the magnification of spatial co-localisation region between vinculin and PI3Kp85 and found that the co-localisation value between them was -0.25 ± 0.28 These experiments were performed four times independently.

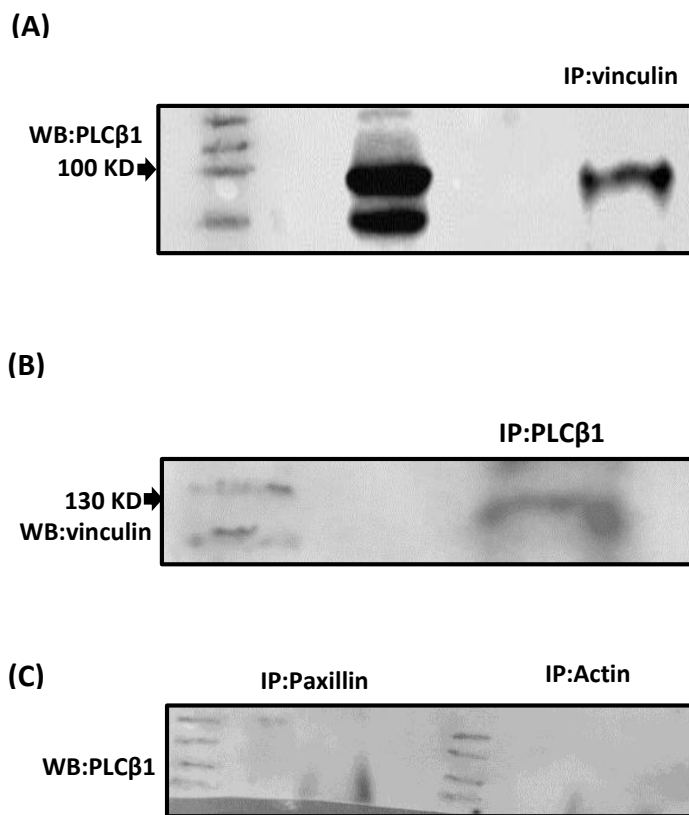


Figure (5.17): co-immunoprecipitates(IP) of PLCβ1 and FAs. A) Proteins were extracted from MDA-MB-231 cells then incubated overnight with primary anti-PLCβ1. Vinculin was precipitated from lysate using mouse anti-vinculin antibody and detected by western blotting using rabbit anti-PLCβ1. **B)** Reverse-IP, PLCβ1 was precipitated from lysate using rabbit anti- PLCβ1 antibody and detected by western blotting using rabbit anti-vinculin antibody and found that PLCβ1 was not bound with vinculin. **C)** Paxillin and actin were precipitated from lysate using mouse anti-paxillin and anti-actin antibody and detected by western blotting using rabbit anti-PLCβ and found that PLCβ1 was not bound with paxillin and actin. These experiments were performed four times independently.

5.3. Discussion:

In order to determine the reasons for the decline of local levels of PtdIns(4,5)P₂ within FA disassembly it is important to study PLC and PI3K signalling as they are two of the main enzymes that metabolise PtdIns(4,5)P₂ (van den Bout and Divecha, 2009).

Our results showed that PLC inhibition significantly reduces the decline in PtdIns(4,5)P₂ levels within the disassembly of a single FA (Figure 5.2), whereas PI3K inhibition had only a small effect (Figure 5.4). This suggests that PLC hydrolyses the majority of PtdIns(4,5)P₂ within a single FA into DAG and IP₃, while PI3K converts a small amount of PtdIns(4,5)P₂ to PtdIns(3,4,5)P₃. It has been shown that PLC increases the concentration of DAG and IP₃ about 10 fold through metabolising of PtdIns(4,5)P₂ (Gericke et al., 2013). Possibly, PLC allows disassembly of FAs either directly through hydrolysis of the local levels of PtdIns(4,5)P₂ or indirectly through its intracellular second messengers which target FA components locally.

Our results showed that both PI3K and PLC inhibition decreased FA turnover time (Figures 5.6 and 5.8). This can be explained by a number of possibilities 1) either through second messengers produced by PI3K and PLC (Figure 5.19), or 2) through decrease in local levels of PtdIns(4,5)P₂ within a single FA (Figure 5.18).

1) Decreased FA turnover due to reduction in the local levels of PtdIns(4,5)P2

PtdIns(4,5)P2 signalling interacts and activates the FAs-integrin signalling pathways (Goni et al., 2014, Thapa et al., 2015, Orłowski et al., 2015, Chinthalapudi et al., 2014). It may also enhance the strength of adhesion between FAs and integrin through recruitment of FA proteins (Le et al., 2015, Gilmore and Burridge, 1996). So, PtdIns(4,5)P2 increases the strength of binding between FAs and integrin during the assembly process (Izard and Brown, 2016, Chandrasekar et al., 2005, Wang, 2012, Yuan et al., 2017). The recruitment of FA proteins into FAs complex is supported by PtdIns(4,5)P2 (Huttelmaier et al., 1998, Carisey and Ballestrem, 2011, Garvalov et al., 2003) which play a role in the regulation of temporal organisation of FA turnover (Wu et al., 2011, Izard and Brown, 2016, Legate et al., 2011). This may suggest that decline of PtdIns(4,5)P2 levels regulate FAs through destabilizing and detaching FAs from the ECM (Goldschmidt-Clermont et al., 1990). So, it can be said that FA turnover depends on decline of local levels of PtdIns(4,5)P2 within FAs (Figure 5.18).

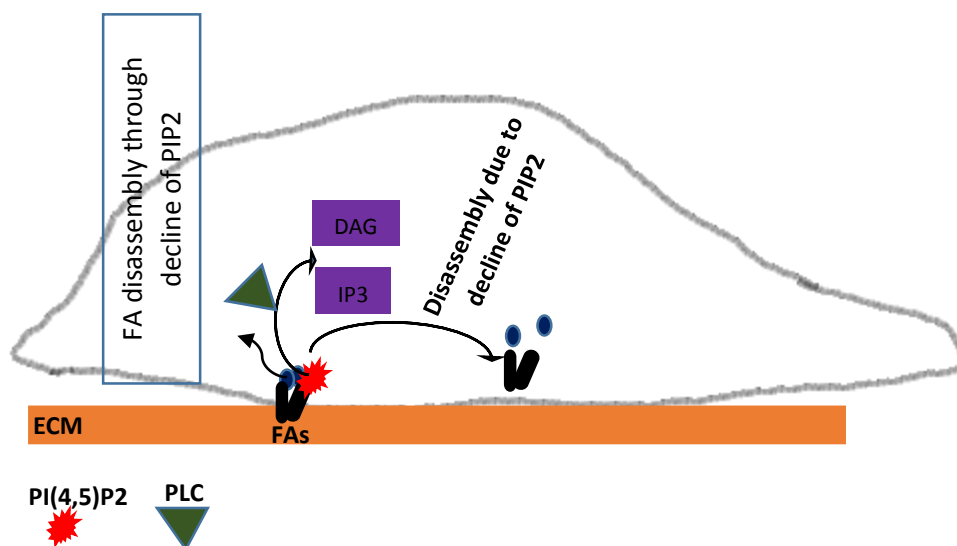


Figure (4.18): A model showing a possible role of PLC within FA disassembly. PLC affects FA disassembly through reduction in the local levels of PtdIns(4,5)P2 within FA.

2) Decreased FA turnover due to production of second messengers

a) PLC signalling

PLC cleaves PtdIns(4,5)P₂ into DAG and IP₃. DAG remains in the cell membrane while IP₃ diffuses away from the cell membrane into the cytoplasm. Eventually, DAG and IP₃ play crucial independent roles by activating the kinases involved in FA disassembly. DAG activates PKC, and IP₃ interacts with IP₃R receptors on the ER. IP₃-bound IP₃Rs release Ca²⁺ into the cytosol which activates the calpains, Pyk2, PKC (Valeyev et al., 2006) and Ca²⁺/calmodulin dependent protein kinase (CaMK-II,) (Easley et al., 2008) which are controlled spatially and temporally by PLC activity (Valeyev et al., 2006) and trigger FA disassembly locally (Figure 5.19) (Tsai et al., 2015).

Activated calpains cleave many important FA proteins, including talin, paxillin and α -actinin (Valeyev et al., 2006, Chen et al., 2013). Calpains also use FA proteins as substrates and degrade them in a limited manner due to targeting distinct sequences. The function of fragmented proteins are different from intact proteins. This proposes that calpains cut their substrate in disordered or distinct regions between structured domains (Tompa et al., 2004, Franco and Huttenlocher, 2005), such as paxillin is targeted at a particular site which is between LD1 and LD2 and produce a C-terminal fragment which acts as paxillin antagonist and affects FA disassembly (Cortesio et al., 2011). The specificity of cleavage of FA proteins is different between cell types (Franco and Huttenlocher, 2005).

It has been shown that PLC enhances cancer cell migration through reduction of PtdIns(4,5)P₂ levels in the cell membrane and releases DAG and IP₃ into the cytoplasm where they regulate FA turnover (Valeyev et al., 2006). Inhibition of IP₃-dependent

calpains leads to the reduction of integrin-mediated cell migration, slow the disassembly rates of the trailing edge of cell and increase the stabilisation and adhesiveness (Franco and Huttenlocher, 2005). The most common calpains which cleave FA components are calpain-1 and calpain-2. Inhibition of calpain-1 reduces FA turnover and cell spreading (Franco and Huttenlocher, 2005). Knockdown of calpain-2 also decreases disassembly of FAs (Franco and Huttenlocher, 2005, Franco et al., 2004b). Knockdown of calpain 2 by RNAi forms large adhesion complexes through the slow rate of FA disassembly (Franco et al., 2004a, Franco and Huttenlocher, 2005). Calpain-resistant talin-1 also decreases FA disassembly rates (Franco and Huttenlocher, 2005). The co-localisation between zyxin and α -actinin is disrupted by inhibition of calpain by calpastatin which leads to translocation of FA to the cell centre. It also modifies localization of α -actinin into FA complexes and then subsequent disassembly (Bhatt et al., 2002). So, calpains regulate cell motility by weakening adhesion to the ECM and enhancing detachment of the trailing edge of cell (Franco and Huttenlocher, 2005).

Even though calpains are implicated in FA disassembly, calpains might also be implicated in FA complex assembly. It has been shown that calpain-1 is implicated in FA assembly at the leading edge of cell through regulation of Rho GTPase activity and enhances FA turnover (Leloup et al., 2010). Calpain-2 allows FA disassembly by cleaving talin, vinculin, FAK and α -actinin at the trailing edge of cell (Leloup et al., 2010). Calpain-mediated cleavage of talin 1 enhances its interaction to integrin β -tails which is important for inside-out activation of integrins (Calderwood, 2004). Inhibition of calpains by calpastatin also prevents microtubule-mediated FA turnover (Bhatt et al., 2002, Franco and Huttenlocher, 2005).

Further, calpain-2 is phosphorylated by ERK on serine 50. Phosphorylated calpain-2 is localised to the cell membrane via interaction with PtdIns(4,5)P₂ through its domain III. The ERK phosphorylation stimulates the interaction of calpain-2 to PtdIns(4,5)P₂ (Leloup et al., 2010). Calpain-2 is spatially co-localised with PtdIns(4,5)P₂ in the cell membrane during growth factor receptor-mediated activation, suggesting that PtdIns(4,5)P₂ might act as docking site or cofactor for the localisation of calpain-2 to the cell membrane for subsequent activation. The binding of PtdIns(4,5)P₂ reduces the requirement of calcium for activation of calpain-2 (Shao et al., 2006). In other study, however, PtdIns(4,5)P₂ promotes the interaction of calcium to domain III of calpain-2 (Shao et al., 2006). It has been shown that the reduction of PtdIns(4,5)P₂ in the cell membrane leads to reduction the activation of EGF-induced calpain-2 (Shao et al., 2006). The activity of EGF-induced calpain-2 is eliminated by inhibiting PtdIns(4,5)P₂ synthesis, while membrane-calpain-2 interaction is eliminated by PLC (Shao et al., 2006). Therefore, Loss of local levels of PtdIns(4,5)P₂ might deactivate calpain and which would no longer have the ability to cleave FA. So, these sequences of events in agreement with our results in chapter 4 showed that the local levels of PtdIns(4,5)P₂ were at a constant level during FA disassembly n= 8 FA of total number n=30 FA (Figure 4.4 A-D). Probably, there are two mechanisms; PtdIns(4,5)P₂-dependent FA turnover and PLC-dependent FA turnover. 74 % of FA turnover depend on the decline in PtdIns(4,5)P₂ levels, while 24% of FA turnover depend on PLC activity (Figure 4.4 C). This may indicate that after FA disassembly through the decline of PtdIns(4,5)P₂ by PLC into DAG and IP₃. IP₃ releases calcium to activate calpain which in turn cleaves the nearby FA (Figure 5.19).

Activated Pyk2 acts as a biochemical bridge between FAs and Ca^{2+} and regulates many important cellular signalling in FA turnover (Chen et al., 2013). Inhibition of Ca^{2+} -dependent Pyk2 inhibits monocyte motility (Watson et al., 2001). It also localises with FA after AngII stimulation and plays a mediator for PDK1 through FA formation (Taniyama et al., 2003).

Activated CaMK-II involves in FA turnover through stimulating tyrosine dephosphorylating of paxillin and FAK. It enhances FA turnover and cell motility via transiently and locally inducing tyrosine dephosphorylating of FA proteins to promote FA turnover and cell Motility (Easley et al., 2008). It also impacts cell adhesion via disturbing of $\beta 1$ integrin through either direct phosphorylation of $\beta 1$ integrin or phosphorylation of integrin cytoplasmic linked protein-1 alpha, ICAP-1 α (Easley et al., 2008). It has been shown that inhibition of CaMK-II increases FA size and reduces cell motility (Easley et al., 2008).

DAG-dependent PKC contributes to FA turnover and forward migration and mediates the signal transformation of inside-outside of $\alpha 4\beta 1$ integrin during FAs formation via its interaction with integrin $\beta 1$ directly (Tsai et al., 2014, Fogh et al., 2014).

PKCs are downstream signalling for both Ca^{+2} and DAG (Mellor and Parker, 1998). PKC α , β I, β II and γ isoforms are activated following interaction with Ca^{+2} and DAG through their C1 and C2 domains (Evans and Falke, 2007). Activated PKCs contribute in the FA turnover through regulation of FA assembly and disassembly in cell migration (Fogh et al., 2014). PKC β determines the direction of cell migration through phosphorylation of myosin II (Murakami et al., 1995, Dulyaninova et al., 2007). They also play a role in breast cancer through localisation with FA complexes and interaction with integrin $\beta 1$ (Bass et al.,

2008). PKC inhibition leads to destabilisation of FA formation (Woods and Couchman, 1992). PKC α and δ inhibition by using specific shRNA leads to inhibition of extracellular signal-regulated kinase (ERK)-mediated phosphorylation of paxillin at Ser¹⁷⁸ which plays role in the regulation of FA disassembly and cell migration in hepatocellular carcinoma cells (Hu et al., 2013, Fogh et al., 2014).

b) PI3K signalling

It has been shown that PI3K plays a role in cancer cell migration through activation of Akt/mTOR signalling (Laplante and Sabatini, 2009, Slomovitz and Coleman, 2012). It has also been shown that PI3K regulate cell migration and cell adhesions either via the direct interaction with proteins, or the indirect interaction with other signalling pathways through its lipid products, such as PtdIns(3,4,5)P3 (Cain and Ridley, 2009). PI3K signalling also participates in the regulation of integrin signalling and FAs complexes (Wegener et al., 2007, Somanath et al., 2007, Tadokoro et al., 2003), via interaction with Src, Ras signalling (Cote and Vuori, 2007, Cain and Ridley, 2009), RhoA signalling (Figure 5.17) (Tadokoro et al., 2003, Graupera et al., 2008) and activate myosin II (Tadokoro et al., 2003, Graupera et al., 2008). PI3K p110 β and p85 α are involved in the disassembly process though interaction with Rab5 that activates endocytosis (Zerial and McBride, 2001, Chamberlain et al., 2004). This leads to internalisation and recycling of integrin and FAs by endocytosis (Jones et al., 2006), from trailing edge to leading edge. This process is regulated by Akt which is downstream of PI3K signalling (Roberts et al., 2004, Chamberlain et al., 2004).

Our results showed that the inhibition of PLC reduces the decline of PtdIns(4,5)P2 level from 43% to 24% (Figure 5.2), still giving a partial decline and not inhibiting it completely. This may indicate there are other factors responsible for generating PtdIns(4,5)P2 including PIP5K1 and PTEN (Min and Abrams, 2009) as mentioned in chapter1.

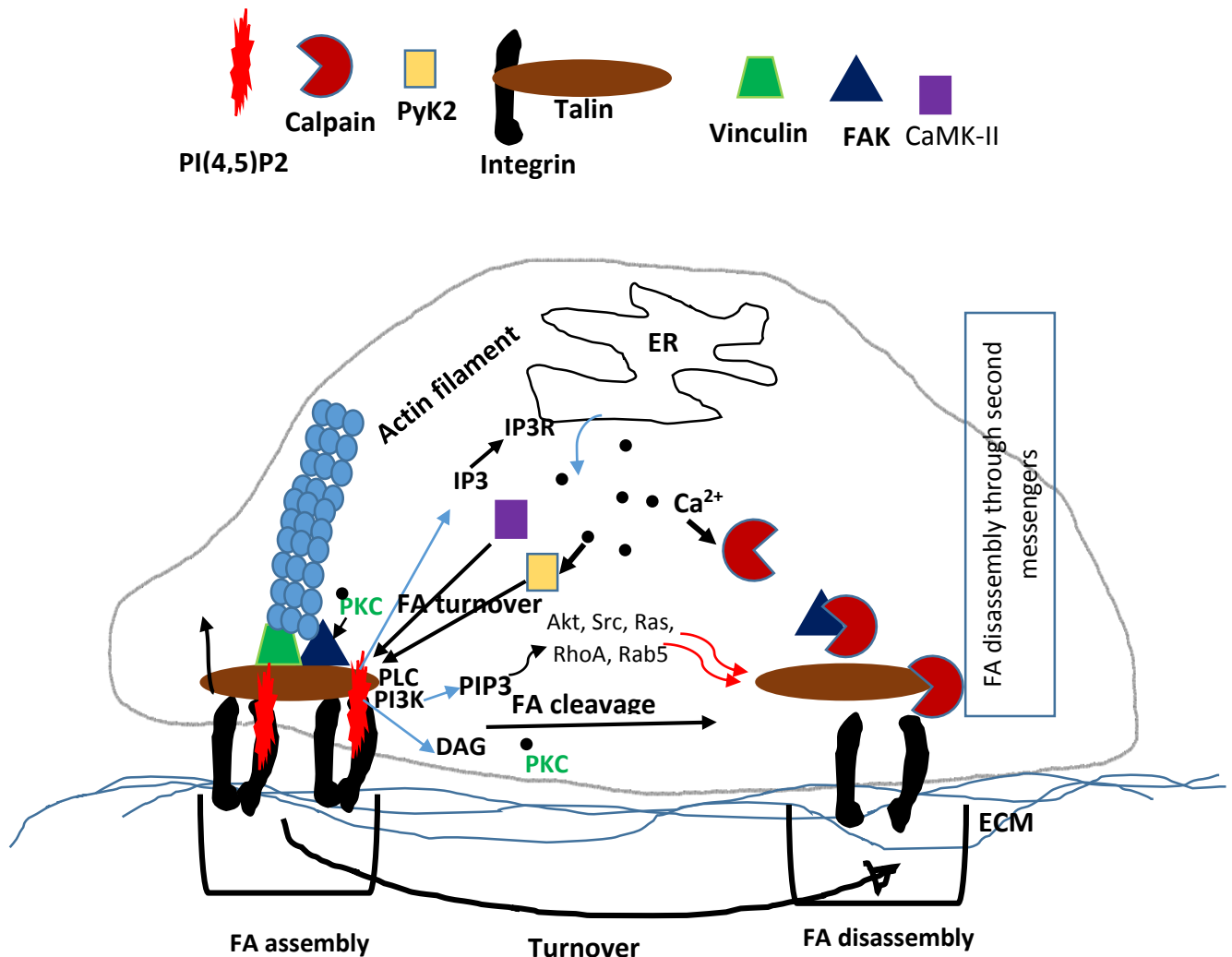


Figure (5.19): A model showing a possible role of PLC and PI3K within FA disassembly. FA disassembly by production of IP3, DAG and PtdIns(3,4,5)P3. PLC metabolises PtdIns(3,4,5)P3 to DAG and IP3, DAG remains in cell membrane and IP3 diffuses away from the cell membrane into cytosol. Eventually IP3 binds to IP3R receptors on the endoplasmic reticulum (ER) to release Ca^{2+} and DAG activates PKC. Cytosolic Ca^{2+} ions activate Calpain, CaMK-11 and PyK2. Activated Calpain cleaves many important focal adhesion proteins, including FAK, talin, vinculin and α -actinin. PI3K converts PtdIns(4,5)P2 to PtdIns(3,4,5)P3 which interacts and activates Akt, src, Ras, RhoA and Rab5 which involved in FA turnover. Cleaved FAs then disassemble.

Our data showed that PLC inhibition affects FA turnover time, while in Figure 5.3 & 5.2 showed that that the PLC inhibition reduces the decline of PtdIns(4,5)P₂ during FA disassembly while zyxin falls off at the same rate in the absence and the presence of the PLC inhibitor. This may have a number of possible interpretations.

One possibility is PtdIns(4,5)P₂ decline is not required for FA disassembly but affect the initiation of the FA turnover process. During FA initiation talin recruits PIP5K γ which increases an enrichment of PtdIns(4,5)P₂ levels (Wu et al., 2011, Izard and Brown, 2016, Legate et al., 2011), then PtdIns(4,5)P₂ recruits and activates additional FA proteins during the early stages of FA initiation , such as vinculin (Izard and Brown, 2016, Chandrasekar et al., 2005, Wang, 2012, Yuan et al., 2017), VASP and zyxin (Garvalov et al., 2003) this interaction might also be supported by PtdIns(4,5)P₂ (Huttelmaier et al., 1998, Carisey and Ballestrem, 2011, Garvalov et al., 2003). So, PtdIns(4,5)P₂ might require for FA initiation through participation in the recruitment, activation of FA proteins (Ling et al., 2002), and increase the strength of binding between FAs and integrin (Saltel et al., 2009). This temporal sequence of PtdIns(4,5)P₂ metabolism might suggest that PtdIns(4,5)P₂ plays an auxiliary role in the activation of FA initiation (Izard and Brown, 2016).

The second possibility is the temporal sequence of PtdIns(4,5)P₂ metabolism contributes to the FA disassembly not by itself but through its second messengers. The products of PtdIns(4,5)P₂ hydrolysis, IP₃ and DAG could in turn function second messengers in the events leading to FA disassembly. DAG and IP₃ could exert their effects by release Ca²⁺ into the cytosol which stimulates the calpains, Pyk2, PKC (Valeyev et al., 2006) and CaMK-II (Easley et al., 2008) which are controlled temporally by PLC

activity (Valeyev et al., 2006) and trigger FA disassembly locally (Tsai et al., 2015). So, inhibition of PLC activity leads to stop PtdIns(4,5)P2 hydrolysis into IP3 and DAG, thus would no longer have the ability to activate the enzymes which trigger and cleave FA disassembly locally (Tsai et al., 2015). This observation might suggest that local levels of PtdIns(4,5)P2 require for FA initiation while its second messenger require for FA disassembly through the release of Ca²⁺ and activation of PKC which lead to affect the zyxin turnover.

Another possibility is the decline of PtdIns(4,5)P2 during FA disassembly might diffuse along the membrane that not correlate with FA turnover (Botelho et al., 2000, Scott et al., 2005).

Furthermore, FA disassembly is still not well understood due to there are several factors involved in FA disassembly, including microtubules (Crowley and Horwitz, 1995, Franco and Huttenlocher, 2005), autophagy (Sharifi et al., 2016), PDK1 (di Blasio et al., 2015), ubiquitination (Teckchandani and Cooper, 2016) and Rab5 (Nagano et al., 2012, di Blasio et al., 2015, Mendoza et al., 2017). So, these series of events may suggest that some FA turnover depends on different factors. Probably this provides a novel insight concerning other mechanisms which may involve in the FA turnover. So, this would be very important to investigate in future which factors are involved in FA disassembly instead lipids pool and why FA disassembly depends on different factors.

Several questions remain to be resolved, which of PtdIns(4,5)P2, IP3 or DAG has most effect on FA turnover. Our results showed that PtdIns(4,5)P2 directly affects FA turnover, while previous studies have shown that IP3 and DAG affect FA disassembly by activation of enzymes involve in FA disassembly, such as CaMK-II (Easley et al., 2008),

calpain (Franco and Huttenlocher, 2005), PKC (Fogh et al., 2014) and Pyk2 (Taniyama et al., 2003). However, little attention has been given to the study of the role of IP3 and DAG and the enzymes activated by them within FA turnover in cancer cell migration. In order to know the dynamics of these second messengers and their function within single FA it is important to investigate their spatial and temporal organisation in cancer cell migration. This study can be carried on by using DAG biosensor and anti-DAG antibody. Studying the role of IP3 and calcium within FA may be it is difficult because IP3 diffuses away from the cell membrane to interact with IP3R and calcium is released to the cytoplasm and do not interact directly with FA.

Effect of PLC and PI3K inhibitors on cell migration and wound healing

Our results showed that PLC and PI3K inhibitors significantly inhibit cell migration and wound healing (Figures 5.9 A-B, 5.10 A-B & 5.11 A-B). There are several reasons behind that; PLC and PI3K signalling play a role in FA turnover and cell migration through their second messengers that interact with other pathways involved in cell migration. PLC cleaves PtdIns(4,5)P₂ into IP₃ and DAG which trigger many cellular processes including cell migration and proliferation (Figure 5.18). Therefore, PLC inhibition leads to blocked Ca²⁺ and DAG signalling (Tsai et al., 2015, Tsai et al., 2014). The Lack of PLC γ influences on FA formation and actin polymerisation via amendment of the RHO family GTPase RAC (Sala et al., 2008, Lattanzio et al., 2013). PLC β 1 promotes cancer cell migration through reduction of PtdIns(4,5)P₂ levels in cell membrane (Sengelaub et al., 2016) which releases PI(4,5)P₂-interacting coniflin into the cytoplasm where it regulates actin turnover (Sengelaub et al., 2016).

PI3K converts PtdIns(4,5)P₂ to PtdIns(3,4,5)P₃ which in turn recruits and activates Akt/mTOR signalling that is involved in the regulation of cell growth, cell survival, wound healing and proliferation (Laplante and Sabatini, 2009, Slomovitz and Coleman, 2012, Castilho et al., 2013), either via the direct interaction with proteins, or the indirect interaction with other signalling pathways (Figure 5.20) (Cain and Ridley, 2009).

The PI3K–Akt–mTOR pathway is often activated in cancer. PtdIns(3,4,5)P₃ activates PDK1 which in turn activates Akt and then Akt activates mTOR. Subsequently, mTOR is implicated in regulation of proliferation, migration and invasion. mTORC2 phosphorylates PKC α , Akt and FA proteins and regulates tumour cell motility through

activation of the small GTPases (RhoA, Cdc42 and Rac1), while mTORC1 phosphorylates S6K1 and 4E-BP1, and FA proteins, such as FAK and paxillin (Zhou and Huang, 2011).

Aberrant activation of the PI3K-Akt-mTOR pathway occurs in many human cancers, including lung (Sarris et al., 2012), breast (Myers and Cantley, 2010) and prostate (Morgan et al., 2009). The molecular alterations and increased activity of this pathway is linked with cancer metastasis and resistance to cancer therapies (Morgan et al., 2009, Sarris et al., 2012). Hyperactivation of Akt may stimulate cell growth and proliferation, and participate in apoptotic resistance (Wan et al., 2007). So, PI3K inhibition blocks PtdIns(3,4,5)P₃ generation which plays an important role in cell migration through activation of Akt/mTOR signalling (Figure 5.20).

At the clinical application level, PLC and PI3K inhibitors have recently been used as drug for cancer. PI3K inhibitors have been used as a novel drug to block cancer through targeting of a specific pathway class II phosphoinositol 3-kinases (Falasca et al., 2017). There are a number of PI3K inhibitors, including the pan-PI3K inhibitor buparlisib (BKM120) and the PI3K α -selective inhibitor alpelisib (BYL719) currently in clinical development may be used as anticancer agents. In addition, isoform-selective inhibitors, include pictilisib, copanlisib, taselisib, Idelalisib and a selective PI3K δ inhibitor are used for hematologic malignancies, including chronic lymphocytic leukemia, relapsed follicular B-cell non-Hodgkin's lymphoma (NHL), and relapsed small lymphocytic lymphoma (Massacesi et al., 2016).

The PI3K-Akt-mTOR pathway may be involved in resistance. The activation of the PI3K pathway has also been involved in de novo and acquired treatment resistance to targeted therapies in multiple tumour types (LoRusso, 2016).

It has been stated that many tumours upregulate Akt in order to obtain resistance to standard chemotherapies (Huang and Hung, 2009). Combination methods that include targeting both the PI3K-Akt-mTOR pathway and other treatment may be applicable strategies to treat resistance mechanisms (Statz et al., 2017, LoRusso, 2016). PLC has also become as a suitable target to prevent breast and melanoma cancer cell invasion via recognition of a specific pathway (PDK1/ PLC γ 1 interaction) by using 2-O-benzyl-myoinositol1,3,4,5,6-pentakisphosphate (2-O-Bn-InsP5) which is small molecule inhibitor (Raimondi et al., 2016). So, probably inhibiting PLC and PI3K signalling leads to block them to regulate FA turnover which plays a role in cell migration.

In this chapter pharmacological inhibitors were used and have limitations. Wortmannin , LY294002 and U73122 inhibitors were used to block PI3K and PLC activity respectively, enabling manipulation of local levels of PtdIns(4,5)P2 and PtdIns(3,4,5)P3 at FA sites and monitoring of their changes during the FA turnover process. However these inhibitors might block other kinases, such as wortmannin may inhibit Pan-PI3K mTOR, DNA-PK and MLCK and the U73122 PLC inhibitor may also inhibit TRPM3. Thus, they might affect other pathways in cells, complicating the interpretation of these experiments. Second, concentrations of these inhibitors might also be toxic, thus altering cell behavior (Kong and Yamori, 2008).

So, in these experiments require appropriate controls to ensure that any effects that are observed are really due to inhibitors which target PI3K and PLC, such as U73343 inhibitor which is inactive analogue of U73122 (Botelho et al., 2000) and LY 303511 which also is inactive analogue of LY 294002 (El-Kholy et al., 2003).

These negative control compounds are structurally distinct inhibitors targeting the same enzyme but inactive variant. So, the cells can be treated with these inactive analogue compounds and inhibitors with same concentrations and examine their effect on PLC and PI3K activity and include curves which contain their concentrations and effects as Grinstein laboratory describing similar things and comparing between U73122 and U73343 and found that U73122 inhibit the lipid levels while U73343 had no effect and explained their concentrations and effects by curve (Botelho et al., 2000). Other PI3K inhibitors could be used due to more selective than wortmannin and LY294002, including A66 (Jamieson et al., 2011), AS 252424 (Condliffe et al., 2005), AS 605240 (Peng et al., 2010), BAG 956 (Stauffer et al., 2008) and 33-Methyladenine (Blommaart et al., 1997).

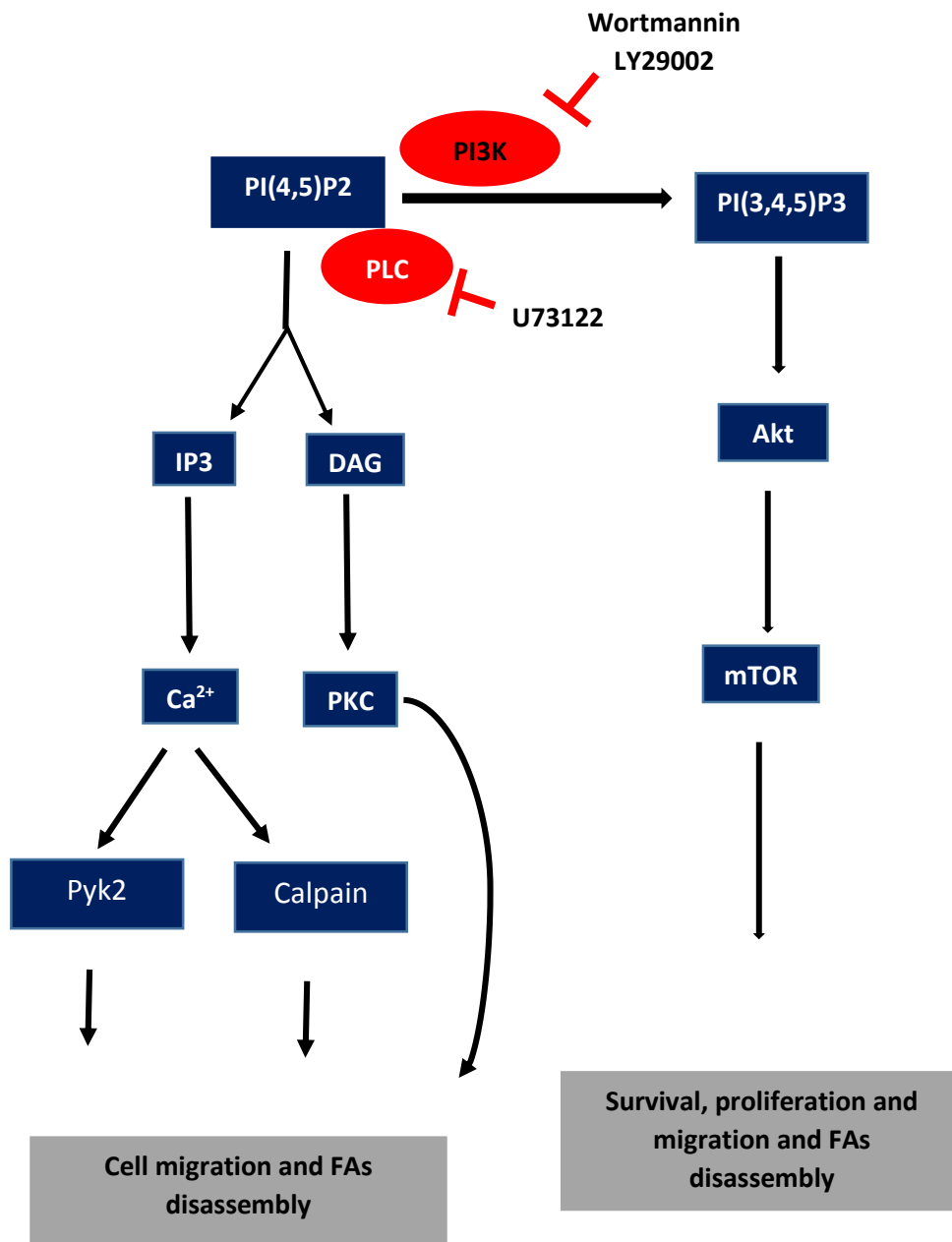


Figure (5.20): PLC and PI3K are activated and recruited by PtdIns(4,5)P2 and FA proteins to cell membrane. PLC cleaves PtdIns(4,5)P2 into IP3 and DAG and PI3K generates PtdIns(3,4,5)P3. IP3, DAG and involved in cell migration and FA turnover through activation of Ca²⁺, calpain and Akt/mTOR. So, the PLC and PI3K inhibition lead to reduction of FA turnover and cell migration.

Interaction of PLC and PI3K with FA

Talin, vinculin, paxillin and actin were used as a control for co- Immunoprecipitation (co-IP) experiments as they are key components of FA complexes as discussed in chapter 3 and 4. Our results showed that vinculin, talin and actin interacted with each other, while paxillin was not directly bound with vinculin and talin. Co-IP studies also showed that the PI3K p110 α and PLC β 1 directly associated with vinculin and talin, while PI3K p85 did not interact with them. Reverse co-IP was used to confirm the interaction between FA proteins and PLC/PI3K. Immunofluorescence co-localisation images were in agreement with IP results which showed that vinculin localised with PI3K p110 α but was not localised with PI3Kp85 (Figures 3.17 & 3.19). PI3Kp85 has previously been shown to be associated with vinculin in OCUM-2MD3 cells (Matsuoka et al., 2012), with paxillin in NMuMG cells (Tsubouchi et al., 2002) and with FAK (Tyr-397) in vitro and in vivo and then activates PI3K during cell adhesion (Chen et al., 1996, Guinebault et al., 1995, Chen and Guan, 1994). PLC- γ 1 was found to be associated with the FAK Tyr-397 site in COS-7 cells (Zhang et al., 1999), and associated with the actin-cytoskeleton (Pei et al., 1996).

These data strongly indicate that both PI3K and PLC signalling associate with FA complexes and can interfere with other signalling, such as integrin signalling through their interaction with FA proteins (Matsuoka et al., 2012, Zhang et al., 1999, Pei et al., 1996). So, it can be said that this interaction may reveal a new mechanism for PLC and PI3K activation at FA complexes and play an important role in signalling events that occur during FA turnover.

In co-IP experiments it would be helpful to include appropriate controls to make sure these kinases associate with FA proteins. Rabbit IgG can be used as negative control. Theoretically, rabbit IgG should not associate any proteins in this sample then, when western blotting is performed, no bands should be seen at the level of the protein of interest. Likewise the co-localisation data would also benefit from suitable controls, such as siRNA or shRNA which selectively impair the expression of PI3K isoforms, then stained with anti-PI3K isoforms to define specificity of the anti-PI3K isoform antibody. This might be important as our data suggests that PI3K p110 α is co-localised with vinculin while PI3K p85 was not co-localised.

In conclusion, our results suggest that PtdIns(4,5)P2 regulates FA turnover to facilitate cancer cell migration. The dynamic change of local levels of PtdIns(4,5)P2 and FAs turnover are important events promoting cell adhesion in cancer. PI3K and PLC signalling are activated and recruited by PtdIns(4,5)P2 and PtdIns(3,4,5)P3 into FA complexes in order to regulate the temporal organisation of PtdIns(4,5)P2 and PtdIns(3,4,5)P3 within a single FA turnover.

Chapter six: General discussion

In this thesis, PtdIns(4,5)P2 and PtdIns(3,4,5)P3 have been studied to investigate their role in the regulation of FAs in cancer cell migration by using the MDA-MB-231 cell line as a model.

Chapter 3 showed that PtdIns(4,5)P2 and PtdIns(3,4,5)P3 moderately co-localised with FA proteins (Figure 3.11 & table1). This may indicate that PtdIns(4,5)P2 and PtdIns(3,4,5)P3 signalling interacts with FA proteins and integrin signalling (Goni et al., 2014, Thapa et al., 2015, Orłowski et al., 2015, Chinthapudi et al., 2014).

Additionally, Chapter 4 showed that the local levels of PtdIns(4,5)P2 within a single FA increased gradually during assembly (Figures 4.2A & 4.3A) and declined gradually during FA disassembly (Figure 4.2A & 4.3A). This may suggest that PtdIns(4,5)P2 plays a role in the modulation and activation of FAs dynamic (Wu et al., 2011, Izard and Brown, 2016, Legate et al., 2011). Thus, PtdIns(4,5)P2 might involves in the strength of interaction between FAs and ECM during the assembly process (Saltel et al., 2009). Chapter 4 also showed that PtdIns(3,4,5)P3 within and around FAs was almost at a constant level during FA assembly and disassembly process (Figure 4.5A-B & 4.6A-B). The percentage change within and around FA was not significantly different between them (Figure 4.5C & 4.6C) as summarised in table4.3& 4.4. This may indicate that PtdIns(3,4,5)P3 is involved in other aspects in cancer migration but is not essential in FA turnover (Qin et al., 2009). So, this might suggest that PtdIns(4,5)P2 and PtdIns(3,4,5)P3 may perform different roles in the cell (Insall and Weiner, 2001) due to differences in their temporal and spatial organisation (Insall and Weiner, 2001).

Finally, chapter 5 showed that PLC inhibition significantly reduces the decline in PtdIns(4,5)P₂ levels within the disassembly of a single FA (Figure 5.2), whereas PI3K inhibition had only a small effect (Figure 5.4). This might suggest that PtdIns(4,5)P₂ can be involved in disassembly of FAs either directly through hydrolysis of the local levels of PtdIns(4,5)P₂ or indirectly through its intracellular second messengers (Gericke et al., 2013). This chapter also showed that both PI3K and PLC inhibition decreased FA turnover time (Figures 5.6 and 5.8). This is possibly due to second messengers produced by PI3K and PLC (Valeyev et al., 2006) or a decrease in local levels of PtdIns(4,5)P₂ within a single FA (Goldschmidt-Clermont et al., 1990)

Co-IP studies in chapter 5 showed that PI3K p110 α and PLC β 1 directly associated with vinculin and talin, while PI3K p85 did not interact with them. Reverse co-IP was used to confirm the interaction between FA proteins and PLC/PI3K. Immunofluorescence co-localisation images were in agreement with the IP results which showed that vinculin localised with PI3K p110 α but was not localised with PI3Kp85 (Figures 3.17 & 3.19). This may suggest that some isoforms of PI3K and PLC associated with FA proteins, such as PI3Kp85 associated with vinculin (Matsuoka et al., 2012), with paxillin (Tsubouchi et al., 2002) and with FAK (Tyr-397) in vitro and in vivo (Chen et al., 1996, Guinebault et al., 1995, Chen and Guan, 1994), and PLC- γ 1 associated with the FAK Tyr-397 site in COS-7 cells (Zhang et al., 1999).

Chapter 5 also showed that PLC and PI3K inhibitors significantly inhibit cell migration and wound healing (Figures 5.9 A-B, 5.10 A-B & 5.11 A-B). This might suggest that PLC and PI3K inhibition plays a role in cell migration through generation of Ca²⁺ and DAG signalling (Tsai et al., 2015, Tsai et al., 2014), and PtdIns(3,4,5)P₃ which in turn recruits and activates Akt/mTOR signalling that is involved in the regulation of cell growth, cell

survival, wound healing and proliferation (Laplante and Sabatini, 2009, Slomovitz and Coleman, 2012, Castilho et al., 2013).

Probably, there are further experiments that could be undertaken to confirm our results. Using a negative control of binding-deficient mutant versions of the probe, such as PLC δ -GFP PH domain mutant (R40L) which is a negative control of PLC δ -PH domain (wild type). Then, measurement the local levels of PtdIns(4,5)P2 within FA sites by using fluorescence recovery after photobleaching (FRAP) which may use to monitor the changes in PtdIns(4,5)P2 levels and the interaction with FA proteins in living cells. The FRAP methodology can also be used to study temporal and spatial of PtdIns(4,5)P2 and PtdIns(3,4,5)P3 within FA sites and identify the changes of PtdIns(4,5)P2 levels within FA turnover not due to membrane changes (Pincet et al., 2016). Another technique which also be applied to visualise and measure the dynamic change in lipid distribution within FA turnover is fluorescence lifetime imaging (FLIM) microscopy. It can be used to monitor the change of PtdIns(4,5)P2 concentration within FA turnover (Stöckl and Herrmann, 2010), to define the amount of membrane in the FAs to be sure that any changes that are observed in PtdIns(4,5)P2 are not a consequence of changes in the shape or amount of membrane.

Possibly, there are several future research areas arising from this work. One question to address is which of PtdIns(4,5)P2, IP3 or DAG has the most effect on FA turnover. Our results showed that PtdIns(4,5)P2 directly affects FA turnover, while previous studies have shown that IP3 and DAG affect FA disassembly by activation of enzymes involve in FA disassembly, such as CaMK-II (Easley et al., 2008), calpain (Franco and Huttenlocher, 2005), PKC (Fogh et al., 2014) and Pyk2 (Taniyama et al., 2003). However, little attention

has been given to the study of the role of IP₃ and DAG and the enzymes activated by them within single FA turnover in cancer cell migration. In order to know the dynamics of these second messengers and their function within single FA it is important to investigate their spatial and temporal organisation during cancer cell migration.

This study can be carried on by using anti-DAG antibody and anti-FA protein antibodies. DAG biosensors can be used in live cells in order to study the temporal organisation within a single FA turnover. Studying the role of IP₃ and calcium within FA might be it is difficult because IP₃ diffuses away from cell membrane to interact with IP₃R and calcium is released to the cytoplasm and do not interact directly with FA. Remus et al. (2006) constructed biosensors for IP₃ and calcium which are fluorescence resonance energy transfer-based InsP₃ biosensors (FIRE) and fluorescent calcium indicator fluo-4/AM to measure their concentration and study their spatiotemporal resolution in cells.

Besides, PKC is activated by DAG and calcium. So, it is important to investigate its spatial and temporal organisation within a single FA in cancer cell migration, and examine its role in FA turnover. This study can also be carried on by using anti-PKC antibody and PKC biosensor to study its spatial and temporal organisation within a single FA.

Further, phosphatidic acid (PA) plays many roles including, biosynthesis of other lipids and recruiting proteins to the cell membrane, such as sphingosine kinase 1 (Delon et al., 2004). PA is formed by phospholipase D (PLD) (Liscovitch et al., 2000) and phosphorylation of DAG by DAG kinase (DAGK)(Merida et al., 2008). So, it is important studying its spatial and temporal organisation within a single FA and examine its role in FA turnover. Likewise, this study can also be carried on by using anti-PA antibody to study its spatial organisation with FA proteins through measurement of co-localisation value between them. In live cells, a PA biosensor can be used in order to study its

temporal organisation within a single FA turnover. Lu et al. (2016) Constructed a new biosensor called PASS derived from PA-associating domain of yeast. So, they developed fluorescence lifetime imaging microscopy (FLIM) and Förster or fluorescence resonance energy transfer (FRET).

Acknowledgements

I would like to express my profound thank to my supervisor Dr Phil Dash for his guidance and efforts in my full 4-year PhD period. I would also like to express my profound gratitude for his recommendations on how to write a thesis and discussion context based on constructive scientific criticism.

I thank my committee members, Dr Mike Fry and Dr Andrew Bicknell, special thanks to Dr Mike Fry for his collaboration in this project and his recommendations and comments in lab meeting were very useful in my project.

I would like to thanks Dr Elizabeth Lander for her help in molecular cloning experiments, my profound thanks to all my friends in cell migration lab.

My sincere gratitude and appreciation to my sponsor, Iraqi ministry of higher education and scientist research.

Last but not least, special thanks must go to my family without whom I cannot finish my PhD.

Bibliography

- ARIAS-SALGADO, E. G., LIZANO, S., SARKAR, S., BRUGGE, J. S., GINSBERG, M. H. & SHATTIL, S. J. 2003. Src kinase activation by direct interaction with the integrin beta cytoplasmic domain. *Proc Natl Acad Sci U S A*, 100, 13298-302.
- ATHERTON, P., STUTCHBURY, B., JETHWA, D. & BALLESTREM, C. 2016. Mechanosensitive components of integrin adhesions: Role of vinculin. *Experimental Cell Research*, 343, 21-27.
- BADER, A. G., KANG, S. & VOGT, P. K. 2006. Cancer-specific mutations in PIK3CA are oncogenic in vivo. *Proc Natl Acad Sci U S A*, 103, 1475-9.
- BADER, A. G., KANG, S., ZHAO, L. & VOGT, P. K. 2005. Oncogenic PI3K deregulates transcription and translation. *Nat Rev Cancer*, 5, 921-9.
- BAE, Y. H., DING, Z., DAS, T., WELLS, A., GERTLER, F. & ROY, P. 2010. Profilin1 regulates PI(3,4)P(2) and lamellipodin accumulation at the leading edge thus influencing motility of MDA-MB-231 cells. *Proceedings of the National Academy of Sciences of the United States of America*, 107, 21547-21552.16
- BAENKE, F., PECK, B., MIESS, H. & SCHULZE, A. 2013. Hooked on fat: the role of lipid synthesis in cancer metabolism and tumour development. *Disease Models & Mechanisms*, 6, 1353-1363.
- BACH, I. 2000. The LIM domain: regulation by association. *Mech Dev*, 91, 5-17.
- BALLA, T. 2013. Phosphoinositides: Tiny Lipids With Giant Impact on Cell Regulation. *Physiological Reviews*, 93, 1019-1137.
- BALLA, T. & VARNAI, P. 2009. Visualization of cellular phosphoinositide pools with GFP-fused protein-domains. *Curr Protoc Cell Biol*, Chapter 24, Unit 24.4.
- BALLESTREM, C., HINZ, B., IMHOF, B. A. & WEHRLE-HALLER, B. 2001. Marching at the front and dragging behind: differential alphaVbeta3-integrin turnover regulates focal adhesion behavior. *J Cell Biol*, 155, 1319-32.

- BASS, M. D., MORGAN, M. R., ROACH, K. A., SETTLEMAN, J., GORYACHEV, A. B. & HUMPHRIES, M. J. 2008. p190RhoGAP is the convergence point of adhesion signals from alpha 5 beta 1 integrin and syndecan-4. *J Cell Biol*, 181, 1013-26.
- BERGERS, G. & BENJAMIN, L. E. 2003. Tumorigenesis and the angiogenic switch. *Nat Rev Cancer*, 3, 401-10.
- BHATT, A., KAVERINA, I., OTEY, C. & HUTTENLOCHER, A. 2002. Regulation of focal complex composition and disassembly by the calcium-dependent protease calpain. *Journal of Cell Science*, 115, 3415-3425.
- BLOMMAART, E. F., KRAUSE, U., SCHELLENS, J. P., VREELING-SINDELAROVA, H. & MEIJER, A. J. 1997. The phosphatidylinositol 3-kinase inhibitors wortmannin and LY294002 inhibit autophagy in isolated rat hepatocytes. *Eur J Biochem*, 243, 240-6.
- BOTELHO, R. J., TERUEL, M., DIERCKMAN, R., ANDERSON, R., WELLS, A., YORK, J. D., MEYER, T. & GRINSTEIN, S. 2000. Localized Biphasic Changes in Phosphatidylinositol-4,5-Bisphosphate at Sites of Phagocytosis. *The Journal of Cell Biology*, 151, 1353-1368.
- BRAKEBUSCH, C. & FASSLER, R. 2003. The integrin-actin connection, an eternal love affair. *Embo j*, 22, 2324-33.
- BROOKS, S. A., LOMAX-BROWNE, H. J., CARTER, T. M., KINCH, C. E. & HALL, D. M. 2010. Molecular interactions in cancer cell metastasis. *Acta Histochem*, 112, 3-25.
- BROWN, M. C., CURTIS, M. S. & TURNER, C. E. 1998. Paxillin LD motifs may define a new family of protein recognition domains. *Nat Struct Biol*, 5, 677-8.
- BROWN, M. C., PERROTTA, J. A. & TURNER, C. E. 1996. Identification of LIM3 as the principal determinant of paxillin focal adhesion localization and characterization of a novel motif on paxillin directing vinculin and focal adhesion kinase binding. *J Cell Biol*, 135, 1109-23.

- BUNNEY, T. D. & KATAN, M. 2011. PLC regulation: emerging pictures for molecular mechanisms. *Trends Biochem Sci*, 36, 88-96.
- BURRIDGE, K., TURNER, C. E. & ROMER, L. H. 1992. Tyrosine phosphorylation of paxillin and pp125FAK accompanies cell adhesion to extracellular matrix: a role in cytoskeletal assembly. *The Journal of Cell Biology*, 119, 893-903.
- BUTCHER, D. T., ALLISTON, T. & WEAVER, V. M. 2009. A tense situation: forcing tumour progression. *Nat Rev Cancer*, 9, 108-22.
- CAILLEAU, R., YOUNG, R., OLIVÉ, M. & REEVES, J. W. J. 1974. Breast Tumor Cell Lines From Pleural Effusions2. *JNCI: Journal of the National Cancer Institute*, 53, 661-674.
- CAIN, R. J. & RIDLEY, A. J. 2009. Phosphoinositide 3-kinases in cell migration. *Biol Cell*, 101, 13-29.
- CALDERWOOD, D. A. 2004. Integrin activation. *Journal of Cell Science*, 117, 657-666.
- CARISEY, A. & BALLESTREM, C. 2011. Vinculin, an adapter protein in control of cell adhesion signalling. *European Journal of Cell Biology*, 90, 157-163.
- CARISEY, A., TSANG, R., GREINER, ALEXANDRA M., NIJENHUIS, N., HEATH, N., NAZGIEWICZ, A., KEMKEMER, R., DERBY, B., SPATZ, J. & BALLESTREM, C. 2013. Vinculin Regulates the Recruitment and Release of Core Focal Adhesion Proteins in a Force-Dependent Manner. *Current Biology*, 23, 271-281.
- CASE, L. B., BAIRD, M. A., SHTENGEL, G., CAMPBELL, S. L., HESS, H. F., DAVIDSON, M. W. & WATERMAN, C. M. 2015. Molecular mechanism of vinculin activation and nanoscale spatial organization in focal adhesions. *Nat Cell Biol*, 17, 880-892.
- CASTILHO, R. M., SQUARIZE, C. H. & GUTKIND, J. S. 2013. Exploiting PI3K/mTOR Signaling to Accelerate Epithelial Wound Healing. *Oral diseases*, 19, 551-558.
- CHAMBERLAIN, M. D., BERRY, T. R., PASTOR, M. C. & ANDERSON, D. H. 2004. The p85alpha subunit of phosphatidylinositol 3'-kinase binds to and stimulates the GTPase activity of Rab proteins. *J Biol Chem*, 279, 48607-14.

- CHAN, K. T., BENNIN, D. A. & HUTTENLOCHER, A. 2010. Regulation of adhesion dynamics by calpain-mediated proteolysis of focal adhesion kinase (FAK). *J Biol Chem*, 285, 11418-26.
- CHANDRASEKAR, I., STRADAL, T. E. B., HOLT, M. R., ENTSCHLADEN, F., JOCKUSCH, B. M. & ZIEGLER, W. H. 2005. Vinculin acts as a sensor in lipid regulation of adhesion-site turnover. *Journal of Cell Science*, 118, 1461-1472.
- CHAO, W. T., ASHCROFT, F., DAQUINAG, A. C., VADAKKAN, T., WEI, Z., ZHANG, P., DICKINSON, M. E. & KUNZ, J. 2010. Type I phosphatidylinositol phosphate kinase beta regulates focal adhesion disassembly by promoting beta1 integrin endocytosis. *Mol Cell Biol*, 30, 4463-79.
- CHEN, C. S., ALONSO, J. L., OSTUNI, E., WHITESIDES, G. M. & INGBER, D. E. 2003. Cell shape provides global control of focal adhesion assembly. *Biochem Biophys Res Commun*, 307, 355-61.
- CHEN, H. C., APPEDDU, P. A., ISODA, H. & GUAN, J. L. 1996. Phosphorylation of tyrosine 397 in focal adhesion kinase is required for binding phosphatidylinositol 3-kinase. *J Biol Chem*, 271, 26329-34.
- CHEN, H. C. & GUAN, J. L. 1994. Association of focal adhesion kinase with its potential substrate phosphatidylinositol 3-kinase. *Proceedings of the National Academy of Sciences*, 91, 10148-10152.
- CHEN, Y. F., CHEN, Y. T., CHIU, W. T. & SHEN, M. R. 2013. Remodeling of calcium signaling in tumor progression. *J Biomed Sci*, 20, 23.
- CHINTHALAPUDI, K., PATIL, D. N., RANGARAJAN, E. S., RADER, C. & IZARD, T. 2015. Lipid-directed vinculin dimerization. *Biochemistry*, 54, 2758-68.
- CHINTHALAPUDI, K., RANGARAJAN, E. S., PATIL, D. N., GEORGE, E. M., BROWN, D. T. & IZARD, T. 2014. Lipid binding promotes oligomerization and focal adhesion activity of vinculin. *The Journal of Cell Biology*, 207, 643-656.

- CONDLIFFE, A. M., DAVIDSON, K., ANDERSON, K. E., ELLSON, C. D., CRABBE, T., OKKENHAUG, K., VANHAESEBROECK, B., TURNER, M., WEBB, L., WYMANN, M. P., HIRSCH, E., RUCKLE, T., CAMPS, M., ROMMEL, C., JACKSON, S. P., CHILVERS, E. R., STEPHENS, L. R. & HAWKINS, P. T. 2005. Sequential activation of class IB and class IA PI3K is important for the primed respiratory burst of human but not murine neutrophils. *Blood*, 106, 1432-40.
- CORTESIO, C. L., BOATENG, L. R., PIAZZA, T. M., BENNIN, D. A. & HUTTENLOCHER, A. 2011. Calpain-mediated Proteolysis of Paxillin Negatively Regulates Focal Adhesion Dynamics and Cell Migration. *The Journal of Biological Chemistry*, 286, 9998-10006.
- COTE, J. F. & VUORI, K. 2007. GEF what? Dock180 and related proteins help Rac to polarize cells in new ways. *Trends Cell Biol*, 17, 383-93.
- CROWLEY, E. & HORWITZ, A. F. 1995. Tyrosine phosphorylation and cytoskeletal tension regulate the release of fibroblast adhesions. *J Cell Biol*, 131, 525-37.
- CZECH, M. P. 2000. PIP2 and PIP3: complex roles at the cell surface. *Cell*, 100, 603-6.
- DEL RIO, A., PEREZ-JIMENEZ, R., LIU, R., ROCA-CUSACHS, P., FERNANDEZ, J. M. & SHEETZ, M. P. 2009. Stretching single talin rod molecules activates vinculin binding. *Science*, 323, 638-41.
- DELON, C., MANIFAVA, M., WOOD, E., THOMPSON, D., KRUGMANN, S., PYNE, S. & KTISTAKIS, N. T. 2004. Sphingosine kinase 1 is an intracellular effector of phosphatidic acid. *J Biol Chem*, 279, 44763-74.
- DI BLASIO, L., GAGLIARDI, P. A., PULIAFITO, A., SESSA, R., SEANO, G., BUSSOLINO, F. & PRIMO, L. 2015. PDK1 regulates focal adhesion disassembly by modulating endocytosis of $\alpha\beta 3$ integrin. *Journal of Cell Science*, 128, 863-877.
- DI PAOLO, G., PELLEGRINI, L., LETINIC, K., CESTRA, G., ZONCU, R., VORONOV, S., CHANG, S., GUO, J., WENK, M. R. & DE CAMILLI, P. 2002. Recruitment and regulation of

- phosphatidylinositol phosphate kinase type 1[gamma] by the FERM domain of talin. *Nature*, 420, 85-89.
- DIGMAN, M. A., BROWN, C. M., HORWITZ, A. R., MANTULIN, W. W. & GRATTON, E. 2008. Paxillin dynamics measured during adhesion assembly and disassembly by correlation spectroscopy. *Biophys J*, 94, 2819-31.
- DORMANN, D., WEIJER, G., PARENT, C. A., DEVREOTES, P. N. & WEIJER, C. J. 2002. Visualizing PI3 kinase-mediated cell-cell signaling during Dictyostelium development. *Curr Biol*, 12, 1178-88.
- DULYANINOVA, N. G., HOUSE, R. P., BETAPUDI, V. & BRESNICK, A. R. 2007. Myosin-IIA heavy-chain phosphorylation regulates the motility of MDA-MB-231 carcinoma cells. *Mol Biol Cell*, 18, 3144-55.
- DUMBAULD, D. W., LEE, T. T., SINGH, A., SCRIMGEOUR, J., GERSBACH, C. A., ZAMIR, E. A., FU, J., CHEN, C. S., CURTIS, J. E., CRAIG, S. W. & GARCIA, A. J. 2013. How vinculin regulates force transmission. *Proc Natl Acad Sci U S A*, 110, 9788-93.
- DUNN, K. W., KAMOCCA, M. M. & MCDONALD, J. H. 2011. A practical guide to evaluating colocalization in biological microscopy. *American Journal of Physiology - Cell Physiology*, 300, C723-C742.
- DURAND, N., BASTEA, L. I., LONG, J., DÖPPLER, H., LING, K. & STORZ, P. 2016. Protein Kinase D1 regulates focal adhesion dynamics and cell adhesion through Phosphatidylinositol-4-phosphate 5-kinase type-I γ . *Scientific Reports*, 6, 35963.
- EASLEY, C. A., BROWN, C. M., HORWITZ, A. F. & TOMBES, R. M. 2008. CaMK-II Promotes Focal Adhesion Turnover and Cell Motility by Inducing Tyrosine Dephosphorylation of FAK and Paxillin. *Cell motility and the cytoskeleton*, 65, 662-674.

- EDLING, C. E., SELVAGGI, F., BUUS, R., MAFFUCCI, T., DI SEBASTIANO, P., FRIESS, H., INNOCENTI, P., KOCHER, H. M. & FALASCA, M. 2010. Key Role of Phosphoinositide 3-Kinase Class IB in Pancreatic Cancer. *Clinical Cancer Research*, 16, 4928-4937.
- EL-KHOLY, W., MACDONALD, P. E., LIN, J. H., WANG, J., FOX, J. M., LIGHT, P. E., WANG, Q., TSUSHIMA, R. G. & WHEELER, M. B. 2003. The phosphatidylinositol 3-kinase inhibitor LY294002 potently blocks K(V) currents via a direct mechanism. *Faseb j*, 17, 720-2.
- ELMORE, S. 2007. Apoptosis: a review of programmed cell death. *Toxicol Pathol*, 35, 495-516.
- EVAN, G. I. & VOUSDEN, K. H. 2001. Proliferation, cell cycle and apoptosis in cancer. *Nature*, 411, 342-8.
- EVANS, J. H. & FALKE, J. J. 2007. Ca²⁺ influx is an essential component of the positive-feedback loop that maintains leading-edge structure and activity in macrophages. *Proc Natl Acad Sci U S A*, 104, 16176-81.
- FALASCA, M., HAMILTON, J. R., SELVADURAI, M., SUNDARAM, K., ADAMSKA, A. & THOMPSON, P. E. 2017. Class II Phosphoinositide 3-Kinases as Novel Drug Targets. *Journal of Medicinal Chemistry*, 60, 47-65.
- FALKE, J. J. & ZIEMBA, B. P. 2014. Interplay between phosphoinositide lipids and calcium signals at the leading edge of chemotaxing ameboid cells. *Chemistry and physics of lipids*, 0, 73-79.
- FALKENBURGER, B. H., JENSEN, J. B. & HILLE, B. 2010. Kinetics of M(1) muscarinic receptor and G protein signaling to phospholipase C in living cells. *The Journal of General Physiology*, 135, 81-97.
- FENG, J. & MERTZ, B. 2015. Novel Phosphatidylinositol 4,5-Bisphosphate Binding Sites on Focal Adhesion Kinase. *PLoS ONE*, 10, e0132833.
- FLEVARIS, P., STOJANOVIC, A., GONG, H., CHISHTI, A., WELCH, E. & DU, X. 2007. A molecular switch that controls cell spreading and retraction. *J Cell Biol*, 179, 553-65.

- FOGH, B. S., MULTHAUPT, H. A. & COUCHMAN, J. R. 2014. Protein kinase C, focal adhesions and the regulation of cell migration. *J Histochem Cytochem*, 62, 172-84.
- FORREST, M. D. 2015. Why cancer cells have a more hyperpolarised mitochondrial membrane potential and emergent prospects for therapy. *bioRxiv*.
- FRANCO, S., PERRIN, B. & HUTTENLOCHER, A. 2004a. Isoform specific function of calpain 2 in regulating membrane protrusion. *Exp Cell Res*, 299, 179-87.
- FRANCO, S. J. & HUTTENLOCHER, A. 2005. Regulating cell migration: calpains make the cut. *J Cell Sci*, 118, 3829-38.
- FRANCO, S. J., RODGERS, M. A., PERRIN, B. J., HAN, J., BENNIN, D. A., CRITCHLEY, D. R. & HUTTENLOCHER, A. 2004b. Calpain-mediated proteolysis of talin regulates adhesion dynamics. *Nat Cell Biol*, 6, 977-83.
- GALBRAITH, C. G. & SHEETZ, M. P. 1998. Forces on adhesive contacts affect cell function. *Curr Opin Cell Biol*, 10, 566-71.
- GARDEL, M. L., SCHNEIDER, I. C., ARATYN-SCHAUS, Y. & WATERMAN, C. M. 2010. Mechanical integration of actin and adhesion dynamics in cell migration. *Annu Rev Cell Dev Biol*, 26, 315-33.
- GARVALOV, B. K., HIGGINS, T. E., SUTHERLAND, J. D., ZETTL, M., SCAPLEHORN, N., KOCHER, T., PIDDINI, E., GRIFFITHS, G. & WAY, M. 2003. The conformational state of Tes regulates its zyxin-dependent recruitment to focal adhesions. *J Cell Biol*, 161, 33-9.
- GEIGER, B., SPATZ, J. P. & BERSHADSKY, A. D. 2009. Environmental sensing through focal adhesions. *Nat Rev Mol Cell Biol*, 10, 21-33.
- GERICKE, A., LESLIE, N. R., LÖSCHE, M. & ROSS, A. H. 2013. PI(4,5)P(2)-Mediated Cell Signaling: Emerging Principles and PTEN as a Paradigm for Regulatory Mechanism. *Advances in experimental medicine and biology*, 991, 85-104.
- GIANNONE, G. 2015. Super-resolution links vinculin localization to function in focal adhesions. *Nat Cell Biol*, 17, 845-847.

- GIANNONE, G., RONDE, P., GAIRE, M., HAIECH, J. & TAKEDA, K. 2002. Calcium oscillations trigger focal adhesion disassembly in human U87 astrocytoma cells. *J Biol Chem*, 277, 26364-71.
- GILMORE, A. P. & BURRIDGE, K. 1996. Regulation of vinculin binding to talin and actin by phosphatidyl-inositol-4-5-bisphosphate. *Nature*, 381, 531-5.
- GOLDSCHMIDT-CLERMONT, P. J., MACHESKY, L. M., BALDASSARE, J. J. & POLLARD, T. D. 1990. The actin-binding protein profilin binds to PIP2 and inhibits its hydrolysis by phospholipase C. *Science*, 247, 1575-8.
- GONI, G. M., EPIFANO, C., BOSKOVIC, J., CAMACHO-ARTACHO, M., ZHOU, J., BRONOWSKA, A., MARTIN, M. T., ECK, M. J., KREMER, L., GRATER, F., GERVASIO, F. L., PEREZ-MORENO, M. & LIETHA, D. 2014. Phosphatidylinositol 4,5-bisphosphate triggers activation of focal adhesion kinase by inducing clustering and conformational changes. *Proc Natl Acad Sci U S A*, 111, E3177-86.
- GOTTLIEB, E., ARMOUR, S. M., HARRIS, M. H. & THOMPSON, C. B. 2003. Mitochondrial membrane potential regulates matrix configuration and cytochrome c release during apoptosis. *Cell Death Differ*, 10, 709-17.
- GRAUPERA, M., GUILLERMET-GUIBERT, J., FOUKAS, L. C., PHNG, L. K., CAIN, R. J., SALPEKAR, A., PEARCE, W., MEEK, S., MILLAN, J., CUTILLAS, P. R., SMITH, A. J., RIDLEY, A. J., RUHRBERG, C., GERHARDT, H. & VANHAESEBROECK, B. 2008. Angiogenesis selectively requires the p110alpha isoform of PI3K to control endothelial cell migration. *Nature*, 453, 662-6.
- GREENBERG, R. A. 2005. Telomeres, crisis and cancer. *Curr Mol Med*, 5, 213-8.
- GREENWOOD, J. A., THEIBERT, A. B., PRESTWICH, G. D. & MURPHY-ULLRICH, J. E. 2000. Restructuring of focal adhesion plaques by PI 3-kinase. Regulation by PtdIns (3,4,5)-p(3) binding to alpha-actinin. *J Cell Biol*, 150, 627-42.

- GUINEBAULT, C., PAYRASTRE, B., RACAUD-SULTAN, C., MAZARGUIL, H., BRETON, M., MAUCO, G., PLANTAVID, M. & CHAP, H. 1995. Integrin-dependent translocation of phosphoinositide 3-kinase to the cytoskeleton of thrombin-activated platelets involves specific interactions of p85 alpha with actin filaments and focal adhesion kinase. *The Journal of Cell Biology*, 129, 831-842.
- GUO, W. H. & WANG, Y. L. 2007. Retrograde fluxes of focal adhesion proteins in response to cell migration and mechanical signals. *Mol Biol Cell*, 18, 4519-27.
- HALET, G. 2005. Imaging phosphoinositide dynamics using GFP-tagged protein domains. *Biol Cell*, 97, 501-18.
- HANAHAN, D. & WEINBERG, R. A. 2011. Hallmarks of cancer: the next generation. *Cell*, 144, 646-74.
- HARBURGER, D. S. & CALDERWOOD, D. A. 2009. Integrin signalling at a glance. *Journal of Cell Science*, 122, 159-163.
- HAUKE, J. & KOSSOWSKI, T. 2011. Comparison of Values of Pearson's and Spearman's Correlation Coefficients on the Same Sets of Data. *Quaestiones Geographicae*.
- HERREROS, L., RODRIGUEZ-FERNANDEZ, J. L., BROWN, M. C., ALONSO-LEBRERO, J. L., CABANAS, C., SANCHEZ-MADRID, F., LONGO, N., TURNER, C. E. & SANCHEZ-MATEOS, P. 2000. Paxillin localizes to the lymphocyte microtubule organizing center and associates with the microtubule cytoskeleton. *J Biol Chem*, 275, 26436-40.
- HILPELA, P., VARTIAINEN, M. K. & LAPPALAINEN, P. 2004. Regulation of the actin cytoskeleton by PI(4,5)P2 and PI(3,4,5)P3. *Curr Top Microbiol Immunol*, 282, 117-63.
- HOFFMAN, B. D., GRASHOFF, C. & SCHWARTZ, M. A. 2011. Dynamic molecular processes mediate cellular mechanotransduction. *Nature*, 475, 316-23.
- HOLT, M. R., CALLE, Y., SUTTON, D. H., CRITCHLEY, D. R., JONES, G. E. & DUNN, G. A. 2008. Quantifying cell-matrix adhesion dynamics in living cells using interference reflection microscopy. *J Microsc*, 232, 73-81.

- HU, C. T., CHENG, C. C., PAN, S. M., WU, J. R. & WU, W. S. 2013. PKC mediates fluctuant ERK-paxillin signaling for hepatocyte growth factor-induced migration of hepatoma cell HepG2. *Cell Signal*, 25, 1457-67.
- HU, Y.-L., LU, S., SZETO, K. W., SUN, J., WANG, Y., LASHERAS, J. C. & CHIEN, S. 2014. FAK and paxillin dynamics at focal adhesions in the protrusions of migrating cells. *Scientific Reports*, 4, 6024.
- HUANG, W. C. & HUNG, M. C. 2009. Induction of Akt activity by chemotherapy confers acquired resistance. *J Formos Med Assoc*, 108, 180-94.
- HUANG, Y. E., IJIMA, M., PARENT, C. A., FUNAMOTO, S., FIRTEL, R. A. & DEVREOTES, P. 2003. Receptor-mediated regulation of PI3Ks confines PI(3,4,5)P3 to the leading edge of chemotaxing cells. *Mol Biol Cell*, 14, 1913-22.
- HUMPHRIES, J. D., WANG, P., STREULI, C., GEIGER, B., HUMPHRIES, M. J. & BALLESTREM, C. 2007. Vinculin controls focal adhesion formation by direct interactions with talin and actin. *The Journal of Cell Biology*, 179, 1043-1057.
- HUTTELMAIER, S., MAYBORODA, O., HARBECK, B., JARCHAU, T., JOCKUSCH, B. M. & RUDIGER, M. 1998. The interaction of the cell-contact proteins VASP and vinculin is regulated by phosphatidylinositol-4,5-bisphosphate. *Curr Biol*, 8, 479-88.
- HUTTENLOCHER, A. & HORWITZ, A. R. 2011. Integrins in cell migration. *Cold Spring Harb Perspect Biol*, 3, a005074.
- HUVENEERS, S. & DANEN, E. H. 2009. Adhesion signaling - crosstalk between integrins, Src and Rho. *J Cell Sci*, 122, 1059-69.
- HYNES, R. O. 2002. Integrins: bidirectional, allosteric signaling machines. *Cell*, 110, 673-87.
- IDEVALL-HAGREN, O. & DE CAMILLI, P. 2015. Detection and manipulation of phosphoinositides. *Biochim Biophys Acta*, 1851, 736-45.
- INSALL, R. H. & WEINER, O. D. 2001. PIP3, PIP2, and Cell Movement—Similar Messages, Different Meanings? *Developmental cell*, 1, 743.

- IZARD, T. & BROWN, D. 2016. Mechanisms and Functions of Vinculin Interactions with Phospholipids at Cell Adhesion Sites. *The Journal of Biological Chemistry*, 291, 2548-55.
- JAALOUK, D. E. & LAMMERDING, J. 2009. Mechanotransduction gone awry. *Nat Rev Mol Cell Biol*, 10, 63-73.
- JAMIESON, S., FLANAGAN, J. U., KOLEKAR, S., BUCHANAN, C., KENDALL, J. D., LEE, W. J., REWCASTLE, G. W., DENNY, W. A., SINGH, R., DICKSON, J., BAGULEY, B. C. & SHEPHERD, P. R. 2011. A drug targeting only p110alpha can block phosphoinositide 3-kinase signalling and tumour growth in certain cell types. *Biochem J*, 438, 53-62.
- JI, C. & LOU, X. 2016. Single-molecule Super-resolution Imaging of Phosphatidylinositol 4,5-bisphosphate in the Plasma Membrane with Novel Fluorescent Probes. *Journal of Visualized Experiments : JoVE*, 54466.
- JI, C., ZHANG, Y., XU, P., XU, T. & LOU, X. 2015. Nanoscale Landscape of Phosphoinositides Revealed by Specific Pleckstrin Homology (PH) Domains Using Single-molecule Superresolution Imaging in the Plasma Membrane. *The Journal of Biological Chemistry*, 290, 26978-26993.
- JI, L., LIM, J. & DANUSER, G. 2008. Fluctuations of intracellular forces during cell protrusion. *Nat Cell Biol*, 10, 1393-400.
- JIANG, G., HUANG, A. H., CAI, Y., TANASE, M. & SHEETZ, M. P. 2006. Rigidity sensing at the leading edge through alphavbeta3 integrins and RPTPalph. *Biophys J*, 90, 1804-9.
- JOHNSON, R. P. & CRAIG, S. W. 1995. The carboxy-terminal tail domain of vinculin contains a cryptic binding site for acidic phospholipids. *Biochem Biophys Res Commun*, 210, 159-64.
- JONES, M. C., CASWELL, P. T. & NORMAN, J. C. 2006. Endocytic recycling pathways: emerging regulators of cell migration. *Curr Opin Cell Biol*, 18, 549-57.

- KADRMAS, J. L. & BECKERLE, M. C. 2004. The LIM domain: from the cytoskeleton to the nucleus. *Nat Rev Mol Cell Biol*, 5, 920-31.
- KANCHANAWONG, P., SHTENGEL, G., PASAPERA, A. M., RAMKO, E. B., DAVIDSON, M. W., HESS, H. F. & WATERMAN, C. M. 2010. Nanoscale architecture of integrin-based cell adhesions. *Nature*, 468, 580-584.
- KANG, S., BADER, A. G. & VOGT, P. K. 2005. Phosphatidylinositol 3-kinase mutations identified in human cancer are oncogenic. *Proc Natl Acad Sci U S A*, 102, 802-7.
- KIRFEL, G., RIGORT, A., BORM, B. & HERZOG, V. 2004. Cell migration: mechanisms of rear detachment and the formation of migration tracks. *Eur J Cell Biol*, 83, 717-24.
- KONG, D. & YAMORI, T. 2008. Phosphatidylinositol 3-kinase inhibitors: promising drug candidates for cancer therapy. *Cancer Sci*, 99, 1734-40.
- KONG, X., WANG, X., MISRA, S. & QIN, J. 2006. Structural basis for the phosphorylation-regulated focal adhesion targeting of type Iγ phosphatidylinositol phosphate kinase (PIPKIγ) by talin. *J Mol Biol*, 359, 47-54.
- LAL, H., GULERIA, R. S., FOSTER, D. M., LU, G., WATSON, L. E., SANGHI, S., SMITH, M. & DOSTAL, D. E. 2007. Integrins: novel therapeutic targets for cardiovascular diseases. *Cardiovasc Hematol Agents Med Chem*, 5, 109-32.
- LAPLANTE, M. & SABATINI, D. M. 2009. mTOR signaling at a glance. *J Cell Sci*, 122, 3589-94.
- LATTANZIO, R., PIANTELLI, M. & FALASCA, M. 2013. Role of phospholipase C in cell invasion and metastasis. *Adv Biol Regul*, 53, 309-18.
- LAUKAITIS, C. M., WEBB, D. J., DONAIS, K. & HORWITZ, A. F. 2001. Differential dynamics of alpha 5 integrin, paxillin, and alpha-actinin during formation and disassembly of adhesions in migrating cells. *J Cell Biol*, 153, 1427-40.

- LAWSON, C., LIM, S.-T., URYU, S., CHEN, X. L., CALDERWOOD, D. A. & SCHLAEPFER, D. D. 2012. FAK promotes recruitment of talin to nascent adhesions to control cell motility. *The Journal of Cell Biology*, 196, 223-232.
- LE CLAINCHE, C. & CARLIER, M. F. 2008. Regulation of actin assembly associated with protrusion and adhesion in cell migration. *Physiol Rev*, 88, 489-513.
- LE, O. T., CHO, O. Y., TRAN, M. H., KIM, J. A., CHANG, S., JOU, I. & LEE, S. Y. 2015. Phosphorylation of phosphatidylinositol 4-phosphate 5-kinase gamma by Akt regulates its interaction with talin and focal adhesion dynamics. *Biochim Biophys Acta*, 1853, 2432-43.
- LEE, S. E., KAMM, R. D. & MOFRAD, M. R. 2007. Force-induced activation of talin and its possible role in focal adhesion mechanotransduction. *J Biomech*, 40, 2096-106.
- LEGATE, K. R., TAKAHASHI, S., BONAKDAR, N., FABRY, B., BOETTIGER, D., ZENT, R. & FÄSSLER, R. 2011. Integrin adhesion and force coupling are independently regulated by localized PtdIns(4,5)(2) synthesis. *The EMBO Journal*, 30, 4539-4553.
- LELOUP, L., SHAO, H., BAE, Y. H., DEASY, B., STOLZ, D., ROY, P. & WELLS, A. 2010. m-Calpain activation is regulated by its membrane localization and by its binding to phosphatidylinositol 4,5-bisphosphate. *J Biol Chem*, 285, 33549-66.
- LEMMON, M. A. 2007. Pleckstrin Homology (PH) domains and phosphoinositides. *Biochemical Society symposium*, 81-93.
- LI, J., YEN, C., LIAW, D., PODSYPANINA, K., BOSE, S., WANG, S. I., PUC, J., MILIARESI, C., RODGERS, L., MCCOMBIE, R., BIGNER, S. H., GIOVANELLA, B. C., ITTMANN, M., TYCKO, B., HIBSHOOSH, H., WIGLER, M. H. & PARSONS, R. 1997. PTEN, a putative protein tyrosine phosphatase gene mutated in human brain, breast, and prostate cancer. *Science*, 275, 1943-7.

- LING, K., DOUGHMAN, R. L., FIRESTONE, A. J., BUNCE, M. W. & ANDERSON, R. A. 2002. Type I gamma phosphatidylinositol phosphate kinase targets and regulates focal adhesions. *Nature*, 420, 89-93.
- LISCOVITCH, M., CZARNY, M., FIUCCI, G. & TANG, X. 2000. Phospholipase D: molecular and cell biology of a novel gene family. *Biochemical Journal*, 345, 401-415.
- LORUSSO, P. M. 2016. Inhibition of the PI3K/AKT/mTOR Pathway in Solid Tumors. *J Clin Oncol*.
- LU, M., TAY, L. W. R., HE, J. & DU, G. 2016. Monitoring phosphatidic acid signaling in breast cancer cells using genetically encoded biosensors. *Methods in molecular biology (Clifton, N.J.)*, 1406, 225-237.
- LUO, B. H., CARMAN, C. V. & SPRINGER, T. A. 2007. Structural basis of integrin regulation and signaling. *Annu Rev Immunol*, 25, 619-47.
- MADUGULA, V. & LU, L. 2016. A ternary complex comprising transportin1, Rab8 and the ciliary targeting signal directs proteins to ciliary membranes. *Journal of Cell Science*, 129, 3922-3934.
- MAEKAWA, M. & FAIRN, G. D. 2014. Molecular probes to visualize the location, organization and dynamics of lipids. *J Cell Sci*, 127, 4801-12.
- MAFFUCCI, T., COOKE, F. T., FOSTER, F. M., TRAER, C. J., FRY, M. J. & FALASCA, M. 2005. Class II phosphoinositide 3-kinase defines a novel signaling pathway in cell migration. *J Cell Biol*, 169, 789-99.
- MAJERUS, P. W. & YORK, J. D. 2009. Phosphoinositide phosphatases and disease. *Journal of Lipid Research*, 50, S249-S254.
- MANNA, D., ALBANESE, A., PARK, W. S. & CHO, W. 2007. Mechanistic basis of differential cellular responses of phosphatidylinositol 3,4-bisphosphate- and phosphatidylinositol 3,4,5-trisphosphate-binding pleckstrin homology domains. *J Biol Chem*, 282, 32093-105.

- MARGADANT, F., CHEW, L. L., HU, X., YU, H., BATE, N., ZHANG, X. & SHEETZ, M. 2011. Mechanotransduction in vivo by repeated talin stretch-relaxation events depends upon vinculin. *PLoS Biol*, 9, e1001223.
- MARTEL, V., RACAUD-SULTAN, C., DUPE, S., MARIE, C., PAULHE, F., GALMICHE, A., BLOCK, M. R. & ALBIGES-RIZO, C. 2001. Conformation, localization, and integrin binding of talin depend on its interaction with phosphoinositides. *J Biol Chem*, 276, 21217-27.
- MASHAGHI, S., JADIDI, T., KOENDERINK, G. & MASHAGHI, A. 2013. Lipid Nanotechnology. *International Journal of Molecular Sciences*, 14, 4242.
- MASSACESI, C., DI TOMASO, E., URBAN, P., GERMA, C., QUADT, C., TRANDAFIR, L., AIMONE, P., FRETAULT, N., DHARAN, B., TAVORATH, R. & HIRAWAT, S. 2016. PI3K inhibitors as new cancer therapeutics: implications for clinical trial design. *OncoTargets and therapy*, 9, 203-210.
- MATSUDA, M., PATERSON, H. F., RODRIGUEZ, R., FENSOME, A. C., ELLIS, M. V., SWANN, K. & KATAN, M. 2001. Real Time Fluorescence Imaging of Plcy Translocation and Its Interaction with the Epidermal Growth Factor Receptor. *The Journal of Cell Biology*, 153, 599-612.
- MATSUOKA, T., YASHIRO, M., NISHIOKA, N., HIRAKAWA, K., OLDEN, K. & ROBERTS, J. D. 2012. PI3K/Akt signalling is required for the attachment and spreading, and growth in vivo of metastatic scirrhous gastric carcinoma. *Br J Cancer*, 106, 1535-1542.
- MCCLATCHEY, A. I. & YAP, A. S. 2012. Contact inhibition (of proliferation) redux. *Curr Opin Cell Biol*, 24, 685-94.
- MELLOR, H. & PARKER, P. J. 1998. The extended protein kinase C superfamily. *Biochem J*, 332 (Pt 2), 281-92.
- MENDOZA, P. A., SILVA, P., DIAZ, J., ARRIAGADA, C., CANALES, J. & CERDA, O. 2017. Calpain2 mediates Rab5-driven focal adhesion disassembly and cell migration. 1-10.
- MERIDA, I., AVILA-FLORES, A. & MERINO, E. 2008. Diacylglycerol kinases: at the hub of cell signalling. *Biochem J*, 409, 1-18.

- MIN, SANG H. & ABRAMS, CHARLES S. 2009. Why do phosphatidylinositol kinases have so many isoforms? *Biochemical Journal*, 423, e5-e8.
- MOFRAD, M. R., GOLJI, J., ABDUL RAHIM, N. A. & KAMM, R. D. 2004. Force-induced unfolding of the focal adhesion targeting domain and the influence of paxillin binding. *Mech Chem Biosyst*, 1, 253-65.
- MORGAN, M. R., HUMPHRIES, M. J. & BASS, M. D. 2007. Synergistic control of cell adhesion by integrins and syndecans. *Nat Rev Mol Cell Biol*, 8, 957-69.
- MORGAN, T. M., KORECKIJ, T. D. & COREY, E. 2009. Targeted therapy for advanced prostate cancer: inhibition of the PI3K/Akt/mTOR pathway. *Curr Cancer Drug Targets*, 9, 237-49.
- MORIMATSU, M., MEKHDJIAN, A. H., CHANG, A. C., TAN, S. J. & DUNN, A. R. 2015. Visualizing the Interior Architecture of Focal Adhesions with High-Resolution Traction Maps. *Nano Letters*, 15, 2220-2228.
- MURAKAMI, N., SINGH, S. S., CHAUHAN, V. P. & ELZINGA, M. 1995. Phospholipid binding, phosphorylation by protein kinase C, and filament assembly of the COOH terminal heavy chain fragments of nonmuscle myosin II isoforms MIIA and MIIB. *Biochemistry*, 34, 16046-55.
- MYERS, A. P. & CANTLEY, L. C. 2010. Targeting a common collaborator in cancer development. *Sci Transl Med*, 2, 48ps45.
- NADER, G., EZRATTY, E. & GUNDERSEN, G. 2016. FAK, talin and PIPKI γ ; regulate endocytosed integrin activation to polarize focal adhesion assembly. *Nature Cell Biology*, 18, 491-503.
- NAGANO, M., HOSHINO, D., KOSHIKAWA, N., AKIZAWA, T. & SEIKI, M. 2012. Turnover of focal adhesions and cancer cell migration. *International journal of cell biology*, 2012.
- NAYAL, A., WEBB, D. J. & HORWITZ, A. F. 2004. Talin: an emerging focal point of adhesion dynamics. *Curr Opin Cell Biol*, 16, 94-8.

- NEWMAN, R. H., FOSBRINK, M. D. & ZHANG, J. 2011. Genetically Encodable Fluorescent Biosensors for Tracking Signaling Dynamics in Living Cells. *Chemical Reviews*, 111, 3614-3666.
- NGUYEN, H.-N., YANG, J.-M., AFKARI, Y., PARK, B. H., SESAKI, H., DEVREOTES, P. N. & IJIMA, M. 2014. Engineering ePTEN, an enhanced PTEN with increased tumor suppressor activities. *Proceedings of the National Academy of Sciences of the United States of America*, 111, E2684-E2693.
- NISHIOKA, T., AOKI, K., HIKAKE, K., YOSHIZAKI, H., KIYOKAWA, E. & MATSUDA, M. 2008. Rapid Turnover Rate of Phosphoinositides at the Front of Migrating MDCK Cells. *Molecular Biology of the Cell*, 19, 4213-4223.
- OLSON, M. F. & SAHAI, E. 2009. The actin cytoskeleton in cancer cell motility. *Clin Exp Metastasis*, 26, 273-87.
- ORŁOWSKI, A., KUKKURAINEN, S., PÖYRY, A., RISSANEN, S., VATTULAINEN, I., HYTÖNEN, V. P. & RÓG, T. 2015. PIP2 and Talin Join Forces to Activate Integrin. *The Journal of Physical Chemistry B*, 119, 12381-12389.
- OWEN, K. A., PIXLEY, F. J., THOMAS, K. S., VICENTE-MANZANARES, M., RAY, B. J., HORWITZ, A. F., PARSONS, J. T., BEGGS, H. E., STANLEY, E. R. & BOUTON, A. H. 2007. Regulation of lamellipodial persistence, adhesion turnover, and motility in macrophages by focal adhesion kinase. *J Cell Biol*, 179, 1275-87.
- PAGEON, S. V., NICOVICH, P. R., MOLLAZADE, M., TABARIN, T. & GAUS, K. 2016. Clus-DoC: a combined cluster detection and colocalization analysis for single-molecule localization microscopy data. *Mol Biol Cell*, 27, 3627-3636.
- PARTRIDGE, M. A. & MARCANTONIO, E. E. 2006. Initiation of attachment and generation of mature focal adhesions by integrin-containing filopodia in cell spreading. *Mol Biol Cell*, 17, 4237-48.

- PASAPERA, A. M., SCHNEIDER, I. C., RERICHA, E., SCHLAEPFER, D. D. & WATERMAN, C. M. 2010. Myosin II activity regulates vinculin recruitment to focal adhesions through FAK-mediated paxillin phosphorylation. *The Journal of Cell Biology*, 188, 877-890.
- PATTERSON, G. H. 2009. Fluorescence microscopy below the diffraction limit. *Seminars in cell & developmental biology*, 20, 886-893.
- PENG, X. D., WU, X. H., CHEN, L. J., WANG, Z. L., HU, X. H., SONG, L. F., HE, C. M., LUO, Y. F., CHEN, Z. Z., JIN, K., LIN, H. G., LI, X. L., WANG, Y. S. & WEI, Y. Q. 2010. Inhibition of phosphoinositide 3-kinase ameliorates dextran sodium sulfate-induced colitis in mice. *J Pharmacol Exp Ther*, 332, 46-56.
- PEI, Z., YANG, L. & WILLIAMSON, J. R. 1996. Phospholipase C- γ 1 Binds to Actin-Cytoskeleton via Its C-terminal SH2 Domain in Vitro. *Biochemical and Biophysical Research Communications*, 228, 802-806.
- PETIT, V. & THIERY, J. P. 2000. Focal adhesions: structure and dynamics. *Biol Cell*, 92, 477-94.
- PINCET, F., ADRIEN, V., YANG, R., DELACOTTE, J., ROTHMAN, J. E., URBACH, W. & TARESTÉ, D. 2016. FRAP to Characterize Molecular Diffusion and Interaction in Various Membrane Environments. *PLoS ONE*, 11, e0158457.
- QIN, J., XIE, Y., WANG, B., HOSHINO, M., WOLFF, D. W., ZHAO, J., SCOFIELD, M. A., DOWD, F. J., LIN, M. F. & TU, Y. 2009. Upregulation of PIP3-dependent Rac exchanger 1 (P-Rex1) promotes prostate cancer metastasis. *Oncogene*, 28, 1853-63.
- RAIMONDI, C., CALLEJA, V., FERRO, R., FANTIN, A., RILEY, A. M., POTTER, B. V. L., BRENNAN, C. H., MAFFUCCI, T., LARIJANI, B. & FALASCA, M. 2016. A Small Molecule Inhibitor of PDK1/PLC γ 1 Interaction Blocks Breast and Melanoma Cancer Cell Invasion. 6, 26142.
- RAUCHER, D., STAUFFER, T., CHEN, W., SHEN, K., GUO, S., YORK, J. D., SHEETZ, M. P. & MEYER, T. 2000. Phosphatidylinositol 4,5-bisphosphate functions as a second messenger that regulates cytoskeleton-plasma membrane adhesion. *Cell*, 100, 221-8.

- REBECCHI, M. J. & PENTYALA, S. N. 2000. Structure, function, and control of phosphoinositide-specific phospholipase C. *Physiol Rev*, 80, 1291-335.
- REDDY, K. B., SMITH, D. M. & PLOW, E. F. 2008. Analysis of Fyn function in hemostasis and α IIb β 3-integrin signaling. *J Cell Sci*, 121, 1641-8.
- REMUS, T. P., ZIMA, A. V., BOSSUYT, J., BARE, D. J., MARTIN, J. L., BLATTER, L. A., BERS, D. M. & MIGNERY, G. A. 2006. Biosensors to measure inositol 1,4,5-trisphosphate concentration in living cells with spatiotemporal resolution. *J Biol Chem*, 281, 608-16.
- REN, X. D., KIOSSES, W. B., SIEG, D. J., OTEY, C. A., SCHLAEPFER, D. D. & SCHWARTZ, M. A. 2000. Focal adhesion kinase suppresses Rho activity to promote focal adhesion turnover. *J Cell Sci*, 113 (Pt 20), 3673-8.
- RID, R., SCHIEFERMEIER, N., GRIGORIEV, I., SMALL, J. V. & KAVERINA, I. 2005. The last but not the least: the origin and significance of trailing adhesions in fibroblastic cells. *Cell Motil Cytoskeleton*, 61, 161-71.
- ROBERTS, M. S., WOODS, A. J., DALE, T. C., VAN DER SLUIJS, P. & NORMAN, J. C. 2004. Protein kinase B/Akt acts via glycogen synthase kinase 3 to regulate recycling of α v β 3 and α 5 β 1 integrins. *Mol Cell Biol*, 24, 1505-15.
- RUBASHKIN, M. G., CASSEREAU, L., BAINER, R., DUFORT, C. C., YUI, Y., OU, G., PASZEK, M. J., DAVIDSON, M. W., CHEN, Y. Y. & WEAVER, V. M. 2014. Force engages vinculin and promotes tumor progression by enhancing PI3K activation of phosphatidylinositol (3,4,5)-triphosphate. *Cancer Res*, 74, 4597-611.
- RUTH, N. 2013. The spatial structure of cell signaling systems. *Physical Biology*, 10, 045004.
- SALA, G., DITURI, F., RAIMONDI, C., PREVIDI, S., MAFFUCCI, T., MAZZOLETTI, M., ROSSI, C., IEZZI, M., LATTANZIO, R., PIANTELLI, M., IACOBELLI, S., BROGGINI, M. & FALASCA, M. 2008. Phospholipase $\text{C}\gamma$ 1 Is Required for Metastasis Development and Progression. *Cancer Research*, 68, 10187-10196.

- SALTEL, F., MORTIER, E., HYTONEN, V. P., JACQUIER, M. C., ZIMMERMANN, P., VOGEL, V., LIU, W. & WEHRLE-HALLER, B. 2009. New PI(4,5)P₂- and membrane proximal integrin-binding motifs in the talin head control beta3-integrin clustering. *J Cell Biol*, 187, 715-31.
- SANTOS, C. R. & SCHULZE, A. 2012. Lipid metabolism in cancer. *FEBS J*, 279, 2610-23.
- SARRIS, E. G., SAIF, M. W. & SYRIGOS, K. N. 2012. The Biological Role of PI3K Pathway in Lung Cancer. *Pharmaceuticals (Basel)*, 5, 1236-64.
- SASAKI, T., TAKASUGA, S., SASAKI, J., KOFUJI, S., EGUCHI, S., YAMAZAKI, M. & SUZUKI, A. 2009. Mammalian phosphoinositide kinases and phosphatases. *Prog Lipid Res*, 48, 307-43.
- SAUNDERS, R. M., HOLT, M. R., JENNINGS, L., SUTTON, D. H., BARSUKOV, I. L., BOBKOV, A., LIDDINGTON, R. C., ADAMSON, E. A., DUNN, G. A. & CRITCHLEY, D. R. 2006. Role of vinculin in regulating focal adhesion turnover. *European Journal of Cell Biology*, 85, 487-500.
- SCHALLER, M. D. 2001. Paxillin: a focal adhesion-associated adaptor protein. *Oncogene*, 20, 6459-72.
- SCHESWOHL, D. M., HARRELL, J. R., RAJFUR, Z., GAO, G., CAMPBELL, S. L. & SCHALLER, M. D. 2008. Multiple paxillin binding sites regulate FAK function. *J Mol Signal*, 3, 1.
- SCHÖBER, M., RAGHAVAN, S., NIKOLOVA, M., POLAK, L., PASOLLI, H. A., BEGGS, H. E., REICHARDT, L. F. & FUCHS, E. 2007. Focal adhesion kinase modulates tension signaling to control actin and focal adhesion dynamics. *J Cell Biol*, 176, 667-80.
- SCOTT, C. C., DOBSON, W., BOTELHO, R. J., COADY-OSBERG, N., CHAVRIER, P., KNECHT, D. A., HEATH, C., STAHL, P. & GRINSTEIN, S. 2005. Phosphatidylinositol-4,5-bisphosphate hydrolysis directs actin remodeling during phagocytosis. *J Cell Biol*, 169, 139-49.

- SENGELAUB, C. A., NAVRAZHINA, K., ROSS, J. B., HALBERG, N. & TAVAZOIE, S. F. 2016. PTPRN2 and PLC β 1 promote metastatic breast cancer cell migration through PI(4,5)P(2)-dependent actin remodeling. *The EMBO Journal*, 35, 62-76.
- SERVANT, G., WEINER, O. D., HERZMARK, P., BALLA, T., SEDAT, J. W. & BOURNE, H. R. 2000. Polarization of chemoattractant receptor signaling during neutrophil chemotaxis. *Science*, 287, 1037-40.
- SHAO, H., CHOU, J., BATY, C. J., BURKE, N. A., WATKINS, S. C., STOLZ, D. B. & WELLS, A. 2006. Spatial localization of m-calpain to the plasma membrane by phosphoinositide biphosphate binding during epidermal growth factor receptor-mediated activation. *Mol Cell Biol*, 26, 5481-96.
- SHARIFI, M. N., MOWERS, E. E., DRAKE, L. E., COLLIER, C., CHEN, H., ZAMORA, M., MUI, S. & MACLEOD, K. F. 2016. Autophagy promotes focal adhesion disassembly and cell motility of metastatic tumor cells through the direct interaction of paxillin with LC3. *Cell reports*, 15, 1660-1672.
- SHARMA, V. P., DESMARAIS, V., SUMNERS, C., SHAW, G. & NARANG, A. 2008. Immunostaining evidence for PI(4,5)P2 localization at the leading edge of chemoattractant-stimulated HL-60 cells. *J Leukoc Biol*, 84, 440-7.
- SHAYESTEH, L., LU, Y., KUO, W. L., BALDOCCHI, R., GODFREY, T., COLLINS, C., PINKEL, D., POWELL, B., MILLS, G. B. & GRAY, J. W. 1999. PIK3CA is implicated as an oncogene in ovarian cancer. *Nat Genet*, 21, 99-102.
- SHEN, B., DELANEY, M. K. & DU, X. 2012. Inside-out, outside-in, and inside-outside-in: G protein signaling in integrin-mediated cell adhesion, spreading, and retraction. *Current opinion in cell biology*, 24, 600-606.
- SHI, Q. & BOETTIGER, D. 2003. A novel mode for integrin-mediated signaling: tethering is required for phosphorylation of FAK Y397. *Mol Biol Cell*, 14, 4306-15.
- SHORT, B. 2014. PIP2 directs vinculin assembly. *The Journal of Cell Biology*, 207, 572-572.

- SLOMOVITZ, B. M. & COLEMAN, R. L. 2012. The PI3K/AKT/mTOR pathway as a therapeutic target in endometrial cancer. *Clin Cancer Res*, 18, 5856-64.
- SOMANATH, P. R., KANDEL, E. S., HAY, N. & BYZOVA, T. V. 2007. Akt1 signaling regulates integrin activation, matrix recognition, and fibronectin assembly. *J Biol Chem*, 282, 22964-76.
- SPIRA, F., MUELLER, N. S., BECK, G., VON OLSHAUSEN, P., BEIG, J. & WEDLICH-SOLDNER, R. 2012. Patchwork organization of the yeast plasma membrane into numerous coexisting domains. *Nat Cell Biol*, 14, 640-648.
- STATZ, C. M., PATTERSON, S. E. & MOCKUS, S. M. 2017. mTOR Inhibitors in Castration-Resistant Prostate Cancer: A Systematic Review. *Target Oncol*, 12, 47-59.
- STAUFFER, T. P., AHN, S. & MEYER, T. 1998. Receptor-induced transient reduction in plasma membrane PtdIns(4,5)P₂ concentration monitored in living cells. *Curr Biol*, 8, 343-6.
- STAUFFER, F., MAIRA, S. M., FURET, P. & GARCIA-ECHEVERRIA, C. 2008. Imidazo[4,5-c]quinolines as inhibitors of the PI3K/PKB-pathway. *Bioorg Med Chem Lett*, 18, 1027-30.
- STEEG, P. S. 2006. Tumor metastasis: mechanistic insights and clinical challenges. *Nat Med*, 12, 895-904.
- STEIMLE, P. A., HOFFERT, J. D., ADEY, N. B. & CRAIG, S. W. 1999. Polyphosphoinositides inhibit the interaction of vinculin with actin filaments. *J Biol Chem*, 274, 18414-20.
- STÖCKL, M. T. & HERRMANN, A. 2010. Detection of lipid domains in model and cell membranes by fluorescence lifetime imaging microscopy. *Biochimica et Biophysica Acta (BBA) - Biomembranes*, 1798, 1444-1456.

- SUN, Y., LING, K., WAGONER, M. P. & ANDERSON, R. A. 2007. Type I γ phosphatidylinositol phosphate kinase is required for EGF-stimulated directional cell migration. *The Journal of Cell Biology*, 178, 297-308.
- SUSANN, S., JENS, E., KATHARINA, K., TRISTAN, N., MAREK, P., HANNAH, E. S., RICHARD, W. T., ELISABETH, G., SÉBASTIEN, L., ISABEL, D. A. & VAHID, S. 2016. Visualization of lipids and proteins at high spatial and temporal resolution via interferometric scattering (iSCAT) microscopy. *Journal of Physics D: Applied Physics*, 49, 274002.
- TADOKORO, S., SHATTIL, S. J., ETO, K., TAI, V., LIDDINGTON, R. C., DE PEREDA, J. M., GINSBERG, M. H. & CALDERWOOD, D. A. 2003. Talin binding to integrin beta tails: a final common step in integrin activation. *Science*, 302, 103-6.
- TANIYAMA, Y., WEBER, D. S., ROCIC, P., HILENSKI, L., AKERS, M. L., PARK, J., HEMMINGS, B. A., ALEXANDER, R. W. & GRIENDLING, K. K. 2003. Pyk2- and Src-Dependent Tyrosine Phosphorylation of PDK1 Regulates Focal Adhesions. *Molecular and Cellular Biology*, 23, 8019-8029.
- TECKCHANDANI, A. & COOPER, J. A. 2016. The ubiquitin-proteasome system regulates focal adhesions at the leading edge of migrating cells. *eLife*, 5, e17440.
- THAPA, N. & ANDERSON, R. A. 2012. PIP2 signaling, an integrator of cell polarity and vesicle trafficking in directionally migrating cells. *Cell Adh Migr*, 6, 409-12.
- THAPA, N., CHOI, S., TAN, X., WISE, T. & ANDERSON, R. A. 2015. Phosphatidylinositol Phosphate 5-Kinase I γ and Phosphoinositide 3-Kinase/Akt Signaling Couple to Promote Oncogenic Growth. *J Biol Chem*, 290, 18843-54.
- THORPE, L. M., YUZUGULLU, H. & ZHAO, J. J. 2015. PI3K in cancer: divergent roles of isoforms, modes of activation, and therapeutic targeting. *Nature reviews. Cancer*, 15, 7-24.
- TOMPA, P., BUZDER-LANTOS, P., TANTOS, A., FARKAS, A., SZILAGYI, A., BANOCZI, Z., HUDECZ, F. & FRIEDRICH, P. 2004. On the sequential determinants of calpain cleavage. *J Biol Chem*, 279, 20775-85.

- THOMPSON, P. M., RAMACHANDRAN, S., CASE, L. B., TOLBERT, C. E., TANDON, A., PERSHAD, M., DOKHOLYAN, N. V., WATERMAN, C. M. & CAMPBELL, S. L. 2017. A Structural Model for Vinculin Insertion into PIP2-Containing Membranes and the Effect of Insertion on Vinculin Activation and Localization. *Structure*, 25, 264-275.
- TRUONG, H. & DANEN, E. H. J. 2009. Integrin switching modulates adhesion dynamics and cell migration. *Cell Adhesion & Migration*, 3, 179-181.
- TSAI, F.-C., SEKI, A., YANG, H. W., HAYER, A., CARRASCO, S., MALMERSJÖ, S. & MEYER, T. 2014. A polarized Ca²⁺, diacylglycerol and STIM1 signalling system regulates directed cell migration. *Nat Cell Biol*, 16, 133-144.
- TSAI, F. C., KUO, G. H., CHANG, S. W. & TSAI, P. J. 2015. Ca²⁺ signaling in cytoskeletal reorganization, cell migration, and cancer metastasis. *Biomed Res Int*, 2015, 409245.
- TSUBOUCHI, A., SAKAKURA, J., YAGI, R., MAZAKI, Y., SCHAEFER, E., YANO, H. & SABE, H. 2002. Localized suppression of RhoA activity by Tyr31/118-phosphorylated paxillin in cell adhesion and migration. *The Journal of Cell Biology*, 159, 673-683.
- TUMBARELLO, D. A., BROWN, M. C. & TURNER, C. E. 2002. The paxillin LD motifs. *FEBS Lett*, 513, 114-8.
- TURNER, C. E., GLENNEY, J. R., JR. & BURRIDGE, K. 1990. Paxillin: a new vinculin-binding protein present in focal adhesions. *J Cell Biol*, 111, 1059-68.
- VALASTYAN, S. & WEINBERG, R. A. 2011. Tumor metastasis: molecular insights and evolving paradigms. *Cell*, 147, 275-92.
- VALEYEV, N. V., DOWNING, A. K., SKORINKIN, A. I., CAMPBELL, I. D. & KOTOV, N. V. 2006. A calcium dependent de-adhesion mechanism regulates the direction and rate of cell migration: a mathematical model. *In Silico Biol*, 6, 545-72.
- VAN DEN BOGAART, G., MEYENBERG, K., RISSELADA, H. J., AMIN, H., WILLIG, K. I., HUBRICH, B. E., DIER, M., HELL, S. W., GRUBMULLER, H., DIEDERICHSEN, U. & JAHN, R. 2011.

- Membrane protein sequestering by ionic protein-lipid interactions. *Nature*, 479, 552-555.
- VAN DEN BOUT, I. & DIVECHA, N. 2009. PIP5K-driven PtdIns(4,5)P₂ synthesis: regulation and cellular functions. *J Cell Sci*, 122, 3837-50.
- VAN DER FLIER, A. & SONNENBERG, A. 2001. Function and interactions of integrins. *Cell Tissue Res*, 305, 285-98.
- VAN ZANTEN, T. S. & MAYOR, S. 2015. Current approaches to studying membrane organization. *F1000Research*, 4, F1000 Faculty Rev-1380.
- VAN ZIJL, F., KRUPITZA, G. & MIKULITS, W. 2011. Initial steps of metastasis: cell invasion and endothelial transmigration. *Mutat Res*, 728, 23-34.
- VÁRNAI, P. & BALLA, T. 1998. Visualization of Phosphoinositides That Bind Pleckstrin Homology Domains: Calcium- and Agonist-induced Dynamic Changes and Relationship to Myo-[³H]inositol-labeled Phosphoinositide Pools. *The Journal of Cell Biology*, 143, 501-510.
- VARNAI, P., ROTHER, K. I. & BALLA, T. 1999. Phosphatidylinositol 3-kinase-dependent membrane association of the Bruton's tyrosine kinase pleckstrin homology domain visualized in single living cells. *J Biol Chem*, 274, 10983-9.
- VICENTE-MANZANARES, M., CHOI, C. K. & HORWITZ, A. R. 2009a. Integrins in cell migration – the actin connection. *Journal of Cell Science*, 122, 199-206.
- VICENTE-MANZANARES, M., MA, X., ADELSTEIN, R. S. & HORWITZ, A. R. 2009b. Non-muscle myosin II takes centre stage in cell adhesion and migration. *Nat Rev Mol Cell Biol*, 10, 778-90.
- VON WICHERT, G., JIANG, G., KOSTIC, A., DE VOS, K., SAP, J. & SHEETZ, M. P. 2003. RPTP- α acts as a transducer of mechanical force on α v β 3-integrin-cytoskeleton linkages. *J Cell Biol*, 161, 143-53.

- WADE, R. & VANDE POL, S. 2006. Minimal features of paxillin that are required for the tyrosine phosphorylation of focal adhesion kinase. *Biochemical Journal*, 393, 565-573.
- WAN, L., PANTEL, K. & KANG, Y. 2013. Tumor metastasis: moving new biological insights into the clinic. *Nat Med*, 19, 1450-1464.
- WAN, X., HARKAVY, B., SHEN, N., GROHAR, P. & HELMAN, L. J. 2007. Rapamycin induces feedback activation of Akt signaling through an IGF-1R-dependent mechanism. *Oncogene*, 26, 1932-40.
- WANG, J. & RICHARDS, D. A. 2012. Segregation of PIP2 and PIP3 into distinct nanoscale regions within the plasma membrane. *Biology Open*, 1, 857-862.
- WANG, J. H. 2012. Pull and push: talin activation for integrin signaling. *Cell Res*, 22, 1512-4.
- WANG, X., HILLS, L. B. & HUANG, Y. H. 2015. Lipid and Protein Co-Regulation of PI3K Effectors Akt and Itk in Lymphocytes. *Frontiers in Immunology*, 6, 117.
- WANG, Y. & GILMORE, T. D. 2003. Zyxin and paxillin proteins: focal adhesion plaque LIM domain proteins go nuclear. *Biochim Biophys Acta*, 1593, 115-20.
- WARREN, S. C., MARGINEANU, A., KATAN, M., DUNSBY, C. & FRENCH, P. M. W. 2015. Homo-FRET Based Biosensors and Their Application to Multiplexed Imaging of Signalling Events in Live Cells. *International Journal of Molecular Sciences*, 16, 14695-14716.
- WATSON, J. M., HARDING, T. W., GOLUBOVSKAYA, V., MORRIS, J. S., HUNTER, D., LI, X., HASKILL, J. S. & EARP, H. S. 2001. Inhibition of the calcium-dependent tyrosine kinase (CADTK) blocks monocyte spreading and motility. *J Biol Chem*, 276, 3536-42.
- WEBB, D. J., DONAIS, K., WHITMORE, L. A., THOMAS, S. M., TURNER, C. E., PARSONS, J. T. & HORWITZ, A. F. 2004. FAK-Src signalling through paxillin, ERK and MLCK regulates adhesion disassembly. *Nat Cell Biol*, 6, 154-61.
- WEGENER, K. L., PARTRIDGE, A. W., HAN, J., PICKFORD, A. R., LIDDINGTON, R. C., GINSBERG, M. H. & CAMPBELL, I. D. 2007. Structural basis of integrin activation by talin. *Cell*, 128, 171-82.

- WEHRLE-HALLER, B. & IMHOF, B. 2002. The inner lives of focal adhesions. *Trends Cell Biol*, 12, 382-9.
- WOODS, A. & COUCHMAN, J. R. 1992. Protein kinase C involvement in focal adhesion formation. *Journal of Cell Science*, 101, 277-290.
- WOZNIAK, M. A., MODZELEWSKA, K., KWONG, L. & KEELY, P. J. 2004. Focal adhesion regulation of cell behavior. *Biochim Biophys Acta*, 1692, 103-19.
- WU, C. 2007. Focal Adhesion: A Focal Point in Current Cell Biology and Molecular Medicine. *Cell Adhesion & Migration*, 1, 13-18.
- WU, Y., EGHBALI, M., OU, J., LU, R., TORO, L. & STEFANI, E. 2010. Quantitative Determination of Spatial Protein-Protein Correlations in Fluorescence Confocal Microscopy. *Biophysical Journal*, 98, 493-504.
- WU, Z., LI, X., SUNKARA, M., SPEARMAN, H., MORRIS, A. J. & HUANG, C. 2011. PIPK γ regulates focal adhesion dynamics and colon cancer cell invasion. *PLoS One*, 6, e24775.
- WUTTKE, A. 2015. Lipid signalling dynamics at the beta-cell plasma membrane. *Basic Clin Pharmacol Toxicol*, 116, 281-90.
- YAMAGUCHI, H. & CONDEELIS, J. 2007. Regulation of the actin cytoskeleton in cancer cell migration and invasion. *Biochim Biophys Acta*, 1773, 642-52.
- YAO, M., GOULT, B. T., CHEN, H., CONG, P., SHEETZ, M. P. & YAN, J. 2014. Mechanical activation of vinculin binding to talin locks talin in an unfolded conformation. *Sci Rep*, 4, 4610.
- YE, X., MCLEAN, M. A. & SLIGAR, S. G. 2016a. Conformational equilibrium of talin is regulated by anionic lipids. *Biochim Biophys Acta*, 1858, 1833-40.
- YE, X., MCLEAN, M. A. & SLIGAR, S. G. 2016b. Phosphatidylinositol 4,5-Bisphosphate Modulates the Affinity of Talin-1 for Phospholipid Bilayers and Activates Its Autoinhibited Form. *Biochemistry*, 55, 5038-48.

- YUAN, Y., LI, L., ZHU, Y., QI, L., AZIZI, L., HYTÖNEN, V. P., ZHAN, C.-G. & HUANG, C. 2017. The molecular basis of talin2's high affinity toward β 1-integrin. *Scientific Reports*, 7, 41989.
- ZAIDEL-BAR, R., COHEN, M., ADDADI, L. & GEIGER, B. 2004. Hierarchical assembly of cell-matrix adhesion complexes. *Biochem Soc Trans*, 32, 416-20.
- ZAMIR, E., KATZ, M., POSEN, Y., EREZ, N., YAMADA, K. M., KATZ, B. Z., LIN, S., LIN, D. C., BERSHADSKY, A., KAM, Z. & GEIGER, B. 2000. Dynamics and segregation of cell-matrix adhesions in cultured fibroblasts. *Nat Cell Biol*, 2, 191-6.
- ZERIAL, M. & MCBRIDE, H. 2001. Rab proteins as membrane organizers. *Nat Rev Mol Cell Biol*, 2, 107-17.
- ZHANG, X., CHATTOPADHYAY, A., JI, Q.-S., OWEN, J. D., RUEST, P. J., CARPENTER, G. & HANKS, S. K. 1999. Focal adhesion kinase promotes phospholipase C- γ 1 activity. *Proceedings of the National Academy of Sciences of the United States of America*, 96, 9021-9026.
- ZHANG, X., JIANG, G., CAI, Y., MONKLEY, S. J., CRITCHLEY, D. R. & SHEETZ, M. P. 2008. Talin depletion reveals independence of initial cell spreading from integrin activation and traction. *Nat Cell Biol*, 10, 1062-8.
- ZHAO, X. & GUAN, J. L. 2011. Focal adhesion kinase and its signaling pathways in cell migration and angiogenesis. *Adv Drug Deliv Rev*, 63, 610-5.
- ZHENG, Y., ADAMS, T., ZHI, H., YU, M., WEN, R., NEWMAN, P. J., WANG, D. & NEWMAN, D. K. 2015. Restoration of responsiveness of phospholipase C γ 2-deficient platelets by enforced expression of phospholipase C γ 1. *PLoS One*, 10, e0119739.
- ZHOU, H. & HUANG, S. 2011. Role of mTOR Signaling in Tumor Cell Motility, Invasion and Metastasis. *Current protein & peptide science*, 12, 30-42.
- ZIEGLER, W. H., GINGRAS, A. R., CRITCHLEY, D. R. & EMSLEY, J. 2008. Integrin connections to the cytoskeleton through talin and vinculin. *Biochem Soc Trans*, 36, 235-9.

ZINCHUK, V., WU, Y. & GROSSENBACHER-ZINCHUK, O. 2013. Bridging the gap between qualitative and quantitative colocalization results in fluorescence microscopy studies. *Scientific Reports*, 3, 1365.